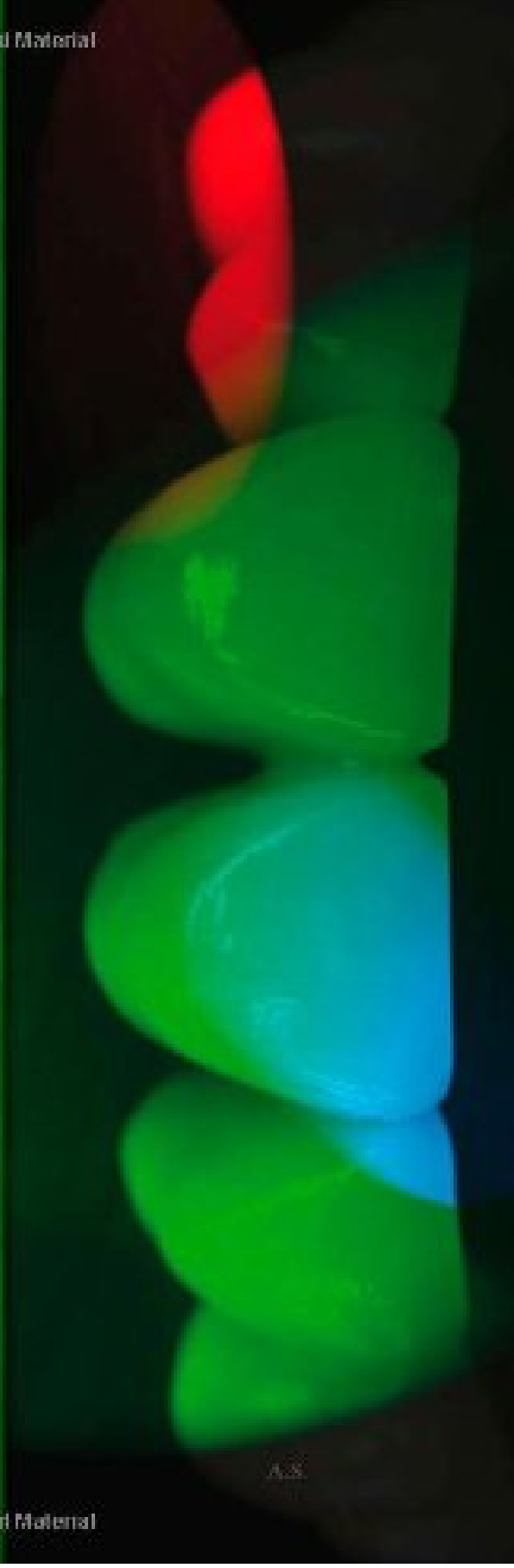
Copyrighted Material

Adhesion Aspects in Dentistry

Edited by
J.P. Matinlinna
K.L. Mittal



VSP

Copyrighted Material

Adhesion Aspects in Dentistry

Edited by

Jukka P. Matinlinna and K. L. Mittal

VSP

LEIDEN • BOSTON
2009

ISBN: 978 90 04 17271 5

© 2009 by Koninklijke Brill NV, Leiden, The Netherlands.
Koninklijke Brill NV incorporates the imprints BRILL, Hotei Publishing,
IDC Publishers, Martinus Nijhoff Publishers and VSP.

All rights reserved. No part of this publication may be reproduced, translated, stored in a retrieval system, or transmitted in any form or by any means, electronic, mechanical, photocopying, recording or otherwise, without prior written permission from the publisher.

Authorization to photocopy items for internal or personal use is granted by Koninklijke Brill NV provided that the appropriate fees are paid directly to The Copyright Clearance Center, 222 Rosewood Drive, Suite 910, Danvers, MA 01923, USA.
Fees are subject to change.

PRINTED IN THE NETHERLANDS

Contents

Preface vii

Part 1: Adhesion and Bonding Aspects

Adhesion to Intraradicular Dentin: A Review
L. Breschi, A. Mazzoni, E. De Stefano Dorigo and M. Ferrari 3

Direct Resin-Based Composite Restorations — Clinical Challenges
J. Perdigão, S. Duarte, Jr. and G. Gomes 35

Important Aspects of Bonding Resin to Dental Ceramics
A. Della Bona 49

Interpenetrating Polymer Networks (IPNs) in Dental Polymers and Composites
P. K. Vallittu 63

Resin Bonding to Oxide Ceramics for Dental Restorations
M. Kern 75

Resin Bonding to Dentine after Casein Phosphopeptide-Amorphous Calcium Phosphate (CPP-ACP) Treatments
V. Sattabanasuk, M. F. Burrow, Y. Shimada and J. Tagami 91

Amorphous Calcium Phosphate Composites and Their Effect on Composite–Adhesive–Dentin Bonding
J. M. Antonucci, J. N. R. O'Donnell, G. E. Schumacher and D. Skrtic 105

Adhesive Cementation and the Strengthening of All-Ceramic Dental Restorations
G. J. P. Fleming and O. Addison 121

Comparison of Different Etching Agents and Repair Materials Used on Feldspathic Porcelain
P. K. Lundvall, E. Ruyter, H. J. Rønold and K. Ekstrand 137

Evaluation of *bis*-GMA/MMA Resin Adhesion to Silica-Coated and Silanized Titanium
M. Puska, L. Lassila, P. K. Vallittu, J. Seppälä and J. Matinlinna 147

XPS Analysis of Silane Films on the Surface of a Dental Ceramic
T. Hooshmand, A. Keshvad and R. van Noort 163

Part 2: Mechanics and Durability Aspects

Numerical Analysis of Biomechanical Response of a Dental Prosthesis with Regard to Bone–Implant Adhesion Phenomena
A. N. Natali, E. L. Carniel and P. G. Pavan 177

Bond-Disruptive Stresses Generated by Resin Composite Polymerization in Dental Cavities
D. C. Watts, L. F. J. Schneider and H. Y. Marghalani 191

Fatigue Resistance of Resin-Bonded Post–Core–Crown Treated Teeth with Flared Root Canal
Q. Xie, W. Wu, P. Liu and P. K. Vallittu 211

Thermocycling Effects on Resin Bond to Silicatized and Silanized Zirconia
T. T. Heikkinen, L. V. J. Lassila, J. P. Matinlinna and P. K. Vallittu 223

Part 3: Adhesion Testing

Adhesion Strength Testing — Time to Fail or a Waste of Time?
B. W. Darvell 235

Navigating the Dentin Bond Strength Testing Highway: Lessons and Recommendations
J. L. Ferracane, J. M. Dossett, F. Pelogia, M. R. P. Macedo and T. J. Hilton 245

Critical Evaluation of Adhesive Test Methods Used in Dentistry
K.-J. M. Söderholm 261

Shear Bond Strength of Cement to Zirconia
M. Rosentritt, M. Behr, J. M. van der Zel and A. J. Feilzer 279

Preface

The phenomenon of adhesion plays a crucial role in modern operative and preventive dentistry. Adequate adhesion between dental tissues and restorations is *sine qua non* for satisfactory performance of restorations. On the other hand, in dental sciences adhesion can be *bête noire* as it can lead to biofilm formation with concomitant undesirable effects, e.g., gingival problems, halitosis, tooth decay and periodontal complications. So an understanding and control of adhesion in the oral milieu is of cardinal importance.

Even a cursory look at the literature will evince that in past decades there has been tremendous interest and high tempo of research activity in the arena of dental adhesion and much effort has been devoted to ameliorating the existing adhesives or devising new and improved adhesive products and techniques. Adhesive dentistry has numerous applications in cariology, prosthodontics, implantology, orthodontics as well as in aesthetic dentistry — in essence in comprehensive dental care. The current developments in adhesive techniques for soft tissues and also some slow-releasing agents have expanded applications to endodontics, periodontology and maxillo-facial surgery as well. Clinicians and researchers are fully aware of such modern motto which is based on minimal invasive dentistry and adhesive techniques: "Seal is the deal". The concept "adhesive dentistry" is profoundly changing the practice in dentistry and all signals indicate that interest in adhesive dentistry will continue unabated.

In light of the importance and wide-ranging applications and implications of adhesion and adhesives in dentistry, we decided to make this book available as a single and easily accessible source of comprehensive information. This book is based on the Special Issue of the *Journal of Adhesion Science and Technology* (*JAST*), Vol. 23, Nos 7–8 (2009). The papers as published in the above-mentioned Issue have been re-arranged and grouped in a more logical fashion in this book.

This book containing a total of 19 papers (reflecting overviews and original research) and covering many ramifications of adhesion in dentistry is divided into three parts. Part 1: Adhesion and Bonding Aspects; Part 2: Mechanics and Durability Aspects; and Part 3: Adhesion Testing. Topics covered include: adhesion to intraradicular dentin; resin-based composite restorations; bonding resins to dental

Adhesion Aspects in Dentistry
© Koninklijke Brill NV, Leiden, 2009

ceramics; surface treatments to improve adhesion of resin composites, including use of silanes; biomechanical response of dental prosthesis; bond-disruptive stresses; thermocycling effects on resin bond; adhesion strength testing; dentin bond strength testing; adhesive test methods used in dentistry.

It is quite patent that many aspects of adhesion and adhesives in dentistry are accorded due coverage in this book; concomitantly, this book represents a comprehensive treatise on this fascinating topic with societal implications. Moreover, this book, containing bountiful information, reflects the cumulative work and wisdom of many (about 50) world-renowned researchers and practitioners and thus should be of interest to anyone interested/involved in any aspects of dentistry. We further hope this book will serve as a fountainhead for new research ideas and new application vistas will emerge as new adhesive materials and techniques become available.

Acknowledgements

Now it is a pleasure to acknowledge all those who helped in many and varied ways. First of all, we profusely thank the authors for their interest, contribution, enthusiasm, and cooperation without which this book would not have seen the light of day. Second, we are most appreciative of the reviewers for their time and efforts in providing many valuable comments which certainly improved the quality of manuscripts. JPM would like to express his sincerest thanks to Profs. Stig Karlsson, Pekka Vallittu, and Lakshman Samaranayake at NIOM, Nordic Institute of Dental Materials, Oslo, Norway; the Institute of Dentistry at the University of Turku, Finland; and the Faculty of Dentistry, The University of Hong Kong, P. R. China, respectively, for providing requisite facilities and atmosphere to enable him to carry out the editorial activity. Last, our appreciation goes to the staff of Brill (publisher) for materializing this book.

JUKKA P. MATINLINNA
University of Hong Kong
Faculty of Dentistry, Dental Materials Science
The Prince Philip Dental Hospital
34 Hospital Road
Hong Kong, P. R. China

K. L. MITTAL
P.O. Box 1280
Hopewell Junction, NY 12533, USA

Part 1
Adhesion and Bonding Aspects

Adhesion to Intraradicular Dentin: A Review

Lorenzo Breschi [a,b], **Annalisa Mazzoni** [c], **Elettra De Stefano Dorigo** [a] **and Marco Ferrari** [d,*]

[a] Department of Biomedicine, University of Trieste, Via Stuparich 1, 34125 Trieste, Italy
[b] IGM-CNR, Unit of Bologna c/o IOR, Via Pupilli 1, 40136 Bologna, Italy
[c] Department of SAU&FAL, University of Bologna, Via Irnerio 48, 40126 Bologna, Italy
[d] Department of Fixed Prosthodontics and Dental Materials, University of Siena, Policlinico Le Scotte, Viale Bracci, 53100 Siena, Italy

Abstract
Luting fiber posts to intraradicular dentin remains an unpredictable goal due to various clinical factors influencing the clinical procedure. Primarily differences can be found between bonding to coronal or to intraradicular dentin due to the different histological characteristics of the substrates, the high C-factor of the endodontic space, the presence of smear layer due to the post preparation technique, incompatibility between some adhesive systems and resin-based cements, and finally the limited access of the post space that may lead the clinician to different mistakes. Thus this article critically evaluates all aspects that may jeopardize the adhesion of luted fiber posts within the endodontic space, suggesting the use of standardized techniques that improve immediate adhesion and stabilize the adhesive interface over time.

The review of the data currently available in peer-reviewed journals suggests that a strict following of a step-by-step clinical standardized technique allows the clinician to minimize bond failure and obtain a clinically reliable durable bond.

Keywords
Dentin, adhesion, dental bonding systems, fiber posts

1. Introduction

Adhesion is a complex phenomenon involving physical and chemical mechanisms that allows attachment of one material to another. The bonding systems allow resistance to separation between the substrate and the adhesive and stress distribution along the adhesive interface [1]. In addition, and pivotal for all dental restorations, adhesion means the possibility to properly seal the interface between the cavity and the restorative material, thus reducing the risk of post-operative sensitivity, marginal staining and recurrent caries [2].

* To whom correspondence should be addressed. E-mail: md3972@mclink.it

Adhesion Aspects in Dentistry
© Koninklijke Brill NV, Leiden, 2009

The modern concepts of adhesive dentistry started a long time ago with the pioneering studies of Dr. Buonocore that revealed how etching with phosphoric acid could increase bond effectiveness, in terms of either bond strength or sealing ability [3]. As the first adhesives were mainly based on bisphenol glycidyl methacrylate (Bis-GMA) [4], the bonding system was extremely hydrophobic (i.e., no compatibility with water) and, thus, no adhesion was possible with the dentin tissue since it is an intrinsically wet substrate. Later on the development and the incorporation within the adhesive systems of more hydrophilic monomers, such as 2-hydroxyethyl methacrylate (HEMA), allowed adhesives to bond also to dentin [5]. The possibility of the dental adhesives to tolerate water is extremely important, particularly after the introduction of the total etch technique (i.e., simultaneous etching of enamel and dentin that removes smear layers and smear plugs funnelling the tubule orifices) [6] since relatively large amount of water permeates throughout the dentin thickness wetting the cavity surface [7].

Despite major simplifications in dental adhesion, bonding to intraradicular dentin remains an unpredictable goal due to various clinical factors influencing the procedure. In particular, several differences can be found between bonding to coronal and to intraradicular dentin due to the relative limited access of the post space that may lead the clinician to different mistakes, finally jeopardizing the adhesion [8]. Thus there is a need for a standardized step-by-step procedure that should be applicable also within the endodontic space.

2. Dental Bonding Systems and Classification

Dental bonding systems are resin blends possessing both hydrophilic and hydrophobic properties, thus, named amphiphilic. In other words, adhesives are compounds containing both hydrophilic monomers that allow bonding with the tooth structure, as well as hydrophobic monomers contributing to coupling with the restorative materials or resin-based cements.

From a physical perspective, bonding is a relation between the free energy of the tooth surface and the wetting ability of the adhesive solution [9]. If the adhesive cannot wet the substrate, no adhesion can occur. The adhesion process involves enhancing the surface free energy of the tooth structure with an acidic solution (e.g., etching) so as to reduce the contact angle with the bonding solution that should also contain a surfactant agent (e.g., primer) to allow proper wetting of the substrate [10].

Despite their different formulations, all adhesive systems involve three cardinal steps which are considered as pivotal in establishing a durable adhesive interface: (1) etching, (2) priming and (3) bonding [2]. The etching involves an acidic solution that demineralises the enamel/dentin surface thus increasing their surface free energy. The primer is composed of a mixture of hydrophilic monomers and solvents aiming to allow the wettability of the tooth surface and to permit substitution of the water retained within the substrate with the resin monomers. The bonding

agent contains the hydrophobic part of the system that allows coupling with the resin-based restorative materials or the resin cements.

Adhesive systems interact with the dentin tissue following two different strategies: they can remove the smear layer (etch-and-rinse technique) or maintain it as the substrate for bonding procedure (self-etch technique) [2]. The etch-and-rinse strategy is characterized by the application of a preliminary and separate etching step (usually with a gel of 35–37% phosphoric acid) that is later rinsed away. Conversely, the self-etch approach refers to the application of an etchant/primer solution that is only air-dried, thus, also named 'etch-and-dry' [11]. As no rinsing occurs after etching, the acidic compound of the self-etch system remains entrapped within the modified smear layer and the acid is buffered by the mineral released from the substrate [12, 13]. The other steps such as priming and bonding can be separate or combined, depending on the adhesive formulation. If the bonding agent is combined with the primer (for the etch-and-rinse technique) or with the self-etching/primer agent (for the self-etch technique) the adhesives are considered as 'simplified' [14].

As all adhesives contain etching, primer and bonding agents in their formulations [2], a classification based on the number and combination of the steps constituting the adhesive system is proposed. Thus we can identify four different classes (Table 1):

1. Etch-and-rinse, three-step: adhesive systems characterized by the sequential application of etching, primer and bonding agents as separate and individual solutions (Fig. 1).

2. Etch-and-rinse, two-step: simplified adhesive systems characterized by the use of a combined primer and bonding agents that is applied on the tooth surface after removal of the etching agent.

3. Self-etch, two-step: adhesive systems characterized by a self-etching primer that is dried on the tooth surface, followed by a separate hydrophobic bonding agent (Fig. 2).

4. Self-etch, one-step: simplified adhesive systems characterized by a combination in a single application solution of the etching/primer/bonding agents. These extremely simplified adhesive systems can be formulated as 'one-bottle' systems or, alternatively, in 'multi-bottle' systems mixed only prior to the clinical application.

When the dentin tissue is instrumented, a smear layer is created on top of the dentin surface [15]. The smear layer is removed by etch-and-rinse adhesive systems during the etching and the following water rinsing and then the sound dentin is surface-demineralized [16]. Since the peritubular dentin is highly mineralized, the use of the etching agent opens the tubules funnelling their orifices and removing all residual smear plugs [17]. The intertubular dentin is demineralized to only a few μm in depth, depending on acid concentration, gel formulation, time and mode of application (e.g., a continuous brushing technique enhances demineralization) [18].

Table 1.
Classification of contemporary dental bonding systems and commercial names of some of the most common adhesive systems

Etch-and-rinse		Self-etch or etch-and-dry	
3-step 4th generation	2-step 5th generation	2-step 6th generation	1-step 7th generation
Etching Apply for 15 s, rinse for 15 s, gentle air-dry keeping dentin moist Priming Apply 1–5 layers, gentle air-dry Bonding Apply 1 layer, gentle air-dry, light cure	Etching Apply for 15 s, rinse for 15 s, gentle air-dry keeping dentin moist Priming & Bonding Apply 1–5 layers, gentle air-dry, light cure	Etching & Priming 1 application without rinsing, gentle air dry Bonding Apply 1 layer, gentle air-dry, light cure	Etching & Priming & Bonding Apply 1–5 layers without rinsing, gentle air-dry, light cure
Adper Scotchbond Multi-Purpose (3M ESPE) All Bond 3 (Bisco) Optibond FL (Kerr) Syntac (Ivoclar Vivadent) Gluma Solid Bond (Heraeus Kulzer)	Prime & Bond NT (Dentsply) XP-Bond (Dentsply) Excite (Vivadent) Adper Scotchbond 1XT (3M ESPE) One-Step Plus (Bisco) PQ1 (Ultradent) Gluma Comfort Bond (Heraeus Kulzer)	AdheSE (Ivoclar Vivadent) Clearfil Protect Bond (Kuraray) One-Step Plus/TYRIAN (Bisco) Peak (Ultradent)	AdheSE One (Ivoclar Vivadent) All-Bond SE (Bisco) Adper Prompt L-Pop (3M ESPE) Clearfil S^3Bond (Kuraray) XENO V (Dentsply) I-Bond (Heraeus Kulzer)

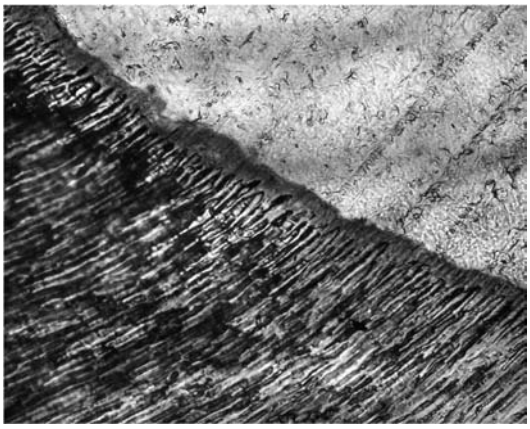


Figure 1. Hybrid layer and resin tag formation created by an etch-and-rinse adhesive system bonded to intraradicular dentin (light microscopy image 100×).

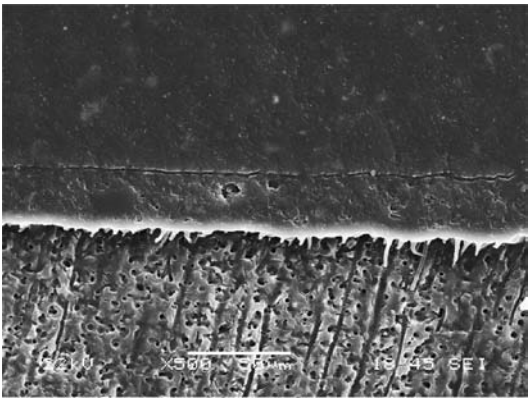


Figure 2. Low magnification view of a self-etching adhesive system bonded within the root canal (SEM image 500×).

The removal of the mineral phase from dentin surface allows to expose the dentin organic matrix, which is constituted by an intricate network of type I-collagen fibrils (90% of the organic matrix) [19] and other non-collagenous proteins, such as proteoglycans, lipids and enzymes [20]. The resin monomers (primer and bonding agent of the adhesive system) should then fully infiltrate this delicate network of demineralized collagen fibrils, creating the so-called hybrid layer [21]. The bond established by the etch-and-rinse adhesive systems relies only on micromechanical retention between the demineralized dentin matrix and the polymerized adhesive system [22]. The penetration of the adhesive into the funnelled dentin tubules creates the so-called resin tags [23], particularly extended when the adhesive is applied in endodontically treated teeth since no adverse pulpal pressure is present. Although resin tags have been morphologically described by several researchers, their active role in adhesion is controversial as bond strength value is reduced in deep dentin

where most of the substrate is represented by dentin tubules [24], confirming that the hybridization of the intertubular dentin is critical for adhesion [25].

When self-etch adhesive systems are used, the smear layer is only partially demineralized, depending on the pH and pKa of the etching acidic solution. In relation to the etching ability of the adhesives, self-etch systems are classified as mild, intermediate and strong [2]. Strong self-etch adhesives are able to completely dissolve the smear layer (i.e., similar to the etch-and-rinse strategy) [26], while intermediate to mild systems modify the smear layer and demineralize the dentin matrix leaving residual hydroxyapatite crystals on the collagen fibrils providing additional chemical bond with adhesive monomer [27], that cannot be obtained with etch-and-rinse adhesives since they fully demineralize the collagen.

While self-etch adhesive systems are characterized by a simultaneous demineralization and infiltration (due to the combination of the primer with the etching agent), impregnation of etch-and-rinse monomers occurs after demineralization. For this reason, etch-and-rinse systems (mainly two-step systems where primer and bonding agent are combined) should be applied on wet dentin to maintain large interfibrillar spaces between the demineralized collagen fibrils, thus facilitating monomer impregnation [28]. The solvent of the bonding agent (usually ethanol, water or acetone) acts as a carrier for the resin monomer that enhances the substitution of the residual dentin water. The air-drying that follows the primer/bonding agent application permits solvent evaporation, leaving the resin material within the collagen network, the bonding agent co-polymerizes with the primer creating a hydrophobic surface that can be polymerized and then coupled with the resin-based material or with the resin-based cement.

3. Substrate: Intraradicular Dentin

The analysis of the radicular portion allows to identify pulpal tissue, predentin and mineralized dentin surrounded by cement tissue. Predentin is a layer of unmineralized organic matrix that lines the innermost pulpal portion and may greatly vary in thickness but still remaining constant during aging since the amount that calcifies is balanced by the addition of newly secreted organic matrix [29]. The synthesis of predentin begins with the production of large-diameter collagen fibrils (called von Korff's fibres) by the odontoblasts, mainly consisting of type III-collagen fibrils [30, 31]. Predentin and dentin are in direct and dynamic contact as the odontoblasts produce type I-collagen fibrils and proteoglycans by extending their processes into the forming extracellular matrix starting dentinogenesis. These forming structures of un-mineralized organic components will constitute the dentin organic matrix which represents approximately 30% in volume of the mineralized sound dentin. The remnants of the dentin tissue are composed of water (approx. 20%) and minerals such as apatite [19].

As predentin is removed by the instrumentation of the pulpal tissue due to the endodontic treatment (associated with sodium hypochlorite rinses) followed by

the use of calibrated burs to prepare the post space, the substrate for any adhesive luting procedure within the roots is represented by mineralized intraradicular dentin [32]. Several studies investigated composition and structure of the intraradicular dentin, and major differences in bond strengths between intraradicular and coronal dentin were demonstrated and only minor morphological and biochemical differences were reported. Similar to coronal dentin, intraradicular dentin is a non-homogeneous tissue characterized by the presence of tubules extending from the pulp to the tooth periphery [32]. For this reason the intraradicular dentin tissue can be classified in peritubular and intertubular depending on the density and distribution of the tubules. Peritubular dentin is characterized by the presence of a collar of hyper-mineralized tissue and low content of type I-collagen fibrils; conversely, the intertubular dentin is mainly composed of mineralized type I-collagen fibrils [17]. As the number of tubules greatly diminishes toward the apical region of the intraradicular dentin, the ratio between peritubular and intertubular dentin greatly varies from the apical to the coronal third [32, 33]. Moving toward the apex, the substrate modification will induce changes in the impregnation pattern of the adhesive system, thus reducing peritubular dentin infiltration and resin tag formation, while increasing intertubular dentin impregnation [34]. Since it is well known that resin tags contribute only minimally to bond strength [25], the greater amount of intertubular dentin available for hybridization should potentially lead to higher bond strength in the apical rather than in the coronal third of the root canal [32]. However, the overwhelming majority of the studies report that bond strength to intraradicular dentin decreases from the coronal to the apical third of the root canal and it has been shown that the thickness of the hybrid layer is significantly reduced in the apical third. The thinning of the hybrid layer observed by some authors toward the apex was considered as responsible for the lower bond strength due to reduced impregnation of the adhesive system at this level of the root canal [32]. However, this issue is still controversial as some studies reported similar or increased bond strength closer to the apical region showing no differences in terms of thickness of the hybrid layer (Table 2).

As both the thickness of the hybrid layer and the morphology of the resin tags (determined by the substrate) have been recently shown to contribute minimally to the bond strength, we may conclude that the reduced bond strength reported in most of the studies on the intraradicular dentin compared to the coronal dentin might probably be attributed to other factors instead of the substrate morphology, such as the high C-factor of the endodontic space and the difficulty in clinical handling due to the limited endodontic space.

4. Clinical Procedures — Factors Affecting Bonding to Intraradicular Dentin

A fundamental prerequisite for adhesion to intraradicular dentin is represented by the ability of the clinician to obtain a perfectly clean post space as the use of sodium hypochlorite rinses, EDTA, endodontic cements, gutta-percha, or other endodontic

Table 2.
Studies reporting bond strength values to intraradicular dentin

Coronal third > apical third	Coronal third ⩾ apical third	Coronal third < apical third
Yoshiyama *et al.*, *J. Dent.* 1998	Yoshiyama *et al.*, *J. Dent.* 1996	Gaston *et al.*, *J. Endodont.* 2001
Bouillaguet *et al.*, *Dent. Mater.* 2003	Burrow *et al.*, *Am. J. Dent.* 1996	Mannocci *et al.*, *Dent. Mater.* 2004
Goracci *et al.*, *Eur. J. Oral Sci.* 2004	Aksornmuang *et al.*, *J. Dent.* 2004	Muniz and Matias, *Oper. Dent.* 2005
Perdigao *et al.*, *Am. J. Dent.* 2004	Foxton *et al.*, *J. Oral Rehabil.* 2005	
Bolhuis *et al.*, *Quintessence Int.* 2004	Ngoh *et al.*, *J. Endodont.* 2001	
Mallmann *et al.*, *Oper. Dent.* 2005	Kanno *et al.*, *Dent. Mater. J.* 2004	
Bolhuis *et al.*, *Oper. Dent.* 2005	Foxton *et al.*, *Oper. Dent.* 2003	
Kalkan, *J. Prosthet. Dent.* 2006		
Perez *et al.*, *Int. J. Prosthodont.* 2006		
de Durâo Mauricio *et al.*, *J. Biomed. Mater. Res.* 2007		
Perdigao *et al.*, *Dent. Mater.* 2007		
Perdigao *et al.*, *J. Prosthodont.* 2007		
Faria Silva *et al.*, *J. Endodont.* 2007		
Boff *et al.*, *Quintessence Int.* 2007		
Wang *et al.*, *Dent. Mater.* 2007		
Ohlmann *et al.*, *J. Dent.* 2007		

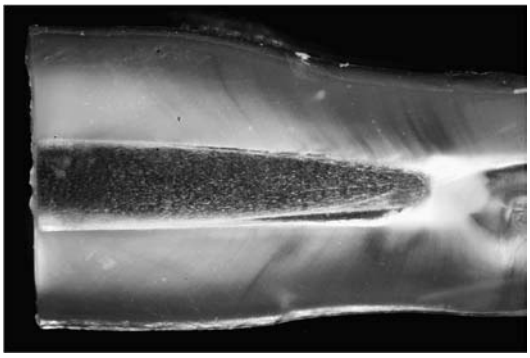


Figure 3. Fiber-reinforced post luted into a root canal (stereomicroscopic image 10×).

filling materials clearly modify the intraradicular dentin environment [35] (Fig. 3). In addition, the difficulty to control the substrate surface and to properly apply the adhesive and the cement inside the narrow endodontic space is evident.

Several factors may affect intraradicular dentin: the presence and thickness of the endodontic smear layer, the method of post space preparation as well as several adverse clinical factors; in addition, the use of irrigants or medicaments during the endodontic treatment, the use of eugenol-based materials or bleaching agents, the influence of endodontic re-treatment, the possible incompatibility between different

resin-based materials, and geometric factors are some of the most important aspects that need to be clarified.

4.1. Endodontic Smear Layer

The theoretical goals of successful endodontic therapy are the disinfection and the complete obliteration of the root canal space with an inert filling material, creating an optimal seal with the tooth structure. The prerequisite for a tight seal is the closed adaptation of the filling material to the canal walls, which, however, is impaired by the presence of the endodontic smear layer, invariably formed after manual and rotary instrumentation [36]. According to its original definition, the smear layer has been defined as 'any debris, calcific in nature, produced by reduction or instrumentation of dentin, enamel or cementum' [37], or as a 'contaminant' [38] that precludes interaction with the underlying pure tooth tissue [1]. The burnishing action of the cutting instruments generates frictional heat and shear forces, so that the smear layer becomes attached to the underlying surface in a manner that prevents it from being rinsed off or scrubbed away [1, 39]. The morphological features, composition and thickness of the smear layer are determined by the type of endodontic instrument used, the method of irrigation and tooth substrate at which it is formed [1, 40].

Coronal smear layers reflect the substructure of dentine matrix composition while endodontic smear layer contains inorganic and organic substances that include also fragments of odontoblastic process, microorganisms and necrotic material [15] (Fig. 4). Despite its different composition the thickness of smear layer ranges from 0.5 to 2 μm, in addition to a deeper layer packed into the dentin tubules to a depth of up to 40 μm, obstructing their orifices thus forming the so-called *smear plugs* (Fig. 5). The smear layer can be detrimental to effective bonding: in early smear layer research, non-acidic adhesives, applied without prior etching, did not penetrate sufficiently enough to establish a bond with intact dentin; such bonds were prone to cohesive failure of the smear layer [24].

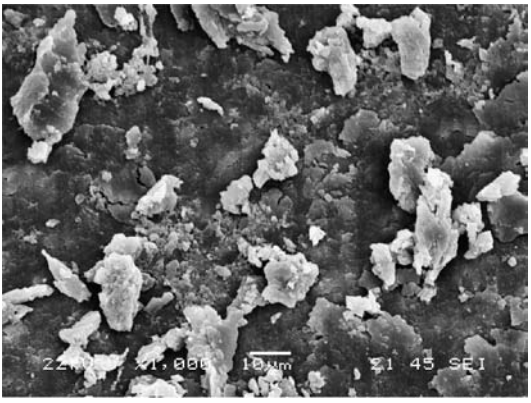


Figure 4. SEM micrograph of smear layer created by instrumentation along the wall of the coronal third (1000×).

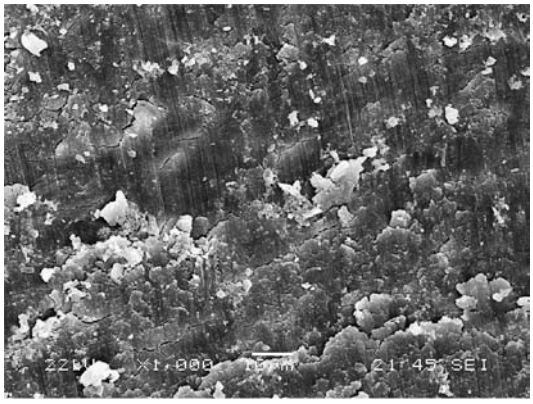


Figure 5. SEM micrograph of dentinal tubules closed by smear plugs and densely packed debris (1000×).

As previously mentioned in the description of the adhesive systems, two bonding strategies are used to overcome the low attachment strengths of the smear layer. With the etch-and-rinse approach the use of the etching followed by extensive rinsing removes the smear layer prior to the bonding, while in the self-etch approach the smear layer is only modified beforehand and it is incorporated within the hybrid layer complex [2, 26]. The more acidic and aggressive the conditioner, the more completely the smear layer and smear plugs are removed [41].

Within the root canal, dentin surfaces covered with debris and remnants of pulp tissue are not likely to achieve effective bonding [35, 42], because the endodontic smear layer acts as a barrier significantly influencing any adhesive bond formed between the instrumented canal walls and the restorative material [2], as well as the resin cementation of fiber posts. Although there is some controversy regarding the desirability of retaining smear layer in adhesive dentistry, in endodontics, its removal is considered to be advantageous and highly desirable [43]. The endodontic smear layer, in fact, may be infected and may protect the bacteria already present in the dentinal tubules; because of these concerns, one may deem it prudent to remove the initially infected root canals and to allow penetration of intraradicular medications into the dentinal tubules [44]. In addition to the reduced penetration of root canal medicaments, several studies have reported also a better adhesion of obturation materials after removal of the smear layer [45] and the penetration depth within the dentinal tubules of different sealers is also consistently increased (by 10–80 μm) once the smear layer is removed [44, 46].

4.2. Post Space Preparation and 'Secondary' Smear Layer

In addition to the 'traditional' smear layer produced by manual or rotary instrumentation of the root canal walls, the subsequent preparation of the post space using post drills resulted in an additional and even thicker smear layer composed of debris and sealer/gutta-percha remnants that significantly influenced the adhesion of

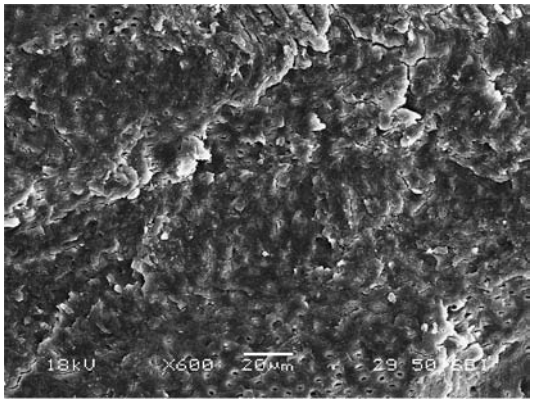


Figure 6. SEM micrograph of smear layer along the root canal walls (600×).

fiber posts [43] (Fig. 6). In fact, the action of the drills used to remove the root-filling material to create post space produces a new smear layer rich in sealer and gutta-percha remnants that are plasticized by the frictional heat of the drill and this may diminish the penetration and chemical action of the agents used to bond fiber posts. In addition, only minimal irrigation can be performed inside the endodontic canal. Thus, achieving clean dentinal surfaces after mechanical post space preparation seems to be a critical step for optimal post retention, in particular, when resin cement is used [47]. It has been reported that the use of phosphoric acid after post space preparation resulted in discontinuous areas of deep intertubular demineralization alternating with areas characterized by open tubules and other areas covered by debris, smear layer and gutta-percha and/or sealer remnants as the result of an incomplete chemical dissolution during the etching procedure, due to the penetration into the dentinal tubules of the sealer and the plasticized material during the condensation procedure [48].

To increase retention when resin cement is used, some authors suggested a pre-treatment with a chelating agent and sodium hypochlorite before post cementation in order to efficiently remove the large areas that are not available for bonding and resin cementation of fiber posts [49]. Others authors suggested also the use of ultrasonic instrumentation in conjunction with EDTA pre-treatment prior to the bonding procedure, resulting in a decrease of debris and open tubules [48]. Although the removal of this tenacious and thick smear layer is enhanced by the suggested combination of EDTA and ultrasonic instrumentation (Fig. 7), the effectiveness in terms of interfacial post bond strength is still related to the bonding strategy selected, i.e., the etch-and-rinse or the self-etch approach [50].

4.3. Negative Clinical Factors

Besides the success of the root canal treatment, a successful final restoration is mandatory for long-term clinical success. Extensive loss of tooth structure may require post core restoration of a root canal filled tooth. However, in these systems,

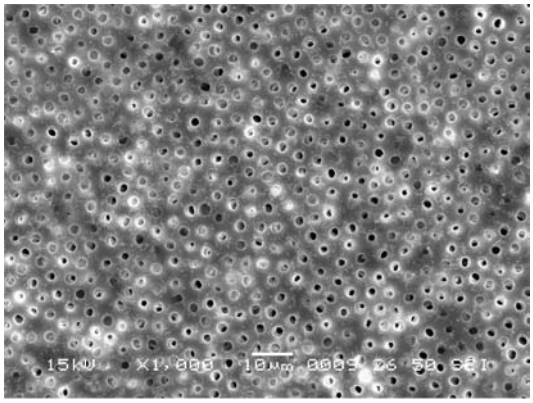


Figure 7. SEM micrograph of the intraradicular dentin substrate after EDTA irrigation and ultrasonic instrumentation (1000×).

lack of adhesion permits apical or coronal microleakage that causes failure of root canal treatment [51]. For this reason, effective adhesion to intraradicular dentin is a fundamental prerequisite to achieve the proper sealing of the endodontic space. However, adhesion to intraradicular dentin may be affected by several factors: the use of certain disinfectant solutions or medications during root canal preparation may have an adverse effect on the bond strength of post to root canal dentin [52] as well as bleaching and re-treatment procedures [42].

4.4. Irrigating Solutions and Medicaments

During irrigation, radicular and coronal dentins are exposed to various solutions used to disinfect the endodontic space. As previously mentioned, this may cause alterations on the dentin surface affecting its interactions with the resin-based materials used either for root canal obturation or for coronal restoration [53].

The effect of some chemicals, such as EDTA and NaOCl, on dentin has been widely investigated [52–55]. Theoretically, NaOCl is an ideal endodontic irrigant, however, despite positive effects, NaOCl causes problems when used in conjunction with resin-based materials due to its strong oxidizing property. NaOCl leaves a dentin surface characterized by an oxygen-rich layer that can significantly reduce bond strength and increase microleakage [52, 54, 55] (Fig. 8). Thus, if resin cements are used to lute endodontic posts, it is important to optimize clinical procedures that result in high bond strength between the adhesive and dentin and between the resin-based material and the post. In this way, adhesion to intraradicular dentin can be favourably influenced with a 10% ascorbic acid and 10% sodium ascorbate after NaOCl irrigation as this additional step has been shown to completely reverse the compromised bond obtained on 5% NaOCl-treated dentin [54]. Interestingly, 10% sodium ascorbate (pH 7) has been reported to be effective and even better than 10% ascorbic acid (pH 4) at restoring high bond strengths to NaOCl-treated dentin, thus, suggesting that ascorbate acts as a reducing agent. It is likely that the oxidizing

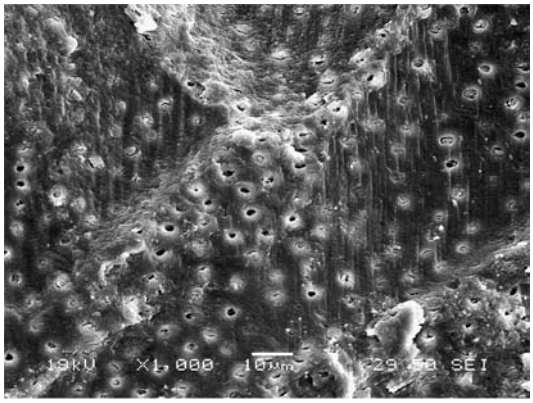


Figure 8. SEM micrograph of the root canal dentin after the use of 5% NaOCl endodontic irrigant (1000×). Tubules appear partially obliterated by smear plugs, the smear layer seems almost completely dissolved.

action of NaOCl leads to residual free oxygen within the dentin matrix that may critically interfere with the initiation of the interfacial polymerization of resin cements, leading to lower bond strengths [54]. According to Morris *et al*. [54], by treating dentin with 10% sodium ascorbate, the intraradicular dentin substrate is converted from an oxidized to a reduced surface, speculating that this treatment restores the redox potential of the dentin and facilitates the polymerization of the resins.

Besides NaOCl and EDTA, the use of hydrogen peroxide (H_2O_2) during canal instrumentation effectively removes remnants of pulp tissue and dentin debris, although the use of 3% H_2O_2 solution has been reported to negatively influence bond strength of resin cement to root canal dentin [51, 52, 56]. Hydrogen peroxide breaks down to water and oxygen thus inducing liberation of oxygen by the chemical reaction of hydrogen peroxide with sodium hypochlorite. Oxygen from such chemicals causes strong inhibition of the interfacial polymerization of resin bonding material [56, 57]. After the use of 3% H_2O_2 alone or in combination with NaOCl, residuals of the chemical irrigants and their products are likely to diffuse into dentin along the tubules, contaminating the dentin surface, which may affect the penetration of resin monomers into the dentin structure or the polymerization of the monomers within the demineralized dentin: this is believed to decrease bond strength to dentin [51, 56].

Reduction in resin bond strength to root dentin is reported to be produced also after the use of RC-Prep (Premier Dental Products, Plymouth, PA) as gliding and demineralizing agent [54]. It has been described that this reduction is the result of concurrently contributing factors. Primarily, the presence of hydrogen peroxide in RC-Prep, that breaks down to oxygen and water during bonding procedure, might generate bubbles or voids altering the resin infiltration process as reported also for bleaching agents and 3% H_2O_2 alone or if used in combination with NaOCl [56, 58]. On the other hand, RC-Prep contains in its formulation the poly(ethylene gly-

col) (PG) vehicle (Carbowax®) to provide lubricating properties which might be difficult to be rinsed off, thus interfering with the polymerization process and preventing a complete polymerization of the resin. However, a plausible restoration of the bond strength to control values can be achieved with a post RC-Prep treatment with 10% ascorbic acid [54].

An additional side effect of these intraradicular irrigating solutions is the significant reduction in microhardness of the root canal dentin walls. Sodium hypochlorite, hydrogen peroxide, EDTA all decreased the microhardness value of root dentin [53, 59]. This reduction after irrigation indicates direct effects of the chemical solutions on the components of dentin structure. Although the relative softening effect exerted by chemical irrigants on the dentinal walls could be of clinical benefit as it permits rapid preparation and facilitates the access to small and tight root canals, these alterations affect adhesion and sealing ability of the sealers to the softened chemically treated dentin surfaces [53, 59]. Based on these observations the use of 0.2% chlorhexidine gluconate has been proposed as an irrigating solution to provide optimal obturation due to its harmless effect on the microhardness and roughness of root canal dentin [59]. Additional positive effects are attributed to chlorhexidine supporting its use as a widely effective irrigating solution during endodontic procedures: higher bond strength compared with other irrigants [51], more effectiveness, more residual antibacterial effect and lower toxicity compared to 5.25% NaOCl with similar clinical timing required to eliminate all microorganisms [60, 61]. Moreover, chlorhexidine absorption by dentin and subsequent release from dentin last for 48 to 72 h after instrumentation [62].

Calcium hydroxide paste is sometimes placed in the root canal for its antimicrobial properties and other desirable effects between endodontic appointments. Moreover, as the complete removal of calcium hydroxide before the obturation is almost impossible, residual particles might interfere with bonding in some areas by acting as a physical barrier [63, 64]. In addition, due to its high pH, calcium hydroxide may also neutralize the self-etching/primer solutions of self-etch adhesives significantly reducing its etching effect, resulting in lower bond strength.

4.5. Eugenol

It is well known that eugenol negatively affects the resin polymerization process thus altering the bonding effectiveness. Sealers and temporary restorative materials such as zinc oxide eugenol contain eugenol in its formulation. The eugenol released from these products can permeate dentin [65] and further interact with resin-based restorative materials. As other phenolitic compounds, eugenol is a radical scavenger that inhibits the polymerization of resin-based materials [66]. The negative chemical reaction involves the hydroxyl group of the eugenol that tends to protonize the free radicals formed during the polymerization of resin-based materials, thereby blocking their reactivity and reducing the degree of conversion of these materials [67, 68].

In order to avoid the sub-optimal polymerization and the related reduced bond strength due to the use of an eugenol-based sealer (or temporary material), a me-

chanical cleaning of the canal walls involving scrubbing with a detergent or alcohol to remove all visible signs of residual material has been proposed [69, 70]. This procedure may help to remove an oily layer debris before performing the bonding procedure [42].

The use of 37% phosphoric acid as etching agent for most of the etch-and-rinse adhesives has been reported to only incompletely remove remnants of the temporary restoration [71]; however, the phosphoric acid pre-treatment eliminates the contaminated smear layer and results in the demineralization of dentin to a depth of 9–10 μm [72]. This depth of demineralization and the water rinsing after etching reduces the amount of free eugenol and temporary restoration remnants on the dentin surface [66]. Studies have, in fact, demonstrated that the three-step etch-and-rinse adhesive systems allow better and more effective bonding to eugenol contaminated dentin surface compared to the self-etch approach due to the non-removal of the eugenol debris entrapped within the smear layer [66, 73].

Therefore, in daily clinical practice when posts are placed after the use of eugenol-based sealer or eugenol-based temporary materials, the clinicians should prefer the use of an etch-and-rinse adhesive system, as self-etch systems incorporate the eugenol-rich smear layer into the hybrid layer rather than removing it [42].

4.6. Bleaching

Tooth discoloration due to endodontic reasons is a severe problem in aesthetic dentistry [74]. Although aesthetic can be improved using a variety of techniques, tooth bleaching is the most conservative and cost-effective alternative to enhance the appearance of non-vital teeth [75]. Besides the satisfactory results, side effects of this therapy have been reported [76, 77] including decrease of the bond strength of resin-based restorative materials [74]. It has been reported that the lower bond strength after bleaching is due to the oxygen-rich surface left behind hydrogen-based peroxide products, that significantly inhibits the polymerization of the adhesive systems [56, 76, 77]. Thus, the bond strength may be improved by replacing the final restoration several days after bleaching to allow the release of the residual oxygen. If immediate bond is needed, extended time of polymerization may reverse part of the polymerization inhibition [57].

In addition, it has been reported that a high concentration of hydrogen peroxide causes great decrease in dentin microhardness [78, 79]. This is an indirect evidence for mineral loss in the dental hard tissue, which may affect adhesion and sealing ability of sealers to the bleached dentin surfaces [53, 59].

4.7. Re-treatment

During endodontic re-treatment procedures, radicular and coronal dentins are sometimes exposed to gutta-percha solvents deposited within the root canal. Chloroform and, more recently, halothane are the most commonly used gutta-percha solvents employed for this purpose [51]. These agents are strong lipid solvents that may alter the chemical composition of the dentin surface and of the dentin organic matrix

thus affecting its interaction with resin-based materials used for restorations. The solvents may redeposit on the root canal surface a waxy film interfering with the resin–dentin bonds [51, 80] and causing significant loss of bond strength [51].

4.8. Incompatibility between Simplified Adhesives and Chemical/Dual-Cured Composites

In response to the increasing demand in procedural simplification in the formulation of adhesives, the classical multi-step dentin adhesives have been replaced by simplified systems that are simpler, faster and more user-friendly [14]. However, incompatibility between simplified adhesives (i.e., two-step etch-and-rinse and one-step self-etch adhesives) and chemical/dual-cured composites has been reported [81–84]. The decrease in bond strength was inversely proportional to the acidity of the adhesives [83–85] and adverse chemical interaction between suboptimally polymerized acidic adhesive resin monomers and the basic tertiary amine catalyst in the composite was thought to be responsible for the observed incompatibility [83]. In the etch-and-rinse strategy, only the two-step process was claimed to show incompatibility, while the conventional three-step total etch involving the use of intermediate resin layer was unaffected [83, 84]. Similarly, within the self-etch bonding strategy, only one-step self-etch adhesives are incompatible with chemical/dual-cured composites [82], due to their more acidic content by virtue of the increased concentration of lower pKa acidic resin monomers, [86] which is responsible for the additional increased permeability shown by one-step self-etch adhesives [82]. These acidic resin monomers can both react with the basic components (aromatic tertiary amine) of the composite, and/or create a hypertonic environment that osmotically draws fluid from the bonded hydrated dentin through the permeable adhesive layer [85, 87, 88]. Tay *et al*. reported that also the increased permeability that characterized these adhesives, due to the higher concentration of the ionic resin monomers, was responsible for the aforementioned incompatibility [82].

Thus, based on these observations, three-step etch-and-rinse and two-step self-etch adhesives do not show incompatibility with chemical/dual-cured resin composites due to the use of intermediate bonding resin layer: this additional coat of less acidic and less hydrophilic resin layer prevents the negative acid–base reaction since the composite layer does not come into direct contact with the acidic monomer components in the primer layer and, thus, reduces permeability of the resin–tooth interfaces [83, 84].

Most clinicians generally use dual-cured adhesives for bonding to root canal dentin because of their ability to self-polymerize in the absence of light in deeper regions of post cavity. However, clinically, incompatibility of one-step self-etch adhesives with chemical/dual-cured composites precludes their use for indirect bonding procedures in such areas that are not accessible to light-activation [83].

For the above-mentioned reasons the use of self-etch one-step adhesives should be avoided, although the use of a ternary catalyst has been proposed to overcome



Figure 9. A fiber post luted within the root canal with all-in-one adhesive system in conjunction with a dual-cured resin cement. The combination of these materials results in incompatibility of curing.

the acid–base reaction [88]. This solution has been formulated in most etch-and-rinse two-step adhesives with the addition of a separate bottle of activator solution containing ternary catalyst, and in some self-etch one-step adhesives by the incorporation of ternary catalyst as adhesive component [88]. Nevertheless, it has been reported that adhesive permeability still occurs when these activated adhesives are employed for bonding to hydrated dentin [82, 88, 89].

In conclusion, within the root canal the use of one-step self-etch adhesives is not recommended (Fig. 9) while the 2-step etch-and-rinse adhesives should be employed only in association with the chemical activator in order to circumvent the adverse acid–base reaction although light curing still remains mandatory to obtain a complete adhesive polymerization, overcoming the chemical interaction with cements and finally avoiding low bond strength and resin leaching.

4.9. Cavity Geometric Factors

The employment of methacrylate-based resin materials in endodontic focuses the attention also on the shrinkage stresses associated with their polymerization. During polymerization process, the intermolecular spaces between the monomers are reduced generating sufficient shrinkage stresses to debond the material from dentin, thereby decreasing retention and increasing leakage [90]. In clinical practice, the polymerization phenomenon leads, in fact, to stress development, gap formation and potential bacterial presence at the tooth/resin material interface; however, in addition to polymerization shrinkage, several other factors may influence shrinkage stress and gap formation. Feilzer *et al.* reported that shrinkage stress is related to the cavity configuration factor (C-factor), defined as the ratio of bonded to unbonded surface areas of the restoration [91], and when the so-called 'C-factor' of a restoration is above a certain limit, the stress development exceeds the bond strength of the bonding agents present [92]. The extent of shrinkage stress is, however, dependent also on the viscoelastic properties of the resin material: at a given polymerization shrinkage, the most rigid resin material will produce the highest shrinkage stress,

and, consequently, increase gap formation at the tooth–resin interface [93, 94]. Only if the shrinkage stress caused by the wall-to-wall contraction of the resin material can be relieved by sufficient elastic yielding of the surrounding materials the bond may survive [95], revealing that a major problem associated with endodontic bonding is the lack of relief of shrinkage stresses created in deep root canals [96, 97] which is strictly dependent on the cavity geometry and the resin film thickness [92]. Within the root canal the cavity geometry is unfavourable, since the unbonded surface area becomes small as a consequence of insufficient stress relief in association with high probability that one or more bonded areas will pull off or debond [90]. Braga *et al*. [98], analyzing the influence of cavity dimensions on shrinkage stress in composite restorations, showed that the cavity depth had a stronger influence than diameter; thus, if we reflect these data to the endodontic cavity configuration, the influence on shrinkage stress is even worse.

Similarly to bonding to root canals, the cementation of endodontic posts to prepared root post spaces is critical for the negative geometric factors, and was described by Feltzer *et al*. as the worst scenario in achieving gap-free interfaces [92]. According to Bouillaguet *et al*. [99], the estimated C-factor in post spaces may, in fact, even exceed 200, compared to the coronal restoration values that range between 1 and 5. More recently, Tay *et al*. [90], using a modelling approach, investigated the geometric variables influencing root-filling bonding adhesive materials to canal walls revealing a negative correlation between C-factor in bonded root canals and sealer thickness: in addition to the C-factor, in fact, the contribution of the other geometric attribute, i.e., the 'S-factor', was taken into consideration. As the thickness of the adhesive layer is reduced, the volumetric shrinkage is reduced, which results in the final reduction in shrinkage stress (S-factor). However, it was concluded that the interaction of these two factors (C- and S-factor) predicts that bonding of adhesive root-filling material is highly unfavourable when compared to indirect intracoronal restoration with similar resin film thickness [90].

All the above-mentioned problems limit bond strength to intraradicular dentin. Recently, some authors hypothesized that the retention of fiber posts into root canals was mainly due to friction of the post itself along the cavity walls through the interposition of luting material [100, 101]. However, as friction occurs only after bonding failure, i.e., until the adhesive interface is effective, friction should not play a significant role in terms of post retention. Friction will improve post luting in case no bonding occurs at the coronal part of the abutment, otherwise, even in the presence of low bond strength, the post will continue to be luted to the dental structure due to the bonding interface with the coronal dentin until debonding of the radicular part of the post occurs. Friction is additionally influenced by the granulometry of the luting material [102]; however, it is still unclear if a macrofilled cement can develop a higher 'bond strength due to friction' or not.

Goracci *et al*. [103] investigating the effect of post luting with and without the employment of adhesive systems reported no statistical differences between the groups, and the results were mainly attributed to the limited number of samples

and, in particular, to the low value recorded in the study. In addition, the standard deviation of the two tested groups was very high, thus, the authors do not believe that it can be assumed that 'retention of fiber posts is mainly due to friction'. More recently, Carvalho *et al*. [104] showed that the application of the adhesive system was mandatory for obtaining high bond strength to root dentin and that the use of unfilled bonding resins used as luting material consistently increased the bond strength to intraradicular dentin. The important role of unfilled resin for luting fiber posts was further supported by recent findings [105].

Considering the main types of failures reported in clinical practice (i.e., debonding), another important issue related to the geometric factors can be related to the circular shape of the posts which does not correspond to the root shape, at least in the oval root canals. In addition, also the post diameter should be taken into account, fitting properly only the most apical part of the root canals while remaining usually too thin in the most coronal compartment. These two aspects determine a wide thickness of luting cement, which becomes the weakest part of the system under occlusal loading; thus, for minimizing the cement's thickness the employment of 'anatomic posts' [106], 'oval posts', indirect luting procedure [107, 108], and/or additional smaller sizes of posts may be useful in clinical practice [109].

4.10. Ethanol-Wet Bonding Technique

An ethanol-wet bonding technique has been recently proposed to improve bonding to dentin [110]. The original wet-bonding technique of etch-and-rinse adhesives requires that water originally present within the interfibrillar spaces of the collagen network be displaced by the polar solvents contained in these adhesives, and ultimately be replaced by pure resins [110]. It has been reported that by replacing water in the demineralized collagen matrix with ethanol, phase separation of the hydrophobic dimethacrylates can be prevented as they are applied to ethanol-saturated instead of water-saturated dentin [110, 111]. Using a macromodel of the hybrid layer to predict how well adhesives can bond to dentin, Pashley *et al*. [110] indicated that the ethanol-wet bonding might be superior to water-wet bonding and several studies evaluated the effectiveness of this technique [111–113].

Few investigations evaluated the effects of the 'ethanol-wet bonding technique' on luting fiber posts revealing that this procedure did not improve bond strength with the fiber post surface [114]; however, it can improve bond strength to intraradicular dentin (Fig. 10).

The main problem to employ this technique is due to the complex clinical procedure based on several steps, to the instability of its component (shelf-life), in addition to the fact that the system is not available on the market yet. In vital teeth, possible pulp damages due to application of pure ethanol on vital dentin for fixing the collagen fibers are theoretically reasonable (thus, several *in vivo* studies are currently ongoing to challenge the pulp effects of this technique). Although the concept of ethanol-wet bonding may sound radical to a clinician who may have doubts on the potential effects on vital pulp, Pashley *et al*. remarked that such a procedure was

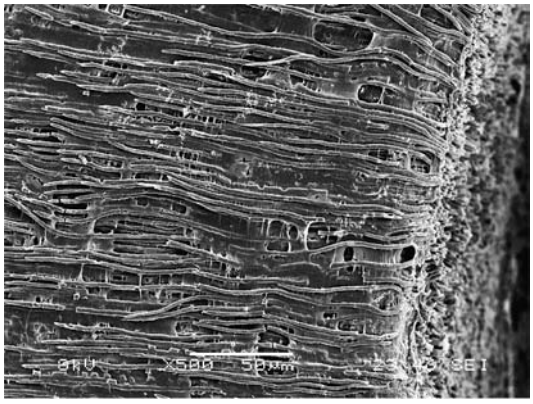


Figure 10. SEM micrograph showing resin tags formed after application of an adhesive system in accordance with the ethanol-wet bonding technique for luting a fiber post: the length of resin tags exceeds 500 μm in depth (SEM 500×).

not so different from the application of acetone-based or ethanol-based primers, as most of these primers may contain up to 85% ethanol or acetone [110]. Based on these observations, further laboratory and clinical studies are needed to test and further validate this procedure.

5. Failure of the Adhesive Interface

As clinical investigation revealed that failure of the bond occurs after some time, researchers recently have focused their attention on the chemical phenomena that occur during aging. Since the hybrid layer is a complex mixture of collagen and adhesive monomers, both components may be affected by aging.

Two degradation patterns were morphologically described within the hybrid layer thickness after storage in water for 1 year: (1) hydrolysis of the resin from interfibrillar spaces and (2) disorganization of collagen fibrils [115]. These phenomena clearly weaken the strength of resin–dentin bond allowing leakage, marginal staining, and finally failure of the adhesive interface with clinical debonding (Fig. 11).

Since resin degradation is related to water sorption within the hybrid layer [116], resin blends characterized by low water sorption result in the formation of bonds that are more stable than hydrophilic adhesive systems which are prone to water sorption. In addition, as the hydrolytic degradation of the resin monomers occurs only in presence of water, adhesive hydrophilicity, water sorption and subsequent hydrolytic degradation are correlated [116–118]. This allowed the researchers to hypothesize that simplified adhesives (i.e., etch-and-rinse two-step, and self-etch one-step that are characterized by the presence of both hydrophilic and ionic resin monomers into the bonding agent) are less stable than un-simplified adhesives (etch-and-rinse three-step and self-etch two-step) which are characterized by the presence of a non-solvated hydrophobic resin coating [11, 119]. The lack of hy-

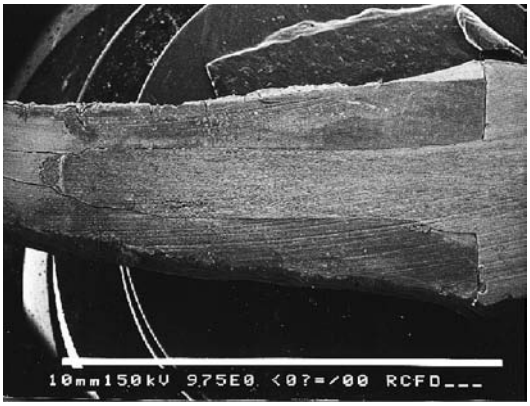


Figure 11. Root section with a luted fiber post after exposure to water for 6 months; after the artificial storage evident degradation of the hybrid layer occurred.

drophobic characteristics exhibited by simplified adhesives has also been revealed by morphological evidences that their hybrid layer behaves as a semi-permeable membrane after polymerization, allowing movement of water throughout the interface [82]. Recent studies also correlated adhesive permeability with its polymerization kinetics [120]. Interestingly, all simplified adhesives exhibited sub-optimal polymerization which was correlated with their high permeability to fluid movement due to the presence of high concentrations of hydrophilic monomers while un-simplified adhesives showed higher extents of polymerization that were correlated with less permeability to water [121]. As the extent of polymerization within the endodontic space may be reduced due to limited access of the tip of the curing light unit, the extension of curing time could be an important clinical tip suggested during luting of the post, in conjunction with the employment of translucent fiber posts: the use of posts made with translucent components permits the curing light to pass through.

Similarly to resin monomers the collagen fibrils constituting the hybrid layer can also degrade after time contributing to the weakening of the hybrid layer structure [122]. In fact, these extrinsic degradation mechanisms of the resin–dentin interface that originate in the adhesive above the hybrid layers are accompanied by intrinsic degradation mechanisms that originate from beneath dentin hybrid layers [7]. The recent reports of collagenolytic and gelatinolytic activities in partially demineralised dentin collagen matrices [122–124] are indirect proofs of the existence of matrix metalloproteinases (MMPs) in human dentin. MMPs are a class of zinc- and calcium-dependent endopeptidases [125] that are trapped within the mineralized dentin matrix during tooth development [125–128]. The release and activation of these endogenous enzymes during dentin bonding [122] are thought to be responsible for the *in vitro* manifestation of thinning and disappearance of collagen fibrils from incompletely infiltrated hybrid layers in aged, bonded dentin [119, 123, 124, 129]. Collagen degradation at the bottom of hybrid layers has been subsequently

confirmed *in vivo* in both primate [130] and human studies [131]. The involvement of host-derived MMPs in this degradation process has also been indirectly confirmed, since the application of chlorhexidine, an inhibitor of MMPs [132], to acid-etched human primary dentin resulted in the preservation of collagen integrity within the hybrid layers after the application of a simplified etch-and-rinse adhesive [131]. Unfortunately, a definitive cause and effect relationship between the different procedures employed in the etch-and-rinse technique and the degradation of the dentin hybrid layers has not been yet established. Presumably, phosphoric acid demineralization could have activated the MMPs, trapped within the mineralized dentin [122], resulting in collagenolytic and gelatinolytic activities identified within the hybridized dentin. However, using fluorescein-labeled collagen enzymatic assay, it was found that treatment of mineralized dentin powder with 37% phosphoric acid gel for 15 s actually reduced the inherent collagenolytic activity of mineralized dentin, probably due to its high acidity (pH 0.7), that partially denatures the MMPs [122] causing confusion as to how dentin hybrid layers could be degraded over time. In a recent study Mazzoni *et al*. [133] revealed the potential roles of the adhesives in dentin proteolytic activities using a modeling approach in which the relative proteolytic activities derived from dentin were quantified before and after the sequential applications of the phosphoric acid etchant and an etch-and-rinse adhesive. Within the limits of the study, it was concluded that simplified etch-and-rinse adhesives can activate new endogenous enzymes present in dentin that counteract the MMPs previously inactivated by phosphoric acid-etching, providing a plausible explanation for both *in vitro* and *in vivo* observations of the degradation of dentin hybrid layers [133]. Similarly, also the less aggressive (i.e., less acidic) versions of self-etch adhesives were tested, highlighting the same effect of activation of endogenous MMPs present in crown dentin [134].

With the increasing popularity in bonding to root canals, it was not known if intraradicular dentin possessed similar intrinsic degradation mechanisms that might adversely affect the longevity of resin–dentin bonds. Thus, Tay *et al*. [135] demonstrated, with the same modelling approach, that intraradicular dentin possesses latent collagenolytic activity which can be activated by mild self-etching adhesives. In fact, in this study the decrease in fluorescence associated with the calcium chelator, EDTA, and the classic MMP inhibitor, chlorhexidine, indirectly showed that latent MMPs were present in the instrumented intraradicular dentin and could be further activated by mild self-etch adhesives, resulting in an increase of the collagenolytic activity up to 15-fold [135]. This is an important finding with potential clinical implications since MMPs are zinc-activated, calcium-dependent enzymes; thus, the use of 17% EDTA as an endodontic irrigant may result in chelation of the calcium ions that are required for functioning of these enzymes. Similarly, the use of chlorhexidine as an endodontic irrigant has potential merits, apart from its well-documented antimicrobial benefits, in inactivating MMP activities. However, as reported by Tay *et al.*, 2% chlorhexidine and 17% EDTA only partially inhibited the MMPs activated by the self-etch adhesives, concluding that time, concentration

and method of delivery to be employed for maximal MMP inactivation have to be optimized in future studies [135].

In conclusion, as several studies stressed the effectiveness of aging process on bonding interfaces and some of them considered the possible detrimental effect of water on bonding interface of luted fiber posts, the role of water within the root canal should be considered. The main hypothesis of water contact along the interface of root dentin/luted post is based on the study by Chersoni *et al*. [136], demonstrating that permeability of simplified adhesives results in water movement, even in root-treated dentin. However, more recently, a similar protocol [137] was repeated demonstrating that under *in vivo* conditions, water was not in direct contact with the bonding/luting/post system (Figs 12 and 13), findings that were further confirmed by several other clinical and laboratory studies [138] (Figs 14 and 15). Thus, we can say that the presence of water blisters detected by Chersoni *et al*.

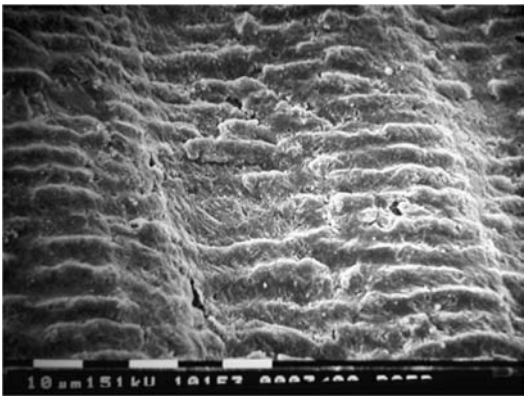


Figure 12. SEM micrograph of root canal dentin after being treated with absolute ethanol for 1 min in accordance with the substrate conditioning of the ethanol-wet bonding technique (500×).

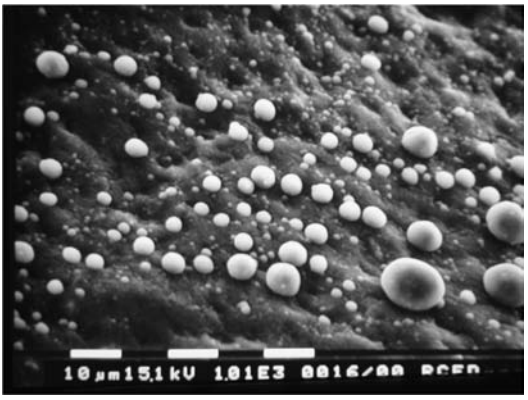


Figure 13. Water droplets imaged with SEM following the replica technique within the endodontic space (2000×).

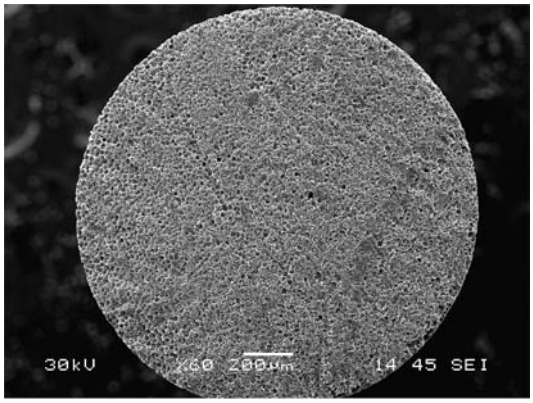


Figure 14. A fiber post luted into a root canal after storage in water for 6 months. No degradation of the post is noticeable (SEM image 60×).

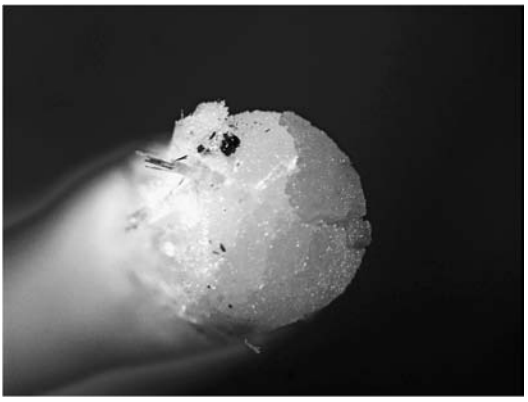


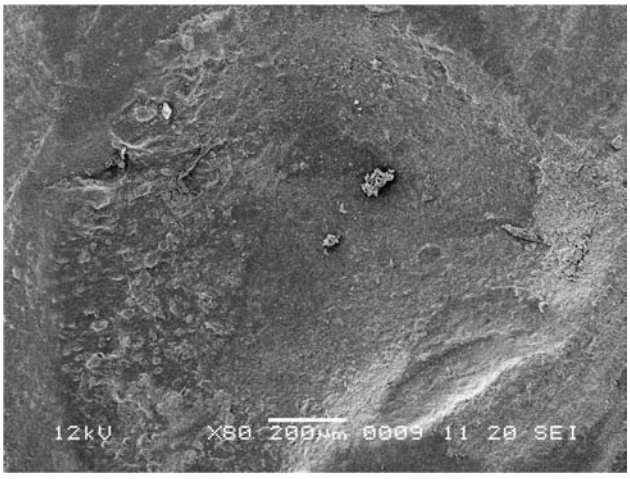
Figure 15. A fiber post after storage in water for 6 months with evident signs of degradation.

[136] may be attributed to the experimental procedure or to incomplete solvent evaporation of the tested adhesives instead of water presence [138, 139].

It should be considered that the aging process occurring at the adhesive interface has been predominantly studied in coronal dentin under simulated laboratory conditions whilst almost no data are available on the aging process affecting bonding to root dentin. As the vitality of the tooth determines fluid movement through the dentinal tubules due to the presence of the pulpal fluid, aging of the adhesive interface in intraradicular dentin cannot be related to water mediated phenomena, while other reasons such as degradation caused *via* the activity of endogenous enzymes such as matrix metalloproteinases can be hypothesized [122, 124]. In fact, a restoration placed on coronal dentin has a bonding interface directly exposed to the oral environment and consequently subjected to 'water aging process', whilst the bonding interface created within the root canal is not in direct contact with water unless a very small amount of intrinsic dentin is formed by water [32]. Moreover,



(a)



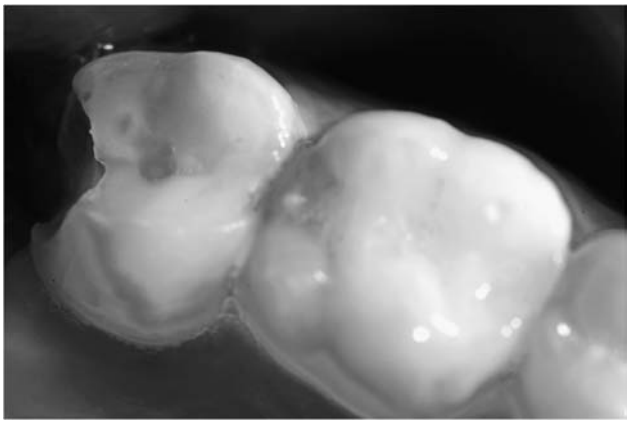
(b)

Figure 16. (a) Fiber posts exposed on the occlusal surface of abutments after 10 years of clinical function. (b) Higher magnification view of Fig. 16a under SEM taken on a replica obtained from pouring the impression in epoxy resin (80×).

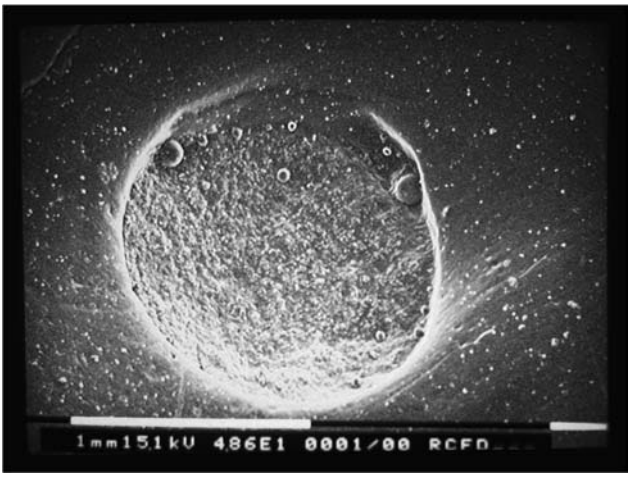
it was recently reported that under *in vivo* conditions (after 5 years of clinical function) post surfaces that remained exposed to oral environment showed only a small amount of wear because of occlusion while no degradation occurred due to water uptake [140] (Figs 16 and 17).

6. Conclusions

Although in the last 15 years fiber posts have been widely investigated with different tecniques and, in many aspects, there has been rapid progress in materials and techniques. Many new developments will take place in the near future before



(a)



(b)

Figure 17. (a) A post exposed on occlusal surface of a second molar after 5 years of clinical function. (b) Higher magnification view of Fig. 17a under SEM (500×).

reaching the most ideal procedure for luting posts into root canals of endodontically treated teeth.

References

1. B. Van Meerbeek, K. Van Landuyt, J. De Munk, S. Inoue, Y. Yoshida, J. Perdigao, P. Lambrechts and M. Peumans, in: *Fundamentals of Operative Dentistry*, J. B. Summitt, J. W. Robbins and R. S. Swartz (Eds), pp. 183–260. Quintessence Books (2006).
2. B. Van Meerbeek, J. De Munck, Y. Yoshida, S. Inoue, M. Vargas, P. Vijay, K. Van Landuyt, P. Lambrechts and G. Vanherle, *Oper. Dent.* **28**, 215–235 (2003).
3. M. G. Buonocore, *J. Dent. Res.* **34**, 849 (1955).
4. R. L. Bowen. U.S. Patent No. 3,066,112 (1962).
5. R. L. Bowen, *J. Dent. Res.* **44**, 903–905 (1965).

6. T. Fusayama, M. Nakamura, N. Kurosaki and M. Iwaku, *J. Dent. Res.* **58**, 1364–1370 (1979).
7. F. R. Tay and D. H. Pashley, *J. Can. Dent. Assoc.* **69**, 726–731 (2003).
8. M. Simonetti, I. Radovic, M. Vano, N. Chieffi, C. Goracci, F. Tognini and M. Ferrari, *J. Adhes. Dent.* **8**, 421–425 (2006).
9. R. E. Baier, *Oper. Dent.* **5** (Suppl.), 1 (1992).
10. J. F. Padday, in: *Handbook of Adhesion*, D. E. Packham (Ed.), p. 88. Longman (1992).
11. L. Breschi, A. Mazzoni, A. Ruggeri Jr., M. Cadenaro, R. Di Lenarda and E. Dorigo, *Dent. Mater.* **24**, 90–101 (2008).
12. J. Perdigao, L. Lopes, P. Lambrechts, J. Leitao, B. Van Meerbeek and G. Vanherle, *Am. J. Dent.* **10**, 141–146 (1997).
13. U. Salz, A. Mucke, J. Zimmermann, F. R. Tay and D. H. Pashley, *J. Adhes. Dent.* **8**, 143–150 (2006).
14. F. R. Tay and D. H. Pashley, *J. Adhes. Dent.* **4**, 91–103 (2002).
15. D. H. Pashley, *Proc. Finn. Dent. Soc.* **88** (Suppl. I), 215–224 (1992).
16. D. H. Pashley, J. A. Horner and P. D. Brewer, *Oper. Dent.* **5** (Suppl.), 137 (1992).
17. J. Perdigão, An ultramorphological study of human dentine exposed to adhesive systems, PhD Thesis, Catholic University of Leuven, Leuven, Belgium (1995).
18. J. Perdigão, P. Lambrechts, B. Van Meerbeek, A. R. Tomé, G. Vanherle and A. B. Lopes, *Dent. Mater.* **12**, 262–271 (1996).
19. G. W. Marshall, S. J. Marshall, J. H. Kinney and M. Balooch, *J. Dent.* **25**, 441–458 (1997).
20. A. Linde, *Anat. Rec.* **224**, 154–166 (1989).
21. B. Van Meerbeek, A. Dhem, M. Goret-Nicaise, M. Braem, P. Lambrechts and G. Vanherle, *J. Dent. Res.* **72**, 495–501 (1993).
22. N. Nakabayashi, K. Kojima and E. Mashuara, *J. Biomed. Mater. Res.* **16**, 1240–1243 (1982).
23. D. H. Pashley, *Trans. Acad. Dent. Mater.* **3**, 55 (1990).
24. L. Tao and D. H. Pashley, *Dent. Mater.* **4**, 371–378 (1988).
25. A. J. Gwinnett, F. R. Tay, K. M. Pang and S. H. Wei, *Am. J. Dent.* **9**, 140–144 (1996).
26. F. R. Tay and D. H. Pashley, *Dent. Mater.* **17**, 296–308 (2001).
27. Y. Yoshida, B. Van Meerbeek, Y. Nakayama, J. Snauwaert, L. Hellemans, P. Lambrechts, G. Vanherle and K. Wakasa, *J. Dent. Res.* **79**, 709–714 (2000).
28. J. Kanca III, *Quintessence Int.* **23**, 39–41 (1992).
29. A. Nanci, *Oral Histology: Development, Structure and Function*, 6th edn, pp. 192–239. Mosby, St. Louis, Missouri (2003).
30. Y. Ohsaki ans K. Nagata, *Anat. Rec.* **240**, 308–313 (1994).
31. Y. Kitasako, S. Shibata, C. F. Cox and J. Tagami, *Int. Endodont. J.* **35**, 996–1004 (2002).
32. M. Ferrari, F. Mannocci, A. Vichi, M. C. Cagidiaco and I. A. Mjor, *Am. J. Dent.* **13**, 255–260 (2000).
33. I. A. Mjor, M. R. Smith, M. Ferrari and F. Mannocci, *Int. Endodont. J.* **34**, 346–353 (2001).
34. F. Mannocci, P. Pilecki, E. Bertelli and T. F. Watson, *Dent. Mater.* **20**, 293–296 (2004).
35. R. S. Schwartz, *J. Endodont.* **32**, 1125–1134 (2006).
36. S. G. Prabhu, N. Rhaim, K. S. Bhat and J. Mathew, *Endodontology* **15**, 20–25 (2003).
37. S. Ishioka and A. A. Caputo, *J. Prosthet. Dent.* **61**, 180–185 (1989).
38. A. J. Gwinnett, *Am. J. Dent.* **6**, 7–9 (1993).
39. D. H. Pashley, L. Tao, L. Boyd, G. E. King and J. A. Horner, *Arch. Oral Biol.* **33**, 265–270 (1988).
40. D. H. Pashley, *Oper. Dent.* **3** (Suppl.), 13–29 (1984).
41. S. D. Meryon, R. S. Tobias and K. J. Jakeman, *J. Prosthet. Dent.* **57**, 174–179 (1987).

42. R. S. Schwartz and R. Fransman, *J. Endodont.* **31**, 151–165 (2005).
43. C. Goracci, F. T. Sadek, A. Fabianelli, F. R. Tay and M. Ferrari, *Oper. Dent.* **30**, 627–635 (2005).
44. M. Torabinejad, R. Handysides, A. A. Khademi and L. K. Bakland, *Oral Surg. Oral Med. Oral Pathol. Oral Radiol. Endodont.* **94**, 658–666 (2002).
45. R. R. White, M. Goldman and P. S. Lin, *J. Endodont.* **10**, 558–562 (1984).
46. A. Pallares, V. Faus and G. N. Glickman, *Int. Endodont. J.* **28**, 266–269 (1995).
47. K. J. Boone, D. F. Murchison, W. G. Schindler and W. A. Walker 3rd, *J. Endodont.* **27**, 768–771 (2001).
48. C. Serafino, G. Gallina, E. Cumbo and M. Ferrari, *Oral Surg. Oral Med. Oral Pathol. Oral Radiol. Endodont.* **97**, 381–387 (2004).
49. J. P. Standlee and A. A. Caputo, *J. Prosthet. Dent.* **68**, 913–917 (1992).
50. I. Coniglio, E. Magni, C. Goracci, I. Radovic, C. A. Carvalho, S. Grandini and M. Ferrari, *J. Endodont.* **34**, 83–86 (2008).
51. A. Erdemir, A. U. Eldeniz, S. Belli and D. H. Pashley, *J. Endodont.* **30**, 589–592 (2004).
52. H. Ari, E. Yaşar and S. Belli, *J. Endodont.* **29**, 248–251 (2003).
53. A. A. Saleh and W. M. Ettman, *J. Dent.* **27**, 43–46 (1999).
54. M. D. Morris, K. W. Lee, K. A. Agee, S. Bouillaguet and D. H. Pashley, *J. Endodont.* **27**, 753–757 (2001).
55. B. Ozturk and F. Ozer, *J. Endodont.* **30**, 362–365 (2004).
56. T. Nikaido, Y. Takano, Y. Sasafuchi, M. F. Burrow and J. Tagami, *Am. J. Dent.* **12**, 177–180 (1999).
57. M. Cadenaro, L. Breschi, A. Antoniolli, A. Mazzoni and R. Di Lenarda, *Eur. J. Oral Sci.* **114**, 257–262 (2006).
58. K. C. Titley, C. D. Torneck and D. C. Smith, *Endodont. Dent. Traumatol.* **5**, 132–138 (1989).
59. H. Ari, A. Erdemir and S. Belli, *J. Endodont.* **30**, 792–795 (2004).
60. O. Oncag, M. Hosgor, S. Hilmioglu, O. Zekioglu, C. Eronat and D. Burhanoglu, *Int. Endodont. J.* **36**, 423–432 (2003).
61. M. E. Vianna, B. P. Gomes, V. B. Berber, A. A. Zaia, C. C. Ferraz and F. J. de Souza-Filho, *Oral Surg. Oral Med. Oral Pathol. Oral Radiol. Endodont.* **97**, 79–84 (2004).
62. M. R. Leonardo, M. Tanomaru Filho, L. A. Silva, P. Nelson Filho, K. C. Bonifacio and I. Y. Ito, *J. Endodont.* **25**, 167–171 (1999).
63. T. Lambrianidis, J. Margelos and P. Beltes, *J. Endodont.* **25**, 85–88 (1999).
64. S. K. Kim and Y. O. Kim, *Int. Endodont. J.* **35**, 623–628 (2002).
65. A. M. Kielbassa, T. Atti and E. Hellwig, *Oper. Dent.* **22**, 15–20 (1997).
66. C. N. Carvalho, J. R. de Oliveira Bauer, A. D. Loguercio and A. Reis, *J. Esthet. Restor. Dent.* **19**, 144–152 (2007).
67. S. Fujisawa and Y. Kadoma, *Biomaterials* **18**, 701–703 (1997).
68. F. Bayindir, M. S. Akyil and Y. Z. Bayindir, *Dent. Mater.* **22**, 592–599 (2003).
69. T. L. Woody and R. D. Davis, *Oper. Dent.* **17**, 175–180 (1992).
70. E. K. Watanabe, A. Yamashita, M. Imai, H. Yatani and K. Suzuki, *Int. J. Prosthodont.* **10**, 440–452 (1997).
71. R. Terata, S. Yoshinaka, K. Nakashima and M. Kubota, *Dental Mater.* **15**, 45–50 (1996).
72. D. H. Pashley and R. M. Carvalho, *J. Dent.* **25**, 355–372 (1997).
73. T. Mayer, T. Pioch, H. Duschner and H. J. Staehle, *Quintessence Int.* **28**, 57–62 (1997).
74. G. M. Arcari, E. Araujo, L. N. Baratieri and G. C. Lopes, *J. Adhes. Dent.* **9**, 333–340 (2007).
75. L. N. Baratieri, A. V. Ritter, S. Monteiro Jr., M. A. Caldeira de Andrada and L. C. Cardoso Vieira, *Quintessence Int.* **26**, 597–608 (1995).

76. D. Heller, J. Skriber and L. M. Lin, *J. Endodont.* **18**, 145–148 (1992).
77. H. Elkhatib, M. Nakajima, N. Hiraishi, Y. Kitasako, J. Tagami and S. Nomura, *Oper. Dent.* **28**, 591–597 (2003).
78. J. D. Pecora, A. M. Cruzfilho, M. D. Sousaneto and R. G. Silva, *Braz. Dent. J.* **5**, 129–134 (1994).
79. H. K. Chng, J. E. Palamara and H. H. Messer, *J. Endodont.* **28**, 62–67 (2002).
80. D. Kaufman, C. Mor, A. Stabholz and I. Rotstein, *J. Endodont.* **23**, 614–615 (1997).
81. E. J. Swift Jr., J. Perdigao, E. C. Combe, C. H. Simpson 3rd and M. F. Nunes, *Am. J. Dent.* **14**, 137–140 (2001).
82. F. R. Tay, D. H. Pashley, B. I. Suh and R. M. Carvalho and A. Itthagarun, *J. Dent.* **30**, 371–382 (2002).
83. C. Cheong, N. M. King, D. H. Pashley, M. Ferrari, M. Toledano and F. R. Tay, *Oper. Dent.* **28**, 747–755 (2003).
84. F. R. Tay, B. I. Suh, D. H. Pashley, C. Prati, S. F. Chuang and F. Li, *J. Adhes. Dent.* **5**, 91–105 (2003).
85. A. M. Sanares, A. Itthagarun, N. M. King, F. R. Tay and D. H. Pashley, *Dent. Mater.* **17**, 542–556 (2001).
86. S. Inoue, M. A. Vargas, Y. Abe, Y. Yoshida, P. Lambrechts, G. Vanherle, H. Sano and B. Van Meerbeek, *J. Adhes. Dent.* **3**, 237–245 (2001).
87. F. R. Tay, D. H. Pashley, C. K. Yiu, A. M. Sanares and S. H. Wei, *J. Adhes. Dent.* **5**, 27–40 (2003).
88. B. I. Suh, L. Feng, D. H. Pashley and F. R. Tay, *J. Adhes. Dent.* **5**, 267–282 (2003).
89. F. R. Tay, N. M. King, B. I. Suh and D. H. Pashley, *J. Adhes. Dent.* **3**, 207–225 (2001).
90. F. R. Tay, R. J. Loushine, P. Lambrechts, R. N. Wellar and D. H. Pashley, *J. Endodont.* **31**, 584–588 (2006).
91. A. J. Feilzer and B. S. Dauvillier, *J. Dent. Res.* **82**, 824–828 (2003).
92. A. J. Feilzer, A. J. De Gee and C. L. Davidson, *J. Dent. Res.* **66**, 1636–1639 (1987).
93. C. L. Davidson and A. J. Feilzer, *J. Dent.* **25**, 435–440 (1997).
94. E. Moreira da Silva, G. O. dos Santos, J. G. Guimaraes, A. Barcellos Ade and E. M. Sampaio, *Oper. Dent.* **32**, 356–362 (2007).
95. C. M. Kemp-Scholte and C. L. Davidson, *J. Dent. Res.* **67**, 841–845 (1988).
96. C. L. Davidson, L. Van Zeghbroeck and A. J. Feilzer, *J. Dent. Res.* **70**, 880–882 (1991).
97. C. L. Davidson and A. J. de Gee, *J. Dent. Res.* **63**, 146–148 (1984).
98. R. R. Braga, L. C. Boaro, T. Kuroe, C. L. Azevedo and J. M. Singer, *Dent. Mater.* **22**, 818–823 (2006).
99. S. Bouillaguet, S. Troesch, J. C. Wataha, I. Krejci, J. M. Meyer and D. H. Pashley, *Dent. Mater*. **19**, 199–205 (2003).
100. C. Pirani, S. Chersoni, F. Foschi, G. Piana, R. J. Loushine, F. R. Tay and C. Prati, *J. Endodont.* **31**, 891–894 (2005).
101. E. A. Bonfante, L. F. Pegoraro, M. F. de Gòes and R. M. Carvalho, *Dent. Mater.* **24**, 483–491 (2008).
102. R. Van Noort, in: *Introduction to Dental Materials*, R. W. Philips (Ed.). Elsevier Health Sciences, London (2002).
103. C. Goracci, A. Fabianelli, F. T. Sadek, F. Papacchini, F. R. Tay and M. Ferrari, *J. Endodont.* **31**, 608–612 (2005).
104. C. A. Carvalho, F. Monticelli, A. Cantoro, L. Breschi and M. Ferrari, *J. Adhes. Dent.* **11**, 65–70 (2008).

105. A. L. F. Silva, D. S. M. Casselli, G. M. B. Ambrosiano and L. R. M. Martins, *J. Endodont.* **33**, 1078–1081 (2007).
106. S. Grandini, C. Goracci, F. Monticelli, A. Borracchini and M. Ferrari, *J. Adhes. Dent.* **7**, 235–240 (2005).
107. S. Bouillaguet, L. Shaw, J. Barthelemy, I. Krejci and J. C. Wataha, *Int. Endodont. J.* **41**, 219–226 (2008).
108. L. A. Jongsma, P. B. Bolhuis, P. Pallav, C. J. Kleverlaan and A. J. Feilzer, in: *IADR-CED and Israel Divisions Annual Meeting*, Thessaloniki, Greece, Abstract #0424 (2007).
109. P. F. Porciani, M. Vano, C. Goracci, S. Grandini and M. Ferrari, *Am. J. Dent.* **21**, 373–376 (2008).
110. D. H. Pashley, F. R. Tay, R. M. Carvalho, F. A. Rueggeberg, K. A. Agee, M. Carrilho, A. Donnelly and F. García-Godoy, *Am. J. Dent.* **20**, 7–20 (2007).
111. F. R. Tay, D. H. Pashley, R. R. Kapur, M. R. Carrilho, Y. B. Hur, L. V. Garrett and K. C. Tay, *J. Dent. Res.* **86**, 1034–1039 (2007).
112. F. T. Sadek, D. H. Pashley, Y. Nishitani, M. R. Carrilho, A. Donnelly, M. Ferrari and F. R. Tay, *J. Biomed. Mater. Res. A* **84**, 19–29 (2008).
113. Y. Wang, P. Spencer, X. Yao and B. Brenda, *J. Biomed. Mater. Res. A* **82**, 975–983 (2007).
114. H. Ounsi, Z. Salameh, C. A. Carvalho, A. Cantoro, S. Grandini and M. Ferrari, *J. Adhes. Dent.*, in press (2009).
115. M. Hashimoto, H. Ohno, H. Sano, M. Kaga and H. Oguchi, *Biomaterials* **24**, 3795–3803 (2003).
116. J. Malacarne, R. M. Carvalho, M. F. de Goes, V. Svizerd, D. H. Pashley, F. R. Tay, C. K. Yin and M. R. Carrilho, *Dent. Mater.* **22**, 973–980 (2006).
117. F. R. Tay, M. Hashimoto, D. H. Pashley, M. C. Peters, S. C. Lai, C. K. Yiu and C. Cheong, *J. Dent. Res.* **82**, 537–541 (2003).
118. S. Ito, M. Hashimoto, B. Wadgaonkar, N. Svizero, R. M. Carvalho, C. Yiu, F. A. Rueggeberg, S. Foulger, T. Saito, Y. Nishitani, M. Yoshiyama, F. R. Tay and D. H. Pashley, *Biomaterials* **26**, 6449–6459 (2005).
119. J. De Munck, K. Van Landuyt, M. Peumans, A. Poitevin, P. Lambrechts, M. Braem and B. Van Meerbeek, *J. Dent. Res.* **84**, 118–132 (2005).
120. M. Cadenaro, F. Antoniolli, S. Sauro, F. R. Tay, R. Di Lenarda, C. Prati, M. Biasotto, L. Contardo and L. Breschi, *Eur. J. Oral Sci.* **113**, 525–530 (2005).
121. L. Breschi, M. Cadenaro, F. Antoniolli, S. Sauro, M. Biasotto, C. Prati, F. R. Tay and R. Di Lenarda, *Dent. Mater.* **23**, 1066–1072 (2007).
122. D. H. Pashley, F. R. Tay, C. Yiu, M. Hashimoto, L. Breschi, R. M. Carvalho and S. Ito, *J. Dent. Res.* **83**, 216–221 (2004).
123. M. Hashimoto, F. R. Tay, H. Ohno, H. Sano, M. Kaga, C. Yiu, H. Kumagai, Y. Kudou, M. Kubota and H. Oguchi, *J. Biomed. Mater. Res. B* **66**, 287–298 (2003).
124. M. Ferrari, P. N. Mason, C. Goracci, D. H. Pashley and F. R. Tay, *J. Dent. Res.* **83**, 414–419 (2004).
125. T. Sorsa, L. Tjäderhane and T. Salo, *Oral Disease* **10**, 311–318 (2004).
126. L. Tjäderhane, H. Larjava, T. Sorsa, V. J. Uitto, M. Larmas and T. Salo, *J. Dent. Res.* **77**, 1622–1629 (1998).
127. A. J. van Strijp, D. C. Jansen, J. De Groot, J. M. ten Cate and V. Everts, *Caries Res.* **37**, 58–65 (2003).
128. S. Martin-De Las Heras, A. Valenzuela and C. M. Overall, *Arch. Oral Biol.* **45**, 757–765 (2000).
129. S. R. Armstrong, M. A. Vargas, I. Chung, D. H. Pashley, J. A. Campbell, J. E. Laffoon and F. Qian, *Oper. Dent.* **29**, 705–712 (2004).

130. K. Koshiro, S. Inoue, H. Sano, J. De Munck and B. Van Meerbeek, *Eur. J. Oral Sci.* **113**, 341–348 (2005).
131. J. Hebling, D. H. Pashley, L. Tjäderhane and F. R. Tay, *J. Dent. Res.* **84**, 741–746 (2005).
132. R. Gendron, D. Greiner, T. Sorsa and D. Mayrand, *Clin. Diagn. Lab. Immunol.* **6**, 437–439 (1999).
133. A. Mazzoni, D. H. Pashley, Y. Nishitani, L. Breschi, F. Mannello, L. Tjaderhane, M. Toledano, E. L. Pashley and F. R. Tay, *Biomaterials* **27**, 4470–4476 (2006).
134. Y. Nishitani, M. Yoshiyama, B. Wadgaonkar, L. Breschi, F. Mannello, A. Mazzoni, R. M. Carvalho, L. Tjäderhane, F. R. Tay and D. H. Pashley, *Eur. J. Oral Sci.* **114**, 60–166 (2006).
135. F. R. Tay, D. H. Pashley, R. J. Loushine, R. N. Weller, F. Monticelli and R. Osorio, *J. Endodont.* **32**, 862–868 (2006).
136. S. Chersoni, G. L. Acquaviva, C. Prati, M. Ferrari, S. Grandini, D. H. Pashley and F. R. Tay, *J. Dent. Res.* **84**, 223–227 (2005).
137. M. Ferrari, I. Coniglio, E. Magni, M. C. Cagidiaco, C. Prati and L. Breschi, *J. Adhes. Dent.* **10**, 211–218 (2008).
138. M. Vano, A. Vichi, C. Goracci and M. Ferrari, *Dent. Mater.*, in press (2009).
139. K. L. Van Landuyt, J. Snauwaert, J. De Munck, E. Coutinho, A. Poitevin, Y. Yoshida, K. Suzuki, P. Lambrechts and B. Van Meerbeek, *J. Dent. Res.* **86**, 739–744 (2007).
140. M. Vano, F. Garcia-Godoy, C. Goracci, A. Vichi and M. Ferrari, *J. Adhes. Dent.*, in press (2009).

Direct Resin-Based Composite Restorations — Clinical Challenges

Jorge Perdigão [a,*], **Sillas Duarte, Jr.** [b] **and George Gomes** [c]

[a] University of Minnesota School of Dentistry, Division of Operative Dentistry, 515 SE Delaware St, 8-450 Moos Tower, Minneapolis, MN 55455, USA

[b] Case Western Reserve University, School of Dental Medicine, Department of Comprehensive Care, 10900 Euclid Avenue, Cleveland, OH 44106, USA

[c] University of Santiago de Compostela, School of Medicine and Dentistry, Entreríos s/n Campus Universitario Sur, 15782 Santiago de Compostela, Spain

Abstract

With the increase in esthetic awareness and the widespread use of adhesive techniques, a resin composite has become the material of choice for anterior and posterior restorations. In spite of its advantages, polymerization shrinkage and the resulting stress are still a concern for clinicians. The shrinkage stress may cause cusp deflection, interfacial debonding or enamel cracks, leading to microleakage, post-operative sensitivity and secondary caries.

The micro-mechanical nature of the interaction of dental adhesives with enamel and dentin is a result of the infiltration of resin monomers into the microporosities left by the acid etching and subsequent enveloping of the exposed enamel hydroxyapatite crystals and the dentin collagen fibers with the resulting polymer. The latest development in dental adhesives is based on simplification and reduced application time of the bonding procedure by using non-rinsing adhesives. These non-rinsing (or self-etch) adhesives do not require a separate acid-etch step as they condition and prime enamel and dentin simultaneously by infiltrating and partially dissolving hydroxyapatite to generate a resin-infiltrated zone with minerals and smear layer incorporated. In spite of their user-friendliness and low technique sensitivity, self-etch adhesives have resulted in low bonding effectiveness, behaving as semi-permeable membranes to allow movement of water across the dentin–resin interface and potentially leading to hydrolytic degradation. Recently, the role of metalloproteinases (MMPs), in inducing degradation of the dentin extracellular matrix components, has been highlighted in the literature along with the potential role of chlorhexidine in inhibiting the deleterious role of MMPs.

The ultimate goal of a bonded restoration is to attain an intimate adaptation of the restorative material with the dental structure. This task is difficult to achieve as the bonding procedure is different for enamel and for dentin. The bonded interface undergoes degradation with time when a hermetic seal is not achieved. On the other hand, an improved sealing results in decreased post-operative sensitivity and higher resistance to the caries process. The stress resulting from the polymerization shrinkage of resin composites is also a factor that interferes with the bonding procedure as it may cause interfacial leakage and cusp deflection.

Keywords

Dental bonding, dental leakage, resin composite, material testing, polymerization shrinkage

* To whom correspondence should be addressed. Tel.: (612) 625-8486; Fax: (612) 625-7440; e-mail: perdi001@umn.edu

Adhesion Aspects in Dentistry

© Koninklijke Brill NV, Leiden, 2009

1. Introduction

The latest development in dental adhesives is based on simplification and reduced application time of the bonding procedure by using non-rinsing adhesives. These non-rinsing (or self-etch) adhesives do not require a separate acid-etch step as they condition and prime enamel and dentin simultaneously by infiltrating and partially dissolving hydroxyapatite to generate a resin-infiltrated zone with minerals and smear layer incorporated. In spite of their user-friendliness and low technique sensitivity, self-etch adhesives have resulted in low bonding effectiveness, behaving as semi-permeable membranes to allow movement of water across the dentin–resin interface and potentially leading to hydrolytic degradation.

Root canal-treated teeth are often restored with a post and core to replace the tooth structure that has been lost by caries, restorative procedures, fractures, or endodontic access preparations. Loss of adhesion at the post–dentin interface is still the main reason why these restorations fail. The use of fiber-reinforced resin posts (or fiber posts) has gained popularity in the last few years as a consequence of several factors, including the enhanced esthetic properties of fiber posts, the use of adhesive techniques, and the elastic modulus of the posts being similar to that of dentin. However, several limitations of this technique have been recently discussed. First, the high C-factor inside the root canal, a confined environment, leads to development of high shrinkage stresses. Secondly, the anatomy of the root canal does not allow for the complete removal of gutta-percha residues leading to areas of debonding of the resin cement.

To obtain a durable and strong bond to dentin clinicians must understand not only the technique-sensitivity of the clinical bonding procedures, but also the biological and mechanical aspects of the bonding substrate, so they can reduce the existing potential for resin–dentin interfaces to undergo degradation.

2. Polymerization Shrinkage

Light-cured resin composites have been widely used in recent years due to their esthetic advantages, ease of use, improved bonding to the tooth structure and enhanced mechanical properties [1]. The polymerization reaction of light-cured composites is faster than that of chemically-polymerized composites, which leads to the development of higher polymerization stresses for the former [2]. The development of internal stresses is due to a volumetric contraction, typically in the order of 2–9%, that occurs during the polymerization of light-cured resin composites [3, 4]. These shrinkage stresses are considered one of the principal mechanisms responsible for interfacial failures [5].

The matrix of most contemporary resin composite materials consists of methacrylate-based monomers. Resin composites shrink during polymerization, because of the tighter packing of the monomer molecules in the resin matrix upon polymerization [6]. During the early stages of polymerization, monomers are converted into polymeric chains. After a certain degree of conversion has been attained, the prime

reaction consists of cross-linking of the polymeric chains. Although the material viscosity increases rapidly during the initial chain-growth period, the polymeric chains can still slide along one another to alleviate the stress created by the new molecule arrangement [6, 7]. When the cross-linking reaction is completed, the ability of individual polymer chains to slide is no longer possible.

The elastic modulus of the shrinking material is a factor on which shrinkage stresses depend. *In vitro* studies have shown that the interfacial stress that develops during the setting of a resin composite is positively correlated with the rigidity of the setting material [8]. The elastic modulus also increases as the polymerization reaction proceeds [9].

At the cross-linking stage, also known as the post-gel phase, the polymeric chains reach a sufficiently high modulus of elasticity to result in a strong, rigid material. Polymer contraction may continue in response to further conversion. At this point the rigidity of the material resists the plastic flow that tries to compensate for the original volume, leading to contraction stresses [5]. When bonded to the walls in the cavity preparation (cavity preparation or preparation is the space created in the tooth crown (by the dentist) to receive a restorative material (or filling)), the stresses are transferred to the tooth–restoration interface [10]. In areas where contraction stresses overcome bond strength, interfacial integrity is lost [11], and the resulting interfacial gap may result in microleakage [12, 13], post-operative sensitivity, marginal staining and recurrent caries [14, 15].

3. Effect of Polymerization Shrinkage on Bonded Interfaces in Crown Dentin

Any adhesive restoration may be subjected to one of two phenomena: (i) the bonded interface resists the shrinkage stress or (ii) the shrinkage stresses surpass the enamel/dentin bond strength [16].

When the bonded interface resists the polymerization shrinkage stresses, the transfer of the stresses to the bonded interface may cause cusp deflection and enamel fractures [13, 17]. The cusps move inward reducing the amount of composite to be inserted into the preparation [16]. In addition, during mastication, the occlusal load results in resin composite deformation, increasing the cusp deflection [18, 19]. As a result, the patient may feel severe discomfort during mastication. Incremental application of resin composite has been advocated to reduce the potential of cusp deflection and decrease the stresses originated from polymerization shrinkage [20–22] (Fig. 1(a–d)). Several other factors are inter-related and play a role in the clinical manifestation of events that develop during the polymerization of the resin composite. Among these factors, cavity dimensions, resin elastic modulus, resin viscosity, shrinkage, contraction stress, tensile modulus and flow are the most relevant [22]. The application of increments of 2 mm or less has been recommended because the C-factor for a small increment is lower than for bulk filling and, therefore, minimizes the harmful effects of stress development at the adhesive interface. Cuspal deflection that results from polymerization shrinkage is reduced by incre-

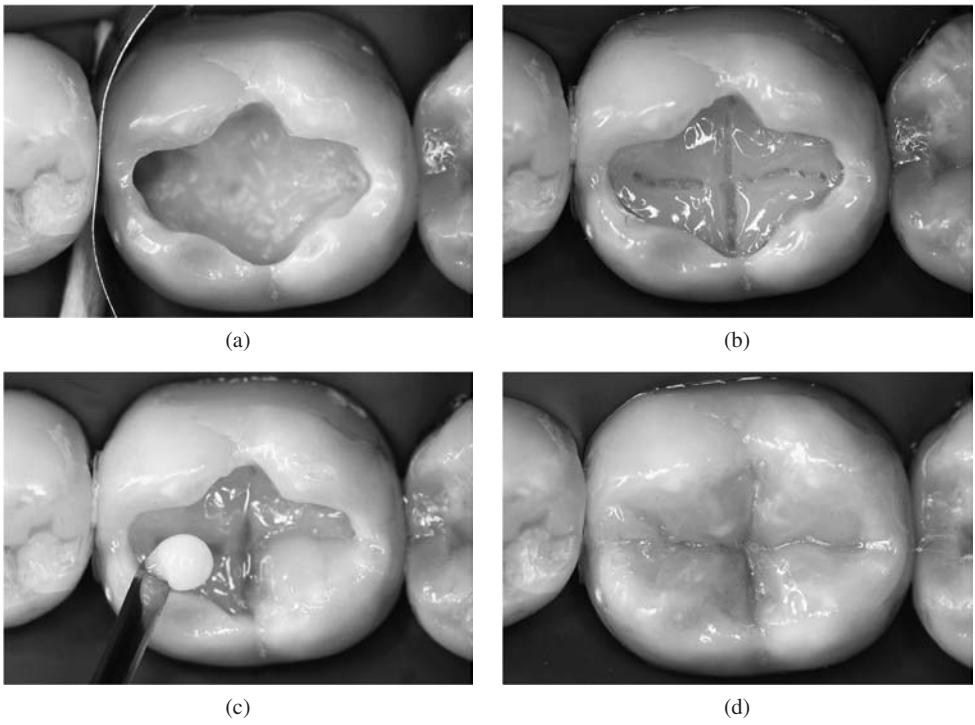


Figure 1. Sequence of incremental application to reduce polymerization stress. (a) Occlusal cavity preparation; (b) after application of the adhesive, the preparation is filled in composite increments from dentin towards enamel; (c) composite (enamel shade) layers being applied and (d) final restoration after finishing.

mental filling techniques compared to bulk filling, regardless of using a horizontal incremental technique or an oblique horizontal technique [23]. A clinical study with class II restorations found significantly less sensitivity to occlusal loading when two composite increments were used as compared to bulk filling [24]. However, the incremental technique has been questioned in view of the fact that even using small increments of resin composite, the amount of material to be inserted into the preparation would be reduced because of dentin deformation [25–29]. Another technique, the trans-enamel polymerization, has also been advocated to reduce the deleterious effects of the contraction stresses by attenuation of the light output. In this technique, the curing energy is transmitted through the enamel and into the preparation [30, 31]. The resin composite is inserted in bulk and polymerized from the buccal and lingual walls. Continued application of energy supposedly penetrates through the tooth substrate into the resin adjacent to the internal surfaces of the preparation, so the bonding forms before the polymerization shrinkage starts developing. A recent study, however, has shown that increasing the enamel thickness resulted in a significant decrease in composite microhardness and cure depth [32]. Additionally, increasing the curing time did not compensate for the light intensity attenuation

effect of the enamel structure [32]. The resulting low degree of conversion might compromise some of the material's properties, including solubility, dimensional stability, color change and biocompatibility of the resin composite [33, 34]. Reducing contraction stress by varying polymerization rate has some limitations [35] and also alters the quality of the formed polymer. It has also been shown that resins cured with low irradiance are more susceptible to degradation as measured by the amount of residual monomers [35, 36]. Another form of light intensity attenuation, the 'soft-start' polymerization, does not result in less cusp deflection or cervical dentin microleakage, as found in a very recent study using mesio-occluso-distal (MOD) restorations in premolars [37]. The degree of conversion is dependent on several other factors [38]. Of all these parameters, the irradiance of the light source and the exposure time are of particular interest since, in practice, these are amenable to manipulation by clinician [39].

It has been described that when a thick layer of a low elastic modulus material is used, the bulk shrinkage of the main restoration may not exert as much stress on the adhesive liner [35, 40]. Attempts to use flowable composites to provide the same effect have been reported. Unfortunately, the elastic modulus of some of the current flowable composites, which manufacturers recommend for use as liners, may not be ideal to behave as 'stress absorbers' [4, 41]. Flowable composites do not necessarily result in stress reduction proportional to the reduction in elastic modulus compared to stiffer composites [42]. Additionally, the higher shrinkage associated with flowable composites, compared to a microfilled composite, may indicate a potential for higher interfacial stresses for the former [4]. Clinical studies with flowable composites have failed to demonstrate any benefits from their use. In one study, the use of flowable composite as a liner under hybrid composite restorations did not improve the clinical performance of class V restorations at 12 months [43]. Another study on teeth scheduled to be extracted for orthodontic reasons did not find better interfacial adaptation of the resin composite in the proximal box of class II restorations when a flowable composite was used in the proximal box [44]. The 2-year clinical performance of occlusal composite restorations in another study did not benefit from the additional use of a flowable composite [45].

In case the composite shrinkage stresses surpass the composite–dentin bond strengths a gap will form (Fig. 2). Marginal gaps may allow the penetration of fluids, bacteria, molecules, and ions to the tooth–restoration interface. During gap formation the resin tags are partially pulled from the tubules, leaving dentin tubules unprotected and susceptible to contamination (Fig. 2). The fluids within the dentinal tubules are challenged by osmotic changes. As a result of fluid movement the nerve receptor is stimulated, generating the sensation of pain [46]. Despite the fact that dentinal hypersensitivity is transient, the sensation is extremely uncomfortable.

The adhesive bond of resin composite to gingival margins is significantly weaker and more susceptible to failure than the bond to the axial walls [47, 48]. Possible explanations for the fact described above are: (i) dentin tubules in the gingival area exhibit the highest density compared to other dentin locations [49]; (ii) during cav-

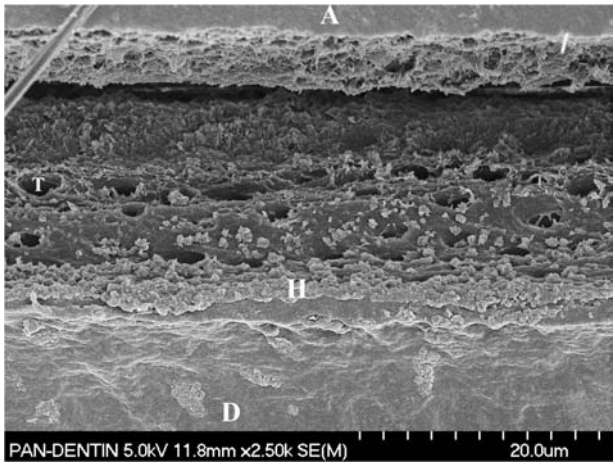


Figure 2. FESEM micrograph showing resin composite debonding from the hybrid layer. Note the patent dentinal tubules. Magnification = ×2500. A — adhesive; H — hybrid layer; D — dentin.

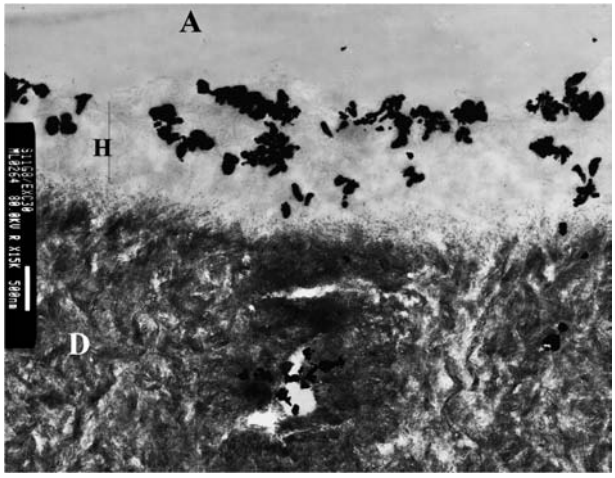


Figure 3. TEM micrograph of reticular pattern of nanoleakage in the hybrid layer obtained after 30 s dentin etching and application of a total-etch ethanol-based adhesive. Magnification = ×15 000. A — adhesive; H — hybrid layer; D — dentin.

ity preparation tubules in the gingival area are cut perpendicular to their long axes [50]; and (iii) the presence of a cementum layer of approximately 150–200 μm at the cervical margins [51]. *In vivo* experiments confirm that the gingival margin represents a serious challenge for reliable bonding [50, 52, 53].

4. Degradation of the Bonded Interfaces

A strongly bonded interface would theoretically be able to resist polymerization stresses. However, the quality of the dentin sealing can be significantly affected by:

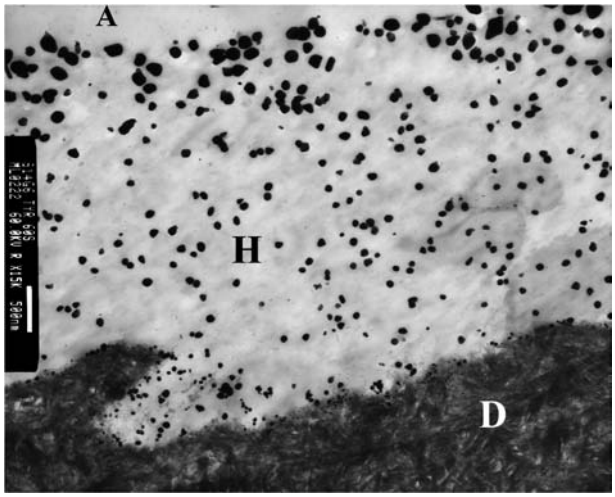


Figure 4. TEM micrograph of spotted pattern of nanoleakage dispersed throughout the hybrid layer after the application of a non-rinsing acidic conditioner. Magnification = ×15 000. A — adhesive; H — hybrid layer; D — dentin.

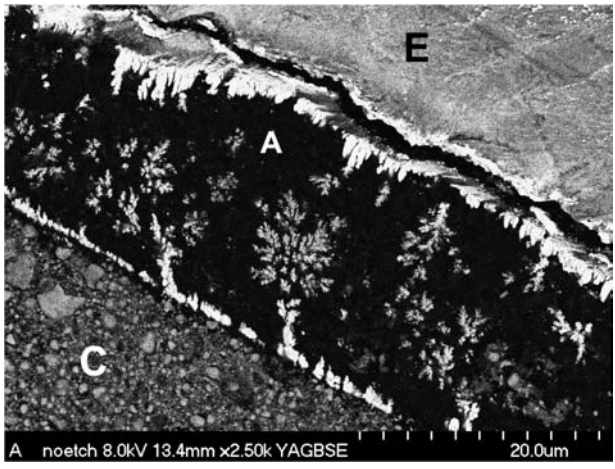
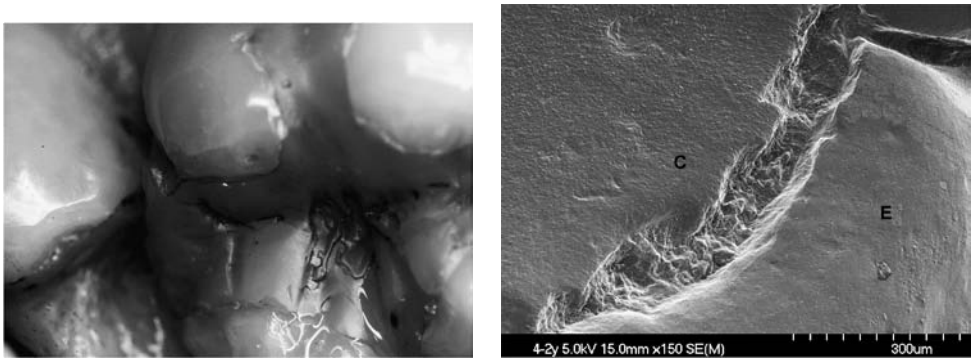


Figure 5. Backscattered FESEM micrograph of nanoleakage (water-tree) in the adhesive layer of an all-in-one self-etch adhesive. Magnification = ×2500. E — enamel; A — adhesive; D — composite resin.

(i) porosity within the hybrid layer (Figs 3–5); (ii) aging of the bonded interfaces (Fig. 6); (iii) the insufficient amount of adhesive used to coat the dentin surface [54, 55]. Even in the absence of marginal gaps, leakage is frequently found within the hybrid layer [56]. Areas of residual water or diffusion of dentinal fluids can be found within the hybrid layer (nanoleakage) (Figs 3–5) or extending from the hybrid layer toward the adhesive layer in form of water-trees [56, 57]. In order to obtain an adequate bond, enamel and dentin surfaces must be modified by phosphoric



(a) (b)

Figure 6. (a) Clinical view of a posterior composite restoration at the 2-year recall. This restoration was placed with a self-etch all-in-one adhesive. (b) FESEM micrograph of the same restoration showing open margins. C — resin composite; E — enamel. Magnification = ×150.

acid-etching or acidic monomer solutions. During the application of the adhesive solution, the role of the adhesive solvent is to displace the fluids located between the individual collagen fibrils to form a homogeneous and compact resin–dentin interdiffusion zone. Evaporation of solvent by air-drying is a critical step regarding the marginal quality of the restorations [58, 59]. In contrast, if the water is shifted from the dentin tubules to the interfibrillar spaces, nanoleakage may increase and bond strength decrease [60]. The complete infiltration of the resin monomers into the collagen network depends on other factors such as monomer molecular weight (61), adhesive composition [62, 63], application technique [54, 55, 60], amount of remaining water [57, 64] and integrity of the dentin collagen [47, 65, 66].

Dentin adhesives can undergo hydrolytic degradation not only immediately after application but also with aging. The discrepancy between the depth of demineralization and resin infiltration results in a basal area of the hybrid layer filled with water [67]. The water present within the nanometric spaces and channels between collagen fibrils may dilute the resin monomers [68]. Thus, the remaining water prevents a complete polymerization of the adhesive, leaving intermittent areas of nanoleakage, which then show as a reticular pattern [67] (Fig. 3). It is speculated that water sorption occurs in localized hydrophilic phases of adhesive matrices causing phase separation of copolymers containing hydrophobic and hydrophilic resins [68] (Fig. 4). Water-trees along the adhesive–dentin junction may result in a rapid deterioration of the mechanical properties of the adhesive resulting in adhesive failure along the surface of the hybrid layer [67] (Fig. 5). In addition, nanoleakage is strongly affected by the depth of the preparation, therefore more nanoleakage (less durability of the bonds) is expected closer to the pulp [53].

Aging significantly increases the degradation of the hybrid layer. Enzymes from the oral environment hydrolytically attack collagen fibrils over time [69]. Simultaneously, areas of unprotect demineralized dentin (‘naked’ collagen) may undergo hydrolysis [70]. As a result, loss of unpolymerized resin from interfibrillar spaces

[71] and disorganization of the collagen network occur [72]. Microvoids in the hybrid layer become wider because the resin undergoes physical separation into hydrophobic- and hydrophilic-rich phases [73]. This phenomenon may result in significant reduction in resin–dentin bond strengths following long-term water immersion. Therefore, the presence of a peripheral enamel bond is crucial to reduce the degradation rate of the resin–dentin interface [74].

A decreased concentration of resin monomer in the acid-etched dentin, and resin elution from hydrolytically unstable polymers within the hybrid layers may leave the collagen fibrils vulnerable to degradation by endogenous metalloproteinases (MMPs) [75], which are enzymes capable of inducing degradation of the extracellular matrix components. Collagenolytic and gelatinolytic activities found in partially demineralized dentine [76] imply the existence of MMP in human dentin. Human dentin contains gelatinases MMP-2 and -9, collagenase (MMP-8), and enamelysin MMP-20 [75, 77, 78]. These enzymes are trapped within the mineralized dentin matrix during odontogenesis [77, 78]. Dentin collagenolytic and gelatinolytic activities can be overcome by protease inhibitors [76], indicating that MMP inhibition could preserve the integrity of the hybrid layer. In fact, the *in vivo* application of chlorhexidine, known to have a MMP-inhibitory effect [79], improved the integrity of the hybrid layer [80]. When chlorhexidine was applied *in vitro*, the integrity of the hybrid layer and the magnitude of bond strengths were preserved in aged dentin–resin interfaces [81]. Apart from having been a commonly known antibacterial element, mainly used in Periodontology, chlorhexidine also functions as a potent MMP inhibitor. When phosphoric acid is applied without the subsequent application of chlorhexidine, it does not inhibit the collagenolytic activity of mineralized dentin, while the use of chlorhexidine after acid-etching, in even very low concentrations, strongly inhibits this activity. The drawback that might be associated with the use of chlorhexidine is the potential discoloration associated with its use [82]. While this staining potential has been widely reported for tooth surfaces, there are no reports dealing with the staining of composite–tooth interfaces that might be wrongly diagnosed as leakage.

5. Bonding to Root Dentin — the Ultimate Challenge

Loss of adhesion at the fiber post–dentin interface is still the main reason why adhesive restorations in the root canal fail [83]. Apart from the difficult access and the lack of direct vision within the root canal, the interaction between the high C-factor inside the canal (ratio of bonded to unbonded surfaces) [20] and polymerization shrinkage of resin materials results in very high stresses that may jeopardize the adhesive cementation of intraradicular posts [84]. The resin material has an opportunity to flow when free surfaces are available, which results in relaxation of stresses that develop in the polymerizing resin [10, 20]. Internal shrinkage stresses in the cement inside the root canal may separate the cement from the dentin wall [85]. These

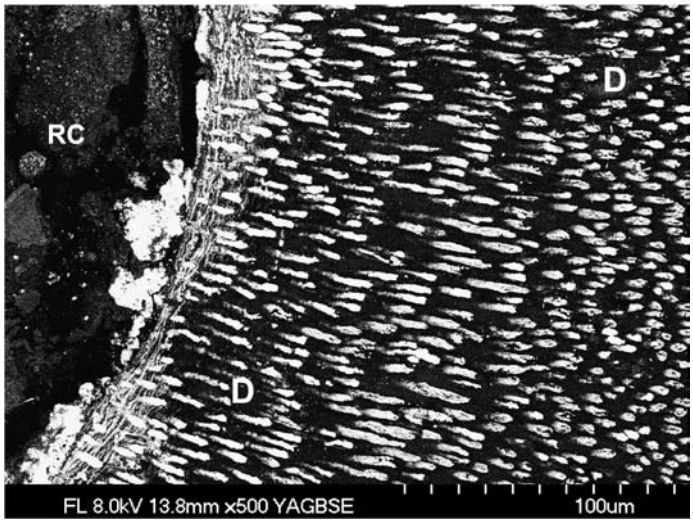


Figure 7. FESEM micrograph (backscattered) of a section of a root canal restored with a fiber post and resin cement (RC). Note the silver leakage associated with air voids in the cement, spreading into the dentinal tubules. Magnification = ×500.

shrinkage stresses were responsible for the resin cement–dentin interface debonded areas observed by different authors [83, 85].

Most adhesive materials used to cement pre-fabricated posts inside the root canal are hand-mixed, which may result in air bubbles entrapped within the cement [85, 86]. The use of a spiral-shaped rotative instrument (lentulo) reduced the prevalence of voids [86]. The incorporation of air in the resin has been shown to inhibit the polymerization of the cement [2, 21]. The deleterious effect of a high C-factor may actually be compensated by the stress relaxation provided by the air present in the resin material [20]. Consequently, the use of hand-mixed resin cements to lute fiber posts may be of some benefit for the mechanical integrity of the resin–dentin interface as it provides an opportunity for the stresses accumulated in the resin cement to dissipate, at least partially [20]. Notwithstanding this benefit, air bubbles may weaken the composite, which explains, in part, the debonding that occurs between the resin cement and the root dentin and the greater microleakage observed at this interface (Fig. 7) [87]. Some of the current cements do not require hand-mixing. For example, the auto-mixing mechanism of some cements and their placement in the root canal with elongated plastic tips may explain the scarcity of voids at the cement–dentin interface in some of the studies performed in our laboratory [87]. It has also been demonstrated that when self-adhesive cements are applied under pressure the number of porosities at the interface decreases [88].

One of the obstacles that clinicians have to overcome when bonding to root canal dentin is the residual gutta-percha that is not removed with the instrumentation and

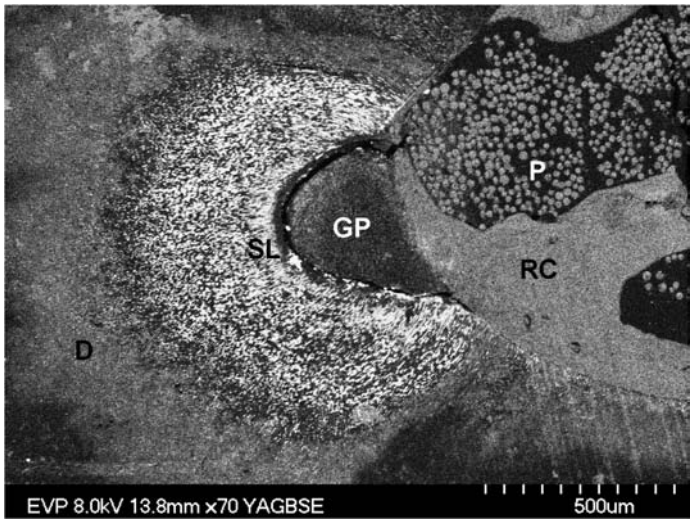


Figure 8. FESEM micrograph (backscattered) of section of a root canal restored with a moldable fiber post (P) and resin cement (RC). Note the silver leakage (SL) between the gutta-percha (GP) and dentin (D). Magnification $= \times 70$.

shaping of the root canal during root canal treatment. These areas around residual gutta-percha may be pathways for leakage (Fig. 8). The unpredictable variation in root canal morphological features [89] may be responsible for the incomplete gutta-percha removal. Adhesion to root dentin requires a surface free of debris and pulpal remnants [90]. Studies have shown that not all walls of the root canal are contacted by instruments [91]. Additionally, the presence of residual gutta-percha in the prepared canals does not allow for adhesion between cement and dentin, leading to debonding at the adhesive interface which prevents a tight seal. In spite of the careful preparation of the canal spaces, some canals had an elliptical shape in cross-section, which resulted in residual gutta-percha in areas that the preparation drill would not reach [87].

6. Summary and Further Studies

Most of the published research on clinically-relevant dental materials is carried out in a laboratory setting. The ultimate test for any dental material is clinical effectiveness and durability. A new version of a specific resin-based dental material is often launched even if the previous one has not been fully tested. As a result, clinicians still rely on data from laboratory tests to predict the clinical behavior of new materials. Future studies must include controlled clinical trials. The obstacles that investigators will need to overcome are (i) clinical trials are more time-consuming for investigators than laboratory research and (ii) there is a shortage of independent funding for clinical studies.

References

1. G. J. Christensen, *J. Am. Dental Assoc.* **134**, 1395–1397 (2003).
2. A. Feilzer, A. de Gee and C. Davidson, *Dental Mater.* **9**, 2–5 (1993).
3. A. J. Feilzer, L. H. Dooren, A. J. de Gee and C. L. Davidson, *Eur. J. Oral Sci.* **103**, 322–326 (1995).
4. R. Labella, P. Lambrechts, B. Van Meerbeek and G. Vanherle, *Dental Mater.* **15**, 128–137 (1999).
5. C. L. Davidson and A. J. Feilzer, *J. Dentistry* **25**, 435–440 (1997).
6. B. Venhoven, A. de Gee and C. Davidson, *Biomaterials* **14**, 871–875 (1993).
7. A. Peutzfeldt, *Eur. J. Oral Sci.* **105**, 97–116 (1997).
8. A. J. Feilzer, A. J. de Gee and C. L. Davidson, *J. Dental Res.* **69**, 36–39 (1990).
9. M. Braem, C. L. Davidson, G. Vanherle, V. Van Doren and P. Lambrechts, *J. Dental Res.* **66**, 1036–1039 (1987).
10. C. L. Davidson and A. J. de Gee, *J. Dental Res.* **63**, 146–148 (1984).
11. C. L. Davidson, A. J. de Gee and A. Feilzer, *J. Dental Res.* **63**, 1396–1399 (1984).
12. K. D. Jörgensen, E. Asmussen and H. Shimokobe, *Scand. J. Dental Res.* **83**, 120–122 (1975).
13. G. J. Fleming, D. P. Hall, A. C. Shortall and F. J. Burke, *J. Dentistry* **33**, 139–146 (2005).
14. M. Brännström, *Oper. Dentistry* **9**, 57–68 (1984).
15. J. D. Eick and F. H. Welch, *Quintessence Int.* **17**, 103–111 (1986).
16. A. Versluis, D. Tantbirojn and W. H. Douglas, *J. Dental Res.* **77**, 1435–1445 (1998).
17. G. Abbas, G. J. Fleming, E. Harrington, A. C. Shortall and F. J. Burke, *J. Dentistry* **31**, 437–444 (2003).
18. S. González-López, M. A. Vilchez Diaz, F. de Haro-Gasquet, L. Ceballos and C. de Haro-Munoz, *J. Adhesive Dentistry* **9**, 11–15 (2007).
19. P. Ausiello, A. Apicella, C. L. Davidson and S. Rengo, *J. Biomech.* **34**, 1269–1277 (2001).
20. A. J. Feilzer, A. J. De Gee and C. L. Davidson, *J. Dental Res.* **66**, 1636–1639 (1987).
21. D. Alster, A. J. Feilzer, A. J. de Gee and C. L. Davidson, *Dental Mater.* **13**, 146–150 (1997).
22. C. J. Kleverlaan and A. J. Feilzer, *Dental Mater.* **21**, 1150–1157 (2005).
23. J. Park, J. Chang, J. Ferracane and I. B. Lee, *Dental Mater.* **24**, 1501–1505 (2008).
24. N. J. M. Opdam, F. J. M. Roeters, A. J. Feilzer and E. H. Verdonschot, *J. Dentistry* **26**, 555–562 (1998).
25. D. Tantbirojn, A. Versluis, M. R. Pintado, R. DeLong and W. H. Douglas, *Dental Mater.* **20**, 535–542 (2004).
26. M. M. Winkler, T. R. Katona and N. H. Paydar, *J. Dental Res.* **75**, 1477–1483 (1996).
27. T. R. Katona and M. M. Winkler, *J. Dental Res.* **73**, 1470–1477 (1994).
28. A. D. Loguercio, A. Reis and R. Y. Ballester, *Dental Mater.* **20**, 236–243 (2004).
29. N. Ilie, K. H. Kunzelmann and R. Hickel, *Dental Mater.* **22**, 593–601 (2006).
30. P. C. Belvedere, *Dental Clin. North Am.* **45**, 49–70 (2001).
31. P. Belvedere, *Northwest Dentistry* **73**, 19–22 (1994).
32. G. Gomes and J. Perdigão, *J. Dental Res.* **87** (Special Issue A): abstract #0847 (2008).
33. N. Silikas, G. Eliades and D. Watts, *Dental Mater.* **16**, 292–296 (2000).
34. G. Pearson and C. Longman, *J. Oral Rehabil.* **16**, 57–61 (1989).
35. C. M. Kemp-Scholte and C. L. Davidson, *J. Dental Res.* **67**, 41–45 (1988).
36. H.-J. Moon, Y.-K. Lee, B.-S. Lim and C.-W. Kim, *J. Oral Rehabil.* **31**, 258–264 (2004).
37. G. J. P. Flemming, R. R. Cara, W. M. Palin and F. J. T. Burke, *Dental Mater.* **23**, 637–643 (2007).
38. N. Emami and K. Söderholm, *Eur. J. Oral Sci.* **11**, 536–542 (2003).
39. R. H. Halvorson, R. L. Erickson and C. L. Davidson, *Dental Mater.* **18**, 463–469 (2002).

40. C. M. Kemp-Scholte and C. L. Davidson, *J. Dental Res.* **69**, 1240–1243 (1990).
41. R. Braga, R. Ballester and J. Ferracane, *Dental Mater.* **21**, 962–970 (2005).
42. R. R. Braga, T. J. Hilton and J. L. Ferracane, *J. Am. Dental Assoc*. **134**, 721–728 (2003).
43. A. D. Loguercio, C. Zago, K. Leal, N. R. Ribeiro and A. Reis, *Clin. Oral Invest.* **9**, 18–20 (2005).
44. A. Lindberg, J. W. van Dijken and P. Horstedt, *Clin. Oral Invest*. **9**, 77–83 (2005).
45. B. G. Efes, C. Dörter, Y. Gömec and F. Koray, *J. Adhesive Dentistry* **8**, 119–126 (2006).
46. M. Brännström and A. Åstrom, *Int. Dental J.* **22**, 219–227 (1972).
47. Y. Yuan, Y. Shimada, S. Ichinose, A. Sadr and J. Tagami, *J. Dental Res.* **86**, 1001–1006 (2007).
48. J. H. Purk, V. Dusevich, A. Glaros, P. Spencer and J. D. Eick, *J. Am. Dental Assoc.* **135**, 185–193 (2004).
49. M. Brännström and R. Garberoglio, *Acta Odontol. Scand.* **30**, 291–311 (1972).
50. M. C. Cagidiaco, M. Ferrari and C. L. Davidson, *ASDC J. Dentistry Child.* **64**, 17–21 (1997).
51. M. Ferrari, M. C. Cagidiaco and C. L. Davidson, *Dental Mater.* **13**, 157–162 (1997).
52. M. Ferrari, F. Mannocci, M. C. Cagidiaco and G. Kugel, *Clin. Oral Investig.* **1**, 61–64 (1997).
53. Y. Yuan, Y. Shimada, S. Ichinose and J. Tagami, *J. Dentistry* **35**, 664–672 (2007).
54. M. Hashimoto, J. De Munck, S. Ito, H. Sano, M. Kaga, H. Oguchi, B. Van Meerbeek and D. H. Pashley, *Biomaterials* **25**, 5565–5574 (2004).
55. S. Ito, F. Tay, M. Hashimoto, M. Yoshiyama, T. Saito, W. W. Brackett, J. L. Waller and D. H. Pashley, *J. Adhesive Dentistry* **7**, 133–141 (2005).
56. H. Sano, T. Takatsu, B. Ciucchi, J. A. Horner, W. G. Matthews and D. H. Pashley, *Oper. Dentistry* **20**, 18–25 (1995).
57. F. R. Tay and D. H. Pashley, *Am. J. Dentistry* **16**, 6–12 (2003).
58. Y. Wang, P. Spencer, X. Yao and B. Brenda, *J. Biomed. Mater. Res. A* **82**, 975–983 (2007).
59. M. Balkenhol, J. Huang, B. Wöstmann and M. Hannig, *J. Dentistry* **35**, 836–844 (2007).
60. M. Hashimoto, F. R. Tay, N. R. Svizero, A. Gee, A. Feilzer, H. Sano, M. Kaga and D. Pashley, *Dental Mater.* **22**, 560–568 (2006).
61. D. H. Pashley, B. Ciucchi, H. Sano and J. A. Horner, *Quintessence Int.* **24**, 618–631 (1993).
62. F. R. Tay, D. H. Pashley, C. K. Y. Yiu, C. H. L. Cheong, M. Hashimoto, K. Itou, M. Yoshiyama and N. M. King, *Am. J. Dentistry* **17**, 182–190 (2004).
63. A. F. Reis, C. A. Arrais, P. D. Novaes, R. M. Carvalho, M. F. De Goes and M. Gianinni, *J. Biomed. Mater. Res. B* **71**, 90–98 (2004).
64. F. R. Tay, M. Hashimoto, D. H. Pashley, M. C. Peters, S. C. Lai, C. K. Yiu and C. Cheong, *J. Dental Res.* **82**, 537–541 (2003).
65. Y. Hosoya, F. R. Tay, M. Miyazaki and T. Inoue, *Dental Mater. J.* **26**, 493–500 (2007).
66. Y. Yuan, Y. Shimada, S. Ichinose and J. Tagami, *Dental Mater.* **24**, 584–593 (2008).
67. F. R. Tay, D. H. Pashley and M. Yoshiyama, *J. Dental Res.* **81**, 472–476 (2002).
68. F. R. Tay, A. J. Gwinnett and S. H. Wei, *Am. J. Dentistry* **9**, 161–166 (1996).
69. M. Hashimoto, H. Ohno, M. Kaga, K. Endo, H. Sano and H. Oguchi, *J. Dental Res.* **79**, 1385–1391 (2000).
70. M. Hashimoto, F. R. Tay, H. Ohno, H. Sano, M. Kaga, C. Yiu, H. Kumagai, Y. Kudou, M. Kubota and H. Oguchi, *J. Biomed. Mater. Res. B* **66**, 287–298 (2003).
71. H. Sano, T. Yoshikawa, P. N. Pereira, N. Kanemura, M. Morigami, J. Tagami and D. H. Pashley, *J. Dental Res.* **78**, 906–911 (1999).
72. M. Hashimoto, H. Ohno, H. Sano, M. Kaga and H. Oguchi, *Biomaterials* **24**, 3795–3803 (2003).
73. Q. Ye, Y. Wang and P. Spencer, *J. Biomed. Mater. Res. B* **88**, 339–348 (2009).
74. J. De Munck, B. Van Meerbeek, Y. Yoshida, S. Inoue, M. Vargas, K. Suzuki, P. Lambrechts and G. Vanherle, *J. Dental Res.* **82**, 136–140 (2003).

75. A. Mazzoni, D. H. Pashley, Y. Nishitani, L. Breschi, F. Mannello, L. Tjäderhane, M. Toledano, E. L. Pashley and F. R. Tay, *Biomaterials* **27**, 4470–4476 (2006).
76. D. H. Pashley, F. R. Tay, C. Yiu, M. Hashimoto, L. Breschi and R. M. Carvalho, *J. Dental Res.* **83**, 216–221 (2004).
77. M. Sulkala, M. Larmas, T. Sorsa, T. Salo and L. Tjäderhane, *J. Dental Res.* **81**, 603–607 (2002).
78. S. Martin-De Las Heras, A. Valenzuela and C. M. Overall, *Arch. Oral Biol*. **45**, 757–765 (2000).
79. R. Gendron, D. Grenier, T. Sorsa and D. Mayrand, *Clin. Diagn. Lab. Immunol.* **6**, 437–439 (1999).
80. J. Hebling, D. H. Pashley, L. Tjäderhane and F. R. Tay, *J. Dental Res.* **84**, 741–746 (2005).
81. M. R. O. Carrilho, R. M. Carvalho, M. F. de Goes, V. di Hipólito, S. Geraldeli, F. R. Tay, D. H. Pashley and L. Tjäderhane, *J. Dental Res.* **86**, 90–94 (2007).
82. J. C. Hase, J. Ainamo, H. Etemadzadeh and M. Åstrom, *J. Clin. Periodontol.* **22**, 533–539 (1995).
83. S. Bouillaguet, S. Troesch, J. C. Wataha, I. Krejci, J.-M. Meyer and D. H. Pashley, *Dental Mater.* **19**, 199–205 (2003).
84. F. Tay, R. Loushine, P. Lambrechts, R. Weller and D. Pashley, *J. Endodont.* **31**, 584–589 (2005).
85. J. Perdigão, G. Gomes and V. Augusto, *J. Prosthodont.* **16**, 154–164 (2007).
86. A. Vichi, S. Grandini, C. L. Davidson and M. Ferrari, *Dental Mater.* **18**, 495–502 (2002).
87. V. Santos, J. Perdigão, G. Gomes and A. L. Silva, *J. Prosthodont.*, in press (2009).
88. J. De Munck, M. Vargas, K. Van Landuyt, K. Hikita, P. Lambrechts and B. Van Meerbeek, *Dental Mater.* **20**, 963–971 (2004).
89. I. A. Mjör, M. R. Smith, M. Ferrari and F. Mannocci, *Int. Endodont. J*. **34**, 346–353 (2001).
90. R. Schwartz, *J. Endodont.* **32**, 1125–1134 (2006).
91. O. Peters, *J. Endodont.* **30**, 559–567 (2004).

Important Aspects of Bonding Resin to Dental Ceramics

Alvaro Della Bona *

Dental School, University of Passo Fundo, Campus I - BR 285, P.O. Box 611, Passo Fundo, RS 99001-970, Brazil

Abstract

The clinical success of resin bonding procedures for indirect ceramic restorations and ceramic repairs depends on the quality and durability of the bond between the resin and ceramic. The quality of this bond will depend on the bonding mechanisms that are controlled, in part, by the surface treatment that promotes micromechanical and chemical bonding to the substrate. The objective of this work was to examine the correlation of interfacial toughness (K_A) with fracture surface morphological parameters of the resin–ceramic systems as a function of ceramic surface treatment. This analysis was designed to identify mechanisms that promoted adhesion of these resin–ceramic systems and an appropriate bond test method to yield relevant adhesion performance data. The rationale used in this work indicates that the quality of the bond should not be assessed based on bond strength data alone. In addition, the mode of failure and fractographic analyses should be used to provide important information leading to predictions of clinical performance limits, which is the ultimate test for any adhesive system.

Keywords

Ceramics, resin, bond strength, interfacial toughness, fracture surface

1. Introduction

The discovery that most dental ceramics could be acid etched to create a micromechanical bond to resin has led to the development of acid-etched and bonded ceramic restorations [1]. This concept was extended to include the repair of fractured dental ceramic restorations in the mouth. Such fractures lead to increased cost, discomfort, time and labor when a replacement is required [2]. The repair of a fractured ceramic restoration is a challenging clinical situation and there is little documentation on the clinical performance of the repaired restorations. Yet, repair would be a more cost effective option, provided the final result is clinically acceptable.

Materials and procedures used either to repair fractured ceramic restorations with a resin composite or to bond indirect ceramic restorations using a resin cement are

* Tel.: 55-54-581-0657; 55-54-311-5142; e-mail: dbona@upf.br

Adhesion Aspects in Dentistry
© Koninklijke Brill NV, Leiden, 2009

based on the results of bond strength tests that exhibit wide variability in both test data and resulting fracture surface characteristics [3–11].

In the search for a method that produces a uniform stress distribution across the interface, investigators have evaluated similar adhesive systems under various bond test configurations [6, 12, 13]. These studies suggest that a tensile test may be more appropriate to evaluate the bond strength of adhesive interfaces because of more uniform interfacial stresses. However, tensile tests require careful alignment of the specimens to minimize the risk of flexure [7].

The physical contribution to the adhesion process is dependent on the surface topography of the substrate and can be characterized by its surface energy. Alteration of the surface topography by etching or airborne-particle abrasion results in changes in the surface area and on the wetting behavior of the ceramic. This also changes the ceramic surface energy and its adhesion potential to resin [14, 15]. Dynamic contact angle (DCA) analysis has been used to evaluate the surface energy of treated ceramic surfaces and their work of adhesion (W_A) to resin. In principle, the work of adhesion can be related to the apparent interface toughness [14].

Fracture mechanics allows quantification of the relationships between material properties such as toughness, stress level, the presence of crack-producing flaws, and crack propagation mechanisms. Another way to assess the integrity of the bond is to estimate the apparent interfacial fracture toughness of the adhesion zone by promoting crack initiation within this zone. The apparent fracture toughness value (K_A) reflects the ability of a material to resist unstable crack propagation [16–19].

The objective of this work was to examine the correlation of apparent interfacial toughness (K_A) with fracture surface morphological parameters of the resin–ceramic systems as a function of ceramic surface treatment. This analysis was designed to identify mechanisms that promoted adhesion of these resin–ceramic systems and an appropriate bond test method to yield relevant adhesion performance data.

2. Effect of Surface Treatment on the Contact Angle and Work of Adhesion

The clinical success of either a repaired ceramic restoration or a resin cemented ceramic restoration will depend on the quality and durability of the bond between the resin and ceramic. The quality of this bond will depend on the bonding mechanisms that are controlled, in part, by the specific surface treatment used to promote micromechanical and chemical retention with the substrate [7]. Structural and surface analyses of etched ceramics have shown that different etching patterns are created depending on the ceramic microstructure and composition, and the concentration, application time and type of etchant [7, 20–26]. Surface defects, often located in the glassy matrix, and phase boundaries of heterogeneous ceramic materials are preferentially etched by the acids. Alteration of the surface topography by etching will result in changes in the surface area and on the wetting behavior of the

porcelain [14, 15, 24]. This may also change the ceramic surface energy and its adhesion potential to resin [14, 27]. Differences in ceramic compositions will also produce unique topographic changes after etching procedures [24]. Thus, the ceramic microstructure, composition, and morphology after surface treatment should yield potentially useful information on the clinical success of the bonding procedures for indirect ceramic restorations and ceramic repairs [24, 28].

It has been reported that the surface changes produced by fluoride-containing etchants such as hydrofluoric acid (HF), ammonium bifluoride (ABF) and acidulated phosphate fluoride (APF) are distinct [24]. HF etching has a very aggressive effect on the surface of most acid-sensitive ceramics, where porosities are scattered uniformly throughout the ceramic surface. This pattern is more evident for leucite-based ceramics than for either single-phase or high-content alumina ceramics (Fig. 1) [7, 20–24, 29–31].

ABF etching produces mostly linear defect patterns that are primarily formed because of the etchant attack on existing surface cracks, leucite-induced cracks, and phase boundaries. This etching pattern is also observed after using HF for reduced times and at lower concentrations, suggesting that ABF acts as a low power HF etchant [23, 24].

The APF etchant seems to build up surface deposits preferentially on the leucite crystal phase [6, 7, 23, 24]. These studies demonstrated that treating the ceramic

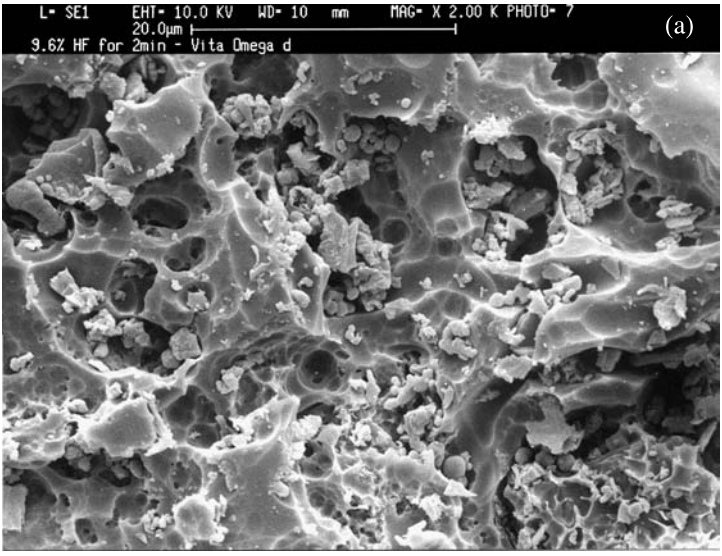


Figure 1. SEM micrographs of HF-etched ceramics. (a) Vita Omega dentine ceramic (Vita Zahnfabrik, Bad Sackingen, Germany), a leucite-based feldspathic ceramic. (b) Duceram-LFC ceramic (Ducera, Rosbach, Germany), a single-phase low-fusing glass. (c) In-Ceram Zirconia ceramic (Vita Zahnfabrik, Bad Sackingen, Germany), a glass-infiltrated zirconia-reinforced ceramic. HF etching produces a very aggressive effect on the surface of most acid-sensitive ceramics (a). The acid effect is reduced for either single-phase (b) or high crystalline content ceramics (c). From Della Bona and Anusavice [24].

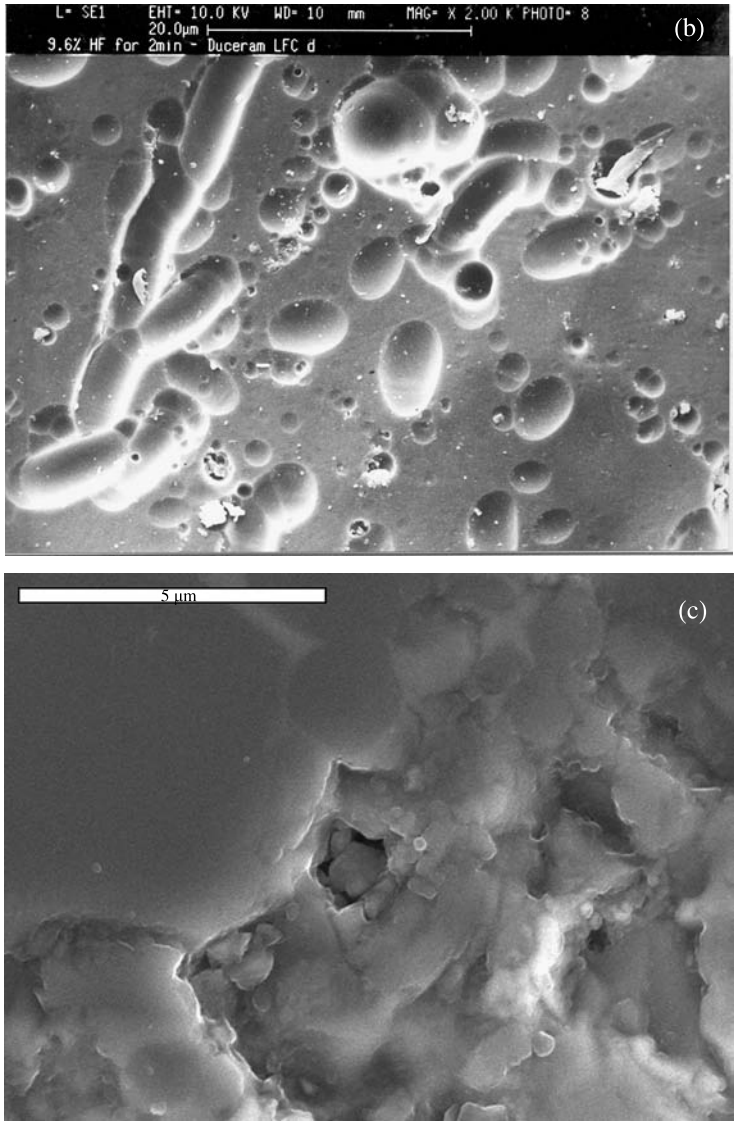


Figure 1. (Continued.)

surface with APF alone produces an insufficient, inconsistent, micromechanically-retentive surface and, as a consequence, the lowest bond strengths were obtained for resin-based composites. Treating the ceramic surface with HF produced a substantial and consistent roughness on acid-sensitive ceramics, mainly because of its action on defects and phase boundaries [7, 23]. These results have a positive correlation with the results from contact angle measurements between the resin and ceramic [14].

The etched ceramic topography can be explained by the chemical reactivity of the crystals of single-phase materials, and this depends on crystallographic orientation. In polycrystalline materials, etching characteristics vary among crystal types. Atoms along the crystal boundaries are more chemically active and dissolve at a greater rate than those within the exposed grain, resulting in the formation of small grooves or linear defects after etching (Fig. 1) [24, 28, 32].

It has, therefore, been suggested that (1) differences in ceramic microstructure and ceramic composition are the controlling factors in the development of micromechanical retention produced by etching, and (2) the etching mechanism is different for different etchants, with HF producing the most prominent etching pattern on most acid-sensitive ceramics [24].

Some clinicians also use coarse diamond rotary instruments or oral gritblaster (airborne-particle abrasion systems) as the first step in the repair of fractured ceramic restorations. It has been shown that other than the scalloped surface created by the rotary instrument, both procedures produce a similar topography. In addition, these methods tend to create more stress and sharp cracks in the ceramic surface, and these are readily attacked by acids and may weaken the substrate [23].

Ceramics with high crystalline content (aluminum and zirconium oxides), also called acid-resistant ceramics, have demonstrated better clinical performance than feldspar-, leucite-, and lithium disilicate-based ceramics, which are known as acid-sensitive ceramics [28]. However, an increase in mechanical strength, by increasing the crystalline content and decreasing the glass content, results in an acid-resistant ceramic whereby any type of acid treatment produces insufficient surface changes for adequate bonding to resin [7, 24, 28, 33–39]. For these acid-resistant ceramics, a silica coating process (silicatization) has been suggested to maximize the bond to resin [28, 36, 37, 39–42]. Coating systems (Rocatec and Cojet, 3M-Espe) create a silica layer on the ceramic surface through high-speed surface impact of alumina particles modified with silica. It has been reported that the airborne particles can penetrate up to 15 μm into ceramic and metal substrates [41]. This tribochemical effect of the silica coating systems may be explained by two bonding mechanisms: (1) the creation of a topographic pattern *via* airborne-particle abrasion allowing for micromechanical bonding to resin; and (2) the promotion of a chemical bond between the silica-coated ceramic surface and the resin-based material, *via* a silane coupling agent. Therefore, a silica–silane chemical bond can occur with acid-resistant ceramics if a silica coating of the ceramic surface is used (Fig. 2) [33, 37, 42–44].

Silanes have been used to enhance the bonding between organic coatings/adhesives and ceramics or metals in various industries since the 1940s [45, 46]. Organosilane coating of inorganic filler particles has improved their bonding to matrix resins [47]. This approach also improves the chemical adhesion of ceramic bonded restorations [48–50] and resin-bonded ceramic repairs [7–9, 22, 25, 26, 51, 52]. However, the long-term stability of such bonding has been challenged [49, 53–56].

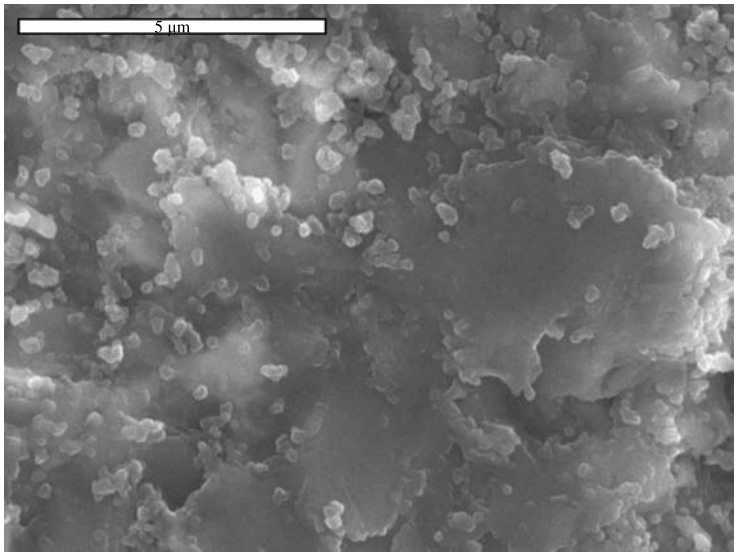


Figure 2. SEM micrograph of a silica-coated In-Ceram Zirconia ceramic (Vita Zahnfabrik, Bad Sackingen, Germany), a glass-infiltrated zirconia-reinforced alumina-based ceramic. The small grains bonded onto the ceramic surface are alumina (Al_2O_3) particles modified by silica that were blasted using the Cojet system (3M-Espe).

Silane coupling agents bond to Si–OH on ceramic surfaces by condensation reactions and methyl methacrylate double bonds provide bonding to the adhesive. As long as there are adequate Si–OH sites on the ceramic surface, satisfactory bonding should be achievable. Therefore, if the goal is to obtain a thin silane coating on any ceramic surface, the protocol should consider the various ceramic microstructures and silane types, and mechanisms to reduce the silane coating thickness, e.g., heat treatment.

Silane commonly used in dentistry is thought to be hydrophobic, and this property is believed to reduce hydrolytic degradation of the bond. It may also improve wetting of the ceramic surface by the adhesive, since the silane-coated surface is organophilic to the adhesive. However, contact angle measurements have shown otherwise [14]. To obtain complete wetting of a surface, the adhesive must initially be of low viscosity and have a surface tension lower than the critical surface tension of the mineral surface [45]. In [57] it has been reported that the surface energy of glass treated with methacryloxy propyl trimethoxy silane — MPTMS is 36.7 mJ/m^2 and the critical surface energy is 28.0 mJ/m^2 at 20°C. Both values are lower than the surface tension of the resin (65% Bis-GMA, 35% TEGDMA: 39.7 mJ/m^2). This should explain the high contact angle values observed for MPTMS treated ceramic surfaces probed using this resin medium [14].

The adhesion between resin-based composites and dental ceramics is the result of a physico-chemical interaction across the interface between the resin (adhesive) and the ceramic (substrate or adherend). The physical contribution to the adhesion

process is dependent on the surface topography of the substrate and can be characterized by its surface energy. Alteration of the surface topography, e.g., by etching and airborne-particle abrasion, will result in changes in the surface area and in the wettability of the substrate [14, 15]. This may also change the surface energy and the adhesion potential [14, 27, 58, 59].

The wetting behavior (wettability) of the resin on the treated ceramic substrate can be characterized using contact angle measurements and surface energy calculations. The wettability of a solid surface by a liquid (e.g., adhesive) can be characterized by Young's equation:

$$\gamma_{SL} = \gamma_{SV} - \gamma_{LV} \cos\theta, \tag{1}$$

where γ_{SV} is the free energy per unit area of the solid surface in equilibrium with vapor, γ_{LV} is the surface tension of liquid in equilibrium with its vapor, γ_{SL} is the interfacial energy, and θ is the contact angle. The work of adhesion (W_A) of the liquid drop on a substrate is expressed by Dupré's equation:

$$W_A = \gamma_{SV} + \gamma_{LV} - \gamma_{SL}. \tag{2}$$

Combining equations (1) and (2) yields the so-called Young–Dupré equation:

$$W_A = \gamma_{LV}(1 + \cos\theta). \tag{3}$$

An increase in the ceramic surface energy can improve the bond strength between resin composite and ceramic. Contact angle values can be used as an indicator of total surface energy and wettability [60]. Dynamic contact angle (DCA) analysis using high-performance liquid chromatography (HPLC) grade water as the probe liquid was used to quantify the influence of surface treatments on contact angle of a feldspathic ceramic [15]. It was found that chemical and mechanical treatments of ceramic surfaces yielded increased total surface area as well as total surface energy. The use of high purity water as a probe liquid is valid for analyzing differences between substrates, such as the effect of etching on dental ceramic surfaces. According to equation (3), W_A is dependent on the surface tension of the liquid (e.g., an adhesive) and its contact angle on the substrate. Thus, the values obtained using water as a probe liquid are not useful to calculate the W_A of resin bonded to ceramic. Instead, an adhesive-equivalent fluid resin should be used, i.e. a resin of similar composition to that of the adhesive. The results of such an approach were that untreated ceramics displayed a larger mean contact angle than the etched ceramics [14]. This improved ceramic wettability by low-viscosity resins is dependent on the increase in surface area, which allows a solid to draw more medium onto its surface and exerts greater interfacial force on the specimen. Consequently, roughened surfaces display smaller contact angles and a greater W_A. A good correlation can be observed between the surface roughness and the resulting contact angle. Thus, the greater the surface roughness, the lower the contact angle and the greater the W_A [14].

3. Bond Strength and Interfacial Fracture Toughness of Resin–Ceramic Systems

Bond strength tests have been used to predict the clinical performance of repaired fractured ceramic restorations and resin-bonded ceramic restorations, although most of these tests exhibit a wide variability in fracture patterns and bond strength values. The commonly used shear bond test often produces fracture at a distance from the resin–ceramic adhesion zone that may lead to erroneous conclusions on bond quality. Such failures of the substrate prevent measurement of interfacial bond strength and limit further improvements in bonding systems [5, 6, 23, 32, 61].

To test the integrity of bonded interfaces one can subject a bonded assembly to a variety of loading conditions to control the crack path along the interface or within the interfacial region. Analyses of bond tests have revealed several problems associated with most common test arrangements and suggest a lack of reliability of such measurements in assessing the adhesive behavior of bonded dental materials. Several studies have identified non-uniform stress distributions along bonded interfaces. These variable stress patterns suggest that a standardized research protocol may address only a part of the problem [6, 61–67].

Studies of similar adhesive systems under different bond test configurations [6, 12, 13] suggest that a tensile bond strength test may be more appropriate to evaluate the bond strength of adhesive interfaces because interfacial stresses are more uniform.

The microtensile test, a tensile bond test with reduced testing area, was developed as an attempt to eliminate non-uniform stress distribution at the adhesive interface and to minimize the influence of interfacial defects [68]. The reduction in the number and size of defects in the adhesion zone is thought to decrease the incidence of bulk cohesive failures and increase the tensile bond strength, regardless of the cross-sectional shape. This test has been used to measure the bond strength of resin composites to dental tissues [13, 68–73] and to ceramics [7, 9, 74].

The non-trimming method to obtain specimens for the microtensile test places less stress on the adhesion zone [71]. As no specimen finishing is necessary, this method also avoids areas of stress concentration produced by polishing materials of different hardness values [7, 9].

The evaluation of the structural integrity of the adhesion zone by Weibull analysis is also an important component for an integral analysis of the bonded interface [7, 9]. The strength values reported using the microtensile test are considered a reliable indicator of the resin composite–ceramic bond quality since all fractures occur within the adhesion zone. In addition, the microtensile test produces variable fracture surface morphology and fracture origins for the same adhesive interfaces within the adhesion zone. Yet, the resin–ceramic interface seems to be the weakest link in this system, and fractures followed a certain mode of failure trend depending on the ceramic surface treatment. The modes of failure were examined and classified (Fig. 3) [9]. Adhesion failures (mode 1) are not common and normally happen during specimen cutting procedures. HF-treated ceramic specimens usually produce

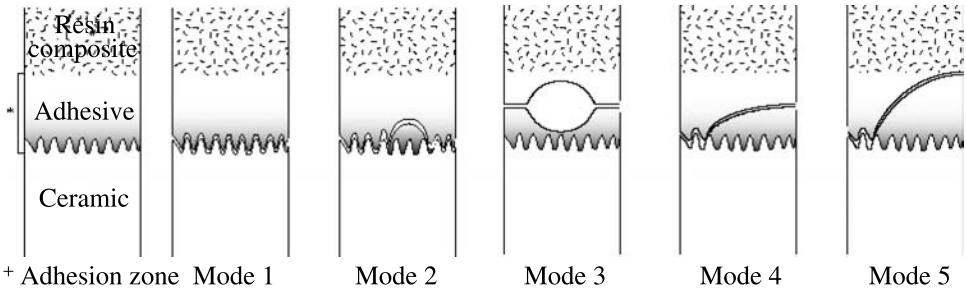


Figure 3. Schematic representation (side view) of the modes of failure for the microtensile bond strength test of ceramic bonded to resin composite, based on crack initiation and principles of fractography. Mode 1: interfacial separation at the ceramic–adhesive resin interface. Mode 2: failure starts at the ceramic–adhesive interface, goes into the adhesive resin and returns to the interface. Mode 3: failure from internal flaw (penny-shape internal crack). Mode 4: failure starts at the ceramic–adhesive interface and propagates through the adhesive resin. Mode 5: failure starts at the ceramic–adhesive interface, goes through the adhesive resin to reach the resin composite–adhesive interface. From Della Bona *et al.* [9].

failures that start at the adhesive–ceramic interface and propagate through the adhesive (mode 4), then either reach the adhesive–resin composite interface (mode 5) or return to the ceramic–adhesive interface (mode 2) [7, 9].

Optical microscopy observation is often not enough to determine the mode of failure of bonded interfaces. A thorough SEM examination of the fracture surfaces following the principles of fractography and confirmation of surface composition through the use of X-ray elemental map analysis (Fig. 4) produce a more consistent and complete description of the fracture initiation, crack propagation, and the modes of failure [8, 9]. These analyses would prevent simplistic comments such as "mixed mode of failure" as an attempt to classify the mode of failure, which often follows the "adhesion" or "cohesive" unscientific determination of the fracture process. Thus, when fractography is correctly used to determine the fracture origin, a proper scientific statement on the mode of fracture can be formulated.

Although the mode of failure is an important aspect of bond strength tests, this behavior is not commonly reported. A detailed inspection of the fracture surfaces can indicate the failure mode of a bonded assembly. The fracture behavior of adhesive interfaces will depend on stress, flaw distribution, material properties, and environmental effects. Therefore, fracture surface characterization (fractography) combined with fracture mechanics inferences are of great importance to understand and predict bonded interface reliability [75].

A careful interpretation of the failure mode is required to prevent inappropriate conclusions about the utility of microtensile testing and adhesion zone phenomena. Several dentin bond strength studies using a microtensile test have reported the modes of failure based on SEM observations [72, 73, 76–81]. These studies have based the failure classification on the location where the fracture has occurred. Examining the information provided in these studies one concludes that most of the

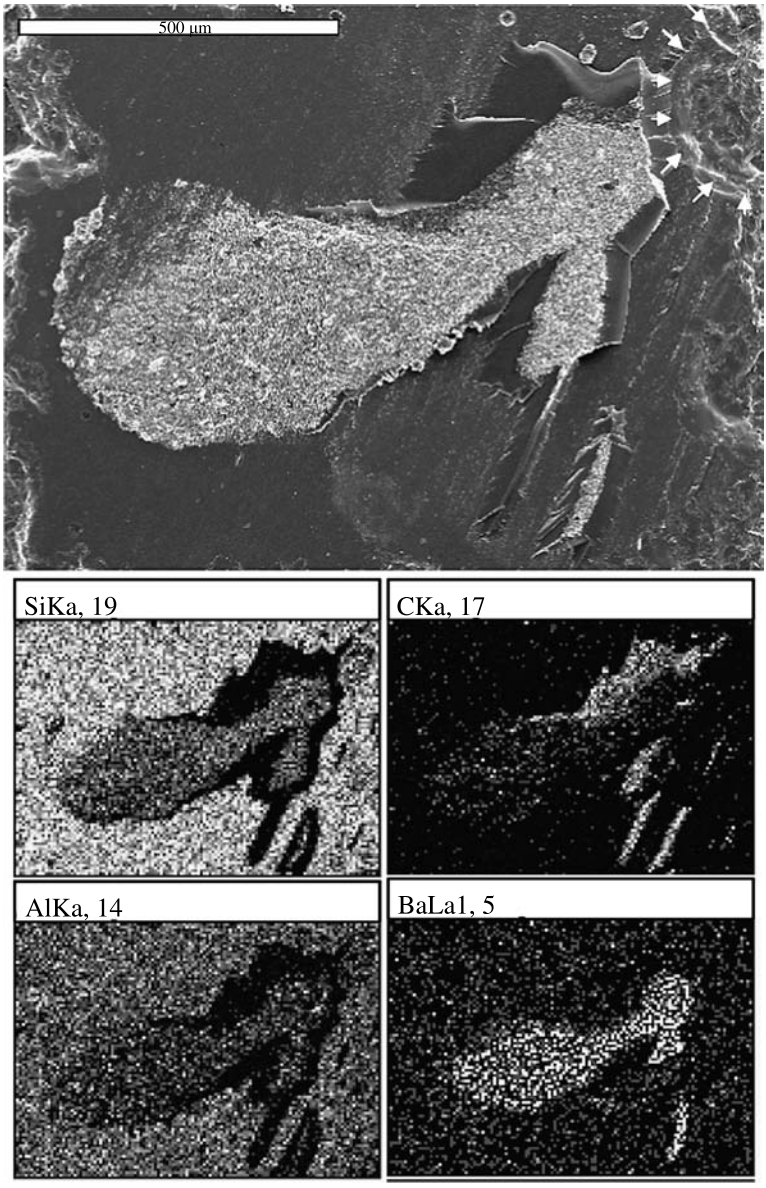


Figure 4. SEM image (top) and X-ray elemental maps of fracture surface of IPS Empress ceramic (Ivoclar AG, Schaan, Liechtenstein) bonded to resin composite (Z100, 3M Dental Products, St. Paul, MN, USA). The label at the top of X-ray maps indicates the elements and their intensity. The critical flaw is indicated by the white arrows at the top right corner of the SEM micrograph (×100). The fracture starts along the ceramic–adhesive interface, propagates through the adhesive resin to reach the resin composite–adhesive interface (Failure mode 5, in Fig. 3). From Della Bona *et al.* [9].

failures occurred within the adhesion zone [9]. Yet, an understanding of the fracture mechanics concepts and the analysis of fracture events on the basis of fractography

will reduce the risk for data misinterpretation such as the inference that the bond strength must exceed the cohesive strength of the ceramic when the fracture initiates away from the interface. Therefore, the classification of the modes of failure based on principles of fractography (Fig. 3) should assist researchers to correctly interpret the fracture phenomena.

As demonstrated by finite element analyses (FEA) of stresses, the non-uniformity of the interfacial stress distribution generated during conventional tensile and shear bond strength testing may lead to fracture initiation from flaws at the interface or within the substrate at areas of high localized stress [6, 67, 82]. To promote crack initiation within the interfacial zone, an interfacial toughness test can be used [9, 18, 19]. These authors used fractography to identify the initial critical flaw and suggested that the interfacial fracture toughness, a more meaningful property than bond strength, could be assessed by employing fracture mechanics principles.

The fracture toughness value (K_{IC}) reflects the ability of a material to resist unstable crack propagation. An extensive literature exists on the various techniques used for measuring the fracture toughness of ceramics [16, 83]. Fracture mechanics allows quantification of the relationships between material properties, stress level, the presence of crack-producing flaws, and crack propagation mechanisms. Another way to assess the strength of the bond is to estimate the apparent interfacial fracture toughness (K_A) of the adhesion zone by promoting crack initiation at the bonding interface. Strictly speaking, measurement of the toughness at the interface in terms of K_{IC} is undefined. However, tensile tests can be performed in which a crack or defect is the source of failure. Therefore, the apparent fracture toughness of the interface can be calculated from the size of the defect and the strength with an appropriate geometric factor. Thus, the apparent fracture toughness value (K_A) reflects the ability of a material to resist unstable crack propagation at the interface [18, 19].

Usually, in order to maintain equal compliances of the specimen halves, i.e. for the two halves to have equal strain energy, most interfacial fracture toughness tests require $E_1 d_1^3 = E_2 d_2^3$, where E is the elastic modulus and d is the depth of the rectangular segment for ceramic and resin composite, subscripts 1 and 2, respectively [9, 18, 19]. As the microtensile test is uniaxial, there is no need to balance the compliance for the two materials to measure K_A. Even so, because the fracture toughness in this form is really a pseudocritical stress-intensity factor, i.e. apparent toughness (K_A), and considering the fact that it is difficult to define stress intensity at an interface, one must still determine an effective modulus for the two materials [18].

Another appropriate way to assess the interfacial bond is to analyze the energy per unit crack surface area, G_{IC}, i.e., the energy required for a crack to advance in the bond plane. The toughness relative to the strain energy release rate (G_{IC}) is an accurate measure of the resistance of the bond to fracture since G_{IC} represents the relative energy required to create the new surfaces [18].

4. Summary and Conclusions

This review suggests that (1) microstructure and composition are the controlling factors in the development of micromechanical retention produced by etching for the acid-sensitive ceramics; (2) roughening the ceramic surface by HF etching and silane coating still yields the highest bond strength values for acid-sensitive ceramics; (3) silica coating of acid-resistant ceramics is effective in improving the bonding to resin; (4) the tensile bond strength and the apparent interfacial fracture toughness of ceramic bonded to resin is affected by the ceramic microstructure and the ceramic surface treatments; (5) the definition of the adhesion zone is critical to classify the modes of failure, which should be an integral component of all failure analyses; (6) tensile bond strength tests may be preferable to conventional shear or flexural tests as an indicator of resin composite–ceramic bond quality, since fracture occurs within the adhesion zone; (7) a careful microscopic analysis of the fracture surfaces and an X-ray elemental map can produce a more consistent and complete description of the fracture process and interpretation of the modes of failure; and (8) there is a positive correlation between the W_A, the tensile bond strength (σ), and K_A, i.e., the greater the mean W_A value, the greater the mean σ and K_A values.

Thus, the quality of the bond should not be assessed based on bond strength data alone. The mode of failure and fractographic analyses can provide important information to predict the clinical performance of adhesive systems. Future studies should also focus on improving surface treatment conditions because of the poor adhesion associated with acid-resistant ceramics.

References

1. M. A. Hussain, E. W. Bradford and G. Charlton, *Br. Dental J.* **147**, 89 (1979).
2. K. J. Anusavice and R. B. Lee, *J. Dental Res.* **68**, 1075 (1989).
3. M. B. Blatz, A. Sadan and M. Kern, *J. Prosthet. Dentistry* **89**, 268 (2003).
4. R. G. Chadwick, A. G. Mason and W. Sharp, *J. Oral Rehabil.* **25**, 610 (1998).
5. A. Della Bona and S. E. Northeast, *J. Dentistry* **22**, 103 (1994).
6. A. Della Bona and R. van Noort, *J. Dental Res.* **74**, 1591 (1995).
7. A. Della Bona, K. J. Anusavice and C. Shen, *J. Adhesive Dentistry* **2**, 305 (2000).
8. A. Della Bona, K. J. Anusavice and J. A. A. Hood, *Int. J. Prosthodont.* **15**, 248 (2002).
9. A. Della Bona, K. J. Anusavice and J. J. Mecholsky, Jr., *Dental Mater.* **19**, 693 (2003).
10. A. Leibrock, M. Degenhart, M. Behr, M. Rosentritt and G. Handel, *J. Oral Rehabil.* **26**, 130 (1999).
11. C. H. Pameijer, N. P. Louw and D. Fischer, *J. Am. Dental Assoc.* **127**, 203 (1996).
12. Y. Kitasako, M. F. Burrow, T. Nikaido, N. Harada, S. Inokoshi, T. Yamada and T. Takatsu, *Dental Mater.* **11**, 298 (1995).
13. R. F. Schreiner, R. P. Chappell, A. G. Glaros and J. D. Eick, *Dental Mater.* **14**, 194 (1998).
14. A. Della Bona, C. Shen and K. J. Anusavice, *Dental Mater.* **20**, 338 (2004).
15. R. D. Phoenix and C. Shen, *Int. J. Prosthodont.* **8**, 187 (1995).
16. A. Della Bona, K. J. Anusavice and J. J. Mecholsky, Jr., *Dental Mater.* **20**, 956 (2004).
17. A. Della Bona, K. J. Anusavice and J. J. Mecholsky, Jr., *J. Dental Res.* **85**, 1037 (2006).

18. J. J. Mecholsky, Jr. and L. M. Barker, in: *Chevron-Notched Specimens: Testing and Stress Analysis*, J. H. Underwood, S. W. Freiman and F. I. Baratta (Eds), STP 855, p. 324. ASTM, Philadelphia (1984).
19. L. E. Tam and R. M. Pilliar, *J. Dental Res.* **72**, 953 (1993).
20. A. al Edris, A. al Jabr, R. L. Cooley and N. Barghi, *J. Prosthet. Dentistry* **64**, 734 (1990).
21. J. H. Chen, H. Matsumura and M. Atsuta, *J. Dentistry* **26**, 53 (1998).
22. J. H. Chen, H. Matsumura and M. Atsuta, *Oper. Dentistry* **23**, 250 (1998).
23. A. Della Bona and R. van Noort, *Am. J. Dentistry* **11**, 276 (1998).
24. A. Della Bona and K. J. Anusavice, *Int. J. Prosthodont.* **15**, 159 (2002).
25. V. Jardel, M. Degrange, B. Picard and G. Derrien, *Int. J. Prosthodont.* **12**, 59 (1999).
26. K. A. Kupiec, K. M. Wuertz, W. W. Barkmeier and T. M. Wilwerding, *J. Prosthet. Dentistry* **76**, 119 (1996).
27. V. Jardel, M. Degrange, B. Picard and G. Derrien, *Int. J. Prosthodont.* **12**, 415 (1999).
28. A. Della Bona, T. A. Donassollo, F. F. Demarco, A. A. Barrett and J. J. Mecholsky, Jr., *Dental Mater.* **23**, 769 (2007).
29. M. Aida, T. Hayakawa and K. Mizukawa, *J. Prosthet. Dentistry* **73**, 464 (1995).
30. T. Hayakawa, K. Horie, M. Aida, H. Kanaya, T. Kobayashi and Y. Murata, *Dental Mater.* **8**, 238 (1992).
31. D. F. Tylka and G. P. Stewart, *J. Prosthet. Dentistry* **72**, 121 (1994).
32. W. D. Callister, *Materials Science and Engineering: An Introduction*. John Wiley, New York (2000).
33. P. Dérand and T. Dérand, *Int. J. Prosthodont.* **13**, 131 (2000).
34. M. Fradeani and M. Redemagni, *Quintessence Int.* **33**, 503 (2002).
35. M. Hayashi, Y. Tsuchitani, Y. Kawamura, M. Miura, F. Takeshige and S. Ebisu, *Oper. Dentistry* **25**, 473 (2000).
36. M. Madani, F. C. S. Chu, A. V. McDonald and R. J. Smales, *J. Prosthet. Dentistry* **83**, 644 (2000).
37. M. Özcan, H. Alkumru and D. Gemalmaz, *Int. J. Prosthodont.* **14**, 335 (2001).
38. J. Tinschert, G. Natt, W. Mautsch, M. Augthun and H. Spiekermann, *Int. J. Prosthodont.* **14**, 231 (2001).
39. A. Della Bona, M. Borba, P. Benetti and D. Cecchetti, *Brazilian Oral Res.* **21**, 10 (2007).
40. N. M. Jedynakiewicz and N. Martin, *Biomaterials* **22**, 749 (2001).
41. R. Sun, N. Suansuwan, N. Kilpatrick and M. Swain, *J. Dentistry* **28**, 441 (2000).
42. L. F. Valandro, A. Della Bona, M. A. Bottino and M. P. Neisser, *J. Prosthet. Dentistry* **93**, 253 (2005).
43. M. Kern and V. P. Thompson, *J. Prosthet. Dentistry* **71**, 453 (1994).
44. M. Kern and V. P. Thompson, *J. Prosthet. Dentistry* **73**, 240 (1995).
45. E. P. Plueddemann, *Silane Coupling Agents*, 2nd edn. Plenum Press, New York (1991).
46. K. L. Mittal (Ed.), *Silanes and Other Coupling Agents*, Vol. 4. VSP/Brill, Leiden (2007).
47. R. L. Bowen, *J. Am. Dental Assoc.* **66**, 57 (1963).
48. K. Kamada, K. Yoshida and M. Atsuta, *J. Prosthet. Dentistry* **79**, 508 (1998).
49. H. Kato, H. Matsumura, T. Tanaka and M. Atsuta, *J. Prosthet. Dentistry* **75**, 163 (1996).
50. K. Sato, H. Matsumura and M. Atsuta, *J. Oral Rehabil.* **26**, 570 (1999).
51. J. H. Bailey, *J. Prosthet. Dentistry* **61**, 174 (1989).
52. M. R. Bouschlicher, J. W. Reinhardt and M. A. Vargas, *Am. J. Dentistry* **10**, 279 (1997).
53. T. Berry, N. Barghi and K. Chung, *J. Oral Rehabil.* **26**, 459 (1999).
54. A. M. Diaz-Arnold and S. A. Aquilino, *J. Prosthet. Dentistry* **62**, 257 (1989).
55. S. Eikenberg and J. Shurtleff, *Gen. Dentistry* **44**, 58 (1996).

56. R. C. Pratt, J. O. Burgess, R. S. Schwartz and J. H. Smith, *J. Prosthet. Dentistry* **62**, 11 (1989).
57. L. H. Lee (Ed.), *Adhesion Science and Technology.* Plenum Press, New York (1975).
58. J. P. Attal, V. Edard and M. Degrange, *J. Biomater. Dent.* **5**, 143 (1990).
59. M. Panighi and C. G'Sell, *J. Biomater. Dent.* **8**, 61 (1993).
60. W. A. Zisman, *Adv. Chem. Ser.* **43**, 1 (1964).
61. A. Versluis, D. Tantbirojn and W. H. Douglas, *J. Dental Res.* **76**, 1298 (1997).
62. K. J. Anusavice, P. H. Dehoff and C. W. Fairhurst, *J. Dental Res.* **59**, 608 (1980).
63. K. J. Anusavice, in: *Dental Ceramics: Proceedings of the First International Symposium on Ceramics*, J. W. McLean (Ed.), pp. 371–414. Quintessence Publishing Co., Chicago (1983).
64. S. Ban and K. J. Anusavice, *J. Dental Res.* **69**, 1791 (1990).
65. P. H. DeHoff, K. J. Anusavice and Z. Wang, *Dental Mater.* **11**, 126 (1995).
66. S. Sudsangiam and R. van Noort, *J. Adhesive Dentistry* **1**, 57 (1999).
67. R. van Noort, S. Noroozi, I. C. Howard and G. Cardew, *J. Dentistry* **17**, 61 (1989).
68. H. Sano, T. Shono, H. Sonoda, T. Takatsu, B. Ciucchi, R. M. Carvalho and D. Pashley, *Dental Mater.* **10**, 236 (1994).
69. R. M. Carvalho, J. S. Mendonca, S. L. Santiago, R. R. Silveira, F. C. Garcia, F. R. Tay and D. H. Pashley, *J. Dental Res.* **82**, 597 (2003).
70. D. H. Pashley, H. Sano, B. Ciucchi, M. Yoshiyama and R. M. Carvalho, *Dental Mater.* **11**, 117 (1995).
71. D. H. Pashley, R. M. Carvalho, H. Sano, M. Nakajima, M. Yoshiyama, Y. Shono, C. A. Fernandes and F. Tay, *J. Adhesive Dentistry* **1**, 299 (1999).
72. S. Phrukkanon, M. F. Burrow and M. J. Tyas, *Dental Mater.* **14**, 120 (1998).
73. Y. Shono, T. Ogawa, M. Terashita, R. M. Carvalho, E. L. Pashley and D. H. Pashley, *J. Dental Res.* **78**, 699 (1999).
74. A. A. El Zohairy, A. J. De Gee, M. M. Mohsen and A. J. Feilzer, *Dental Mater.* **19**, 575 (2003).
75. Z. Chen and J. J. Mecholsky, Jr., *J. Mater. Res.* **8**, 2362 (1993).
76. S. R. Armstrong, D. B. Boyer and J. C. Keller, *Dental Mater.* **14**, 44 (1998).
77. M. Nakajima, H. Sano, I. Urabe, J. Tagami and D. H. Pashley, *Oper. Dentistry* **25**, 2 (2000).
78. S. Phrukkanon, M. F. Burrow and M. J. Tyas, *J. Dentistry* **27**, 265 (1999).
79. H. Sano, T. Yoshikawa, P. N. Pereira, N. Kanemura, M. Morigami, J. Tagami and D. H. Pashley, *J. Dental Res.* **78**, 906 (1999).
80. M. Tanumiharja, M. F. Burrow and M. J. Tyas, *Dental Mater.* **16**, 180 (2000).
81. T. Yoshikawa, H. Sano, M. F. Burrow, J. Tagami and D. H. Pashley, *J. Dental Res.* **78**, 898 (1999).
82. R. van Noort, G. Cardew, I. C. Howard and S. Noroozi, *J. Dental Res.* **70**, 889 (1991).
83. R. W. Hertzberg, *Deformation and Fracture Mechanics of Engineering Materials.* John Wiley, New York (1996).

Interpenetrating Polymer Networks (IPNs) in Dental Polymers and Composites

Pekka K. Vallittu *

Department of Prosthetic Dentistry and Biomaterials Science, Institute of Dentistry, Lemminkäisenkatu 2, University of Turku, FI-20520 Turku, Finland

Abstract

An interpenetrating polymer network (IPN) is a material containing two polymers, each in network form. In biomaterials used in dentistry, the IPN-like nanostructures are used in denture base polymers, denture teeth and fibre-reinforced composites. IPN structures provide the specific and desired properties for the resin system prior to and after polymerization. At adhesive interfaces, IPN polymers and composites provide good interfacial adhesion for adhering and veneering resin composites based on the so-called secondary-IPN bonding formation due to swelling of the IPN nanostructure. Good interfacial adhesion is a requirement for the success of modern adhesive dentistry.

Keywords

Interpenetrating polymer network, IPN, composites, biomaterials, fibre-reinforced composites

1. Introduction

Modern dentistry utilizes polymers and composites in dental treatments. The use of natural rubber and thereafter synthetic polymers as denture base polymers started in the 1860s. The introduction of a denture base polymer of poly(methyl methacrylate) (PMMA) occurred in the late 1930s [1]. Since then, the thermoplastic PMMA denture base polymer has been multiphasic, i.e., it has been made by mixing methylmethacrylate monomer liquid and PMMA beads. In free radical polymerization, the highly viscous resin dough formed the multiphase denture base polymer. The dough-like consistency enabled packing of the resin into the denture moulds and reduced polymerisation contraction of the resin. Since the introduction of cross-linking thermoset monomers in dentistry by Bowen [2], cross-linking dimethacrylate monomers became available also for monomer liquids of denture base resins and, thus, in multiphase denture base polymers. This can be considered the start of the use of IPN-like structures of various kinds in dentistry.

* To whom correspondence should be addressed. E-mail: pekka.vallittu@utu.fi

Adhesion Aspects in Dentistry
© Koninklijke Brill NV, Leiden, 2009

Table 1.
Definitions of mixed polymers [3]

Name of mixture	Description
Polymer blend	One or more polymers are mixed together without a resulting strong chemical bonding between the phases, and in such a way that the phases be separated from each other
Graft polymer	Strong chemical bonding between some portion of polymer I and the end of polymer II
Copolymer	Strong chemical bonding of the end of polymer to the end of polymer II
Interpenetrating polymer network (IPN)	Polymers I and II are at least partially interlaced at molecular level but are not covalently bonded to each other, and cannot be separated unless chemical bonds are broken

IPNs were used for the first time in 1914 by Alysworth, who combined phenol-formaldehyde compositions with natural rubber and sulphur to make the first rubber-toughened plastic. By definition, an IPN is a combination of two or more polymers in network form that are synthesized in juxtaposition [3]. IPNs do not interpenetrate by chemical reactions on a molecular scale, but are composed of finely divided phases of 5–10 nm. IPNs differ from polymer blends which are less homogeneous in structure. They differ from copolymers which are based on chemical reactions of monomers and polymer backbones (Table 1). The rationale for using IPNs instead of homopolymers and copolymers is in the improved handling properties, toughness and mechanical interlocking at nanometer level of resin adhesives to IPN-like polymers and composites. The interlocking of resin adhesives to polymers and composites plays an important role in the clinical success of dental treatments carried out with composite resin restorations. The bonding of resin adhesives to a composite (particulate filler or fibre-reinforced composite) transfers stresses from the restoration to the teeth. Without adequate interlocking of materials, the loads and stresses debond the restoration and the treatment fails.

Currently, the IPN-like structures can be found in nanostructures in denture base polymers, denture teeth, fibre-reinforced composites (FRCs), and very recently, in the restorative composite resins [4–9] which are described and discussed in this review. Structurally, several adhesive interfaces between natural and synthetic biomaterials and adhesive resins by means of primers or coupling agents can also be considered IPNs. Examples of these are the dentine bonding hybrid layer and the silane coupling agent-promoted adhesive interphases between metal and ceramics and adhesive resins.

2. IPNs

There are several kinds of IPNs which differ in terms of structure. These include:

– sequential IPN

– gradient IPN
– thermoplastic IPN
– semi-IPN
– simultaneous IPN.

The dental IPN structures are semi-IPNs in which one or more polymers are cross-linked, and one or more polymers are linear or branched. More precisely, the IPNs belong to the group of non-covalent semi-IPNs where only one of the polymer systems is cross-linked, in contrast to non-covalent full IPNs in which the two separate polymers are independently cross-linked. Dimethacrylate monomers or multifunctional monomers and dendrimers form the cross-linked part of the semi-IPN, while the monofunctional MMA forms the non-cross-linked part of the semi-IPN system. In dental semi-IPNs, due to the fabrication processes of dental materials and devices, the MMA is first polymerized and then swelled and dissolved by the monomers of the cross-linker system, or with a separate solvent. In polymerization of the cross-linking monomers in the presence of swelled and dissolved polymer chains of the PMMA, a semi-IPN structure is formed. The components of current dental semi-IPNs are, therefore, not cross-linked from monomers as in the IPNs according to the definition of the IUPAC (International Union of Pure and Applied Chemistry). However, the dental IPNs fulfill the structural requirements of the IUPAC for the IPN, i.e., the IPN swells but does not dissolve into solvents, the two polymers are not phase separated, and the polymers are interlaced on a molecular level.

In dental IPNs, solid PMMA is often used in powder form in denture base resins and in porous polymer form in preimpregnated glass-fibre reinforcements [10]. Depending on the capability of dimethacrylate monomers like bisphenol-A-diglycidyldimethacrylate (bisGMA) or triethyleneglycol dimethacrylate (TEGDMA), or ethyleneglycol dimethacrylate (EGDMA) to swell and dissolve the PMMA, the contact wetting time of the liquid dimetharylate monomers, and the temperature, and the penetration depth of the cross-linking monomers into the PMMA, the semi-IPN varies. After polymerization, two or three of the following phases occur: cross-linked matrix, semi-IPN phase and linear polymer phase. Thus, the whole polymer is not necessarily a semi-IPN, but there are nano or microstructures of semi-IPNs in the polymer or composites.

Although the IUPAC Comission on Macromolecular Nomenclature has not given a statement on the nomenclature of IPNs, the above-mentioned semi-IPN made of bis-GMA and PMMA can be written as [3]

net-poly(methyl methacrylate)–*inter-net*-poly(bis-glycidyl-A-dimethacrylate),

which is a semi-IPN made of PMMA beads and bis-GMA monomer. If the cross-linking monomer system is diluted by another monomer, like TEGDMA, in order

to achieve a copolymer for the cross-linked polymer, the semi-IPN is written as:

> *net*-poly(methyl methacrylate)–*inter-net*-copoly(bis-glycidyl-A-dimethacrylate)-triethyleneglycol dimethacrylate.

For IPN formation, certain requirements have to be fulfilled to differentiate the IPN from polymer blends. If the IPN is made of photopolymerizing dimethcarcylate monomers and monofunctional methacrylates, the polymerization could occur simultaneously, but without the formation of copolymer of the dimethacrylate and monomethahacrylate. Because of the generally known low reactivity of monofunctional methacrylates in photoinduced free radical polymerization, the monofunctional methacrylates first need to be prepolymerized by other means. By mixing polymerized monofunctional methacrylates and cross-linking dimethacrylates, a polymer blend is obviously formed, unless the cross-linking dimethacrylate monomers, or other solvents, swell and dissolve the monofunctional polymer, which results in molecular-level interlacing and IPN formation.

For interlacing, the solubility parameter of the solvent monomer should match the solubility parameter of the polymer phase. It was known hundreds of years ago by Paracelsus that *similia similibus solvuntur*, *like dissolves like*. Qualitatively, 'like' may be defined variously in terms of similar chemical groups or similar polarities in the molecular structure. Quantitatively, the solubility of one component in another is governed by the equation of free energy of mixing, and, as a result, there will be an increase in the entropy [11]. The solubility parameter of a polymer can be determined by swelling experiments or by measuring the intrinsic viscosity of the polymer in the solvents. Values for the solubility parameter can be calculated; the unit of solubility parameter (δ) is $(\text{cal/cm}^3)^{1/2}$. The solubility parameter for PMMA is 9.45 $(\text{cal/cm}^3)^{1/2}$, for MMA 8.8 $(\text{cal/cm}^3)^{1/2}$, for solvent tetrahydrofuran (THF): 9.1 $(\text{cal/cm}^3)^{1/2}$, and for solvent acetone 9.9 $(\text{cal/cm}^3)^{1/2}$. In comparison to these good solvents for PMMA, the solubility parameters of poor solvents for PMMA are water ($\delta = 23.4$ $(\text{cal/cm}^3)^{1/2}$) and methanol ($\delta = 14.5$ $(\text{cal/cm}^3)^{1/2}$).

A polymer dissolves in two stages. First, solvent molecules diffuse into the polymer, swelling it to a gel state. Then the gel gradually disintegrates and the molecules diffuse into the solvent-rich regions. Linear amorphous polymers can be fully dissolved whereas cross-linked polymers may reach the gel state but they do not dissolve. The concentration of the final solution depends on the relative proportions of polymer and solvent. The molecular size of the solvent needs to allow diffusion into the interchain spacing of the polymer, which in typical engineering polymers varies between 5 and 10 Å.

3. Denture Base Polymers and IPN Structure

Polymers used in baseplates of complete dentures and removable partial dentures, as well as in extension bases of metal framework removable partial dentures, are made of denture base polymers. Denture base polymers are mixed from PMMA

powder (typically M_w: 200 000, particle size: 50 μm) and methyl methacrylate monomer (MMA) liquid. The monomer system contains on average 10 wt% of cross-linking dimethacrylate monomers like EGDMA. Before polymerization, the MMA dissolves the PMMA beads only from the surface, or entire beads. The degree of dissolution or swelling depends on the contact wetting time with MMA in its liquid form, i.e., as a solvent capable of dissolving the PMMA beads. In heat-cured denture base resins, the dough time of 30–60 min allows PMMA beads to be almost fully dissolved by the monomers; whereas in autopolymerizing denture base resins, the polymerization reaction is initiated within a few minutes from mixing the powder and liquid, and putting the initiator and activator together. By rapid solidification of the monomers of the autopolymerizing resins, the penetration depth is limited to a few micrometres. However, in both cases, the monomer system containing the cross-linking agent partly or fully dissolves the linear PMMA beads and forms a semi-IPN structure once it is polymerized.

The semi-IPN structure of denture base polymers increases their creep resistance [12, 13]. In comparison with heat-cured and autopolymerized denture base polymers, the heat-cured polymers have higher mechanical strength and creep resistance than the autopolymerized polymers. The average critical strain values, which correlate with the ultimate failure values, were increased by adding cross-linking monomers to the denture base polymer. This demonstrates the effect of the semi-IPN structure in the interphase of the PMMA beads and the cross-linked matrix on improving mechanical strength. On the other hand, semi-IPN in the denture base polymer does not influence water sorption but increases the solvent resistance [14].

In repairs of fractured pieces of acrylic polymers of linear or semi-IPN type, the adhesion of new resin is also based on dissolving the pieces of denture base polymer by monomer systems of the repair acrylic resin. It has been shown that the wetting time of the acrylic surface with the repair resin is of importance for achieving the swelling and dissolving of the surface of the denture base resin [15]. A three-minute contact wetting time of the denture base polymer of semi-IPN type with the MMA-EGDMA monomer system results in durable adhesion of the repair resin to the pieces of denture base polymer. The bonding mechanism is called *secondary-IPN formation* to differentiate it from the semi-IPN structure of the actual substrate material. Requirements for the secondary-IPN formation are swelling of the substrate, and interlacing of the polymer chains of the repair resin and the old resin together. In this context, the MMA fulfills the requirements for a good solvent for PMMA.

There are two kinds of denture base polymers classified according to the initiation of the polymerization reaction. These are heat-cured and autopolymerized denture base polymers. They differ in terms of the homogeneity of the semi-IPN structure and the quantity of residual monomers in the polymer. Heat-cured denture base polymers are more homogeneous due to the longer dough time of the powder–liquid mixture before polymerization than of the autopolymerized polymers. The PMMA beads in the denture base polymer are predominantly attached to the matrix by a semi-IPN layer. However, at higher temperatures (above 70°C) in the heat-

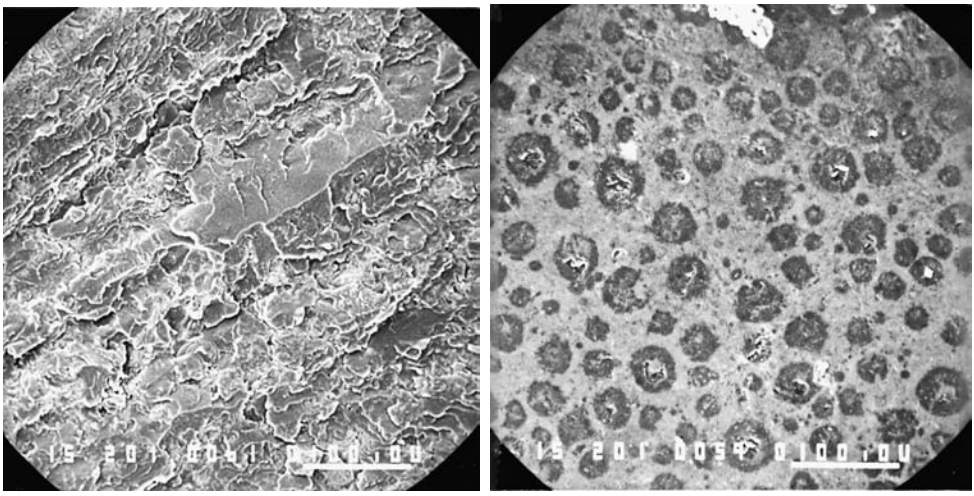
cured denture base resins, the PMMA beads are also bonded to the matrix from MMA by chemical means involving unsaturated double bonds in the PMMA backbones after the termination stage of the polymerization reaction in manufacturing the beads. The quantity of residual monomers in the denture base polymer is around 0.2 wt% in heat-cured polymers and ca. 4 wt% in autopolymerized polymers [15]. Three factors, the homogeneity of the semi-IPN structure, the quantity of residual monomers in the denture base polymer and the polymerisation temperature have been shown to affect the formation of the secondary-IPN between the repair acrylic resin and the denture base polymer. Autopolymerized denture base polymers allow monomers of the repair acrylic resin to penetrate more deeply, thus forming a thicker secondary-IPN layer between the repair resin and the denture base polymer.

During swelling of the polymer surface, the diffusion of monomers takes place in two directions: the monomers of the repair resin to the polymer and *vice versa* [3]. The rate of diffusion of small molecules like MMA is faster than that of PMMA. If the polymer is glassy, like PMMA at room temperature or at mouth temperature, the MMA lowers the glass transition temperature (T_g) of the PMMA by a plasticizing action. The rate of diffusion is, therefore, related to the T_g of the polymer. A linear relationship exists between the time and rate of diffusion at temperatures below the T_g of a polymer [11].

The T_g value for heat-cured PMMA powder varies from 117°C to 122°C, whereas the T_g of the matrix between the PMMA beads varies from 97°C to 100°C [17]. The T_g of the autopolymerized PMMA is substantially lower, varying from 67°C to 78°C. Therefore, the swollen secondary-IPN layer is thicker in the autopolymerized denture base polymers than in the heat-cured polymers. This enables easier secondary-IPN bonding of repair acrylic resin to the denture base polymer in the case of autopolymerized denture base polymer than with heat-cured polymer. On the other hand, it needs to be emphasized that denture base polymers, regardless of whether they are heat-cured or autopolymerized, provide a good adhesive substrate for repair acrylic resins, which is not the case with cross-linked polymers and composites. Examples of cross-linked composites are composite dental fillings and prefabricated fibre-reinforced composite root-canal posts which do not allow secondary-IPN formation and, thus, adhere with difficulty to adhesive resins.

4. Denture Teeth and IPN Structure

The composition of acrylic resin polymer teeth is essentially poly(methyl methacrylate) beads and colour pigments in a cross-linked polymer matrix. There is a semi-IPN layer between the PMMA bead and the cross-linked matrix. The cross-linked polymer matrix of a good quality tooth is usually not evenly distributed in the tooth structure. For example, the gingival ridge-lap area may not be as highly cross-linked as the incisal or occlusal area of the tooth. The less cross-linked structure in the area of the ridge-lap facilitates better bonding of the polymer tooth to the denture base polymer by secondary-IPN formation. Moreover, the cores of the PMMA beads,



(a) (b)

Figure 1. SEM micrographs of fractured bonding surfaces of polymeric denture teeth that have been bonded to (a) a heat-cured denture base polymer and (b) to an autopolymerized denture base polymer. Note how the intact linear polymer phase in the centre of the PMMA bead into the denture base polymer has formed the secondary-IPN structure (Bar = 100 μm) [9].

which have not been affected by the monomers of the matrix, i.e., have not formed a semi-IPN structure, are appropriate sites for the denture base resin to bond. This was clearly demonstrated by a scanning electron microscopy study which showed good bonding of the denture base resin to the linear polymer cores of the PMMA beads of denture teeth (Fig. 1) [9].

The bonding of denture base resin to the denture teeth occurs *via* secondary-IPN formation. In the case of denture base polymer and tooth bonding, the polymerization activation temperature plays a significant role because of the relationship between the temperature and the rate of diffusion. It is known that heat-cured denture base polymers bond better to the denture teeth than autopolymerizing denture base polymers (Fig. 1). The activation of intiators of heat-cured resins occurs at temperatures above 75°C up to 100°C when the bezoyl and phenyl radicals are formed to initiate polymerization of the resin. On the other hand, activation of the radical formation from initiator benzoyl peroxide in autopolymerized denture base resins occurs at lower temperatures with the help of amine activators. Typically, the polymerization temperature is around 45°C.

It has been shown that the polymerization activation temperature affects the bonding of the denture base polymer to denture teeth. At higher temperatures, regardless of the type of denture base polymer (heat-cured or autopolymerized), the bond strengths are increased. This was shown to be due to the deeper penetration of the monomers of the denture base polymers into the denture teeth, showing thicker secondary-IPN layer formation, which resulted in the higher bond strength values.

The critical polymerization temperature to avoid adhesional failures between the denture base polymer and denture teeth is 55°C [9].

5. Fibre-Reinforced Composites and IPN Sturucture

One new group of non-metallic dental biomaterials is fibre-reinforced composites (FRCs) which were first tested as a reinforcement of denture bases in the early 1960s [18]. In principle, an FRC could even then have offered already a durable and tough tooth-coloured material for several applications by combining it with Bowen's resin. Because there were some problems in combining the resin systems with reinforcing fibres and there were difficulties in handling the FRC clinically and technically, the material was not made available until recently. Development of the FRCs with new types of resins systems and an understanding of the design principles behind the devices have led to the use of FRCs in a variety of disciplines and applications: in removable prosthodontics, restorative dentistry, periodontology, orthodontics, and in repairs of fractured porcelain veneers [19–29]. An FRC is a material combination of polymer matrix and reinforcing fibres. The fibres of the composite reinforce the phases when the load is applied to the composite. Load is transferred to be carried by the fibres. The reinforcing fibres can be continuous unidirectional (rovings), continuous bidirectional (weaves), continuous random oriented (mat), or short random-oriented fibres.

Of the many types of fibres, the clinically most suitable have been proved to be glass fibres which can be silanized and, thus, adhere well to the resin matrix of the FRC [30–32]. Glass fibres vary according to their composition, the most commonly used fibre being E-glass (electrical glass) which offers a chemically stable and durable glass in the pH range 4–11 [33].

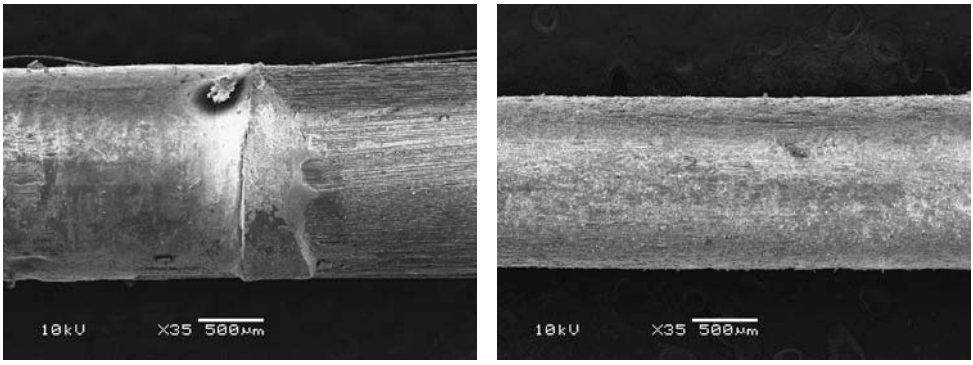
In dental appliances of relatively small size, the quality of the load-bearing FRC substructure is important. For example, an FRC-reinforced root-canal–post system consists of dentine, composite resin cement, a core built-up composite resin and, as a load-bearing material, there is the FRC root-canal post. All these phases need to have adequate strength, and the phases need to adhere well to each other. By increasing the fibre quantity in the resin matrix, the strength of the FRC and the flexural modulus are increased. An important parameter responsible for the strength of the FRC is impregnation of the fibres with resin. Reinforcing fibres are difficult to impregnate with resin systems of high viscosity [34–36].

Such highly viscous resin systems are especially those made from a mixture of polymer powder and monomer liquid which are used in denture bases, provisionally fixed partial dentures, and removable orthodontic appliances, or those made of light-curing resins and particulate fillers. The resin impregnation of fibres by the manufacturers is recommended to ensure complete impregnation of the fibres by the resin in mechanically demanding dental applications. The complete impregnation of fibres by the resin allows the resin to come into contact with every fibre. If complete impregnation is not achieved due to the high viscosity or polymerisation

shrinkage of the resin, the mechanical properties of FRC do not reach the optimal values as calculated by the laws of mixture.

Two types of resins, the cross-linked (thermoset) or linear (thermoplastic) polymer matrix, can be used in FRCs. The cross-linked matrix is formed from multifunctional or dimethacrylate resins, whereas monofunctional methacrylates form the linear (non-cross-linked) polymer matrix. There are also impregnation methods based on using a combination of thermoset and thermoplastic types of resins. The polymer matrix is multiphase in nature, and it is a semi-IPN having the cross-linked polymer and the linear polymer mixed together. The semi-IPN forms in the polymerization of the dimethacrylate monomers with swelled linear polymer poly(methyl methacrylate) (PMMA). The modulus of elasticity of the cross-linked polymer matrix FRC is higher than that of the semi-IPN or linear polymer matrix FRC [37–39]. On the other hand, linear and semi-IPN polymer matrices provide greater toughness than FRCs made of cross-linked thermosets. The semi-IPN polymer matrix of FRC provides benefits over the cross-linked dimethacrylate or epoxy-type of polymer matrices in handling properties and in the bonding of dental laboratory made restorations and root-canal posts to resin-luting cements and veneering composites [40]. Figure 2 shows the bonding of composite resin-luting cement to root-canal posts with a cross-linked or semi-IPN resin matrix.

The adhesion of particulate filler composite (PFC) resin (resin-luting cement, veneering composite) plays an important role in the load transfer from the surface of the device to the FRC framework and tooth. FRC as a bonding substrate contains different types of materials, from polymers to inorganic glass-fibre fillers and even particulate fillers. The internal adhesion of the FRC, influencing its cohesional strength, is based on the bonding of the fibres to the matrix polymer. In this respect, the most suitable fibres are of the OH-group containing glass and silica fibres which can be silanated to produce the adequate adhesion to the polymer matrix [30–32].



(a) (b)

Figure 2. SEM micrographs of the surface of an FRC root-canal post after being pushed out from the composite resin-luting cement. Post with (a) semi-IPN polymer matrix and (b) cross-linked matrix. Note good bonding of cement to semi-IPN post by secondary-IPN bonding mechanism and poor bonding to cross-linked post [40].

Less suitable fibres are ultra-high molecular weight polyethylene (UHMWP) fibres which have been proved to be difficult to adhere to resins even though the fibre surface has been activated with, e.g., various types of high energy treatments [41].

In bonding new resin to FRC, exposed fibres and polymer matrix are the substrates for adhesion. If the fibres of the FRC are exposed on the bonding surface, the adhesional properties of the fibres themselves play a role in adhering the adhesive resin and composite resin-luting cement to the FRC: glass fibres can be adhered to PFC (particulate filler composite) by silanation. Due to the cross-linked nature of the polymer matrix of most dental FRC materials, there are two possibilities to obtain adhesion of the PFC to the FRC. These are mechanical interlocking, and adhesion based on the ongoing polymerisation of the resin matrix of the FRC. If the FRC contains non-cross-linked polymer phases, i.e., they are made of thermoplastics or semi-IPN polymers, the adhesion can also be achieved *via* secondary-IPN formation by diffusion of the monomers of the new resin or resin composite into the non-cross-linked polymer matrix (Table 2) [6, 42]. This requires that the solubility parameter of the linear polymer is close to that of the monomer system of the PFR. In polymerisation of the resin, an adhesion bond based on a secondary-IPN structure is formed.

The adhesion of PFC to directly made (in patient's mouth) or chair-side-made FRC differs from that of FRC made indirectly in the dental laboratory. It is known that in the polymerisation of resins and resin-based composites or FRCs in air, a non-polymerised surface layer, the so-called oxygen inhibited layer, is formed

Table 2.
Summary of the bonding mechanisms for composite resin-luting cements to the FRC root-canal post

Type of post	Type of fibre	Type of polymer matrix	Bonding mechanism
Prefabricated	Carbon/graphite	Cross-linked	– Mechanical retention
Prefabricated	Glass or quartz	Cross-linked	– Mechanical retention – Silane-promoted adhesion
Individually formed (laboratory made)	UHMWP	Cross-linked	– Mechanical retention
Individually formed (laboratory made)	Glass or quartz	Cross-linked	– Mechanical retention – Silane-promoted adhesion
Individually formed (laboratory made)	Glass	Semi-IPN	– Mechanical retention – Silane-promoted adhesion – Secondary IPN adhesion
Individually formed (chair-side made)	UHMWP, Glass or quartz	Cross-linked Semi-IPN	– Mechanical retention – Silane-promoted adhesion – Secondary-IPN adhesion – Free radical polymerisation based adhesion

on the surface [43]. PFCs can adhere to this layer by free radical polymerization of the PFR and form a durable bond. However, with indirectly made restorations, old restorations and prefabricated FRC root-canal posts, a durable bond between new resins and the polymer matrices of the composites can be achieved by the introduction of a linear or semi-IPN polymer matrix into the polymer matrix of the composite [44, 45].

6. Conclusions

Interpenetrating polymer network (IPN) structures of two or more polymers are utilized in dental polymers and composites, although the processing of the IPNs may vary from that generally used in polymer chemistry. Interlaced polymers at the molecular level of dental IPNs provide increased toughness for the polymer and allow the bonding of additional resins to the IPN-containing polymer *via* a secondary-IPN mechanism, i.e., interlacing the polymeric materials together.

References

1. W. T. Sweeney and H. J. Caul, *J. Amer. Dental Assoc.* **27**, 1446 (1940).
2. R. L. Bowen, *J. Amer. Dental Assoc*. **66**, 57 (1963).
3. L. H. Sperling, in: *Interpenetrating Polymer Networks*, D. Klemper, L. H. Sperling and L. A. Utracki (Eds), pp. 3–11. American Chemical Society, Washington, DC (1994).
4. S. Garoushi, P. K. Vallittu, D. C. Watts and L. V. J. Lassila, *Dental Mater.* **24**, 211 (2008).
5. R. G. Jagger and R. Huggett, *Dental Mater.* **6**, 276 (1990).
6. T. Lastumäki, L. V. J. Lassila and P. K. Vallittu, *J. Mater. Sci. Mater. Med.* **14**, 803 (2003).
7. P. K. Vallittu, I. Kangasniemi and A. Yli-Urpo, US Patent No. 6,197,410 B1 (2001).
8. I. E. Ruyter and I. J. Sjövik, *Acta Odontol. Scand.* **39**, 133 (1981).
9. P. K. Vallittu, *Acta Odontol. Scand.* **53**, 99 (1995).
10. P. K. Vallittu, US Patent No. 08/809,488 (1998).
11. L. H. Sperling, *Introduction to the Physical Polymer Science*, pp. 97–119. Wiley, New York, NY (1986).
12. H. Öysaed and I. E. Ruyter, *J. Biomed. Mater. Res.* **23**, 719 (1989).
13. H. Öysaed and I. E. Ruyter, *J. Mater. Sci.* **22**, 3373 (1987).
14. R. G. Jagger and R. Huggett, *Dental Mater.* **6**, 276 (1990).
15. P. K. Vallittu, V. P. Lassila and R. Lappalainen, *J. Prosthet. Dentistry* **72**, 639 (1994).
16. P. K. Vallittu, I. E. Ruyter and S. Buykuilmaz, *Eur. J. Oral Sci.* **106**, 588 (1998).
17. I. E. Ruyter and S. A. Svendsen, *J. Prosthet. Dentistry* **43**, 95 (1980).
18. D. C. Smith, *J. Prosthet. Dentistry* **12**, 1066 (1962).
19. P. K. Vallittu, *Quintessence Int.* **28**, 39 (1997).
20. Y. Y. Cheng and T. W. Chow, *J. Prosthodont.* **8**, 268 (1999).
21. N. H. Ladizesky, *Clin. Mater.* **6**, 181 (1990).
22. N. H. Ladizesky, T. W. Chow and I. M. Ward, *Clin. Mater.* **6**, 209 (1990).
23. N. H. Ladizesky, C. F. Ho and T. W. Chow, *J. Prosthet. Dentistry* **68**, 934 (1992).
24. N. H. Ladizesky, T. W. Chow and Y. Y. Cheng, *Int. J. Posthodont.* **7**, 307 (1994).
25. H. K. Körber and S. Körber, *Quintess. Zahntechik* **24**, 43 (1998).
26. C. Kolbeck, M. Rosentritt, M. Behr, R. Lang and G. Handel, *J. Prosthodont.* **11**, 248 (2002).

27. T. N. Göhring, P. R. Schmidlin and F. Lutzt, *Am. J. Dentistry* **15**, 35 (2002).
28. M. A. Freilich, A. C. Karmarker, C. J. Burstone and A. J. Goldberg, *J. Prosthet. Dentistry* **80**, 311 (1998).
29. M. A. Freilich, J. C. Meiers, J. P. Duncan, K. A. Eckrote and A. J. Goldberg, *J. Amer. Dental Assoc.* **133**, 524 (2002).
30. M. R. Rosen, *J. Coatings Technol.* **50**, 70 (1978).
31. J. P. Matinlinna, S. Areva, L. V. J. Lassila and P. K. Vallittu, *Surface Interface Anal.* **36**, 1314 (2004).
32. P. K. Vallittu, *J. Oral Rehabil.* **20**, 533 (1993).
33. A. Norström, H. Watson, B. Engström and J. Rosenholm, *Colloids Surfaces* **194**, 143 (2001).
34. P. K. Vallittu, *J. Oral Rehabil.* **22**, 257 (1995).
35. P. K. Vallittu, *Appl. Composite Mater.* **2**, 51 (1995).
36. P. K. Vallittu, *J. Oral Rehabil.* **25**, 100 (1998).
37. L. V. J. Lassila, J. Tanner, A.-M. Le Bell, K. Narva and P. K. Vallittu, *Dental Mater.* **20**, 29 (2004).
38. L. V. J. Lassila, T. Nohrström and P. K. Vallittu, *Biomaterials* **23**, 2221 (2002).
39. S. Bouillaguet, A. Schutt, P. Alander, P. K. Vallittu, P. Schwaller, G. Buerki, J. Michler, M. Cattani-Lorente and I. Krejci, *J. Biomed. Mater. Res. B (Appl. Biomater.)* **76**, 98 (2006).
40. A. M. Le Bell, J. Tanner, L. V. J. Lassila, I. Kangasniemi and P. K. Vallittu, *J. Adhesive Dentistry* **6**, 319 (2004).
41. K. Takagi, H. Fujimatsu, H. Usami and S. Ogasawara, *J. Adhesion Sci. Technol.* **9**, 869 (1996).
42. T. T. Kallio, T. M. Lastumäki and P. K. Vallittu, *Dental Mater.* **17**, 80 (2001).
43. P. K. Vallittu, *J. Mater. Sci. Mater. Med.* **8**, 489 (1997).
44. M. S. Keski-Nikkola, P. M. Alander, L. V. J. Lassila and P. K. Vallittu, *J. Oral Rehabil.* **31**, 1178 (2004).
45. M. S. Keski-Nikkola, L. V. J. Lassila and P. K. Vallittu, *Eur. J. Prosthodont. Restorative Dentistry* **12**, 80 (2004).

Resin Bonding to Oxide Ceramics for Dental Restorations

Matthias Kern *

Department of Prosthodontics, Propaedeutics and Dental Materials, School of Dentistry, Christian-Albrechts University, Arnold-Heller-Str. 16, D-24105 Kiel, Germany

Abstract

Bonding to silica-based dental ceramics using etching techniques and silanization is well established, but for bonding of dental oxide ceramics with little or no silica no particular method is generally accepted. Therefore, the purpose of this review is to summarize the current knowledge on bonding to dental oxide ceramics. Approved bonding methods to dental oxide ceramics require first cleaning, roughening and chemical activation through air-abrasion by pure alumina or silica-coated alumina particles. Secondly, chemical coupling agents such as phosphate monomers or silanes are used depending on the surface composition after air-abrasion. Although a large number of laboratory bonding studies on dental oxide ceramics exist, clinical long-term studies on bonded oxide ceramic restorations without mechanical retention are still needed to prove whether laboratory bonding methods provide long-term durable adhesion under clinical conditions.

Keywords

Adhesion, alumina, ceramic primer, dental oxide ceramics, silica coating, zirconia

1. Introduction

In dentistry silica-based ceramics have been used for dental restorations reinforced with metal substructure and luted to the teeth with conventional cements for decades [1–4]. Using adhesive luting techniques silica-based ceramics have also been used for all-ceramic restorations without metal substructure since the 1970s. Due to high content of silica in these ceramics, organosilanes have been successfully used to promote the bond between the silica ceramic and the luting resin usually after roughening the ceramic surface by hydrofluoric acid etching or airborne particle abrasion [5].

Only at the beginning of the 1990s oxide ceramics which contain only little or no silica were introduced into restorative dentistry. By definition oxide ceramics contain less than 15 wt% silica and only a small or no glass phase [6]. Dental oxide ceramics were first glass-infiltrated or densely sintered alumina ceramics, followed by zirconia reinforced glass-infiltrated alumina ceramic, and since the turn of the century numerous densely sintered zirconia ceramic systems have been introduced

* Tel.: +49 431 597 2874; Fax: +49 431 597 2860; e-mail: mkern@proth.uni-kiel.de

Adhesion Aspects in Dentistry
© Koninklijke Brill NV, Leiden, 2009

Table 1.
Typical composition of popular dental oxide ceramics in wt%

Oxides	Product names					
	Glass-infiltrated oxide ceramics			Glass-free oxide ceramics		
	In-Ceram Alumina Classic[1]	In-Ceram Zirconia Classic[1]	In-Ceram Spinell Classic[1]	In-Ceram 2000 AL[1]	DCS Zirkon[3]	Cercon[6]
						e.max Zir-CAD[5]
					Cerapost[4]	In-Ceram 2000 YZ[1]
				Procera Alumina[2]		Lava[7]
					Cosmopost[5]	Procera Zirconia[2]
						Zerion[8]
SiO_2	4–5	3–4	3–4	–	–	–
Al_2O_3	82	57	61	>99.9	–	–
ZrO_2	–	26	–	–	95–96	95–97
MgO	–	–	23	–	–	–
Y_2O_3	–	–	–	–	4–5	3–5
La_2O_3	12	7	6	–	–	–
Others	1–2	6–7	5–6	<0.1	<0.005	<3

Data provided by the manufacturers. [1]Vita Zahnfabrik, Bad Säckingen, Germany; [2]Noble Biocare, Goteborg, Sweden; [3]DCS Dental, Allschwil, Switzerland; [4]Brasseler, Lemgo, Germany; [5]Ivoclar Vivadent, Schaan, Liechtenstein; [6]DeguDent, Hanau, Germany; [7]3M Espe, Seefeld, Germany; [8]Etkon, Gräfelfing near Munich, Germany.

[7, 8]. Current dental oxide ceramics consist mostly of alumina, magnesia, zirconia and yttria (Table 1). Because of their high strength, oxide ceramics are used as frameworks and replacing alloys not only in crowns but also in fixed dental prostheses. In addition, because of their strength, adhesive luting techniques are not required for oxide ceramic dental restorations when the abutment teeth provide adequate mechanical retention for conventional cements.

Nevertheless, adhesive luting techniques for oxide ceramics can provide significant clinical advantages over conventional cementation of dental restorations. A adhesive luting can provide gap-free restoration margins, minimizing microleakage and thereby reducing the risk of secondary caries [9]. In addition, esthetics might be improved by using tooth colored transparent resin luting agents as compared to opaque conventional cements. So tooth colored restorative materials, e.g., ceramics or composite resins, can be bonded to the teeth without visible cementation line [10]. Most importantly, adhesive luting does not require retentive tooth preparation, which often causes invasive removal of sound tooth structure. So adhesive bonding of oxide ceramics allowed the introduction of new non-invasive

treatment modalities for tooth replacement by resin bonding all-ceramic fixed partial dental prostheses to lingual surfaces of teeth adjacent to an edentulous area [11, 12]. Furthermore, adhesive bonding might provide stabilization of the remaining tooth structure when oxide ceramics are used for post and core restorations of structurally severely compromised teeth after endodontic treatment [13, 14]. Adhesive luting can strengthen the restored tooth through a strong bond between the oxide ceramic restoration and the remaining tooth structure [15].

However, bonding methods used for conventional silica-based dental ceramics are not suitable for oxide dental ceramics [16]. Etching oxide ceramics with hydrofluoric acid does not create adequate surface roughness for resin bonding [17, 18] (Figs 1–4). In addition, the most often used coupling agent for silica-based ceramics, 3-methacryloxypropyltrimethoxysilane (MPS), might help in surface-wetting on oxide ceramics [17], but it does not promote adequate bonding to alumina or zirconia ceramics [19–22]. Therefore, alternative bonding techniques are needed to be developed for dental oxide ceramics. Microscopically, densely sintered alumina and zirconia ceramics offer very similar bonding substrates which are completely free of a glassy phase with grains sintered into a dense and homogeneous structure. Chemically, their surfaces consist mainly of either aluminum oxide or zirconium dioxide to which specific adhesive monomers seem to bond equally well [20, 21, 23, 24].

Ceramic bonding surfaces conditioned in the dental laboratory should not be compromised by clinical try-in of the dental restorations with unavoidable contamination caused by saliva and/or silicone disclosing media. Disclosing media are applied to check the internal fit of dental restorations, by revealing the thickness of the luting gap and internal contacts between the restoration and the prepared tooth,

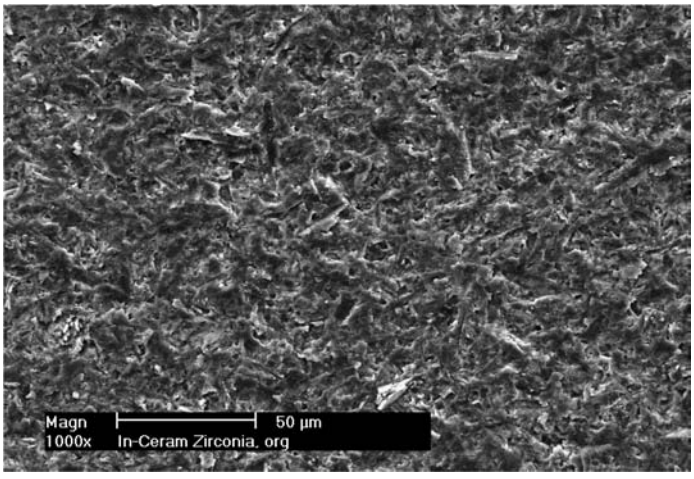


Figure 1. SEM micrograph of the surface of zirconia reinforced glass-infiltrated (In-Ceram Zirconia, Vita) alumina ceramic without additional surface conditioning after the fabrication process (magnification 1000×).

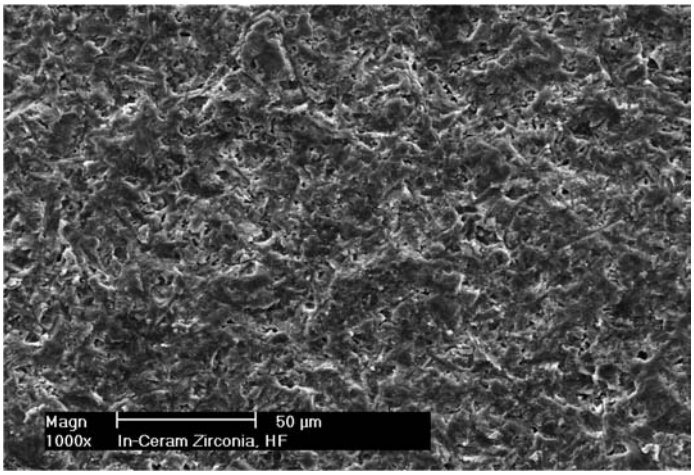


Figure 2. SEM micrograph of the surface of zirconia reinforced glass-infiltrated alumina ceramic (In-Ceram Zirconia, Vita) after additional etching with 9.6% hydrofluoric acid for 3 min (magnification 1000×). No etching pattern is noticeable (surface texture comparable to Fig. 1).

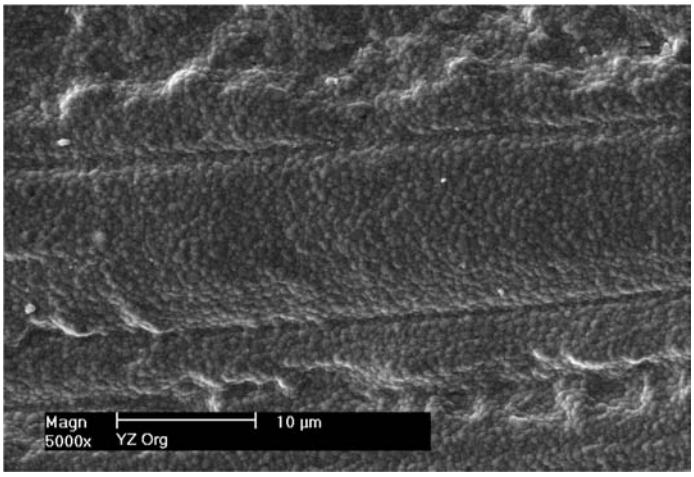


Figure 3. SEM micrograph of the surface of densely sintered zirconia ceramic (YZ Cubes, Vita) after machining without surface conditioning (magnification 5000×). Note the grooves and surface irregularities caused by the milling procedure.

which might prevent the restoration from complete seating. Such contacts are reduced prior to cementation by surface grinding. Therefore, ceramic conditioning methods applied chair-side in the dental office should be able to remove any surface contamination and should be applicable in short time.

The purpose of this article is to summarize the current knowledge on bonding to dental oxide ceramics. Thus for dental restorations the equally important adhesion of the bonding agent to the tooth substrate (enamel–dentine bonding) is not covered

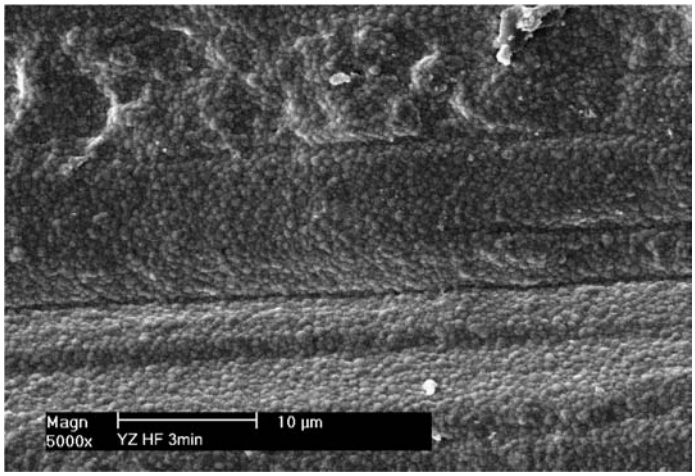


Figure 4. SEM micrograph of the surface of densely sintered zirconia ceramic (YZ Cubes, Vita) after etching with 9.6% hydrofluoric acid for 3 min (magnification 1000×). No etch patterns are noticeable (surface texture comparable to Fig. 3).

in this article. A PubMed database search was conducted for *in vitro* studies pertaining to the resin bond to oxide dental ceramic materials, i.e., alumina and zirconia ceramics. The search was limited to peer-reviewed articles published in English between 1966 and March 2008. Additional references already available in the author's electronic database were included when considered meaningful to the topic.

2. Bonding Methods for Dental Oxide Ceramics

Bonding to dental oxide ceramics essentially requires two steps. First, the bonding surface should be cleaned of contaminants, roughened to increase the bonding surface and to provide micromechanical interlocking, and activated for chemical bonding. Second, bifunctional molecules which promote chemical bonding between the surface oxides and double bonds of the luting resin should be used. Without adequate surface roughening/activation, bonded specimens usually debonded already during artificial aging with water storage and thermal cycling [21, 23, 25, 26]. However, such bonding methods are still recommended by some dental oxide ceramic manufacturers [26].

2.1. Oxide Ceramic Conditioning Methods

Ceramic conditioning methods suggested in the literature include hydrofluoric acid etching, grinding with diamond burs [22], airborne particle abrasion [19–21, 25, 27, 28], tribochemical silica coating [19, 27, 29–32], plasma spraying with hexamethyldisiloxane [22], applying low fusing porcelain pearl layer [22], or a so-called selective infiltration–etching technique [33]. While the first four methods can be applied either in the dental laboratory or in the dental office, the other methods have to be used during the manufacturing process, which makes them less suitable for daily

practice, especially as intraoral try-in of dental restorations is regularly needed in clinical dentistry.

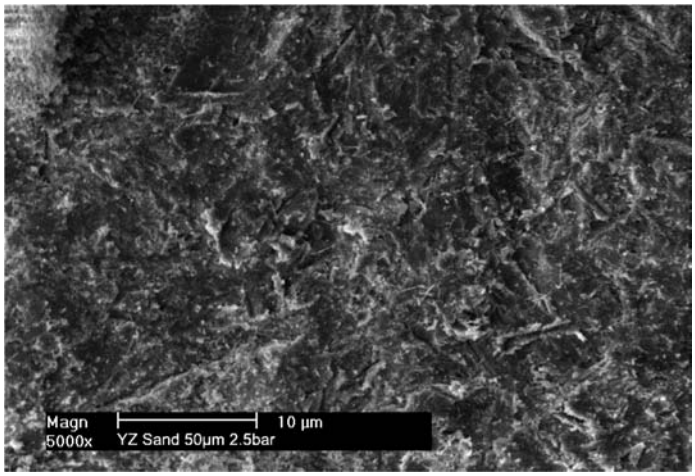
However, adequate micromechanical retention to oxide ceramics would be advantageous because without sufficient micromechanical bonding, the chemically promoted adhesive bonding is prone to contamination and is, therefore, a technique-sensitive process, which might result in some failure rate when carried out in an individual clinical setting. In addition, if bonding is solely based on chemical bonds but not on adequate micromechanical retention debonding will occur when hydrolysis of water degradable chemical bonds takes place. Therefore, under identical ceramic surface conditions only luting resins containing specific adhesive monomers achieved hydrolytically durable bonding to densely sintered alumina and zirconia ceramics while resins without adhesive monomers debonded spontaneously during artificial aging [20, 21, 23, 25].

2.1.1. Airborne Particle Abrasion

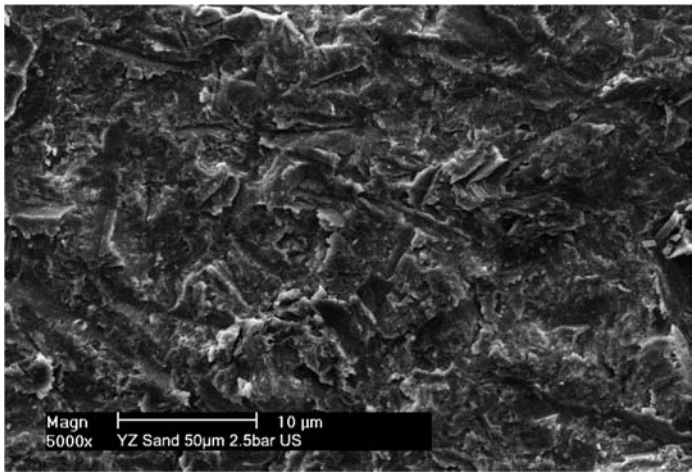
While hydrofluoric acid etching and diamond grinding do not create a micromechanical retention on oxide ceramics [25, 28, 34], airborne particle abrasion with 50–110 μm alumina particles at 0.25 MPa (Fig. 5(a, b)) has been found to be effective in cleaning and roughening the surface of various dental oxide ceramics [19–21, 25, 27, 28, 35]. The substance loss caused by airborne particle abrasion does not alter the clinical fit of dental oxide ceramic restorations significantly [27]. However, it seems important to remove loose particles not firmly attached to the ceramic surface after air-abrasion by ultrasonic cleaning prior to bonding [19–21, 27]. Using unconditioned ceramic controls (as produced from manufacturing a dental restoration) after isopropanol cleaning or after cleaning by air–powder–water spraying with sodium hydrocarbonate, which is often used for tooth cleaning intraorally, resulted in debonding during artificial aging, even when the same luting agents were used which created a durable resin bond to air-abraded surfaces [21, 25, 36].

However, currently there is a controversy whether airborne particle abrasion alters the strength of oxide ceramic restorations on a clinically relevant level. While some studies showed even a strengthening effect of airborne particle abrasion on oxide ceramics [37–40], others reported a strength reducing effect [41–43]. There are no controlled clinical studies yet showing whether airborne particle abrasion influences the clinical outcome of dental oxide restorations negatively. However, a long-term study on resin-bonded oxide ceramic fixed partial dental prostheses revealed no deleterious effect of air-abrading on the bonding surfaces of the retainers over up to 12 years observation time [12].

Nevertheless, it might be advantageous to minimize surface defects by using smaller particles for air-abrasion and/or reducing the blasting pressure (Fig. 6(a, b)). Preliminary laboratory results showed that air-abrasion with 50 μm alumina particles at 0.05 MPa pressure reduced the surface roughness on zirconia ceramic without compromising resin bonding when proper coupling agents were used [44].



(a)

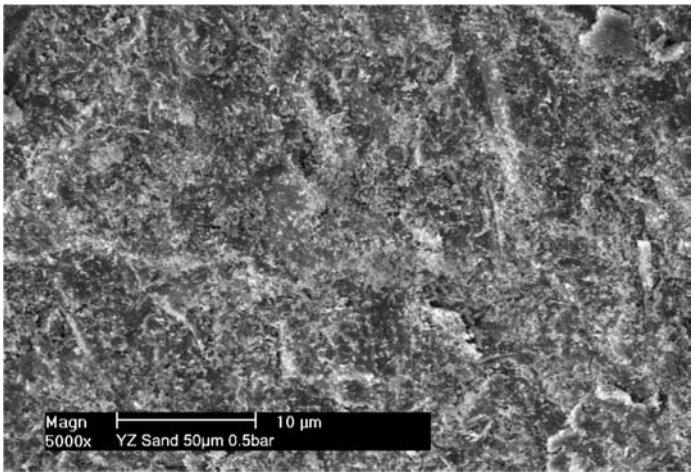


(b)

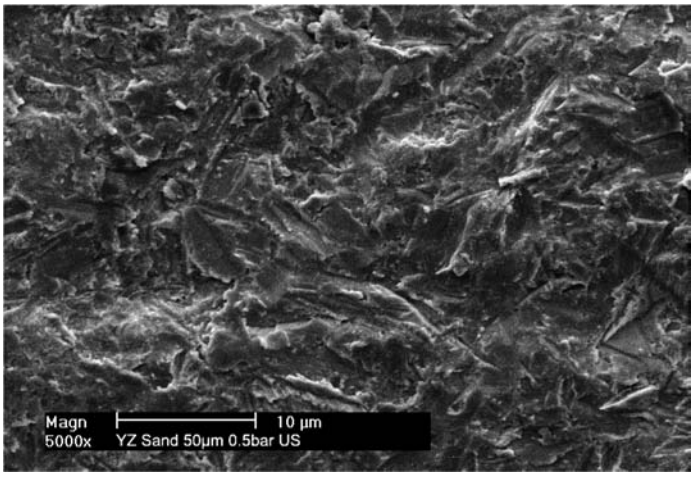
Figure 5. SEM micrograph of the surface of densely sintered zirconia ceramic (YZ Cubes, Vita) after air-abrasion with 50 µm alumina particles at 0.25 MPa for 15 s (magnification 5000×). (a) Visible dust resulting from the air-abrasion was removed by blasting with compressed air. Compared to Fig. 3, the increase of surface irregularities is clearly visible. (b) Visible dust resulting from the air-abrasion was removed by blasting with compressed air, thereafter the sample was ultrasonically cleaned in 96% isopropanol. Compared to Fig. 5(a), obviously loose surface particles have been removed by ultrasonic cleaning.

2.1.2. Tribochemical Silica Coating

Airborne particle silica coating systems (e.g., Rocatec System and Cojet System; 3M Espe, Seefeld, Germany) were originally developed for conditioning metals for bonding by forming a silica layer by air-abrasion with silica-coated alumina particles [45]. MPS silane is then applied that bonds chemically to the silica layer and creates bonds to the subsequently applied luting resin [46]. This method has



(a)



(b)

Figure 6. SEM micrograph of the surface of densely sintered zirconia ceramic (YC Cubes, Vita) after air-abrasion with 50 µm alumina particles at 0.05 MPa for 15 s (magnification 5000×). (a) Visible dust resulting from the air-abrasion was removed by blasting with compressed air. Compared to Fig. 5(a), the surface irregularities are smaller. (b) Visible dust resulting from the air-abrasion was removed by blasting with compressed air, thereafter the sample was ultrasonically cleaned in 96% isopropanol. Compared to Fig. 6(a), obviously loose surface particles have been removed by ultrasonic cleaning.

been used on oxide ceramics with varying results [19–21, 28–30, 35, 47–56]. As a general rule, silica-coating provides a stable bonding basis on glass-infiltrated oxide ceramics [19, 27, 28, 49, 51, 52, 54–56], as the glassy phase is predominantly removed by the air-abrasion with silica containing particles and the silica layer can mechanically interlock with the surface.

However, on glass-phase-free oxide ceramics the results are conflicting for silica-coating, which might be related to the existence of surface porosities and/or the

degree of sintering density. So for a pure alumina ceramic (Procera Alumin; Noble Biocare, Goteborg, Sweden) which contains surface porosities, silica coating followed by silanization provided durable resin bonding [23, 28, 57, 58]. Also for some zirconia ceramics, silica coating produced durable resin bonding [29, 35]. However, for denser alumina or zirconia ceramic surfaces silica coating seems to be less suitable resulting in reduced bond strengths after artificial aging [20, 28, 47, 48, 53, 59] or even in spontaneous debonding during aging [21, 59]. An explanation presented in one study was that the silica-coverage originating from the coating particles appeared, to a large extent, not to be really firmly attached to the hard zirconia surface [59]. Therefore, the weakly attached silica layer seems to be the weak link when bonding to silica coated densely sintered oxide ceramics.

Using silica-coated zirconia particles for silica-coating did not improve bonding to densely sintered zirconia ceramic as compared to using silica-coated alumina particles [48]. However, a recent laboratory study revealed [60] that the operating air pressure of the tribochemical silica-coating process had a significant effect on bond strength to dental oxide ceramics. When increasing the air pressure of silica-coating from 0.15 MPa to 0.45 MPa, bond strength to zirconia and alumina ceramics increased from 11.2 MPa up to 30.5 MPa. However, regarding the suggested deleterious effects of airborne particle abrasion [41–43], an increase of operating pressure for silica coating might have a conflicting effect on the structural subsurface integrity of the oxide ceramic and might ultimately reduce the fracture strength of the restoration itself. These possible negative side-effects must be taken into consideration before recommending increased operating pressures for silica coating of dental oxide ceramics.

2.1.3. Alternate Surface Conditioning Methods

Alternate surface conditioning methods might be utilized in the dental laboratory during the manufacturing process of the dental oxide restorations to avoid air-borne particle abrasion. These surface conditioning methods include plasma spraying with hexamethyldisiloxane [22], applying low fusing porcelain pearl layer [22], a so-called selective infiltration–etching technique [33], or new patented modified ceramic surfaces (NobelBond; Nobel Biocare, Goteborg, Sweden) [61]. In creating microretention and/or the bonding basis for silane coupling agents these methods seem to be quite effective. However, it remains unclear to what extent the conditioned ceramic bonding surfaces are negatively altered by clinical try-in procedures of the dental restorations with unavoidable contaminations or by clinically needed surface adjustments to improve the internal fit of the restorations.

2.2. Chemical Bonding to Oxide Ceramics

In addition to micromechanical retention though surface roughness, chemical bonds between the oxide ceramic surface and the luting agent should be achieved to prevent microleakage which might result in reduced retention and also in discoloration of the bonding margins [62].

As described above, a frequently used method for chemical bonding to oxide ceramics utilizes silica coating followed by MPS silane application as a coupling agent between the silica-enriched surface and the luting resin — however with varying success depending on the oxide ceramic type, operating pressures and silane used. Therefore, silica-coating followed by silanization cannot be recommended as a general method to achieve hydrolytically stable resin bonding to oxide ceramics (see above).

However, results of numerous laboratory studies with glass-infiltrated alumina ceramic and also with densely sintered alumina or zirconia ceramics show that phosphate monomer containing composite resins and primers provide a strong and durable resin bond to these ceramics if used after airborne particle abrasion of the ceramic bonding surface with alumina particles [19–21, 23, 35, 47, 48, 63–65]. The phosphate monomer promoting chemical bonding to oxide ceramics is 10-methacryloxydecyl-dihydrogenphosphate (MDP). This bifunctional molecule contains a phosphate ester group which bonds directly to surface oxides and a methacrylate group which bonds to the resin matrix of the luting resin (Fig. 7) [66]. The MDP monomer is contained in the luting resins of the Panavia product family (auto-curing Panavia or Panavia 21 and dual-curing Panavia F 2.0, all from

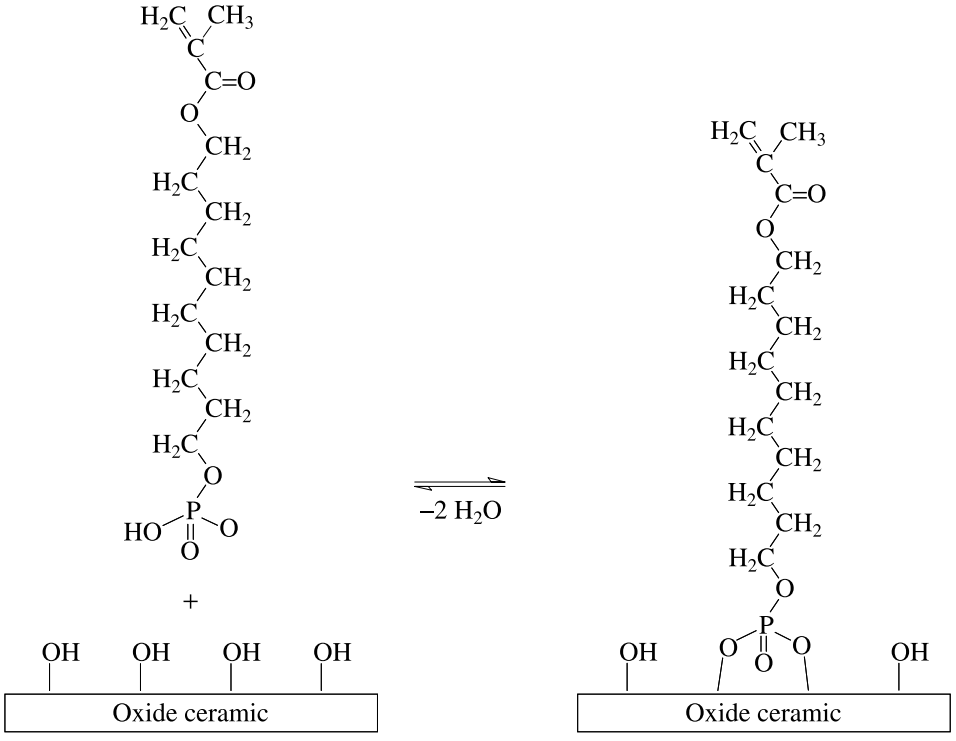


Figure 7. Suggested chemical bonding of the bifunctional phosphate monomer 10-methacryloxydecyl-dihydrogenphosphate (MDP) to oxide ceramics.

Kuraray, Osaka, Japan) and in primers of the same company (Alloy Primer, Clearfil SE Bond/Porcelain Bond Activator and Clearfil Ceramic Primer) [23, 44, 67, 68]. The last product contains both MDP and MPS silane and, therefore, seems to have the potential to act as a universal ceramic primer as it can be used not only on oxide ceramics but also on silica-based ceramics [67]. A long-term clinical study on resin-bonded fixed partial dental prostheses (retained by bonded lingual veneers of oxide ceramic without any mechanical retention) proved the clinical efficiency of bonding using MDP containing resins on air-abraded zirconia ceramic as no debonding occurred over up to 12 years of clinical service [12].

Other luting resins and primers which contain either 4-methacryloxyethyltrimellitate-anhydride (4-META; Superbond C&B, Sun Medical, Kyoto, Japan) or phosphorylated methacrylates, such as RelyX Unicem (3M Espe) or Metal/Zirconia Primer (Ivoclar Vivadent, Schaan, Liechtenstein) show also promising results when used on air-abraded dental oxide ceramics [23, 29, 35, 44, 53, 69, 70]. However, in most studies with these bonding systems, the initially achieved bond strength decreased during artificial aging significantly. Without air-abrading the ceramic surface prior to bonding, usually debonding occurred during artificial aging.

Artificial aging with thermal cycling significantly stresses the adhesive joint [71] because the expansion coefficients of the bonded materials differ considerably. Dental luting composite resins typically have a coefficient of thermal expansion (CTE) of more than 25×10^{-6}/°C [72–74], while the CTE is only $11–12 \times 10^{-6}$/°C for tooth structure [75], $7–8 \times 10^{-6}$/°C for alumina and $9–10 \times 10^{-6}$/°C for zirconia ceramics [76, 77]. Therefore, temperature differences during intake of cold and hot foods will stress the tooth–cement–ceramic system significantly as the CTE of the bonding materials is twice that of the tooth and ceramic materials which results in long-term debonding if the bond is not strong and durable.

2.3. Cleaning Methods After Clinical Try-in

Finished dental oxide ceramic restorations have to be tried clinically prior to adhesive luting. After clinical try-in, the ceramic bonding surface usually is contaminated by saliva, blood and/or silicone fit-indicators. The use of a silicone disclosing medium allows the dentist to improve the fit of dental restorations by detecting interference spots on the internal restoration surfaces before cementation [78]. However, residual organic and silicone contaminants will compromise bonding and, therefore, must be removed from the surface before being able to bond chemically to the ceramic surface [24, 79–81].

Airborne-particle abrasion with alumina particles has always been the most effective cleaning method, resulting in bonds comparable to the uncontaminated controls when using MDP monomer containing resins for bonding [24, 81]. In contrast, water spaying, alcohol and acetone application were ineffective cleaning methods to remove organic contaminations. Although phosphoric acid etching provided some cleaning effect, it cannot be recommended clinically as airborne-particle abrasion is far superior [79, 81]. Therefore it is recommended to use airborne-particle abrasion

with alumina particles directly prior to bonding and not to condition the bonding surface prior to clinical try-in.

2.4. Suggested Bonding Methods to Dental Oxide Ceramics

The partially conflicting results of the above cited laboratory bond strength studies show that these *in vitro* results must be interpreted with caution. Minor variations in bonding procedures and aging methods [48, 82] or differences in bond strength test methods might influence the obtained results significantly [83–88]. In addition, possible deleterious effects of conditioning methods on the ceramic restorative materials and the manageability in the dental office, e.g. simplicity of removing contaminations, must be taken into consideration.

Therefore, oxide ceramic bonding methods approved in clinical long-term studies regarding bonding and ceramic failures [12, 89] should be considered first followed by bonding methods approved in laboratory studies stressing the bonded interface by long-term artificial aging [47, 48]. Lastly, and with caution, bonding methods for which conflicting laboratory results have been reported should be considered. For some bonding methods, e.g., silica coating, the type of oxide ceramic seems to play a significant role. Therefore, such method might be used successfully on one but not on certain other oxide ceramics (see above). Based on these assumptions and the above review of the literature, bonding methods currently recommended for bonding to dental oxide ceramics are listed in Table 2. With additional confirming data on low pressure air-abrasion it might be possible that in the near future the suggested blasting pressure might be reduced to 0.05 MPa.

Table 2.
Recommended bonding methods to dental oxide ceramics

Functional steps	First choice		Second choice		Third choice
Cleaning, Roughnening, chemical activation	Air-abrasion with 50 µm alumina particles at 0.25 MPa		Air-abrasion with 50 µm alumina particles at 0.25 MPa		Silica coating by air-abrasion with 30–110 µm silica-coated alumina particles at 0.25–0.45 MPa
Chemical coupling/ bonding	MDP monomer containing luting resin	MDP monomer containing primer	4-META or phosphorylated methacrylates containing luting resin	Phosphorylated methacrylates containing primer	MPS silane
Luting		Any dental luting resin		Any dental luting resin	Any dental luting resin

MDP = 10-methacryloxydecyl-dihydrogenphosphate, 4-META = 4-methacryloxyethyl-trimellitate-anhydride, MPS = 3-methacryloxypropyltrimethoxysilane.

3. Conclusions

The reviewed literature reveals a vast amount of laboratory bonding studies on dental oxide ceramics, while clinical long-term studies on bonded oxide ceramic restorations without mechanical retention are rare. However, only clinical trials with bonded oxide ceramic restorations without mechanical retention can verify whether a specific bonding method can provide long-term durable adhesion under humid and stressful oral conditions.

Acknowledgement

The author thanks Frank Lehmann, Department of Prosthodontics, Propaedeutics and Dental Materials, School of Dentistry, Christian-Albrechts University at Kiel, for preparation of the SEM micrographs Figs 1–6.

References

1. J. R. Kelly, I. Nishimura and S. D. Campbell, *J. Prosthetic Dentistry* **75**, 18 (1996).
2. A. J. E. Qualtrough and V. Piddock, *J. Dentistry* **25**, 91 (1997).
3. J. R. Kelly, *Dental Clin. North Am.* **48**, 513 (2004).
4. M. B. Blatz, A. Sadan and M. Kern, *Compend. Contin. Educ. Dentistry* **25**, 412 (2004).
5. M. B. Blatz, A. Sadan and M. Kern, *Quintessence Dental Technol.* **25**, 54 (2002).
6. K. H. Schüller and H. W. Hennicke, *Ceram. Forum Int.* **62**, 259 (1985).
7. A. J. Raigrodski, *J. Prosthetic Dentistry* **92**, 557 (2004).
8. I. Denry and J. R. Kelly, *Dental Mater.* **24**, 299 (2008).
9. X.-H. Gu and M. Kern, *Int. J. Prosthodont.* **16**, 109 (2003).
10. S. J. Paul, P. Pliska, N. Pietrobon and P. Schärer, *Int. J. Periodont. Restorative Dentistry* **16**, 165 (1996).
11. M. Kern and R. Gläser, *J. Esthet. Dentistry* **9**, 255 (1997).
12. M. Kern, *Quintessence Int.* **36**, 141 (2005).
13. S. O. Koutayas and M. Kern, *Quintessence Int.* **30**, 383 (1999).
14. S. J. Paul and P. Werder, *Int. J. Prosthodont.* **17**, 524 (2004).
15. F. J. T. Burke, *Quintessence Int.* **26**, 293 (1995).
16. M. B. Blatz, A. Sadan and M. Kern, *J. Prosthetic Dentistry* **89**, 268 (2003).
17. W. Awliya, A. Odén, P. Yaman, J. B. Dennison and M. E. Razzoog, *Acta Odontol. Scand.* **56**, 9 (1998).
18. B. K. Kim, H. E. Bae, J. S. Shim and K. W. Lee, *J. Prosthetic Dentistry* **94**, 357 (2005).
19. M. Kern and V. P. Thompson, *J. Prosthetic Dentistry* **73**, 240 (1995).
20. M. Kern and S. M. Wegner, *Dental Mater.* **14**, 64 (1998).
21. R. Friederich and M. Kern, *Int. J. Prosthodont.* **15**, 333 (2002).
22. T. Derand, M. Molin and K. Kvam, *Dental Mater.* **21**, 1158 (2005).
23. M. Hummel and M. Kern, *Dental Mater.* **20**, 498 (2004).
24. B. Yang, H. C. Lange-Jansen, M. Scharnberg, S. Wolfart, K. Ludwig, R. Adelung and M. Kern, *Dental Mater.* **24**, 508 (2008).
25. M. Wolfart, F. Lehmann, S. Wolfart and M. Kern, *Dental Mater.* **23**, 45 (2007).
26. M. Özcan, S. Kerkdijk and L. F. Valandro, *Clin. Oral Investig.* **12**, 279 (2008).

27. M. Kern and V. P. Thompson, *J. Prosthetic Dentistry* **71**, 453 (1994).
28. M. Özcan and P. K. Vallittu, *Dental Mater.* **19**, 725 (2003).
29. A. Piwowarczyk, H. C. Lauer and J. A. Sorensen, *Oper. Dentistry* **30**, 382 (2005).
30. S. S. Atsu, M. A. Kilicarslan, H. C. Kucukesmen and P. S. Aka, *J. Prosthetic Dentistry* **95**, 430 (2006).
31. L. F. Valandro, M. Özcan, M. C. Bottino, M. A. Bottino, R. Scotti and A. D. Bona, *J. Adhesive Dentistry* **8**, 175 (2006).
32. J. P. Matinlinna, L. V. Lassila and P. K. Vallittu, *Acta Odontol. Scand.* **65**, 44 (2007).
33. M. N. Aboushelib, C. J. Kleverlaan and A. J. Feilzer, *J. Prosthetic Dentistry* **98**, 379 (2007).
34. P. Dérand and T. Dérand, *Int. J. Prosthodont.* **13**, 131 (2000).
35. M. B. Blatz, G. Chiche, S. Holst and A. Sadan, *Quintessence Int.* **38**, 745 (2007).
36. Y. Tsuo, K. Yoshida and M. Atsuta, *Dental Mater. J.* **25**, 669 (2006).
37. T. Kosmac, C. Oblak, P. Jevnikar, N. Funduk and L. Marion, *Dental Mater.* **15**, 426 (1999).
38. T. Kosmac, C. Oblak, P. Jevnikar, N. Funduk and L. Marion, *J. Biomed. Mater. Res.* **53**, 304 (2000).
39. M. Guazzato, L. Quach, M. Albakry and M. V. Swain, *J. Dentistry* **33**, 9 (2005).
40. C. Oblak, P. Jevnikar, T. Kosmac, N. Funduk and L. Marion, *J. Prosthetic Dentistry* **91**, 342 (2004).
41. M. Guazzato, M. Albakry, L. Quach and M. V. Swain, *Biomaterials* **25**, 2153 (2004).
42. Y. Zhang, B. R. Lawn, E. D. Rekow and V. P. Thompson, *J. Biomed. Mater. Res.* **71B**, 381 (2004).
43. Y. Zhang, B. R. Lawn, K. A. Malament, V. P. Thompson and E. D. Rekow, *Int. J. Prosthodont.* **19**, 442 (2006).
44. M. Kern, A. Barloi and B. Yang, *J. Dental Res.* **88**, in press (2009).
45. R. Guggenberger, *Dtsch. Zahnärztl. Z.* **44**, 874 (1989).
46. E. P. Plueddemann, *Silane Coupling Agents*, 2nd edn. Plenum, New York, NY (1990).
47. S. Wegner and M. Kern, *J. Adhesive Dentistry* **2**, 139 (2000).
48. S. M. Wegner, W. Gerdes and M. Kern, *Int. J. Prosthodont.* **15**, 267 (2002).
49. L. F. Valandro, F. P. Leite, R. Scotti, M. A. Bottino and M. P. Niesser, *J. Adhesive Dentistry* **6**, 327 (2004).
50. A. Piwowarczyk, P. Ottl, K. Lindemann, H. Zipprich, R. Bender and H. C. Lauer, *Dtsch. Zahnärztl. Z.* **60**, 314 (2004).
51. M. A. Bottino, L. F. Valandro, R. Scotti and L. Buso, *Int. J. Prosthodont.* **18**, 60 (2005).
52. R. Amaral, M. Ozcan, M. A. Bottino and L. F. Valandro, *Dental Mater.* **22**, 283 (2006).
53. H. Lüthy, O. Loeffel and C. H. F. Hammerle, *Dental Mater.* **22**, 195 (2006).
54. V. H. Kiyan, C. H. Saraceni, B. L. da Silveira, A. C. Aranha and P. Eduardo Cda, *Oper. Dentistry* **32**, 457 (2007).
55. L. F. Valandro, M. Özcan, R. Amaral, F. P. Leite and M. A. Bottino, *Int. J. Prosthodont.* **20**, 70 (2007).
56. R. Amaral, M. Ozcan, L. F. Valandro, I. Balducci and M. A. Bottino, *J. Biomed. Mater. Res. B Appl. Biomater.* **85**, 1 (2008).
57. M. Blixt, E. Adamczak, L.-Å. Lindén, A. Odén and K. Arvidson, *Int. J. Prosthodont.* **13**, 221 (2000).
58. M. B. Blatz, A. Sadan and U. Blatz, *Quintessence Int.* **34**, 542 (2003).
59. J. P. Matinlinna, T. Heikkinen, M. Ozcan, L. V. Lassila and P. K. Vallittu, *Dental Mater.* **22**, 824 (2006).
60. T. T. Heikkinen, L. V. J. Lassila, J. P. Matinlinna and P. K. Vallittu, *Acta Odontol. Scand.* **65**, 241 (2007).
61. J. H. Phark, S. Duarte, Jr., M. Blatz and A. Sadan, *J. Prosthetic Dentistry* **101**, 29 (2009).

62. M. Peumans, J. De Munck, S. Fieuws, P. Lambrechts, G. Vanherle and B. Van Meerbeek, *J. Adhesive Dentistry* **6**, 65 (2004).
63. M. Kern, M. J. Neikes and J. R. Strub, *Dtsch. Zahnärztl. Z.* **46**, 758 (1991).
64. M. B. Blatz, A. Sadan, J. Martin and B. Lang, *J. Prosthetic Dentistry* **91**, 356 (2004).
65. A. Piwowarczyk, H. C. Lauer and J. A. Sorensen, *J. Prosthetic Dentistry* **92**, 265 (2004).
66. T. Wada, in: *Proceedings of the International Symposium on Adhesive Prosthodontics*, L. Gettleman, M. M. A. Vrijhoef and Y. Uchiyama (Eds), pp. 9–18. Academy of Dental Materials, Chicago (1986).
67. K. Yoshida, Y. Tsuo, X. Meng and M. Atsuta, *J. Prosthodont.* **16**, 370 (2007).
68. M. Özcan, H. Nijhuis and L. F. Valandro, *Dental Mater. J.* **27**, 99 (2008).
69. G. M. Dias de Souza, N. Silva, M. Goes, E. Rekow and V. P. Thompson, *J. Dental Res.*, Abstr. No. 324 (2006), available at: http://iadr.confex.com/iadr/2006Orld/techprogram/ abstract_75149.htm
70. F. Lehmann and M. Kern, *J. Dental Res.* **86**, Abstr. No. 0829 (2007).
71. G. A. Crim, M. L. Swartz and R. W. Phillips, *J. Prosthetic Dentistry* **53**, 50 (1985).
72. D. T. Hashinger and C. W. Fairhurst, *J. Prosthetic Dentistry* **52**, 506 (1984).
73. K.-J. M. Söderholm, *J. Dental Res.* **63**, 1321 (1984).
74. R. Yamaguchi, J. M. Powers and J. B. Dennison, *Oper. Dentistry* **14**, 64 (1989).
75. R. G. Craig, *Restorative Dental Materials*. Mosby, St. Louis, MO (1993).
76. M. Andersson and A. Odén, *Acta Odontol. Scand.* **51**, 59 (1993).
77. M. Yoshinari, S. Kim and T. Dérand, *J. Jpn Dental Mater.* **13**, 170 (1994).
78. S. N. White, J. A. Sorensen and S. K. Kang, *Int. J. Prosthodont.* **4**, 323 (1991).
79. A. C. Quaas, B. Yang and M. Kern, *Dental Mater.* **23**, 506 (2007).
80. B. Yang, M. Scharnberg, S. Wolfart, A. C. Quaas, K. Ludwig, R. Adelung and M. Kern, *J. Biomed. Mater. Res. B Appl. Biomater.* **81**, 283 (2007).
81. B. Yang, S. Wolfart, M. Scharnberg, K. Ludwig, R. Adelung and M. Kern, *J. Dental Res.* **86**, 749 (2007).
82. J. C. Chang, J. M. Powers and D. Hart, *J. Prosthodont.* **2**, 110 (1993).
83. R. Van Noort, S. Noroozi, I. C. Howard and G. Cardew, *J. Dentistry* **17**, 61 (1989).
84. G. Øilo, *Int. Dental J.* **43**, 492 (1993).
85. G. Øilo and E. K. Austrheim, *Acta Odontol. Scand.* **51**, 263 (1993).
86. K. L. De Vries and P. R. Borgmeier, in: *Handbook of Adhesive Technology*, A. Pizzi and K. L. Mittal (Eds), pp. 65–91. Marcel Dekker, New York, NY (1994).
87. A. Della Bona and R. Van Noort, *J. Dental Res.* **74**, 1591 (1995).
88. S. Sudsangiam and R. van Noort, *J. Adhesive Dentistry* **1**, 57 (1999).
89. M. Kern and J. R. Strub, *J. Dentistry* **26**, 245 (1998).

Resin Bonding to Dentine after Casein Phosphopeptide-Amorphous Calcium Phosphate (CPP-ACP) Treatments

Vanthana Sattabanasuk [a,*], **Michael F. Burrow** [b], **Yasushi Shimada** [c] **and Junji Tagami** [c]

[a] Department of Conservative Dentistry and Prosthodontics, Faculty of Dentistry, Srinakharinwirot University, Sukhumvit 23, Wattana District, Bangkok 10110, Thailand

[b] Melbourne Dental School, The University of Melbourne, 720 Swanston Street, Melbourne 3010, Victoria, Australia

[c] Cariology and Operative Dentistry, Tokyo Medical and Dental University, 1-5-45, Yushima, Bunkyo-ku, Tokyo 113-8549, Japan

Abstract

Casein phosphopeptide-amorphous calcium phosphate (CPP-ACP) has the ability to enhance enamel and dentine remineralisation and thus has been incorporated in new medicaments for such clinical problems as tooth hypersensitivity and early carious lesions. The current study investigated whether the application of CPP-ACP in the proprietary paste, Tooth Mousse™, would influence the subsequent resin adhesion to dentine. Bonding effectiveness was assessed by microtensile bond strength test and scanning electron microscopy. A three-step etch-and-rinse adhesive (OptiBond FL) or a two-step self-etch adhesive (Clearfil SE Bond) was bonded to three groups of dentine surfaces: no treatment; 5 min or 5 days CPP-ACP application. The microtensile test was performed and bond strength data were analysed using ANOVA and Tukey–Kramer *post hoc* test. Etching characteristics on respective dentine surfaces and resin–dentine interface were observed under SEM. Bond strengths of Clearfil SE Bond to dentine appeared to be similar for all tested groups. OptiBond FL, however, showed lower bond strengths following the application of CPP-ACP for both time periods. Under SEM observations, the CPP-ACP treated dentine displayed a layer of residue or precipitate attached to the surface after the phosphoric acid treatment. The sectioned specimens also showed the resin–dentine interface with less intertubular linking of resin tags, which could mean mineralisation of these channels, hence preventing resin infiltration. The presence of CPP-ACP on the dentine surface, therefore, may compromise bonding effectiveness of etch-and-rinse adhesive system. However, CPP-ACP application may be beneficial to the dentine bonding of self-etch adhesive system, as the chemical interactions between calcium and functional monomers of the adhesives might be enhanced to some degree.

* To whom correspondence should be addressed. Tel.: +66-2-649-5212; Fax: +66-2-649-5212; e-mail: vanthana@swu.ac.th

Adhesion Aspects in Dentistry

© Koninklijke Brill NV, Leiden, 2009

Keywords
Casein phosphopeptide-amorphous calcium phosphate (CPP-ACP), dentine bonding, etch-and-rinse adhesive, self-etch adhesive, microtensile bond strength

1. Introduction

Dentine hypersensitivity is a common clinical condition of transient tooth pain associated with various exogenous stimuli, e.g., temperature change, osmotic gradients, or tactile stimulation [1]. The major underlying factor for dentine hypersensitivity is exposed dentinal tubules. This clinical condition allows fluid movement within the tubules, which results in pressure changes that excite the sensory nerve endings in dentine or pulp tissues [2]. At present, clinicians have used many materials and techniques to manage tooth sensitivity [3, 4]. Topical application of calcium phosphate is one treatment modality that has been reported to relieve the hypersensitivity of dentine [5–7].

Casein phosphopeptide-amorphous calcium phosphate (CPP-ACP) is a form of calcium and phosphate reservoir when placed onto a tooth surface. By aggregating calcium and phosphate with milk-derived protein, casein phosphopeptides, the CPP-ACP acts as a calcium phosphate delivery vehicle [8]. The CPP-ACP complexes release calcium and phosphate ions to maintain a supersaturated environment, therefore reducing demineralisation and enhancing remineralisation [8]. A number of studies have demonstrated that CPP-ACP can promote remineralisation of demineralised enamel and dentine surfaces and shows anticariogenic activity both in the laboratory as well as in *in situ* studies [8–12]. It has also been reported that, in addition to its remineralising ability, CPP-ACP was able to alleviate dentine hypersensitivity [13, 14]. Incorporation of CPP-ACP into dental products is now commercially available in several forms such as a topical paste and mouthrinse [11, 12]. Moreover, addition of CPP-ACP to a temporary luting cement has also been advocated to promote the closure of dentinal tubules during the time that the permanent restoration is being fabricated in the laboratory [15].

Tooth Mousse™ (GC Corp., Tokyo, Japan) is one over-the-counter product containing Recaldent® CPP-ACP in water-based sugar-free cream formulation. According to the manufacturer, Tooth Mousse™ is recommended for daily use at home or following clinical treatments, e.g., tooth preparation, in order to reduce tooth sensitivity [16]. Tooth substrate covered by the precipitation of calcium phosphate, however, may possibly affect the subsequent clinical steps, especially adhesive procedures, as the application of CPP-ACP results in more acid-resistant enamel and dentine surfaces [8–10, 12]. Variations in the outcome of resin adhesion to CPP-ACP treated enamel have been previously stated with the use of a self-etch adhesive [17, 18]. However, there is still no published report to document such an effect on CPP-ACP treated dentine surface.

The present study, therefore, aimed to evaluate the effect of CPP-ACP application on microtensile bond strengths and micromorphological features of dentine surfaces

using two 'gold standard' adhesive systems: a three-step etch-and-rinse system and a two-step self-etch system. The null hypothesis tested was that the presence of CPP-ACP would exert no influence on resin adhesion to dentine.

2. Experimental

2.1. Dentine Specimen Preparation

Intact, non-carious, non-restored human molars extracted as part of a clinical treatment plan for which patients had given prior verbal consent were used for this study. The teeth were stored in 0.1% thymol at 4°C and used within approximately six months of extraction. The occlusal enamel of each tooth was partially removed using a slow-speed diamond saw (IsoMet; Buehler, Lake Bluff, IL, USA) under water-cooling. The cut surface was further ground with wet 600-grit silicon carbide abrasive paper on a table-top grinding/polishing machine (EcoMet 4; Buehler) until all remnants of enamel were removed, exposing flat mid-coronal dentine.

Adhesive restorative materials and Recaldent® CPP-ACP-containing paste and application procedures are listed in Table 1. The teeth were randomly divided into three experimental groups:

- Group 1: No treatment (control). The teeth were bonded with either three-step etch-and-rinse adhesive, OptiBond FL, or two-step self-etch adhesive, Clearfil SE Bond, according to the manufacturers' instructions;
- Group 2: A CPP-ACP-containing paste, Tooth Mousse™, was applied to the dentine surfaces and left in place for 5 min as recommended by the manufacturer [16]. The teeth were kept in a closed chamber at 100% relative humidity and maintained at ambient temperature during the application time. After completion, a copious amount of water was used to rinse off the CPP-ACP-containing paste for 10 s and bonded with each adhesive;
- Group 3: A CPP-ACP-containing paste was applied and left undisturbed for 5 days to prolong the effect of CPP-ACP on dentine surfaces. The teeth were kept in 100% relative humidity and remained in the incubator at 37°C throughout the duration of the treatment. The treated dentine surfaces were rinsed with water and subsequently bonded with each adhesive.

Three horizontal consecutive layers of Clearfil AP-X hybrid resin-based composite, each approximately 1 mm thick, were built up and individually light-cured for 40 s. Light-polymerisation was performed using a quartz–tungsten halogen curing unit (Optilux 501; Kerr, Orange, CA, USA) with a light output no less than 550 mW/cm^2. The bonded teeth were stored in 37°C distilled water for 24 h.

2.2. Microtensile Bond Strength Testing

After storage, each tooth was sectioned perpendicular to the adhesive–tooth interface using a slow-speed diamond saw with water-cooling into approximately

Table 1.
List of materials used in the study

Material	Batch number	Components	Procedures
OptiBond FL (Kerr, Orange, CA, USA)	Etchant: 301194	37.5% phosphoric acid, water, silica thickener, dye colorant	Etch 15 s; rinse 15 s; blot with lint-free absorbent paper, leaving the surface visibly moist
	Primer: 25881	HEMA, GPDM, PAMM, ethanol, water, photoinitiators	Apply 15 s with light scrubbing action; air dry 5 s
	Bond liquid: 25882	Bis-GMA, UDMA, GPDM, HEMA, TEGDMA, ytterbium trifluoride, fillers, photoinitiators, stabilizers	Apply and thin with a new applicator; light-cure 30 s
Clearfil SE Bond (Kuraray Medical, Okayama, Japan)	Primer: 00539A	MDP, HEMA, hydrophilic dimethacrylate, photoinitiators, water	Apply 20 s; air dry
	Bond liquid: 00760A	MDP, Bis-GMA, HEMA, hydrophobic dimethacrylate, photoinitiators, filler	Apply and thin with a new applicator; light-cure 10 s
Tooth Mousse (GC Corp., Tokyo, Japan)	051005M	Recaldent® CPP-ACP, glycerol, D-sorbitol, water, sodium carboxymethyl cellulose, propylene glycol, xylitol, sodium saccharine, phosphoric acid, guar gum, silicon dioxide, titanium dioxide, zinc oxide, ethyl paraben, butyl paraben, propyl paraben	Apply and leave in place for either 5 min or 5 days
Clearfil AP-X (Kuraray Medical, Okayama, Japan)	01112A	Bis-GMA, TEGDMA, barium glass filler, silanated colloidal silica, photoinitiators, pigments	Apply approximately 1 mm thickness increments; light-cure 40 s for each increment

Bis-GMA = bisphenol A diglycidylmethacrylate; CPP-ACP = casein phosphopeptide-amorphous calcium phosphate; GPDM = glycerol phosphate dimethacrylate; HEMA = 2-hydroxyethyl methacrylate; MDP = 10-methacryloyloxydecyl dihydrogen phosphate; PAMM = phthalic acid monoethyl methacrylate; TEGDMA = triethylene glycol dimethacrylate; UDMA = urethane dimethacrylate.

1 mm thick slabs. The tooth was then rotated 90° on the cutting machine and, again, sectioned lengthwise. By this second cut, 6–9 rectangular sticks, with a mean cross-sectional area of 1.00 ± 0.03 mm^2, were obtained from each tooth. The specimens were fixed with cyanoacrylate glue (Model Repair II Blue; Dentsply-Sankin, Tochigi, Japan) to the testing jig and stressed in tension at a crosshead speed of

1 mm/min in a universal testing machine (EZTest; Shimadzu, Kyoto, Japan). The microtensile bond strength was expressed in MPa, as derived from dividing the maximum load (N) at the time of fracture by the cross-sectional area of the bonded surface (mm^2).

2.3. Scanning Electron Microscopy (SEM)

After debonding, all fractured specimens were dried, mounted on aluminum stubs and gold sputter-coated. The fractured surfaces were observed microscopically using SEM (JSM-5410LV; JEOL, Tokyo, Japan). Categories of failure modes were recorded as: 'cohesive failure in dentine', 'cohesive failure in resin', 'failure at resin–dentine interface', or 'mixed failures'. Mixed failures were further classified by their predominant zone of fracture, i.e., dentine, resin, or the resin–dentine interface.

Additional teeth were used for SEM observations. Dentine surface preparation and CPP-ACP treatments were performed as previously described. To observe the etching characteristics on respective dentine surfaces, the 37.5% phosphoric acid or the acidic primer of Clearfil SE Bond was applied as recommended by the manufacturers. Aqueous 37.5% phosphoric acid obtained from a standard phosphoric acid solution was used instead of a commercial etching gel to avoid the precipitation of silica particles on the dentine surface [19]. After application, the phosphoric acid was rinsed with water for 15 s; whereas the monomer components of the acidic primer were removed by rinsing the specimens with 100% ethanol for 5 min and placed in distilled water for further 5 min [20]. The specimens were fixed in 10% neutral buffered formalin overnight at 4°C and washed in running water for 15 min, then dehydrated in an ascending series of ethanol concentrations (10%, 20%, 30%, 50%, 70% and 90% ethanol for at least 30 min per step) and three times in 100% ethanol. The dehydrated specimens were immersed in hexamethyldisilazane solution (Merck KGaA, Darmstadt, Germany) for 30 min, placed on a filter paper, and dried at room temperature [19]. The specimens were gold sputter-coated and observed using SEM.

For the investigation of the resin–dentine interface, the teeth were prepared in the same manner as for the bond strength measurement. After resin-based composite build-up and overnight storage in 37°C distilled water, the bonded teeth were sectioned occluso-gingivally into halves and embedded in an epoxy resin in order to ease manipulation. The sectioned surfaces were ground with a series of increasingly finer silicon carbide abrasive papers under running water and polished with a flannel cloth impregnated with a diamond suspension (CAMEO; Leco, St Joseph, MI, USA), down to a 1 μm particle size. The specimens were immersed in 5 N HCl for 30 s, followed by immersion in 5% NaOCl for 30 min. Following rinsing, the specimens were dried, gold sputter-coated, and the resin–dentine interface was observed under SEM.

2.4. Statistical Analysis

Mean bond strengths and standard deviations for each group were calculated and the data were analysed using two-way analysis of variance (ANOVA). Comparisons between and within experimental groups for differences in microtensile bond strength were carried out using one-way ANOVA and Tukey–Kramer multiple comparison test. The failure mode frequencies were analysed using Fisher's Exact probability test. All statistical analyses were carried out using statistical software system (SPSS version 13.0 for Windows; SPSS Inc., Chicago, IL, USA), at a significance level of 0.05.

3. Results

Mean microtensile bond strengths and standard deviations are shown in Table 2. None of the specimens debonded before actual testing, denoted as 'pre-testing failures'. Unequal numbers of tested specimens are due to human error in specimen handling, or specimen inclusion criteria not being met, e.g., inadequate remaining dentine thickness. Two-way analysis of variance revealed that microtensile bond strength results were significantly influenced by the interaction between CPP-ACP applications and adhesives tested ($p = 0.007$). One-way ANOVA and Tukey–Kramer *post hoc* test showed the reduction in dentine bond strengths with OptiBond FL following the application of CPP-ACP paste both for 5 min ($p = 0.040$) and for 5 days ($p = 0.028$). There is, however, no statistically significant difference between the two CPP-ACP treated groups ($p = 1.000$). For Clearfil SE Bond, no statistical difference was detected for all experimental groups ($p = 0.728$).

Table 3 summarises the fracture patterns of debonded specimens for all groups. No statistically significant difference in failure distributions was found for the specimens bonded using both adhesives ($p = 0.146$ for OptiBond FL and $p = 0.836$ for Clearfil SE Bond). Following CPP-ACP application for 5 days, OptiBond FL specimens were more likely to have failure pathway in dentine than Clearfil SE Bond specimens ($p = 0.005$).

Table 2.
Mean microtensile bond strengths and standard deviations for all specimen groups (MPa)

Group	Adhesive	
	OptiBond FL (No. of specimens tested)	Clearfil SE Bond (No. of specimens tested)
(1) Control	90.6 ± 17.5 (18)	59.9 ± 11.5 (19)[b]
(2) 5 min CPP-ACP application	77.4 ± 14.5 (19)[a]	60.1 ± 13.7 (20)[b]
(3) 5 days CPP-ACP application	77.0 ± 11.3 (20)[a]	66.0 ± 11.1 (17)[b]

Mean values designated with the same superscript letters are not statistically different ($p > 0.05$).

Table 3.
Failure mode results as reported in terms of number of specimens for each failure type

Group	OptiBond FL						Clearfil SE Bond					
	1	2	3	4	5	6	1	2	3	4	5	6
(1) Control	8	0	4	4	0	2	8	0	6	0	1	4
(2) 5 min CPP-ACP application	12	1	3	2	0	1	7	0	3	1	2	7
(3) 5 days CPP-ACP application	16	0	0	1	1	2	5	0	3	1	1	7

Type 1: cohesive failure in dentine.
Type 2: cohesive failure in resin.
Type 3: failure at the resin–dentine interface.
Type 4: mixed failure involving more than 50% dentine fracture.
Type 5: mixed failure involving more than 50% resin fracture.
Type 6: mixed failure involving more than 50% fracture at the resin–dentine interface.

Regarding the SEM observations of the control group, 37.5% phosphoric acid completely removed the smear layer and smear plugs on the dentine surface, exposing patent dentinal tubules and collagen fibril networks (Fig. 1(a)). The formation of a resin–dentine interdiffusion zone created by OptiBond FL, which was approximately 5 μm in thickness, and the penetration of resin into the dentinal tubules could be clearly observed (Fig. 1(b)). The acidic primer of Clearfil SE Bond dissolved the smear layer on the dentine surface, partially exposing the microporosities of the intertubular dentine (Fig. 1(c)). The resin–dentine interdiffusion zone and resin tags were thinner compared with those of OptiBond FL (Fig. 1(d)).

Figures 2 and 3 display the micromorphological characteristics of dentine surfaces and interfaces between resin and dentine after CPP-ACP treatment. There was a residual layer, possibly remnant of the CPP-ACP-containing paste, covering the dentine surfaces after phosphoric acid application (Figs 2(a) and 3(a)). Surprisingly, no remnants were detected on the dentine surfaces treated with acidic primer of Clearfil SE Bond (Figs 2(c) and 3(c)). The resin–dentine interdiffusion zone and resin tags could also be discerned for all CPP-ACP treated groups; however, lateral branches linking the intertubular resin tags were less likely to be observed compared with those seen in the control groups (Figs 2(b), 2(d), 3(b) and 3(d)).

4. Discussion

An assessment of bonding effectiveness between adhesives and tooth substrates can be performed in many ways. One of the common methodologies for evaluating the adhesive properties is the interfacial strength determination. Conventional bond tests, however, require large bonded surface area of specimens that probably contains intrinsic defects. As a result, there is a high concentration of stress at the flaws during the test, initiating the unfavourable stress distribution patterns

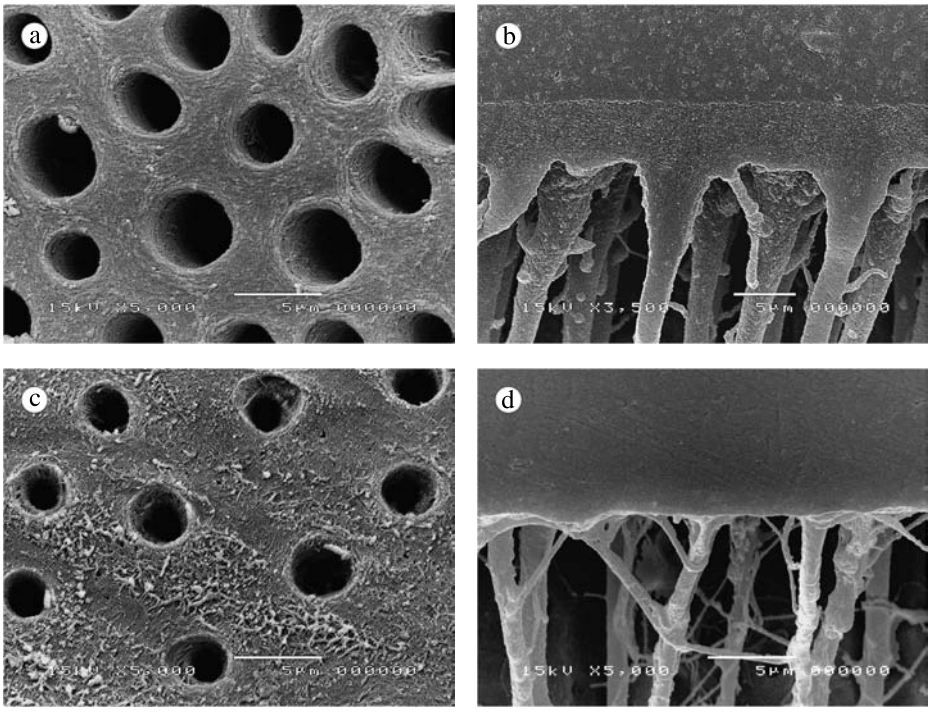


Figure 1. Representative SEM images of the specimens with no CPP-ACP treatment (control group). (a) Phosphoric acid treated dentine surface. Both smear layer and smear plugs are completely removed, showing patent dentinal tubules. (b) Resin–dentine interface created by OptiBond FL. The resin infiltrated zone is approximately 5 µm thick. The resin tags are pronounced after acid–base treatment. (c) Acidic primer treated dentine surface. The smear layer on the dentine surface is removed, exposing the intertubular microporosities. (d) Resin–dentine interface created by Clearfil SE Bond. The thin resin–dentine interdiffusion zone is observed with lateral branches to the thin resin tags are also clearly seen.

[21, 22]. In 1994, the microtensile test was developed to overcome these limitations [22]. Using specimens with small bonding area, a more uniform stress distribution across the interface was reported, which provided reliable information with respect to the bonding potential of adhesive systems [21–23]. A number of studies have used this methodology, with a variety of specimen designs and fabrications, to evaluate the ultimate bond strengths of adhesives to various dental substrates [24–27]. Rectangular stick-shaped specimens were used in the current investigation, as this design of specimen has been shown to present more homogeneous stress distribution than other quadrangular specimen configurations, i.e., dumbbell, and hourglass shapes [24, 25]. Even though the microtensile bond test is a versatile method, the manipulation, however, it requires great care and is technique-sensitive and time-consuming [23]. Furthermore, it has also been suggested that the bond strength values are influenced, in part, by specimen geometry and the manner of attachment of specimen to gripping device [24, 25]. The data from different laboratories, there-

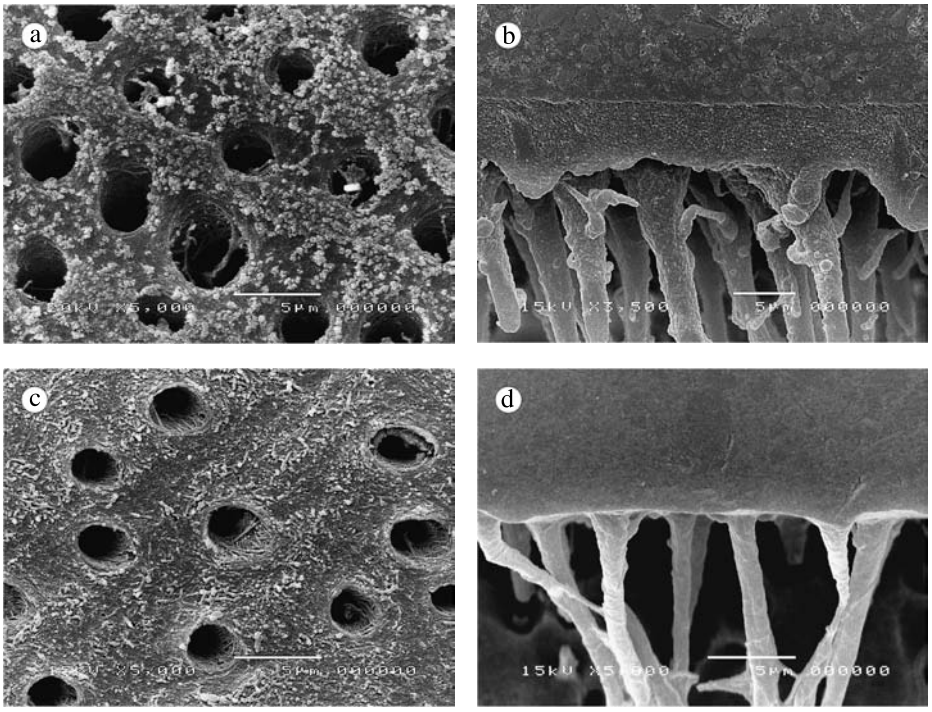


Figure 2. Representative SEM images of the specimens following the application of CPP-ACP for 5 min. (a) Phosphoric acid treated dentine surface. Cross-sectioned tubules show intertubular microporosities and peritubular collagen fibres. A layer of residual material covering the surface is observed. (b) Resin–dentine interface created by OptiBond FL. The thickness of the resin–dentine interdiffusion zone is about 5 μm. (c) Acidic primer treated dentine surface. Entrance of dentinal tubules and porous intertubular dentine can be seen without residual layer of CPP-ACP-containing paste. (d) Resin–dentine interface created by Clearfil SE Bond. The resin–dentine interdiffusion zone appears to be very thin with only a few lateral branches being observed.

fore, might not be directly comparable. Standardisation of the testing methodology is yet to be completely defined.

The results of this laboratory study revealed that dentine bonding of the two tested adhesive systems was dependent on the adhesive used and the application of CPP-ACP. The microtensile bond strengths of self-etch adhesive, Clearfil SE Bond, to dentine following the CPP-ACP treatment remained stable. However, those of etch-and-rinse adhesive, OptiBond FL, to dentine decreased following the application of CPP-ACP-containing paste. Therefore, the hypothesis that CPP-ACP treatment would have no effect on dentine adhesion has to be discarded.

When the CPP-ACP-containing paste is applied, the protein component readily binds to the tooth surface and consequently provides a reservoir of calcium and phosphate ions [8–10]. High concentration gradients of these ions on the tooth surface have been reported and, hence, have been correlated with an increase in surface hardness due to mineral deposition [8, 28]. Using an ultrasonic device, Yamaguchi

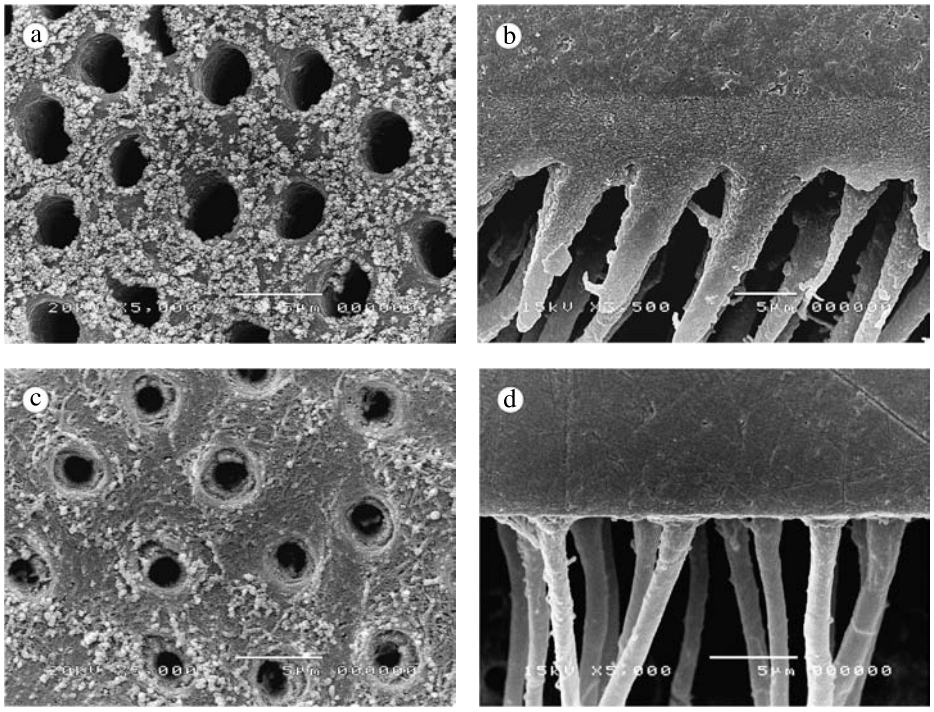


Figure 3. Representative SEM images of the specimens following the application of CPP-ACP for 5 days. (a) Phosphoric acid treated dentine surface. Opening of the dentinal tubules is observed with residual particles present on the surface. (b) Resin–dentine interface created by OptiBond FL. The resin–dentine interdiffusion zone is about 5 μm thick with only a few lateral branches linking intertubular resin tags are evident. (c) Acidic primer treated dentine surface. The intertubular dentine is conditioned, exposing the collagen fibril network. (d) Resin–dentine interface created by Clearfil SE Bond. Lateral branches to the resin tags are rarely observed beneath the resin–dentine interdiffusion zone.

et al. [29] reported that application of CPP-ACP increased the transmission velocity of sonic waves in enamel, implying an enhancement of remineralisation tendency. Also, only relatively minor changes in the morphological features of enamel after immersion in the demineralising solution have been observed using scanning electron microscopy [10, 29]. The enamel surface might have been more resistant to acid demineralisation following CPP-ACP treatment [8, 10, 12, 28, 29]. Based on the concept of enamel bonding, it is widely accepted that the formation of resin microtags within the irregular enamel surface is responsible for the principal adhesion mechanism [1, 30]. Reduction in etching capacity of the acid conditioners, especially of the mild acidic primer used in self-etch adhesives, on the CPP-ACP treated enamel, therefore, might be one possible explanation for the reduction in resin–enamel adhesion [17, 18].

Similar to enamel, the application of CPP-ACP on dentine surfaces might suppress the demineralisation caused by acid treatment [9, 10, 31]. From Fourier

Transform Infrared Spectroscopy (FT-IR) investigations, Rahiotis and Vougiouklakis [9] reported that the percentage of the extent of dentine demineralisation was reduced by one-third following CPP-ACP treatment. Deposition of calcium and phosphate ions on the dentine surface might have occurred and the subsequent dentine might not have been as readily etched by the acid conditioner as in the control groups. Interestingly, as clearly seen in the SEM images, deposition of certain materials on the dentine surface even after the phosphoric acid treatment was evident. Such a finding was not observed in the previous studies, possibly because a diluted solution of CPP-ACP was used instead of the remineralising paste in the current investigation [10, 31]. It is possible that this residual layer is a remnant of the CPP-ACP-containing paste, in which some components in the Tooth Mousse™ might remain after rinsing off the paste. This feature was believed to have reduced resin infiltration into the etched enamel and dentine surface and might have influenced the resin adhesion [17]. Furthermore, it was also noted on the sectioned specimens that lateral branches linking the intertubular resin tags were less following CPP-ACP treatment, which may indicate some mineralisation and occlusion of these channels. Dentine bond strength of the etch-and-rinse adhesive decreased with prior CPP-ACP treatment and an increased tendency for dentine failure after testing was also recorded. These results might indicate that the penetration of resin monomers into the filigree of collagen fibres left exposed by acid conditioning was hampered. Since the bonding mechanism of etch-and-rinse adhesive system depends primarily on the micromechanical interlocking created in resin–dentine interdiffusion zone [1, 30], the presence of a layer of residue, together with the reduction in the etching effect of phosphoric acid on the CPP-ACP treated dentine, therefore, could have influenced the retention of OptiBond FL adhesive.

For the specimens bonded with Clearfil SE Bond, there were, however, no significant differences in dentine bond strengths following the CPP-ACP treatments. On closer inspection, a slight increase in dentine bond strengths was observed, though this was not statistically significant. This finding was unexpected and contrary to the previous studies on enamel adhesion [17, 18]. While the mild acidity of the primer supplied with self-etch adhesive might not be effective enough to etch enamel, resulting in unfavourable bond strengths, bonding to dentine, on the other hand, could reach satisfactory outcomes with the use of self-etch adhesive in spite of the presence of small hybrid layer and thin resin tags [1, 30]. Besides the micromechanical interlocking, chemical adhesion has also been shown to be particularly advantageous as an additional mechanism of dentine bonding with the self-etch adhesive system [30, 32]. Specific chemical interactions between the functional monomers and calcium of the tooth have been demonstrated, and are believed to enhance the bonding performance to dentine [32]. Application of CPP-ACP might supply further calcium to the surface of dentine that may enhance the potential for better adhesion. With respect to SEM observations, the collagen fibril network was evident with no residual CPP-ACP complexes on the acidic primer treated dentine surfaces. The disappearance of this residue might be due to the chemical interac-

tion with the functional monomer used in Clearfil SE Bond, or possibly because the application technique of brushing the surface might have dislodged the residual particles. This finding, however, needs to be further investigated.

The remineralising properties of CPP-ACP have been determined and validated for many years. Tooth Mousse™, a topical cream with bio-available calcium and phosphate, is recommended for preventive therapy from tooth hypersensitivity, treatment of fluorosed teeth, or management of early carious lesions in elderly patients or patients with dry mouth [13, 16]. These clinical problems, however, sometimes end up with surgical treatments requiring restorative procedures with adhesive materials. Selection of materials used and concern for subsequent bonding steps should be carefully considered. The current study demonstrated that the prior application of CPP-ACP-containing paste to dentine as an auxiliary treatment is unlikely to affect the subsequent bonding procedures with Clearfil SE Bond self-etch adhesive. However, care needs to be taken with the use of OptiBond FL etch-and-rinse adhesive. Basically, adhesion to such clinical problems as fluorosed teeth or carious dentine also seems promising with the use of self-etch adhesives [26, 27]. Preliminary CPP-ACP treatment, therefore, might be of benefit to patients prior to the adhesive procedures, if necessary. Further studies into the effect of CPP-ACP on resin bonding, however, are required to provide more definitive recommendations and determine whether this effect would be legitimate for other self-etch adhesives.

5. Conclusion

Prior application of CPP-ACP-containing paste, Tooth Mousse™, to dentine did not affect the microtensile bond strength of Clearfil SE Bond self-etch adhesive. However, significant reduction in microtensile bond strength was shown when OptiBond FL etch-and-rinse adhesive was bonded to CPP-ACP treated dentine.

References

1. J. Perdigão and E. J. Swift, Jr., in: *Sturdevant's Art and Science of Operative Dentistry*, T. M. Roberson (Ed.), 5th edn, pp. 243–279. Mosby, St Louis, MO (2006).
2. M. Brännström, *Oral Surg. Oral Med. Oral Pathol.* **21**, 517–526 (1966).
3. P. M. Bartold, *Aust. Dental J.* **51**, 212–218 (2006).
4. R. Orchardson and D. G. Gillam, *J. Am. Dental Assoc.* **137**, 990–998 (2006).
5. A. M. Cherng, L. C. Chow and S. Takagi, *Arch. Oral Biol.* **49**, 91–98 (2004).
6. S. Geiger, S. Matalon, J. Blasbalg, M. Tung and F. C. Eichmiller, *Oper. Dentistry* **28**, 496–500 (2003).
7. T. Suge, K. Ishikawa, A. Kawasaki, K. Suzuki, T. Matsuo, Y. Noiri, S. Imazato and S. Ebisu, *Am. J. Dentistry* **15**, 220–226 (2002).
8. E. C. Reynolds, *J. Dental Res.* **76**, 1587–1595 (1997).
9. C. Rahiotis and G. Vougiouklakis, *J. Dentistry* **35**, 695–698 (2007).
10. M. Oshiro, K. Yamaguchi, T. Takamizawa, H. Inage, T. Watanabe, A. Irokawa, S. Ando and M. Miyazaki, *J. Oral Sci.* **49**, 115–120 (2007).
11. E. C. Reynolds, F. Cai, P. Shen and G. D. Walker, *J. Dental Res.* **82**, 206–211 (2003).

12. P. Shen, F. Cai, A. Nowicki, J. Vincent and E. C. Reynolds, *J. Dental Res.* **80**, 2066–2070 (2001).
13. F. Ng and D. J. Manton, *Aust. Dental J.* **52**, 243–248 (2007).
14. A. Kowalczyk, B. Botuliński, M. Jaworska, A. Kierklo, M. Pawińska and E. Dabrowska, *Adv. Med. Sci.* **51** (Suppl. 1), 40–42 (2006).
15. K. J. Cross, N. L. Huq and E. C. Reynolds, *Curr. Pharm. Des.* **13**, 793–800 (2007).
16. GC Corp., GC Tooth Mousse (2004), available at: http://www.gcasia-mi.com/GC_tm.pdf
17. O. A. Adebayo, M. F. Burrow and M. J. Tyas, *J. Dentistry* **35**, 862–870 (2007).
18. C. A. Moule, F. Angelis, G. H. Kim, S. Le, S. Malipatil, M. S. Foo, M. F. Burrow and D. Thomas, *Aust. Dental J.* **52**, 133–137 (2007).
19. J. Perdigão, P. Lambrechts, B. Van Meerbeek, A. R. Tomé, G. Vanherle and A. B. Lopes, *Dental Mater.* **12**, 262–271 (1996).
20. S. S. Oliveira, S. J. Marshall, J. F. Hilton and G. W. Marshall, *Biomaterials* **23**, 4105–4112 (2002).
21. D. H. Pashley, H. Sano, B. Ciucchi, M. Yoshiyama and R. M. Carvalho, *Dental Mater.* **11**, 117–125 (1995).
22. H. Sano, T. Shono, H. Sonoda, T. Takatsu, B. Ciucchi, R. M. Carvalho and D. H. Pashley, *Dental Mater.* **10**, 236–240 (1994).
23. D. H. Pashley, R. M. Carvalho, H. Sano, M. Nakajima, M. Yoshiyama, Y. Shono, C. A. Fernandes and F. Tay, *J. Adhesive Dentistry* **1**, 299–309 (1999).
24. C. J. Soares, P. V. Soares, P. C. F. Santos-Filho and S. R. Armstrong, *J. Dental Res.* **87**, 89–93 (2008).
25. N. Betamar, G. Cardew and R. Van Noort, *J. Adhesive Dentistry* **9**, 159–168 (2007).
26. P. G. Waidyasekera, T. Nikaido, D. D. Weerasinghe and J. Tagami, *J. Dentistry* **35**, 915–922 (2007).
27. V. Sattabanasuk, M. F. Burrow, Y. Shimada and J. Tagami, *Aust. Dental J.* **51**, 162–169 (2006).
28. D. Tantbirojn, A. Huang, M. D. Ericson and S. Poolthong, *J. Dentistry* **36**, 74–79 (2008).
29. K. Yamaguchi, M. Miyazaki, T. Takamizawa, H. Inage and B. K. Moore, *J. Dentistry* **34**, 230–236 (2006).
30. B. Van Meerbeek, J. De Munck, Y. Yoshida, S. Inoue, M. Vargas, P. Vijay, K. Van Landuyt, P. Lambrechts and G. Vanherle, *Oper. Dentistry* **28**, 215–235 (2003).
31. K. Yamaguchi, M. Miyazaki, T. Takamizawa, H. Inage and H. Kurokawa, *Caries Res.* **41**, 204–207 (2007).
32. Y. Yoshida, K. Nagakane, R. Fukuda, Y. Nakayama, M. Okazaki, H. Shintani, S. Inoue, Y. Tagawa, K. Suzuki, J. De Munck and B. Van Meerbeek, *J. Dental Res.* **83**, 454–458 (2004).

Amorphous Calcium Phosphate Composites and Their Effect on Composite–Adhesive–Dentin Bonding

J. M. Antonucci [a], **J. N. R. O'Donnell** [b], **G. E. Schumacher** [b] **and D. Skrtic** [b,*]

[a] Polymers Division, National Institute of Standards and Technology, Gaithersburg, MD 20899, USA
[b] American Dental Association Foundation, Paffenbarger Research Center, Gaithersburg, MD 20899, USA

Abstract

This study evaluates the bond strength and related properties of photo-polymerizable, remineralizing amorphous calcium phosphate (ACP) polymeric composite–adhesive systems to dentin after various periods of aqueous aging at 37°C. An experimental ACP base and lining composite was made from a photo-activated resin comprising 2,2-bis[p-(2′-hydroxy-3′-methacryloxypropoxy)phenyl]propane (Bis-GMA), triethylene glycol dimethacrylate (TEGDMA), 2-hydroxyethyl methacrylate (HEMA) and zirconyl dimethacrylate (ZrDMA); designated BTHZ. An experimental orthodontic composite was formulated from a photo-activated resin comprising ethoxylated bisphenol A dimethacrylate (EBPADMA), TEGDMA, HEMA and methacryloxyethyl phthalate (MEP); designated ETHM. In both composite series three fillers were compared: (i) freshly precipitated zirconium-modified ACP (as-prepared Zr-ACP), (ii) milled Zr-ACP and (iii) an ion-leachable fluoride glass. In addition to the shear bond strength (SBS), work to fracture and failure modes of the orthodontic composites were determined. The SBS of the base and lining ACP composites appeared unaffected by filler type or immersion time. In the orthodontic ACP composite series, milled ACP composites showed initial mechanical advantages over as-prepared ACP composites and produced higher incidence of a failure mode consistent with stronger adhesion. After six months of aqueous exposure, 80% of specimens failed at the dentin–primer interface, with a 42% overall reduction in bond strength. BTHZ and ETHM based ACP composites are potentially effective anti-demineralizing–remineralizing agents with possible clinical utility as protective base-liners and orthodontic cements, respectively. The analysis of the bond strength and failure modalities suggests that milled ACP composites may offer greater potential in clinical applications.

Keywords

Amorphous calcium phosphate, photo-polymerizable composites, shear bond strength, dentin

* To whom correspondence should be addressed. Tel.: 301 975 3541; Fax: 301 963 9143; e-mail: drago.skrtic@nist.gov

Official contribution of the National Institute of Standards and Technology; not subject to copyright in the United States.

Adhesion Aspects in Dentistry
© Koninklijke Brill NV, Leiden, 2009

1. Introduction

Calcium phosphate-based restoratives are generally appealing due to their biocompatibility. Specifically, amorphous calcium phosphate (ACP)-containing dental materials may provide an extended supply of Ca and PO_4 ions needed to re-form damaged mineral structures, thus counteracting the recurrent decay that is known to develop near the surfaces of teeth in contact with conventional fillings (almost 50% of all dental fillings require replacement because of recurrent caries). Such cariostatic ACP composites may be particularly useful for patients who are susceptible to caries as a result of radiation therapy and diseases or medications that cause dry mouth. When embedded in polymerized methacrylate matrices and exposed to an aqueous environment, ACP releases sufficient remineralizing Ca and PO_4 ions in a sustained manner to promote redeposition of thermodynamically stable, apatitic tooth mineral [1, 2].

A problem with dental composites of all types is their inability to resist cracking under masticatory stress due to their relatively low strength and toughness. In the case of ACP composites the uncontrolled aggregation of ACP particles was identified as one of the main reasons for a poor interfacial interaction with dental resins that contributes to the mechanical instability of these materials [3] and their inferiority when compared with silanized glass-reinforced composites. To overcome this shortcoming we have focused on developing strategies for improving the ACP filler/polymer matrix interfacial properties (and, in turn, composite properties) by better controlling the particle size distribution and surface properties of ACP fillers or by fine-tuning the resin [4–8]. Formulating ACP base and lining material and developing ACP adhesive cements capable of minimizing the demineralization that frequently occurs under orthodontic brackets are major goals of this ongoing research. Towards this end, extensive physicochemical studies have been and continue to be performed in our group on various ACP polymeric composites.

In this study, we report on the adhesive properties of experimental, photopolymerizable ACP composites formulated for base and lining and orthodontic applications. The first working hypothesis was that bioactive, hybridized ACP filler, when used in composites, will not adversely affect the strength of the composite–adhesive–dentin bond in comparison with similar glass-filled composites based on the same resins after various periods of aqueous immersion. Both as-prepared and milled ACP composites were used in this study to assess the possible correlation between the ACP particle size and state of agglomeration and the composite adhesive properties. The second working hypothesis was that the improvements offered by milling ACP will increase the uniformity at the adhesive–composite interface, reduce the incorporation of flaws and aid maintenance of the bond strength over longer periods of aqueous immersion. The work to fracture and failure modality of de-bonded composites also were utilized to differentiate the more subtle variations in mechanical and fracture behavior of these composites.

2. Materials and Methods

2.1. Resin Formulations

Two matrix resins were formulated from commercially available monomers (Esstech, Essington, PA, USA). The chemical nomenclature and the corresponding acronyms used here of the resin and photo-initiator system components are listed in Table 1. The compositions of the resins are provided in Table 2. Both BTHZ and ETHM resins were photo-activated by the addition of CQ and 4EDMAB (Aldrich Chemical Company, Milwaukee, WI, USA) as photo-activator and photo-reductant components, respectively, of the photo-initiator system.

2.2. Synthesis and Physicochemical Characterization of ACP Fillers

ACP fillers were synthesized following a modified preparation protocol proposed by Eanes *et al.* [9]. The hybridizing agent, $ZrOCl_2$ was used to introduce zirconia

Table 1.
Monomers and components of photo-initiator system employed in the study

Chemical name	Acronym	Type or function
2,2-Bis[p-(2′-hydroxy-3′-methacryloxypropoxy)phenyl]propane	Bis-GMA	Base monomer
Ethoxylated bisphenol A dimethacrylate	EBPADMA	
Triethylene glycol dimethacrylate	TEGDMA	Diluent monomer
2-Hydroxyethyl methacrylate	HEMA	Surface active monomer
Methacryloxyethyl phthalate	MEP	
Zirconyl dimethacrylate	ZrDMA	
Camphorquinone	CQ	Photo-activator
Ethyl-4-N,N-dimethylaminobenzoate	4EDMAB	Photo-reductant

Table 2.
Composition (mass fraction, %) of the resins evaluated in the study

Component	BTHZ* resin	ETHM** resin
Bis-GMA	35.5	–
EBPADMA	–	62.8
TEGDMA	35.5	23.2
HEMA	27.0	10.4
ZrDMA	1.0	–
MEP	–	2.6
CQ	0.2	0.2
4EDMAB	0.8	0.8

*, ** Resin acronyms are obtained by combining the initial letter of the acronym for each monomeric constituent of the matrix.

into precipitating ACP at a mole fraction of 10% based on Ca content. The resulting zirconia-hybridized filler is designated Zr-ACP. To avoid exposure to moisture that may lead to the premature conversion of ACP into crystalline apatite, the filler was kept over anhydrous calcium sulfate under vacuum (2.7 kPa) until used in composite formulation (as-prepared Zr-ACP) or after being milled (milled Zr-ACP). The amorphous state of the as-prepared Zr-ACP was verified by powder X-ray diffraction (XRD; Rigaku X-ray diffractometer; Rigaku-USA Inc., Danvers, MA, USA) and Fourier-transform spectroscopy (FTIR; Nicolet Magna-IR FTIR System 550, Nicolet Instrument Corporation, Madison, WI, USA). Wet ball-milling of Zr-ACP powder was performed as follows: 25 g Zr-ACP, 500 g high density ZrO_2 grinding balls (diameter = 2 mm; Glen Mills Inc., Clifton, NJ, USA) and 150 ml analytical grade isopropanol (J. T. Baker, Phillipsburg, NJ, USA) were sealed in the grinding jar and milled for 2 h at 400 rpm with rotation direction being reversed every 15 min (programmable planetary mill PM100; Retch Inc., Newton, PA, USA). Milled Zr-ACP was separated from the grinding balls by sieving and the remaining isopropanol was evaporated in a vacuum oven (24 h at 70°C). The dry milled powder was then screened by XRD and FTIR to verify that no detectable conversion to apatite had occurred during the milling process, examined by scanning electron microscopy (SEM), and its particle size distribution (PSD) was determined. Fluoride-releasing, strontium glass (Sr-glass) was used as received from the manufacturer (Caulk Dentsply, Milford, DE, USA). The particle size distribution (PSD) of the fillers was determined using laser obscuration concurrently with a computerized inspection system (CIS-100 Particle Size Analyzer; Ankersmid Ltd., Yokneam, Israel). Approximately 3 mg of filler was dispersed in 3 g of ETHM resin and the suspension briefly ground with a mortar and pestle to simulate the effect of hand spatulation. Five replicate measurements were performed for each filler type.

2.3. Preparation of Composites

The photo-polymerizable ACP composite pastes were made by hand-blending the BTHZ or ETHM resin (mass fraction 60%) with as-prepared Zr-ACP and milled Zr-ACP (mass fraction 40%). Almost double the amount of Sr-glass (mass fraction 75%) was combined with the resins (mass fraction 25%) to achieve the same consistency of the glass-filled composite pastes. The homogenized pastes were kept under a moderate vacuum (2.7 kPa) overnight to reduce the air entrained during mixing.

2.4. Bonding Protocol

To test the shear bond strength (SBS) of the experimental composites to dentin through an adhesive system, the occlusal surfaces of extracted, caries-free, human molars were removed and their roots embedded in polycarbonate holders with chemical curing poly(methyl methacrylate) tray resin (Bosworth Fastray Powder and Liquid, Bosworth Company, Skokie, IL, USA). The exposed dentin surfaces were ground flat perpendicular to the longitudinal axis of the teeth with 320 grit silicon carbide paper (Fig. 1(a)). The bonding protocol included the following steps.

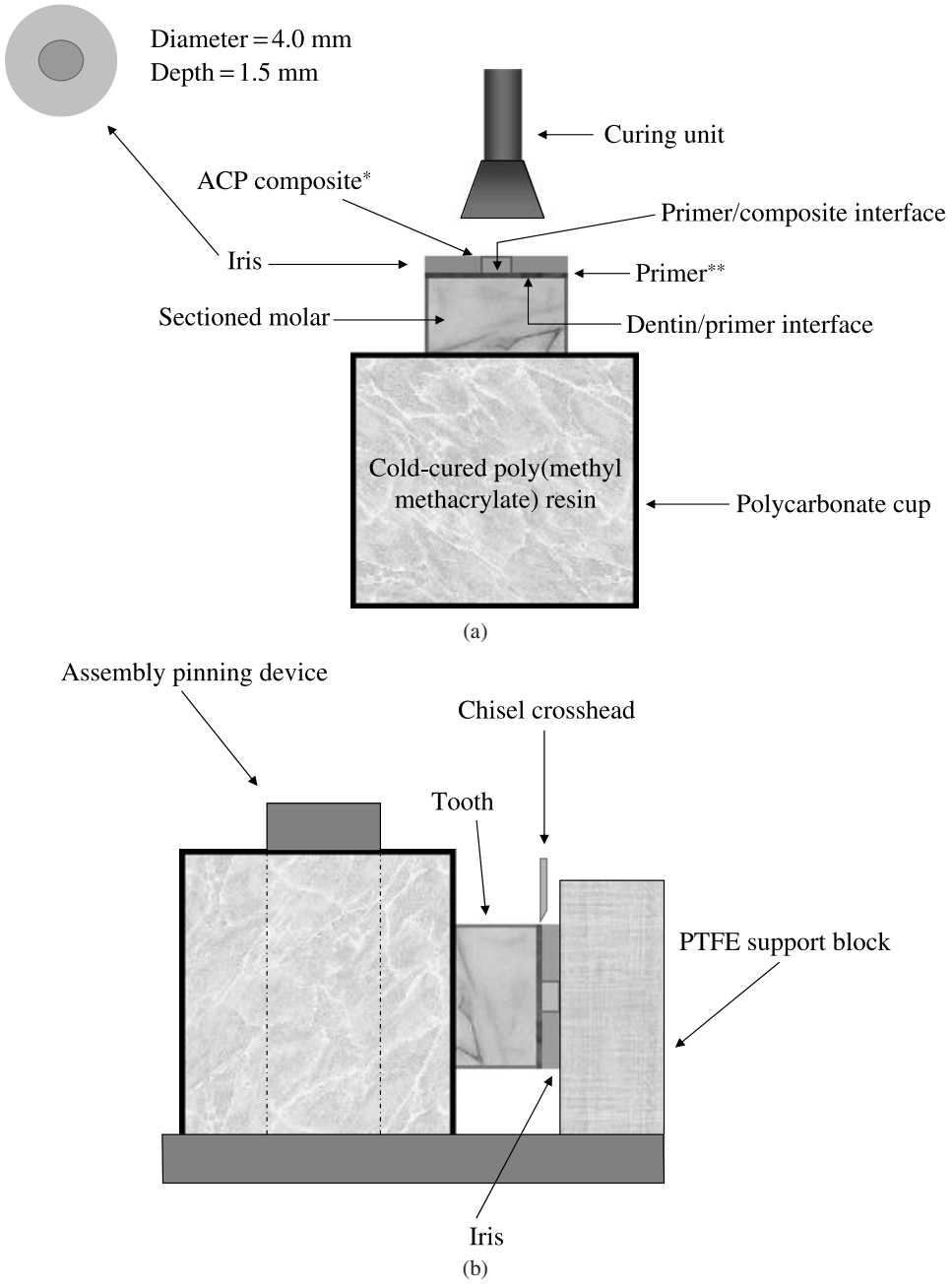


Figure 1. Schematic of bonding protocol (a) and the shear bond strength measurement assembly (b). *ACP base-lining composite plus TPH or orthodontic ACP composite alone: **NPG + PMDMA (base-lining ACP composite specimens) or PMDMA only (orthdodontic ACP composite specimens).

Ground dentin surfaces were first dried, then etched for 15 s with phosphoric acid gel (mass fraction H_3PO_4 38%; Etch-Rite®, Pulpdent Corporation, Watertown, MA, USA). The acid was rinsed away with distilled water for 10 s, and a moistened paper towel (Kimwipes®; Kimberly-Clark Global Sales, Inc., Roswell, GA, USA) was used to blot the surface to a near-dry condition. Two protocols were used to prime the moist dentin surfaces. In the ACP base-lining composite series, dentin surfaces were sequentially primed first with N-phenylglycine (NPG; mass fraction 5%) solution in acetone for 30 s, and then with five consecutive coats of pyromellitic glycerol dimethacrylate (PMGDMA; mass fraction 20%) in acetone solution and camphorquinone (CQ; mass fraction 0.028%) as photo-activator. In the ACP orthodontic composite series, only one coating of PMGDMA-acetone primer (DenTASTIC UNO, Pulpdent Corporation, Watertown, MA, USA) was applied. Following the application of NPG and PMGDMA, or PMGDMA alone, the surfaces were air-dried for 10 s to remove acetone and visible-light cured for 10 s (Spectrum Curing Light, Dentsply Caulk Limited, Milford, DE, USA). A poly(tetrafluoroethylene) (PTFE)-coated iris (4 mm in diameter and 1.5 mm thick) that defined the bonding area was positioned on the tooth surface, filled by the experimental composite and light-cured for 20 s for the experimental base-liner composites and 60 s for the orthodontic composites. ACP base-liner specimens were completed by applying a commercial resin-based composite (TPH, Dentsply Caulk, Milford, DE, USA), which was cured for an additional 60 s. The assemblies were then exposed to air for 5 min to allow further dry-curing at room temperature, after which they were immersed at 37°C in either distilled water (ACP base-liner series) or a saliva-like solution [10] (orthodontic ACP series) for up to 6 months.

2.5. Shear Bond Strength (SBS) Measurements

De-bonding was performed by using the shear test method [11] with a computer-controlled universal testing machine (Instron 5500R, Instron Corp., Canton, MA, USA). Specimens were placed in the test apparatus and fixed such that their iris surface was flush against the PTFE support block (Fig. 1(b)). The SBS was determined normal to the longitudinal axis of the tooth, at a crosshead speed of 0.5 mm/min. It was calculated according to the following equation:

$$\mathrm{SBS} = \frac{4P}{\pi D^2}, \tag{1}$$

where P = applied load at failure and D = diameter of the cured composite as defined by the inner diameter of the iris.

2.6. Fracture Surface Evaluation

Initial qualitative assessments of specimen fracture surfaces (tooth and iris) were made immediately after testing using a stereomicroscope at various magnifications (Leica StereoZoom 6, Leica Microsystems, Wetzlar, Germany), and any observations regarding the surface condition (i.e., irregularities, general mode of failure) were recorded. Tooth and iris surfaces were then digitally photographed (Leica

MZ16 Optical Stereomicroscope, Wetzlar, Germany; QCapture Pro, QImaging Corporation, Surrey, British Columbia, Canada) and imaging software was used to measure the surface areas of different failure modes (ImageJ, National Institutes of Health, Bethesda, MD, USA).

2.7. Statistical Analysis

Experimental data were analyzed by ANOVA ($\alpha = 0.05$). Significant differences between specific groups were determined by all pair-wise multiple comparisons (two-tail t-test; unequal variances). One standard deviation (SD) is given in this paper for comparative purposes as the estimated standard uncertainty of the measurements.

3. Results

The amorphous character of the as-prepared and unmilled ACP fillers utilized in the study was verified by XRD and FTIR analysis (spectra not shown). Their XRD patterns consisted of two diffuse broad bands in $2\theta = 4$–$60°$ region, while the FTIR spectra showed wide absorbance bands typical for non-crystalline phosphates in the 1200–900 cm^{-1} and 630–500 cm^{-1} regions. PSD data (Fig. 2) indicate that the milling process reduced the median diameter (d_m) of ACP by almost 95%, i.e., from 58.23 ± 14.44 μm for as-prepared Zr-ACP to 3.10 ± 0.88 μm for milled Zr-ACP. The Sr-glass filler had a d_m of 2.64 ± 0.86 μm and its volume distribution was close to that of the milled Zr-ACP.

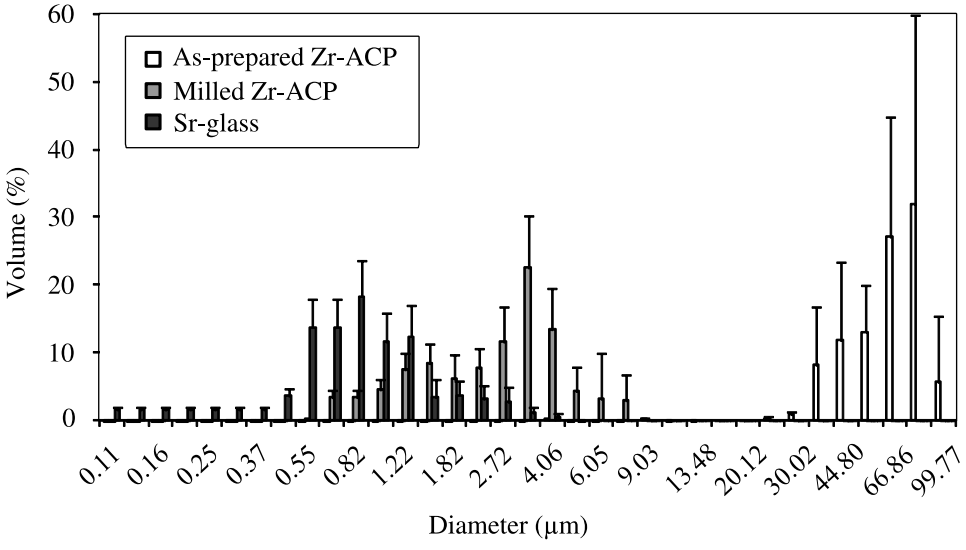


Figure 2. Differential volume particle size distributions of as-prepared Zr-ACP, milled Zr-ACP and Sr-glass used in the study. Indicated values represent the means of five replicate runs in each group. Standard deviation (SD) is indicated by bars.

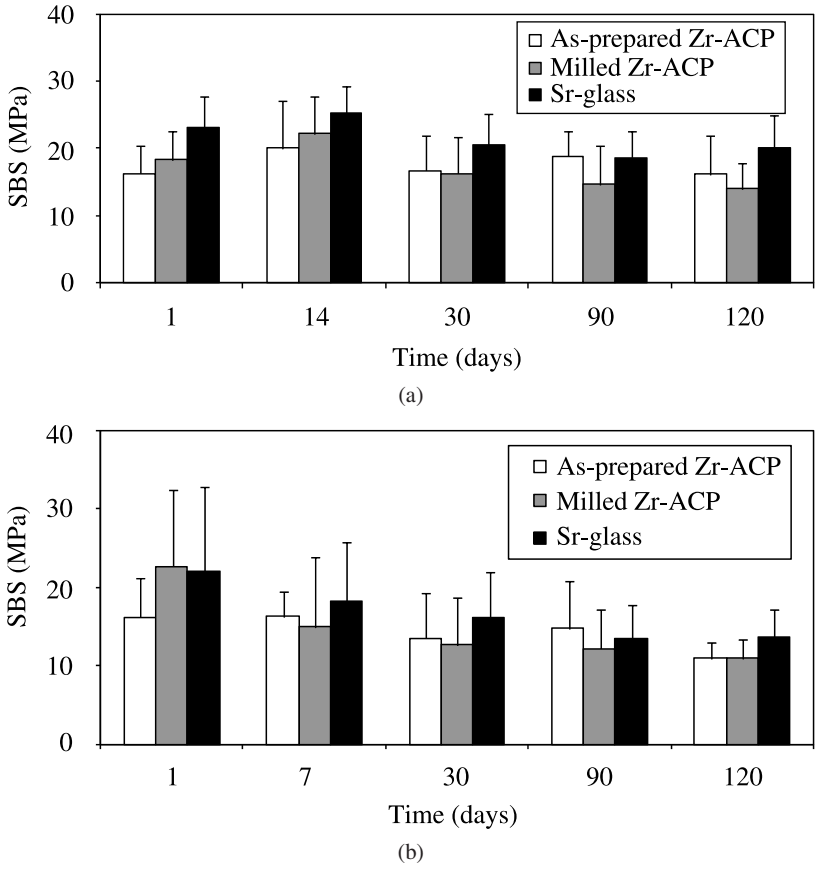


Figure 3. Shear bond strength (SBS) of the base-lining experimental composites (a) and the orthodontic experimental composites (b) as a function of aging time. Indicated are the mean values + one standard deviation (SD) for the number of specimens $n \geqslant 7$ (a) and $n \geqslant 5$ (b).

The aging-related changes in the SBS values of the experimental base-lining composites (BTHZ resin matrix; Fig. 3(a)) and of the experimental orthodontic composites (ETHM resin matrix; Fig. 3(b)) showed identical patterns. All-pair comparisons revealed stronger bonds for Sr-glass composite groups compared with both types of ACP composite only for the 24 h immersion data. At longer time intervals, the differences in mean values between the filler groups were not statistically significant.

The failure analysis by optical microscopy of de-bonded specimens in base-lining composite group was performed on a limited number of specimens (8/group). After 2 weeks of water storage failures occurred predominantly at the dentin–adhesive resin interface regardless of the type of the filler. Further study of the fracture surfaces obtained upon de-bonding of the experimental orthodontic composites pointed to three distinct modes of failure: cohesive failure within the composite and adhesion failures at either the dentin–primer or primer–composite interface. Typ-

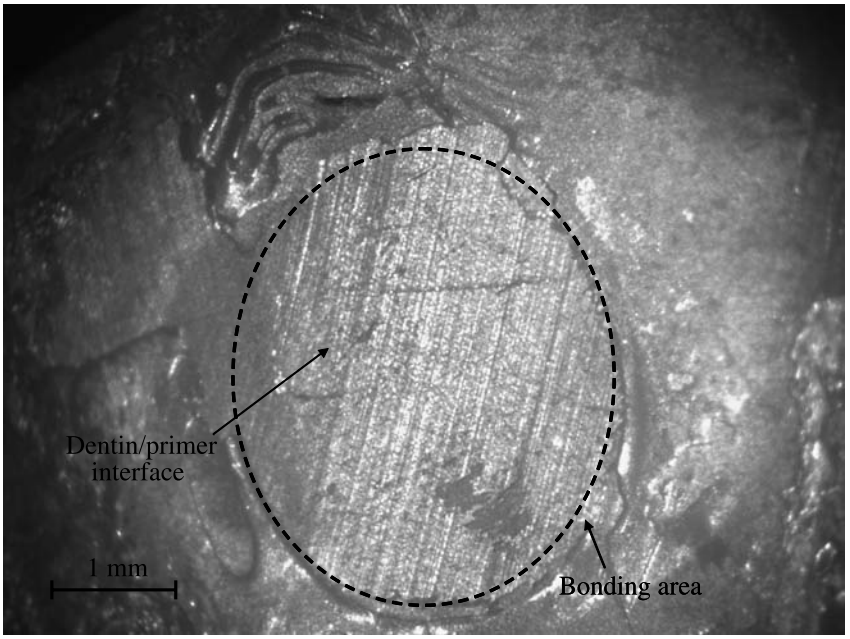
ical examples of different fracture surfaces are shown in Fig. 4(a–d). The failure modes were broken down into two subcategories: complete, in which the fracture surface showed only composite or adhesive interface, and dominant, in which the fracture surface showed mixed adhesive and composite interfaces, with the majority occupied by composite or an adhesive interface. The distinction between complete and dominant was made in order to shed light on differences in mechanical behavior brought about by the transition from complete to mixed interfacial failures. A breakdown of the observed failure modes for the orthodontic composites is provided in Fig. 5.

A fracture surface common to both complete and most dominant dentin–primer failures is illustrated in Fig. 4(a). Regions of visible dentin are denoted as 'dentin–primer interface'. The parallel grinding lines that continue outside of the dotted circle that delineates the bond area are referred to as a 'peel layer'. Fig. 4(b) is typical of the primer–composite failure mode. In this type of failure, primer appears on the surface in the form of parallel or fanned striations, possibly indicating that the primer itself had failed cohesively. Striations are distinguishable from the grinding lines by their visibly raised surfaces (grinding lines are shallow enough that areas on which they occur appear flat). Aside from containing all three distinct failure modes, the bond area shown in Fig. 4(c) shows a region of flat, uniform primer surface suggestive of de-lamination at the interface and indicates poor adherence of the composite. Fig. 4(d) is representative of a complete cohesive failure, marked by the raised, irregular surface of the composite.

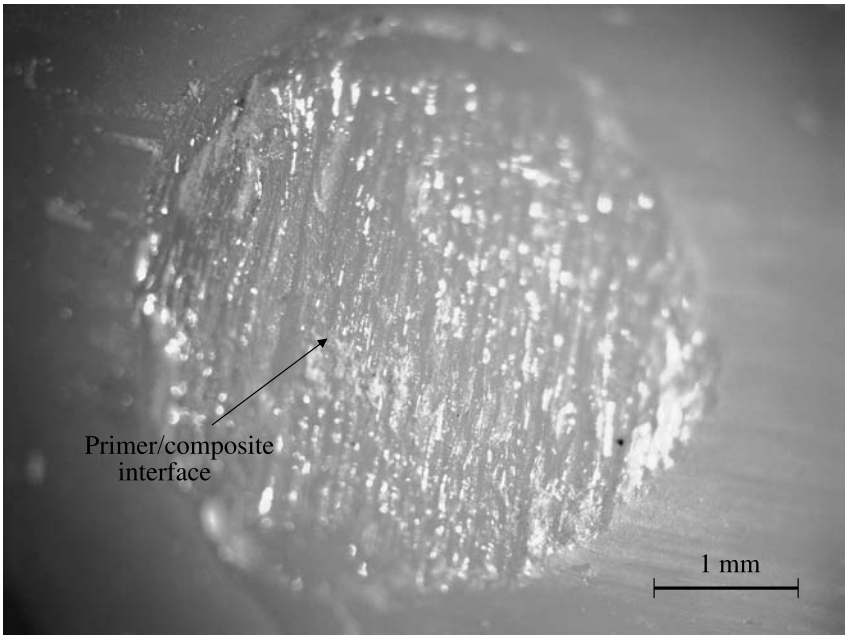
Dominant failure at the dentin–primer interface occurred in 43% of all specimens. The corresponding complete interfacial failures accounted for 22% of the observed fracture surfaces. Complete failure at the primer/composite interface accounted for less than 7% of failures, and did not occur at every immersion time. The same is true of complete and dominant cohesive failures within the composite, which accounted for 5% of the observed failures. However, cohesive failures occurred only for Sr-glass composites, with the SBS of complete cohesive failures consistently in the top 15% of all treatments at corresponding immersion times.

4. Discussion

To obtain a dental resin with a tractable viscosity for composite formulation we have included into BTHZ formulation considerable amounts of the more flexible TEGDMA and HEMA (an adhesion-to-dentin-promoting co-monomer). The additive ZrDMA was included to improve inorganic–organic interface coupling. The fluid nature of BTHZ plus the intensified hydrogen bonding that occurs in matrices with relatively high HEMA contents (BTHZ resin contained mass fraction of 27% HEMA) favor formation of highly-converted, densified polymeric matrices [12] that also may have an important role in determining the bonding properties of their composites.

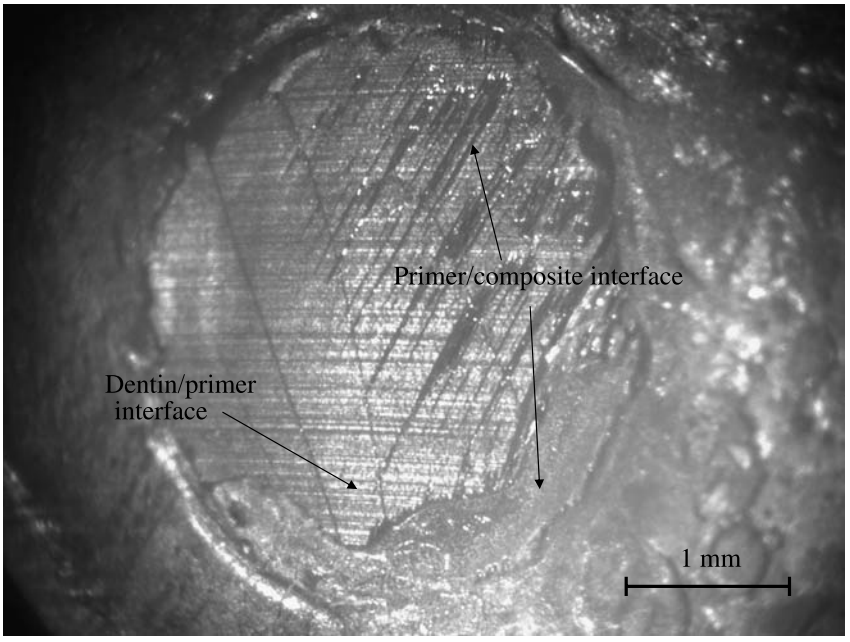


(a)

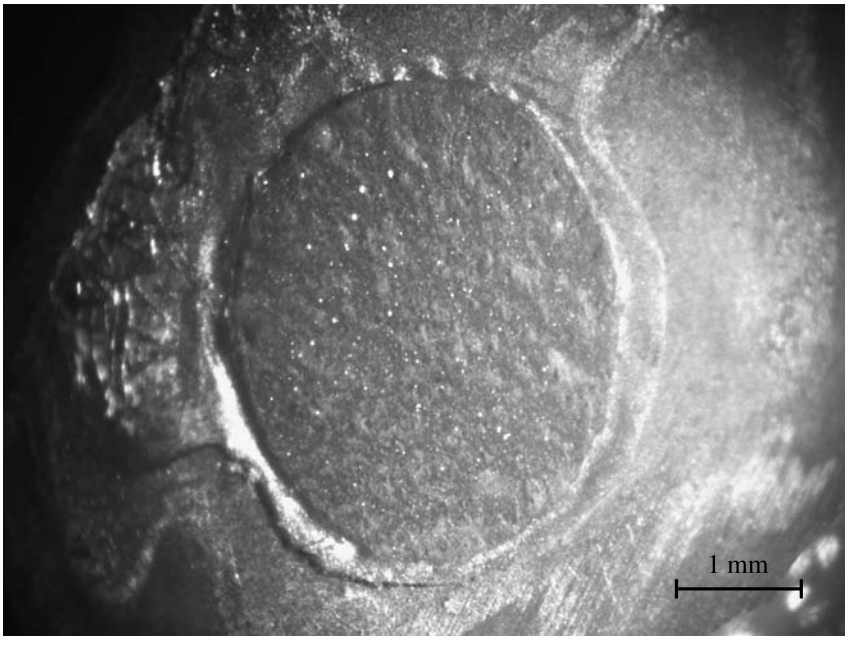


(b)

Figure 4. Typical examples of an adhesion failure at the dentin–primer interface (a), failure at the primer–composite interface (b), adhesion failure at both interfaces, as well as cohesive failure within the composite (c) and a cohesive failure within the composite (d).



(c)



(d)

Figure 4. (Continued.)

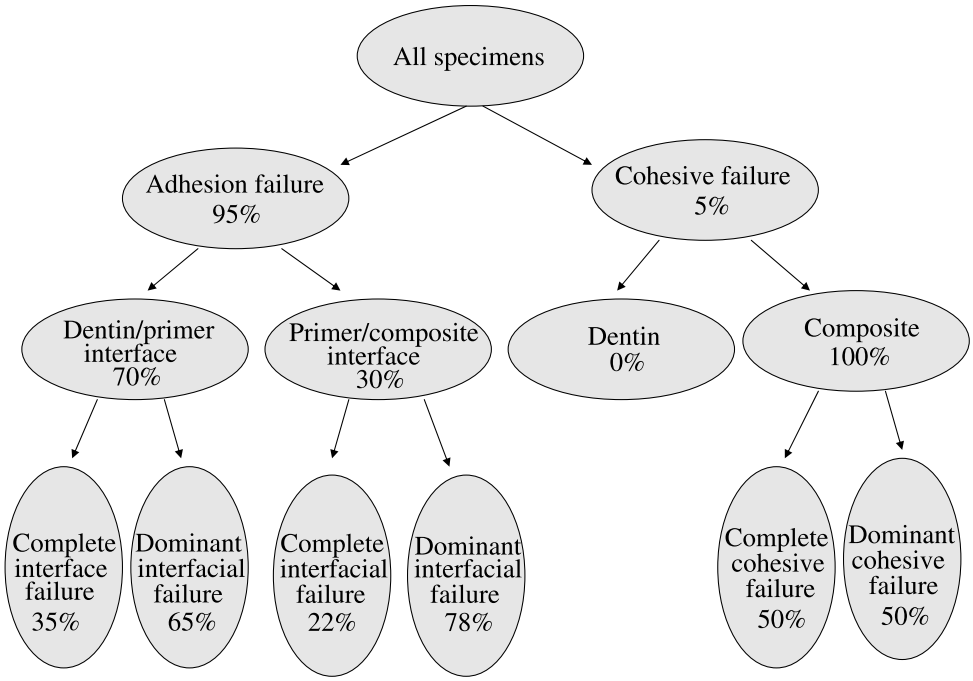


Figure 5. A breakdown of the observed failure modes for the orthodontic composites (as-prepared Zr-ACP, milled ACP and Sr-glass formulations combined) indicating the percentage of specimens that fall under each category.

We have shown [3, 5, 13] that as-prepared Zr-ACP, which is highly agglomerated, disperses unevenly throughout matrices regardless of the compositional makeup of the resin. The existence of large agglomerates in the resin leads to inadequate wetting of the filler and results in composite surface irregularities. Additionally, the ACP filler–matrix interface is predisposed to random spatial and other changes during water sorption as a result of continuous mineral ion release from composites. As a result, composites formulated with the as-prepared Zr-ACP generally exhibit lower strength and are more affected by water exposure than the corresponding unfilled copolymer resins [1]. In recent studies it was shown [14] that employing resin matrices based on the use of the more flexible, low viscosity, EBPADMA instead of the rigid, high viscosity, and somewhat more hydrophilic Bis-GMA along with milled Zr-ACP instead of as-prepared Zr-ACP, resulted in composites of improved mechanical stability, even under aqueous challenge. Contrary to that study, the SBS results reported here showed practically no improvement with the use of milled Zr-ACP filler.

It is generally accepted that, in addition to the chemical and physical bonding to the substrate, gradients in fracture toughness and elastic modulus across the bonded interface are most likely the governing factors in the joint strength and durability of the composite–dentin bond. Another factor may be the adhesion

test methodology. The chisel-on-iris shear method used here may not be sensitive enough to detect subtle differences in the adhesiveness of the tested materials and, perhaps, the wire-loop-on-composite shear bond test, which would involve much higher stress concentrations, might be a more appropriate test to discriminate the adhesive properties of the composites. Uniaxial tensile test methods such as the micro-tensile method also should have greater sensitivity than shear methods in elucidating dentin adhesion. Although other factors, such as tooth-intrinsic flaws and the method of dentin pre-treatment, may have a decisive function in determining the strength of the composite–adhesive–dentin bond, the possible role of the filler type certainly cannot be ignored. However, the results of this study have shown that as-prepared and milled Zr-ACP, despite the flaws that as-prepared ACP filler may introduce into the microstructure of composites, did not adversely affect their short and mid-term bonding behavior to adhesive resins. Composites formulated with either type of Zr-ACP performed at least as well as Sr-glass-reinforced composites, while providing an additional bioactive component that may arrest demineralization and possibly promote remineralization of enamel and dentin. This study suggests that the experimental Zr-ACP–BTHZ resin composite may be a suitable lining or base material with the viscosity of a flowable composite and sufficient strength to serve as a base material [2]. The Zr-ACP–ETHM formulation may be well suited as a cement for orthodontic application, aiding in minimizing the demineralization of enamel often seen adjacent to and under the brackets.

Testing the SBS of strong adhesives commonly produces cohesive failures in dentin [15, 16], a failure mode not usually observed in clinical settings. In this study, the majority of failure modes were observed to occur at the interface between the primer and dentin substrate, and very rarely within the composite itself (indeed, never for milled ACP composites). This suggests strongly that some critical discrepancies exist between the test methods and the clinical situations they are intended to mimic. It follows, then, that an entirely new adhesion test needs to be developed or that existing methods need to be altered to improve their clinical relevance. Additionally, the high degree of scatter inherent in shear bond test methods is a problem that continues to require attention. The biological variability of the human species and anisotropic nature of the tooth itself both present significant obstacles to accurate, reliable measurements, and though widespread test standardization (loading mechanism, crosshead speed, etc.) may achieve some progress in this direction, altering the test method in the interest of clinical relevance might prove more beneficial in the long run. Therefore, modifying the SBS test method to include a fatigue component [17–20] or combined fatigue and modified-bond-geometry (e.g., micro-shear and micro-tensile) approach may be indicated for future studies.

5. Conclusions

The type of bioactive ACP filler and its particle size distribution did not significantly affect the strength of the composite–adhesive–dentin bond for these experimen-

tal, anti-demineralizing–remineralizing resin composites. Composites formulated with milled ACP produced a higher incidence of the failure mode consistent with stronger adhesion, thus offering a potential advantage in clinical bonding applications.

Acknowledgements

Reported work was supported by the National Institute of Dental and Craniofacial Research (NIDCR: grant DE 13169 to the American Dental Association Foundation (ADAF) and the National Institute of Standards and Technology (NIST)/NIDCR Interagency Agreement YI-DE-7005-01). It is a part of the dental material research program conducted by NIST in cooperation with ADAF and was also supported by both NIST and ADAF. Generous contribution of the monomers from Esstech, Essington, PA, USA, is gratefully acknowledged.

Disclaimer

Certain commercial materials and equipment are identified in this article to specify the experimental procedure. In no instance does such identification imply recommendation or endorsement by NIST or ADAF or that the material and equipment identified is necessarily the best available for the purpose.

References

1. D. Skrtic, J. M. Antonucci and E. D. Eanes, *J. Res. (Natl. Inst. Stands. Technol.)* **108**, 167 (2003).
2. J. M. Antonucci and D. Skrtic, in: *Polymers for Dental and Orthopedic Applications*, S. W. Shalaby and U. Salz (Eds), pp. 217–242. CRC Press, Boca Raton, FL (2007).
3. D. Skrtic, J. M. Antonucci, E. D. Eanes and N. Eidelman, *Biomaterials* **25**, 1141 (2004).
4. J. M. Antonucci, D. Skrtic, A. W. Hailer and E. D. Eanes, in: *Polymeric Drugs & Drug Delivery Systems*, R. M. Ottenbrite and S. W. Kim (Eds), pp. 301–310. Technomics Publ. Co., Lancaster, PA (2000).
5. J. M. Antonucci and D. Skrtic, *J. Bioact. Compatible Polym.* **20**, 29 (2005).
6. J. M. Antonucci, D. W. Liu and D. Skrtic, *J. Dispersion Sci. Technol.* **28**, 819 (2007).
7. D. Skrtic, J. M. Antonucci, E. D. Eanes and R. T. Brunworth, *J. Biomed. Mater. Res.* **59**, 597 (2002).
8. D. Skrtic, J. M. Antonucci and D. W. Liu, *Acta Biomaterialia* **2**, 85 (2006).
9. E. D. Eanes, I. H. Gillessen and A. S. Posner, *Nature* **208**, 365 (1965).
10. J. M. Ten Cate and P. P. E. Duijsters, *J. Caries Res.* **16**, 201 (1982).
11. S. Venz and B. Dickens, *J. Dental Res.* **72**, 582 (1993).
12. D. Skrtic, J. W. Stansbury and J. M. Antonucci, *Biomaterials* **24**, 2443 (2003).
13. S. Y. Lee, W. F. Regnault, J. M. Antonucci and D. Skrtic, *J. Biomed. Mater. Res.* **80B**, 11 (2007).
14. D. Skrtic and J. M. Antonucci, *J. Biomater. Appl.* **21**, 375 (2007).
15. A. Versluis, D. Tantbirojn and W. H. Douglas, *J. Dental Res.* **76**, 1298 (1997).
16. D. H. Pashley, H. Sano, B. Ciucchi, M. Yoshiyama and R. M. Carvalho, *Dental Mater.* **11**, 117 (1995).

17. R. Frankenberger, N. Krämer and A. Petschelt, *Clin. Oral Invest.* **3**, 11 (1999).
18. R. Frankenberger, W. O. Strobel, N. Krämer, U. Lohbauer, J. Winterscheidt, B. Winterscheidt and A. Petschelt, *J. Biomed. Mater. Res.* **67B**, 712 (2003).
19. R. Frankenberger, D. H. Pashley, S. M. Reich, U. Lohbauer, A. Petschelt and F. R. Tay, *Biomaterials* **26**, 2043 (2005).
20. M. J. Soappman, A. Nazari, J. A. Porter and D. Arola, *Dental Mater.* **23**, 608 (2007).

Adhesive Cementation and the Strengthening of All-Ceramic Dental Restorations

Garry J. P. Fleming [a,*] **and Owen Addison** [b]

[a] Materials Science Unit, Division of Oral Biosciences, Dublin Dental School & Hospital, Trinity College Dublin, Dublin, Ireland

[b] Biomaterials Unit, School of Dentistry, University of Birmingham, St. Chad's Queensway, Birmingham B4 6NN, UK

Abstract

Dental ceramics are extensively used to restore damaged or missing tooth structure but these fracture in service. Finite element analysis and quantitative fractography of failed restorations have demonstrated that all-ceramic crowns fracture due to the extension of pre-existing surface defects that occupy the inner 'fit' surface of the restoration under tensile loading. Clinically the environment of the inner surface defects is influenced by the dental cement used to retain the restoration on the prepared tooth structure. The use of methacrylate resin-based cements is associated with enhanced clinical performance and *in vitro* laboratory investigations have demonstrated that thin coatings of resin-based cements can significantly increase the flexural strength of a number of all-ceramic crown materials. Mechanisms to account for the apparent strengthening have been proposed including the generation of crack closure stresses, crack 'healing' effects and the creation of a 'hybrid layer' which radically modifies the stress patterns in the region of the critical defect. However, conjecture remains regarding the basis of the strengthening mechanism, thereby preventing the optimisation of resin-based cementation materials and clinical techniques. The aim of the current article is to provide an insight into resin cementation and the mechanisms by which adhesive cements may determine all-ceramic restoration performance.

Keywords

Dental ceramics, adhesion, resin-based cements, fracture

1. Introduction

Missing or damaged tooth structure is routinely replaced to prevent dental pain, sensitivity and infection, in addition to restoring masticatory function and aesthetics. Operative dental procedures to restore natural dentition are classified as direct or indirect techniques. Direct techniques require the placement, manipulation and finishing of the restorative material *in situ* within the oral cavity [1]. In contrast,

* To whom correspondence should be addressed. Tel.: 00 353 1 612 7371; Fax: 00 353 1 612 7297; e-mail: garry.fleming@dental.tcd.ie

Adhesion Aspects in Dentistry

© Koninklijke Brill NV, Leiden, 2009

indirect techniques require preparation of the tooth or teeth to a desired form prior to obtaining a physical or optical impression from which a bespoke prosthesis is designed and fabricated, usually within the environment of a dental laboratory. Finally, the manufactured prosthesis is cemented, a procedure traditionally described as 'luting', onto the prepared tooth to complete the restoration. Indirect operative techniques facilitate improved control over restoration shape and form and enable the use of a broader range of materials with varying mechanical and aesthetic properties [1]. Of the materials currently available to the dental practitioner to indirectly restore natural dentition, dental ceramics are most ideally equipped to mimic tooth structure in form, shade, translucency and lustre [2]. Dental ceramics are chemically stable, biocompatible, corrosion resistant and can be glazed to prevent the adherence of plaque and extrinsic staining. The highly abrasion resistant ceramic surface prevents the loss of surface texture and contour. In addition, the thermal conductivity and thermal expansion coefficient are comparable with natural tooth structure so that the marginal seal between restoration and tooth is less likely to be compromised during intra-oral thermal changes in service. The cementation of all-ceramic restorations involves the application of a small quantity of cement to the inner 'fit' surface(s) of the ceramic restoration prior to seating onto the prepared tooth under localised pressure. The cement sets due to a chemically and/or photo-initiated reaction and any excess cement exuded from the restoration margins is subsequently removed. The ideal dental cement requires a low film thickness to allow full seating of the ceramic restoration; a long working time to enable effective mixing and application of the cement; a short setting time so that the ultimate material properties are achieved quickly; a high compressive strength to prevent deterioration of the cement under occlusal loading; low solubility preventing wash out, marginal gap formation and microleakage in the oral environment; and the cement should be highly retentive preventing loss of the restoration in service [3]. In addition, the dental cement should not cause pulpal irritation thereby necessitating a low setting exotherm and thus a chemical composition that initiates a minimal response from pulpal and periodontal tissues is preferred [3].

2. The Development of All-Ceramic Restorations and Placement Techniques

The mechanical properties of dental ceramics are only partially adequate for the fabrication of dental restorations [4]. Although strong in compression, the traditionally utilised feldspathic dental ceramics have low tensile strength and lack fracture toughness [5]. Failure may be manifested by the development of unaesthetic fracture lines which can stain over time and act as a potential route for microleakage. Alternatively, fracture may be associated with a partial loss of ceramic fragments or the total loss of the restoration from the underlying tooth structure. Both scenarios can lead to unacceptable aesthetics, dentine sensitivity and the impairment of masticatory function. Axisymmetric finite element analysis [6] and quantitative fractography [7–10] have demonstrated that all-ceramic crown restorations commonly fail

from the extension of pre-existing defects present on the internal 'fit' surfaces of the restoration under tensile loading. In the latter half of the twentieth century two different approaches to prevent all-ceramic crown fracture were adopted. Advances in dental ceramic formulations and the introduction of novel processing routes resulted in improvements in the fracture toughness and average fracture strengths of ceramic materials used in crown manufacture [10]. Average flexure strengths, as reported by various investigators, have increased from 61 to 87 MPa for a traditional feldspathic dental ceramic [11–14], 70–229 MPa for a micaceous tetrafluorosilicate castable glass [5, 11, 12, 15, 16], 84–182 MPa for a leucite-reinforced glass ceramic [5, 12–14, 16–19], 236–547 MPa for a lanthanum aluminosilicate glass infused alumina [5, 12, 15, 16, 18, 19], 464–687 MPa for a sintered high purity alumina, and 800 to 1200 MPa for yttria stabilized zirconia [20] (Table 1). However, a disadvantage of many of the high strength ceramic systems is that the additional reinforcement is achieved at a cost of inferior aesthetics and in particular difficulties are associated with shade variation and a loss of translucency due to a volumetric increase in the ceramic crystalline phase [21]. As a result, additional processes are required to fulfil the aesthetic restorative requirements and include the application of extrinsic stains or, more commonly, the addition of an outer layer of a matched thermal expansion veneering ceramic. The thickness of the veneering ceramic is determined by the need to mask the high strength ceramic core but it has been suggested that bilayered ceramic restorations should be constructed from the strongest core material available, employed in the maximum achievable thickness and in contrast the veneer layer should be as thin as possible [22]. It has been demonstrated that an excessive thickness of veneering ceramic can result in ceramic chipping as a result of Hertzian contact damage at the veneering ceramic surface [23]. Despite the increased tensile strength and fracture toughness there has been no increase in clinical performance and the retrospective clinical data for these materials suggest the annual failure rates for all-ceramic crowns to be in the region of 3% [24].

An alternative approach to improving all-ceramic restoration performance became available as a consequence of improvements in dental adhesive technologies that allowed the development of operative procedures to intimately bond certain classes of dental ceramic materials, often in thin sections, to tooth structure. It was recognised that despite the minimal thicknesses of the inherently brittle dental ceramic employed the fracture resistance of the completed adhesively bonded restorations was surprisingly high. The aim of the current article is to provide an insight into the development of adhesively cemented all-ceramic dental restorations and the mechanism by which adhesive cements may determine all-ceramic restoration performance.

3. Cementation of All-Ceramic Restorations

The dental practitioner has a choice of a number of materials with which to cement all-ceramic restorations including zinc phosphate, zinc polycarboxylate, conven-

Table 1.
Flexural strength (MPa) of a feldspathic ceramic (Vita α dentine), micaceous tetrafluorosilicate castable glass ceramic (Dicor®), a heat-pressed leucite reinforced ceramic (IPS Empress®), a lanthanum aluminosilicate glass infused ceramic (Vita In-Ceram) and a high purity sintered aluminous core ceramic (Procera®) determined from three point bending (3PB), four point bending (4PB) and bi-axial flexure (BF) tested by various investigators a–j. Numbers in parentheses represent standard deviations. * number of samples not disclosed

Investigator	a [16]	b [5]	c [15]	d [11]	e [17]	f [12]	g [18]	h [19]	i [13]	j [14]
Strength determination	3PB ($n = 12$–20)	3PB (*)	4PB ($n = 15$)	3PB ($n = 10$–22)	3PB ($n = 10$)	4PB ($n = 30$)	BFS ($n = 10$)	3PB ($n = 5$)	3PB ($n = 20$)	BFS ($n = 20$)
Vita α dentine				63 (9)		61 (7)			61 (10)	68 (10)
Dicor®	229 (11)	114 (24)	72 (7)	125 (19)		70 (12)				
IPS Empress®	97 (19)	182 (26)			177 (13)	84 (11)	134 (22)	102 (10)	117 (32)	134 (22)
Vita In-Ceram	446 (44)	419 (62)	236 (22)		323 (52)	429 (87)	352 (113)	547 (75)		
Procera®					464 (41)		687 (58)			

tional glass-ionomer, resin modified glass-ionomer, and methacrylate resin-based cements [3, 25]. Traditionally zinc phosphate cements have been advocated for cementing all-ceramic restorations and are frequently described as 'luting' agents mediating restoration retention by acting as a space filler, micromechanically retained with no true adhesion to either the overlying ceramic or underlying tooth structure [26–28]. In contrast, zinc polycarboxylate cements were specifically engineered for dental applications and are adhesive to dental enamel and dentine. Adhesion is achieved as the polycarboxylate cement forms complexes with calcium ions present at the surface of hydroxyapatite crystals, the major inorganic component of tooth structure [26]. Adhesion to the underlying tooth structure is considered highly desirable by dental practitioners not only to enhance retention but to also prevent post-operative sensitivity and minimise the risk of bacterial microleakage. Glass-ionomer cements (glass polyalkenoate cements) are similarly adhesive to tooth structure by chelating with surface calcium ions and are increasingly favoured by dental operatives due to continued ion leaching of cariostatic fluoride ions [26]. However, zinc phosphate, zinc polycarboxylate and conventional glass-ionomer cements which are classified as acid–base cements [27, 28], exhibit a low pH after initial manipulation which increases towards neutrality during the setting reaction [29]. It has been demonstrated that initial acidity of the mixed cement and the subsequent setting kinetics influencing pH are sensitive to the mixing ratio of the powder and liquid cement components [27]. Furthermore, it has been suggested that the low pH associated with unset acid–base cements may contribute to the extension of flaws occupying the inner 'fit' ceramic surface and therefore weakening the restoration [27]. Resin modified glass-ionomer cements were developed to increase the setting time of conventional glass-ionomer cements [26]. The introduction of a mixture of polymerisable monomers and/or polycarboxylic acid along with a photo-initiator facilitated a 'command set' cement. However, the materials are not commonly employed to cement all-ceramic restorations due to the excessive levels of hygroscopic expansion which has been implicated in the premature failure of all-ceramic restoration as a result of the creation of detrimental tensile stresses at the internal ceramic surface [30]. In contrast, methacrylate resin-based cements have become increasingly popular for the cementation of all-ceramic restorations and provide improved retention due to the reliable bonding achievable at both resin–ceramic and resin–tooth interfaces [24, 31]. Resin-based cements have low solubility and high compressive strengths relative to acid–base cements and in combination with the improved bonding potential provide a superior seal at the tooth/restoration interface thereby preventing bacterial microleakage. Furthermore, resin-based cements can be shade-matched to correct colour discrepancies in the overlying ceramic and can aesthetically fill deficiencies at the margin between the restoration and tooth structure. The setting reaction of resin-based cements may be light-initiated, chemically-initiated or a combination therefore providing the operator with considerable versatility and control over the cementation process.

4. The Development of the Adhesively Cemented All-Ceramic Restorations

The development of acrylic resins more suitable for placement in the oral environment by Bowen in 1956 resulted in methacrylate resin-based composite dental materials [32]. 'Bowen's resins' in combination with the discovery of acid-etch bonding to enamel by Buonocore in 1955 [33] led to a variety of novel techniques to improve the aesthetics of anterior dentition on a permanent basis. Resin-based composite materials could be directly built-up on the enamel surface or used to bond custom-made acrylic facings (veneers) to the tooth surface [34]. However, early resin-based composite materials and adhesively cemented acrylic veneers were associated with excessive colour modification and staining, loss of surface lustre, poor wear characteristics, inflammation of gingival tissues and debonding. In 1983, Horn described a technique of utilising a glazed porcelain laminate veneer (PLV) as an alternative to an acrylic resin veneer [35]. Horn identified that following the application of 10% hydrofluoric (HF) acid to the internal 'fit' surface of the restoration a surface roughness was created that was conducive to bonding with the methacrylate resin-based cements. Subsequently, an extension of the PLV concept was described by Rezinkor in 1987 as the dentine bonded crown (DBC) [36] and is considered as full or partial coverage of all-ceramic restoration, relying on adhesive bonding to the underlying enamel and/or dentine utilising a resin-based cement [37]. The clinical success of PLVs and DBCs is surprisingly high and it has been suggested that the prepared tooth acts as a reinforcing core whereby the strengthening of the overlying ceramic is imparted by a synergistic bond achieved between the ceramic and the tooth structure mediated by the resin-based cement [38]. The technique had considerable advantages over traditionally prepared and cemented all-ceramic restorations [39]. Retention is not solely dependent on the form of the prepared tooth and thus enables a more conservative tooth preparation, thereby reducing the adverse biological impact of tooth preparation on pulpal tissues [40].

5. Adhesive Cementation of All-Ceramic Restorations

Resin-based luting cements are composite materials and consist of an organic resin matrix, inorganic fillers, initiator(s), and tints to modify the shade [41]. The resin matrix is most commonly based on Bisphenol A glycol dimethacrylate (Bis-GMA) but additional monomers including 2-hydroxyethyl methacrylate (HEMA), urethane dimethacrylate (UDMA), triethyleneglycol dimethacrylate (TEGDMA), amongst others, are blended to modify the mechanical properties and rheological characteristics. Inorganic fillers are added to improve the mechanical properties and are coupled using organofunctional silanes to allow covalent bonding to the resin matrix. The inorganic fillers vary between manufacturers in type, shape, size and volumetric or weight loading [41]. An important balance is required in optimising the resin and filler components to allow for ease of manipulation and achievement of a thin film thickness in the unset state and to maximise the me-

chanical response and resistance to deterioration in oral environment following activation [41]. Activation of the cement occurs by a free-radical polymerisation of the resin matrix and is either 'command set' following photo-initiation using visible light, or chemically activated following mixing of two pastes [41]. Clinically, the cementation procedure requires isolation of the tooth to prevent contamination with saliva prior to acid-etching of the enamel and dentine with 30–40% phosphoric acid and subsequent placement of a dentine bonding agent [1]. The dentine bonding agent mediates bonding between the partially decalcified etched enamel and dentine and the resin-based cement. The mechanisms underlying the adhesion mediated by dentine bonding agents are complex but are extensively reported within the dental literature [42, 43]. The resin-based cement is applied to the inner surfaces of the all-ceramic restoration and/or tooth structure prior to seating under adequate pressure to ensure an accurate fit but not excessive so as to result in the restoration fracture. Clinically, the cement thickness has been characterised between 50 and 150 μm but will vary over the cross section of the restoration due to the inherent inaccuracies of the previous procedures leading up to the delivery of the restoration [44]. An essential step in determining the success of adhesively cemented all-ceramic restorations is the pre-cementation surface conditioning of the inner 'fit' surface(s) of the ceramic which is commonly roughened to promote bonding to the resin-based cement [38, 40]. Pre-cementation surface roughening of dental ceramic surfaces to enhance bonding was first conceived by Rochette in 1975 [45] and fully documented by Horn [35] and Calamia [46]; however, different techniques have since been adapted as novel ceramic materials and cements have been developed. Ceramic surface roughening may be achieved by selective surface grinding, acid-etching [35] or by airborne particle abrasion [47] or a combination [48]. Surface roughening increases the effective surface area available for bonding and creates undercuts that increase the degree of micromechanical interlocking of a resin-based cement with the ceramic surface. Acid-etching with HF or its derivatives results in the preferential dissolution of different ceramic phases resulting in undercuts, thereby creating a surface more conducive to bonding [49]. The microstructural and surface analyses of etched dental ceramics have demonstrated different etching patterns according to the type of acid-etchant, the relative acid concentration and the etching time employed. Differences in ceramic composition, microstructure and the presence of surface irregularities will also produce unique topographic changes after etching procedures [50]. Etching is particularly influenced by the distribution of the crystalline and glassy phases comprising the microstructure of many multicomponent dental ceramic systems. Dental ceramics containing a large crystalline volume, such as high purity alumina or zirconia, are resistant to etching with HF-acid. As a consequence, airborne particle abrasion is employed to create a roughened ceramic surface conducive to bonding [47]. The quantifiable roughness of air abraded dental ceramic surfaces can be significantly influenced by the size of the airborne particle, the distance of delivery, the air pressure, the angle of incidence of particle delivery, and the duration of appli-

cation [4, 51]. A number of concerns with this technique have been highlighted including difficulties in producing a consistent surface roughness, the inability to create significant undercuts in the ceramic surface and concerns over the potential damage to margins which may result in poor fit of the restoration and the potential loss of restoration integrity. Further enhancement of the resin–ceramic bond is achieved with pre-cementation by the application of an organofunctional silane which is recommended prior to the resin cementation of silicaceous all-ceramic materials [52]. In the absence of silane priming the chemical interaction between resin-based cements and silicaceous dental ceramics is weak and consists largely of van der Waals forces and hydrogen bonding. Silanes (organofunctional trialkoxysilanes) comprise a large group of organic compounds capable of mediating covalent bonding between organics and inorganic substrates [52]. Silanol groups (formed after hydrolysis of the silane, i.e. of ethoxy or methoxy groups) react with the OH groups on the ceramic surface, and the organic moiety or group (e.g. vinyl, epoxy, amino, etc.) reacts with organic resin or organic cement. Silane primers for dental purposes most commonly contain pre-hydrolysed silanes in water or an alcohol-based solution, are applied to the clean inner 'fit' surfaces of a ceramic restoration and are allowed to dry before resin-based cement application [52]. The silane coating ideally forms a monomolecular layer on the ceramic surface but in practice multi-molecular layers of 50–100 nm form as a result of the self-condensation of the multi-methoxy or ethoxy functionalities within the silane molecules [52]. The thickness of the silane layer has been shown to be dependent on the drying regimen and the concentration of the active silane in the ceramic primer [53]. Pre-cementation surface conditioning radically alters both the ceramic surface flaw distribution and the subsequent interaction with the resin-based cement and, therefore, may impact restoration performance. It has been demonstrated that HF-acid etching and alumina airborne particle abrasion have a detrimental effect on the strength of certain dental ceramic substrates attributed to the extension of pre-existing surface flaws or the introduction of a new defect population, respectively [51, 54]. Furthermore, it has also been reported that that the macroscopic roughness of a ceramic surface may act to concentrate stress near or at the tips of critical surface flaws resulting in a reduction in strength [55, 56]. Alteration of the surface texture results in both a modification of the surface area available for bonding and the wettability of the ceramic whereby increasing the ceramic surface roughness may be associated with enhanced or reduced wetting by a resin-based cement, depending on the resultant surface topography [57, 58]. Silane priming has been demonstrated to have no significant impact on ceramic strength but will occupy the region of the crack tips and will modify the subsequent interaction with the resin-based cement [59].

6. Clinical Performance of Adhesively Cemented All-Ceramic Restorations

Clinical studies have demonstrated that all-ceramic restorations cemented with methacrylate resin-based cements exhibit lower numbers of premature failures

when compared with those cemented with zinc phosphate and conventional glass-ionomer cements [60–63]. The strengthening of all-ceramic restorations with resin-based cements has also been demonstrated in *in vitro* load to failure mechanical testing of clinically representative restorations by numerous researchers. Bernal *et al.* reported that significantly increased loads were required to initiate the fracture of castable glass crowns cemented with resin-based cements when compared with zinc phosphate and conventional glass-ionomer luting agents [64]. Behr *et al.* measured the load required to initiate fracture in heat-pressed ceramic crowns luted with different cement types and reported significantly increased fracture strengths when a resin-based cement was utilised [65]. Similarly, Yoshinari and Derand reported significantly increased loads to failure for resin cemented feldspathic, castable glass, heat-pressed and glass-infiltrated crowns cemented with resin-based materials when compared with a zinc phosphate cemented control [66]. Burke *et al.* reported that the load required to fracture clinically representative crowns adhesively cemented to prepared maxillary premolar teeth was significantly increased when compared with unbonded controls for both feldspathic porcelain and heat-pressed ceramic restorations [40]. In addition, researchers have attempted to quantify the strengthening achieved following resin cementation by calculating the failure stresses in flexural tests on clinically relevant test specimens. Rosensteil *et al.* calculated the maximum bi-axial failure stress of a castable glass ceramic coated with a thin layer of resin-based cement and reported significant strengthening when compared with an uncoated control [67] (Table 2). The authors suggested that the significant strengthening observed in the absence of a supporting tooth substrate demonstrated that the strengthening of resin cemented all-ceramic restorations was not solely due to improved load transfer to the underlying tooth substrate [67]. Mesaros *et al.* reported that the flexural strength of ceramic beams resin cemented to bovine dentine was significantly increased by the use of a dentine bonding agent and a resin-based cement [68]. Pagniano *et al.* reported that the application of a thin layer of resin cement was associated with a significant increase in the Weibull characteristic strength derived from bi-axial flexure loading a heat-pressed leucite reinforced and heat-pressed lithium disilicate ceramic [69] (Table 2).

7. Mechanisms Underlying the Strengthening of All-Ceramic Restorations with Resin-Based Cements

To optimise the strengthening conferred by resin-based cements on dental ceramic materials it is essential to characterise the strengthening mechanism. Within the dental literature the interaction between resin-based cements and dental ceramics has been extensively discussed in the context of bond strengths. However, little attention has been given to the impact the resin-based cement has on the mechanical integrity of the completed restoration in service. In contrast, the strengthening of glass and ceramic substrates with thin polymeric coatings has been explored in detail within the industrial glass literature in attempts to enhance the perfor-

Table 2.
Percentage strengthening following resin-based cement application to a leucite reinforced ceramic (IPS Empress®), a lithium disilicate ceramic (IPS Empress® 2), a micaceous tetrafluorosilicate castable glass ceramic (Dicor®), an aluminous core ceramic (Vitadur α core) and a feldspathic ceramic (Vita α dentine) determined from bi-axial flexure strength (BFS) testing by various investigators k–o. * for a range of surface treatments

Investigator	k [69]		l [67]	m [78]		n [59]	o [44]		
Strength determination	BFS ($n = 18$)		BFS ($n = 8$–10)	BFS ($n = 20$)		BFS ($n = 20$)	BFS ($n = 60$)		
Ceramic substrate	IPS Empress®	IPS Empress® 2	Dicor®	Vitadur α core		Vitadur α dentine	Vitadur α dentine		
Resin-based cement	Nexus 1		Dicor LA	Compolute aplicap	Unicem aplicap	Adper adhesive	Flowline	Rely X Veneer	Clearfil APX
Cement thickness (μm)	100		100	75–100	75–100	20–50	120		
Ceramic thickness (μm)	1500		1300	2000	2000	900	900		
Strengthening (%)	46	48	49	28	48	20–53*	35	46	106

mance of glassware. Both sol–gel-based coatings and resin-based coatings have been reported and are associated with the strengthening of glass substrates [70]. There is conjecture as to the mechanisms responsible for strengthening and alternative mechanisms suggested include crack length reduction [71, 72], Poisson ratio effects [73] and the generation of crack closure stresses [70, 74]. Fractographic investigations have demonstrated that surface defects are at least partially infiltrated by coatings, however, there is little understanding of how filling a crack with a material with a significantly different elastic response on loading (when compared with the glass bulk) can confer strengthening [70]. Investigators have suggested that the restriction of a resin-based coating to thin layers in a surface defect results in an apparent increase in the elastic modulus of the coating infiltrating the defect [73]. During loading, the coating within a crack extends perpendicular to the crack face producing a compensating Poisson contraction parallel to the crack surface [73]. The contraction is restricted by the resin thickness compared with the stiffer bulk ceramic which also has a lower Poisson's ratio, effectively increasing the stiffness of the resin. As a result, the mechanical response of the coating approaches the mechanical response of the bulk glass. The strengthening mechanism relies on assumptions that the critical surface flaws are infiltrated and that there is durable interfacial bonding between the coating and glass [70]. A strengthening mechanism based on crack 'healing' has been applied to sol–gel coatings on glass [72, 73]. The investigators suggested that the infiltration of surface cracks by a surface coating partially healed and, therefore, reduced the crack length. However, for a reduced crack length to be associated with significant reduction in stress intensity, the elastic response of the coating to load must be similar to that of the glass bulk [70]. Furthermore, fractographic analysis of solvent based coatings on glass substrates has demonstrated complete crack infiltration and that the equivalent flaw sizes cannot be related to either the observed degree of crack filling or to the locus of failure which remained unaltered by surface coating [70]. Alternatively, it has been suggested that compressive stresses may be exerted by the coating on the glass surface as a consequence of a thermal expansion mismatch between the bulk glass and bulk coating [75]. However, investigators calculated the compressive stresses generated in epoxy based coatings on glass substrates and suggested that the stresses generated were insufficient to explain the degree of strengthening observed [70]. It is also conceivable that when a crack is entirely filled by a coating the crack is bridged and a closure stress is generated, thereby retarding crack propagation under tensile loading [74]. However, the origins of the closure stresses have not been identified although it has been suggested that stresses may arise due to thermal expansion mismatches or due to shrinkage during setting [74]. The induction of thermally derived closure stresses is somewhat unlikely within the dental context as the setting reaction of resin-based cements is associated with small exotherms. Within the dental literature a number of mechanisms have been proposed to explain the apparent strengthening effect observed following methacrylate resin-based cement coating of ceramic restorative materials. Marquis also suggested a crack 'healing' mecha-

nism whereby the resin-based cement coating partially or fully infiltrated surface defects thereby reducing the effective crack length and hence the stress intensity at the crack tip [76]; however, the elastic modulus of resin-based cements is reported to range between 5 and 11 GPa [44]. When compared with the elastic modulus of dental ceramic materials ranging in excess of 60 GPa, it is uncertain how such relatively elastic materials could significantly influence the stress intensity of an individual defect. In contrast, Nathanson suggested that the polymerisation shrinkage associated with the setting of resin-based cements exerted a stabilising compressive stress on the surface defect population, thereby resulting in an increased energy requirement to reach the critical tensile stress in the ceramic and initiate failure [77]. Dental resin-based luting cements exhibit polymerisation shrinkage on setting but no association between the magnitude of strengthening and shrinkage-stress generation by the resin-based cement has been made [44]. In addition, both mechanisms imply a sensitivity to defect geometry whereby flaws of variable size would be expected to be differentially strengthened on resin coating. Fleming *et al.* examined the impact of resin cement coating on aluminous core ceramic disc-shaped specimens which had been polished or polished and centrally indented thereby creating a large controlled defect [78] (Table 2). A similar increase in the bi-axial flexure strength following resin cement coating on both the polished and polished indented surfaces was observed and the authors concluded that as the strengthening on both surfaces was of a similar magnitude despite the presence of critical defects of dissimilar geometries, the strengthening mechanism was independent of defect severity [78]. Most recently investigators have demonstrated that the strengthening imparted by the adhesive resin-based cement was independent of individual defect severity but a relationship was observed between the magnitude of strengthening and the macroscopic roughness of the dental ceramic surface [59]. The authors concluded that the infiltration of the ceramic surface by the resin-based cement creates a ‘resin–ceramic hybrid layer’ in which the stress patterns during tensile loading are radically modified [59]. Using Weibull statistics to analyse large sample size fracture strength data ($n = 60$) investigators demonstrated that the distribution of the fracture strength data was unaltered by resin-based cement coating a dental ceramic, despite a significant reinforcement being observed (>100% of the uncoated failure stress) [44]. This observation further suggests that the strengthening mechanism acts across the global surface defect population rather than by ‘healing’ or stabilising individual flaws. Utilising multilayered analytical solutions to calculate the bi-axial failure stresses in a dental ceramic coated with thin layers of methacrylate resin-based cements, the magnitude of strengthening has been reported to be a function of resin-based cement elasticity [44]. The impact of the quality of adhesive bonding between the resin-based cement and ceramic substrate on the magnitude of strengthening is uncertain however, as significant strengthening is reported on highly polished ceramic substrates where micromechanical retention has been minimised [78]. In addition, silane priming, demonstrated to enhance bonding between resin-based materials and silicaceous ceramics, in combination with a highly elastic

unfilled resin provides no further strengthening when compared with the unprimed condition [58]. In contrast, silane priming prior to coating with a less elastic filled resin-based cement results in an increased strengthening when compared with the unprimed state [58]. It has been proposed that under loading, the highly elastic response of the unfilled resin occupying the resin–ceramic hybrid layer permits a critical strain and associated stress to be generated within a surface defect before the critical bond stress between the ceramic and the unfilled resin is exceeded. As a consequence, the improvement of the bonding between ceramic and unfilled resin mediated by the silane is associated with no further strengthening. In contrast, the generation of the strain within the less elastic filled resin-based cement was found to be associated with a stress generation that exceeded the critical bonding stress between resin-based cement and the ceramic and hence the strengthening associated was enhanced by silane priming [58, 79].

8. Conclusions

Strengthening of dental ceramic materials by resin-based cements has the potential to impact clinical performance of indirect all-ceramic restorations. The magnitude of strengthening has been demonstrated to be dependent on the type of ceramic substrate, the pre-cementation ceramic surface conditioning regimen, adhesion between the ceramic and resin-based cement, and the mechanical properties of the resin-based cement itself. The mechanism underlying the strengthening is insensitive to individual defect severity, sensitive to the macroscopic roughness of the ceramic surface and dependent on the elasticity of the resin-based cement. The development of resin-based cement materials has traditionally focused solely on enhancing adhesion to the underlying tooth structure and the overlying restoration. In contrast, the development of resin-based cement materials, specifically to optimise the mechanical response of the restoration under loading, will result in increased clinical confidence.

References

1. T. J. Hilton, in: *Fundamentals of Operative Dentistry — A Contemporary Approach*, 2nd edn, J. B. Summitt, J. W. Robbins, T. J. Hilton and R. S. Schwartz (Eds), pp. 260–305. Quintessence, Chicago, Illinois (2001).
2. V. Piddock and A. J. E. Qualtrough, *J. Dentistry* **18**, 227 (1990).
3. S. F. Rosensteil, M. F. Land and B. J. Crispin, *J. Prosthet. Dentistry* **80**, 281 (1998).
4. B. W. Darvell, in: *Material Science for Dentistry*, 9th edn, pp. 483–502. B. W. Darvell, Hong Kong, China (2002).
5. J. R. Kelly, I. Nishimura and S. D. Campbell, *J. Prosthet. Dentistry* **75**, 18 (1996).
6. K. J. Anusavice and B. Hojjatie, *Int. J. Prosthodont.* **5**, 351 (1992).
7. J. B. Quinn, G. D. Quinn, J. R. Kelly and S. S. Scherrer, *Dental Mater.* **21**, 920 (2005).
8. J. R. Kelly, *J. Prosthet. Dentistry* **81**, 652 (1999).
9. J. R. Kelly, S. D. Campbell and H. K. Bowen, *J. Prosthet. Dentistry* **62**, 536 (1989).

10. S. S. Scherrer, J. B. Quinn, G. D. Quinn and J. R. Kelly, *Int. J. Prosthodont.* **19**, 185 (2006).
11. R. R. Seghi, T. Daher and A. A. Caputo, *Dental Mater.* **6**, 181 (1990).
12. J. Tinschert, D. Zwez, R. Marx and K. J. Anusavice, *J. Dentistry* **28**, 529 (2000).
13. M. J. Cattell, R. L. Clarke and E. J. R. Lynch, *J. Dentistry* **25**, 399 (1997).
14. M. J. Cattell, R. L. Clarke and E. J. R. Lynch, *J. Dentistry* **25**, 409 (1997).
15. R. Giordano, L. Pelletier, S. Campbell and R. Pober, *J. Prosthet. Dentistry* **73**, 411 (1995).
16. R. R. Seghi and R. J. Sorenson, *Int. J. Prosthodont.* **8**, 239 (1995).
17. J. F. Esquivel-Upshaw, J. Chai, S. Sansano and D. Shonberg, *Int. J. Prosthodont.* **14**, 284 (2001).
18. W. C. Wagner and T. M. Chu, *J. Prosthet. Dentistry* **76**, 140 (1996).
19. A. S. Riskalla and D. W. Jones, *Dental Mater*. **20**, 207 (2004).
20. A. R. Curtis, A. J. Wright and G. J. P. Fleming, *J. Dentistry* **34**, 317 (2005).
21. J. W. McLean and M. I. Kedge, *Quintessence Int.* **18**, 97 (1987).
22. S. N. White, A. A. Caputo, F. M. A. Vidjak and R. R. Seghi, *Dental Mater.* **10**, 52 (1994).
23. M. N. Aboushelib, N. de Jager, C. J. Kleverlaan and A. J. Feilzer, *Dental Mater.* **23**, 952 (2006).
24. F. J. T. Burke, G. J. P. Fleming, D. Nathanson and P. M. Marquis, *J. Adhesive Dentistry* **4**, 7 (2002).
25. A. M. Diaz-Arnold, M. A. Vargas and D. R. Haselton, *J. Prosthet. Dentistry* **81**, 135 (1999).
26. B. W. Darvell, in: *Material Science for Dentistry*, 9th edn, pp. 190–220. B. W. Darvell, Hong Kong, China (2002).
27. G. J. P. Fleming and O. Narayan, *Dental Mater.* **19**, 69 (2003).
28. G. F. Kantorowicz, L. C. Howe, A. C. Shortall and D. S. Shovelton, in: *Inlays, Crowns and Bridges: A Clinical Handbook,* 5th edn, G. F. Kantorowicz (Ed.), pp. 57–60. Butterworth-Heinemann, Oxford, UK (1993).
29. D. C. Smith and N. D. Ruse, *J. Amer. Dental Assoc.* **112**, 654 (1986).
30. J. Sidel, F. Frankenberger, K. Krämer and A. Petschelt, *J. Dentistry* **27**, 175 (1999).
31. F. S. Michelini, U. C. Besler, S. S. Scherrer and W. G. De Rijk, *Int. J. Prosthodont.* **8**, 234 (1995).
32. R. L. Bowen, *J. Dental Res.* **35**, 361 (1956).
33. M. G. Buonocore, *J. Dental Res.* **34**, 49 (1955).
34. F. R. Faunce and D. R. Myers, *J. Amer. Dental Assoc.* **93**, 790 (1976).
35. H. R. Horn, *Dental Clin. North Amer.* **27**, 671 (1983).
36. H. Rezinkor, *Clinical Procedures Manual*. Dental Prosthetic Services Inc., Cedar Rapids, Indiana (1987).
37. A. J. R. Crowthers, R. W. Wassell and P. F. Allen, *Dental Update* **20**, 388 (1993).
38. J. W. McLean, *Br. Dental J.* **164**, 187 (1998).
39. F. J. T. Burke, A. J. E. Qualtrough and R. W. Hale, *Br. Dental J.* **179**, 58 (1995).
40. F. J. T. Burke, A. J. E. Qualtrough and R. W. Hale, *J. Amer. Dental Assoc.* **129**, 455 (1998).
41. B. W. Darvell, in: *Material Science for Dentistry*, 9th edn, pp. 115–145. B. W. Darvell, Hong Kong, China (2002).
42. J. D. Eick, A. J. Gwinnett, D. H. Pashley and S. J. Robinson, *Crit. Rev. Oral Biol. Med.* **8**, 306 (1997).
43. J. Perdigao, *Dental Clin. North Amer.* **46**, 277 (2002).
44. O. Addison, P. M. Marquis and G. J. P. Fleming, *J. Dental Res.* **86**, 519 (2007).
45. A. L. Rochette, *J. Prosthet. Dentistry* **33**, 287 (1975).
46. J. R. Calamia, *Quintessence Int.* **16**, 5 (1985).
47. D. M. Wolf, J. M. Powers and K. L. O'Keefe, *Dental Mater.* **8**, 158 (1992).
48. M. Özcan and P. K. Vallitu, *Dental Mater.* **19**, 725 (2003).
49. I. Stangel, D. Nathanson and C. S. Hsu, *J. Dental Res.* **66**, 1460 (1987).
50. A. Della Bona and K. J. Anusavice, *Int. J. Prosthodont.* **15**, 159 (2002).

51. O. Addison, P. M. Marquis and G. J. P. Fleming, *Dental Mater.* **23**, 1332 (2007).
52. J. P. Matinlinna, L. V. Lassila, M. Ozcan, A. Yli-Urpo and P. K. Vallitu, *Int. J. Prosthodont.* **17**, 164 (2004).
53. S. Debnath, S. L. Wunder, J. I. McCool and G. R. Baran, *Dental Mater.* **19**, 441 (2003).
54. O. Addison, P. M. Marquis and G. J. P. Fleming, *Dental Mater.* **23**, 461 (2006).
55. N. de Jager, A. J. Feilzer and C. L. Davidson, *Dental Mater.* **16**, 381 (2000).
56. H. Fischer, M. Schafer and R. Marx, *J. Dental Res.* **82**, 972 (2003).
57. W. S. Oh, C. Shen, B. Alegre and K. J. Anusavice, *J. Prosthet. Dentistry* **88**, 616 (2002).
58. G. Aksoy, H. Polat, M. Polat and G. Coskun, *Colloids Surfaces B: Biointerfaces* **53**, 254 (2006).
59. O. Addison, P. M. Marquis and G. J. P. Fleming, *J. Dentistry* **35**, 416 (2007).
60. K. A. Malament and D. G. Grossman, *J. Dental Res.* **71**, 321 (1992).
61. K. A. Malament and S. S. Socransky, *J. Prosthet. Dentistry* **81**, 23 (1999).
62. K. A. Malament and S. S. Socransky, *J. Prosthet. Dentistry* **81**, 662 (1999).
63. K. A. Malament and S. S. Socransky, *J. Prosthet. Dentistry* **86**, 511 (2001).
64. G. Bernal, R. M. Jones, D. T. Brown, C. A. Munoz and C. J. Goodacre, *Int. J. Prosthodont.* **6**, 286 (1993).
65. M. Behr, M. Rosentrit, M. Mangelkramer and G. Handel, *Int. J. Prosthodont.* **16**, 538 (2003).
66. M. Yoshinari and T. Derand, *Int. J. Prosthodont.* **7**, 329 (1994).
67. S. F. Rosenstiel, P. K. Gupta, R. A. Van der Sluys and M. H. Zimmerman, *Dental Mater.* **9**, 274 (1993).
68. A. J. Mesaros, D. B. Evans and R. S. Schwartz, *Amer. J. Dentistry* **7**, 137 (1994).
69. R. P. Pagniano, R. R. Seghi, S. F. Rosenstiel, R. Wang and N. Katsube, *J. Prosthet. Dentistry* **93**, 459 (2005).
70. R. J. Hand, B. R. Ellis, B. R. Whittle and F. H. Wang, *J. Non-Cryst. Solids* **315**, 276 (2003).
71. B. D. Fabes and G. D. Berry, *J. Non-Cryst. Solids* **121**, 357 (1990).
72. B. D. Fabes and D. R. Uhlmann, *J. Amer. Ceram. Soc.* **73**, 978 (1990).
73. F. H. Wang, R. J. Hand, B. Ellis and A. B. Seddon, *Phys. Chem. Glasses* **36**, 201 (1995).
74. D. H. Roach, S. Lathabai and B. R. Lawn, *J. Amer. Ceram. Soc.* **71**, 97 (1988).
75. T. H. Wang and P. F. James, *J. Mater. Sci.* **26**, 354 (1991).
76. P. M. Marquis, *Bioceramics* **5**, 317 (1992).
77. D. Nathanson, in: *Porcelain and Composite Inlays and Onlays: Esthetic Posterior Restorations*, D. A. Gaber and R. E. Goldstein (Eds), pp. 23–32. Quintessence, Chicago, Illinois (1993).
78. G. J. P. Fleming, R. F. Maguire, G. Bhamra, F. M. Burke and P. M. Marquis, *J. Dental Res.* **85**, 272 (2006).
79. O. Addison, P. M. Marquis and G. J. P. Fleming, *J. Adhesive Dentistry* **10**, 285 (2008).

Comparison of Different Etching Agents and Repair Materials Used on Feldspathic Porcelain

Per Kristian Lundvall [a], **Eystein Ruyter** [b,*], **Hans Jacob Rønold** [a] **and Karl Ekstrand** [a]

[a] Department of Prosthetic Dentistry, Faculty of Dentistry, University of Oslo, Boks 1109 Blindern, NO-0317 Oslo, Norway

[b] NIOM, PO Box 70, NO-1305 Haslum, Norway

Abstract

When fractures of fixed partial dentures occur, they cause an aesthetic and functional dilemma both for the patient and the dentist. Re-make of the entire restoration is an option, but not always desirable. Previous studies have provided several options for ceramic reparation, but there is limited consensus about this issue.

The aim of this study was to test the shear bond strength due to four different etching agents for ceramic repair. The goal was to find a substitute for hydrofluoric acid as etching agent with less toxicity. Ideally, the repair of ceramics must meet both functional and aesthetic requirements.

A total of 70 square shaped feldspathic porcelain disks of dimensions 10 mm × 10 mm × 3 mm were produced and embedded in cylindrical polyethylene walled poly(methyl methacrylate) (PMMA) blocks (16 mm diameter and 12 mm thick). All specimens were wet-ground with silicon carbide papers down to P4000. For one of the groups ten cylindrical ceramic specimens (diameter 5 mm and 2.5 mm high) were made and wet-ground to P4000. The blocks were divided into 7 groups with 10 specimens for each group. In six of the groups composite cylinders were bonded to the porcelain with different pretreatments of the porcelain. As etching agents 9% hydrofluoric acid (HF), 35% phosphoric acid (PO), 15% hydrochloric acid (HCl) and 15% potassium fluoride/hydrogen fluoride (KF·HF) were tested. This study compared a one-part (activated) silane and a new two-part silane. In one group two porcelain specimens were bonded with composite veneer cement. All the specimens were thermocycled for 5000 cycles from 5°C to 55°C before shear bond test.

The best overall result was obtained in group 6 (two porcelain specimens bonded with veneer cement), and the mean shear bond strength was 24.5 MPa. The lowest values were obtained in group 4 with 35% phosphoric acid, and group 5 with 15% hydrochloric acid as the etching agent (6.5 and 0.8 MPa, respectively).

Pretreatment with either 9% HF or 15% KF·HF as the etching agent combined with two-part silane gave good adhesion for porcelain reparations.

Keywords

Adhesion, ceramic, composite, etching, fluorides, shear bond strength, silane

* To whom correspondence should be addressed. Tel.: +4767512200; Fax: +4767512209; e-mail: eystein.ruyter@niom.no

Adhesion Aspects in Dentistry

© Koninklijke Brill NV, Leiden, 2009

1. Introduction

Crowns and bridges made of porcelain fused to metal or other core materials such as alumina and zirconia are widely accepted and used in clinical practice. Despite good long-term success rates they occasionally demonstrate fracture of the brittle ceramic veneer. Longitudinal studies have shown that failures resulting from porcelain fracture or chipping range from 2.4% to 8% [1, 2]. Walton *et al.* [3] described worn or lost veneers as the most frequent mechanical problem encountered with fixed partial dentures. Furthermore, failures occur most frequently in regions that are visible, compromising aesthetics in the anterior region. The fractures are mainly in the maxilla, and predominantly on the labial surface. Fractures of porcelain on crowns and bridges are multifactorial. Lack of a proper framework to support the porcelain, intraceramic defects, or parafunctional occlusion can cause this inconvenient problem [4]. Re-make of the restoration is possible, but it is not always the first choice for practical and economical reasons. The ability to repair a ceramic defect after chipping is more beneficial. The clinical success of the porcelain repair is almost entirely dependent on the integrity of the bond between the ceramic and the composite resin. The bond is achieved either by chemical or mechanical method, or both. Several studies have described different ceramic surface treatments to optimize bond strength at the ceramic–composite interface [5, 6]. In a study by Suliman *et al.* [7] the highest bond strength (19.7 MPa) was achieved with diamond roughening followed by hydrofluoric acid etching and Clearfil bonding agent. Leibrock *et al.* [8] claimed that hydrofluoric acid caused no increase in adhesion to porcelain when compared with phosphoric acid. The intra-oral application of the toxic hydrofluoric acid is very undesirable. Özden *et al.* [9] achieved 11.5 MPa bond strength with a diamond bur roughening and silane application only. The specimens were thermocycled for 100 cycles. There is evidence that thermocycling and hydration decreases the bond strength by weakening the interface due to different thermal expansion coefficients of materials involved [10–12]. Sun *et al.* [13] used a four-point bending test and showed a significantly higher bond strenth after preparing the specimens with tribochemical sandblasting (Co-jet, ESPE, Bavaria, Germany) as compared with simple gritblasting.

The bond strength is achieved by the combination of mechanical and chemical bonds using surface roughening and silane coupling agents. It has recently been shown by Matinlinna and coworkers that different silanes show differences in their adhesion promotion properties [14–16]. It has been claimed that a silane provides chemical covalent as well as hydrogen bonding and also improves the wettability [17].

The aim of this study was to evaluate the shear bond strength due to four different etching agents, and compare a new two-part silane to a one-part (activated) silane. In addition to testing composite bond strength to ceramic, it was also important to test the strength of two ceramic specimens bonded with composite cement as a technique for porcelain repair.

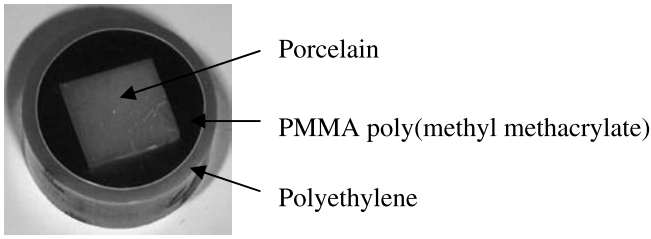


Figure 1. Specimen prior to bonding procedure.

2. Materials and Methods

A total of 70 square shaped feldspathic porcelain specimens (Hera-ceram®, Heraeus Kulzer, Germany) of dimensions 10 mm × 10 mm × 3 mm were produced and embedded in cylindrical polyethylene walled PMMA blocks (16 mm diameter and 12 mm thick) (Fig. 1). All specimens were wet-ground with silicon carbide papers down to P4000 (<5 μm) on a rotating grinding machine (Struers, Denmark). Ten cylindrical ceramic specimens (diameter 5 mm and 2.5 mm high) (ISO 10477) [18] were made and wet-ground in the same manner. The blocks were divided into 7 groups with 10 specimens for each group and the production of the specimens was as follows.

Group 1 (HF–BS–C) $n = 10$. The porcelain surfaces were etched for 60 s with 9% hydrofluoric acid (Porcelain Etch®, Ultradent, USA) followed by water rinsing for 30 s and air drying. A two-part silane (Bis-Silane, Bisco, USA) was activated by mixing equal parts of part A (3-methacryloyloxypropyltrimethoxysilane (5%) in ethanol) and part B (acetic acid), applied with a microbrush, and air blown for 60 s. Adhesive resin, PBR (Porcelain Bonding Resin, Bisco, USA), was applied and the excess resin removed with air. Finally the composite (Charisma, Heraeus Kulzer, Germany) was applied and light cured for 80 s (Demetron, VCL 400, Kerr, USA).

Group 2 (HF–C) $n = 10$. As group 1, but without silane coupling agent.

Group 3 (HF–S–C) $n = 10$. As group 1. The specimens were coated with a one-part silane (Silane, Ultradent Products, Inc., USA) for 60 s and air-dried.

Group 4 (PO–BS–C) $n = 10$. The porcelain surfaces were etched for 180 s with 35% phosphoric acid (Ultra-Etch®, Ultradent Products, Inc., USA), water rinsed for 30 s and dried, followed by application of two-part silane, PBR, composite and light-cured as in previous groups.

Group 5 (HCl–BS–C) $n = 10$. The porcelain surfaces were etched for 300 s with 15% HCl (prepared in the laboratory), water rinsed and dried, followed by application of two-part silane, PBR, composite and light cured as in previous groups.

Group 6 (HF–BS–VC) $n = 10$. Porcelain was used as the repairing material and the cylindrical porcelain specimens were wet-ground (P4000 silicon carbide papers) before the bonding procedure. The following procedure was used for both

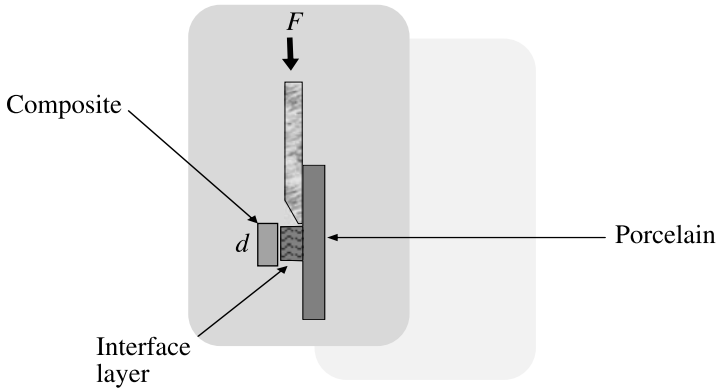


Figure 2. Schematic illustration of the setup for shear bond strength test. The specimen was loaded with a force, F, d is the diameter of the rod.

porcelain plate and porcelain cylinder: 60 s etching with 9% HF (Porcelain Etch®, Ultradent, USA), followed by water rinsing and air drying. Two-part silane (Bis-Silane, Bisco, USA) was activated, applied for 60 s and dried. PBR was applied on both specimens, and cemented with composite cement (Choice 2® light-cured veneer cement, Bisco, USA). Each specimen was light-cured for 80 s.

Group 7 (KF·HF–BS–C) $n = 10$. The porcelain surfaces were treated for 180 s with an aqueous solution of 15% KF·HF (potassium fluoride/hydrogen fluoride), and carboxymethylcellulose prepared in the laboratory. Then followed by application of Bis-silane, PBR and composite.

To ensure complete curing, all specimens were stored dry at (22 ± 1)°C for 24 h before being thermocycled between 5°C and 55°C for 5000 cycles with a 30-s dwell time, according to ISO 10477 [18].

After thermocycling, the specimens were stored in distilled water before being subjected to shear load at a displacement rate of (1 ± 0.3) mm/min. The mean bonded area was measured for each specimen before mounting in the test machine (Lloyd LRX, Lloyd Instruments Ltd, Fareham, UK). The shear load at the point of failure was noted, and shear bond strength calculated according to ISO 10477 [18] (Fig. 2).

The abbreviations used, materials used, and production procedures for various groups are presented in Tables 1, 2 and 3, respectively.

3. Results

The statistical analysis showed that differences existed among the means: The statistical analyses were performed using one-way analysis of variance (ANOVA).

The results of this study are presented in Table 4 and Fig. 3. For each group standard deviation and confidence interval were calculated.

Table 1.
Abbreviations used in the text

HF	9 wt% hydrofluoric acid
HCl	15 wt% hydrochloric acid
PO	35 wt% phosphoric acid
KF·HF	15 wt% potassium fluoride/hydrogen fluoride
S	Silane, one-part
BS	Silane, two-part
PBR	Porcelain bonding resin
C	Composite veneer cement

Table 2.
Materials used in the study

Product	Composition	Manufacturer	Lot nr.
Hera-ceram	Feldspathic porcelain	Heraeus Kulzer, GmBH, Hanau, Germany	
Porcelain Etch	9 wt% hydrofluoric acid	Ultradent Products, Inc., South Jordan, Utah, USA	b3pkt
HCl	15 wt% hydrochloric acid	Laboratory prepared	–
UltraEtch	35 wt% phosphoric acid	Ultradent Products, Inc., South Jordan, Utah, USA	b3qct
KF·HF*	15 wt% potassium fluoride/ hydrogen fluoride	Laboratory prepared	–
Bis-silane	Silane, two-part	Bisco, Inc., Schaumburg, IL, USA	0600010784
Silane	Silane, one-part	Ultradent Products, Inc., South Jordan, Utah, USA	b3n6j
Porcelain bonding resin	Bonding resin, HEMA free	Bisco, Inc., Schaumburg, IL, USA	080009554
Charisma	Composite, hybrid	Heraeus Kulzer, GmBH, Hanau, Germany	010055
Choice 2	Veneer cement	Bisco, Inc., Schaumburg, IL, USA	0600010895

* KF·HF (15 wt% HF) was dissolved in an aqueous solution of carboxymethylcellulose (Sigma-Aldrich Norway AS).

Group 6 had the best overall result (Mean: 24.5 MPa, SD: 7.0) and had significantly higher shear bond strength ($p < 0.001$) than the other groups except group 1 (Mean: 19.0 MPa, SD: 5.0) and group 7 (Mean: 18.4 MPa, SD: 7.1). The lowest shear bond strength was obtained in group 5. (Mean: 0.8 MPa, SD: 1.8). This was significant lower ($p < 0.0001$) than all groups except group 4 (Mean: 6.5 MPa, SD:

Table 3.
Materials and methods used for production of different groups

Materials and methods	Group 1	Group 2	Group 3	Group 4	Group 5	Group 6	Group 7
Specimens	$n = 10$	$n = 10$	$n = 10$	$n = 10$	$n = 10$	$n = 10$	$n = 10$
Feldspathic porcelain (square) wet-ground to P4000	•	•	•	•	•	•	•
Feldspathic porcelain (cylindrical) wet-ground to P4000						•	
Composite, hybrid (C)	•	•	•	•	•		•
9 wt% hydrofluoric acid (HF) 60 s	•	•	•			•	
15 wt% hydrochloric acid (HCl) 300 s					•		
35 wt% phosphoric acid (PO) 180 s				•			
15 wt% potassium fluoride/ hydrogen fluoride (KF·HF) 180 s							•
Silane, two-part (BS) 60 s	•			•	•	•	•
Silane, one-part (S) 60 s			•				
Porcelain bonding resin, HEMA free (PBR)	•	•	•	•	•	•	•
Composite veneer cement (C)						•	
Light-cured 80 s	•	•	•	•	•	•	•
Thermocycling 5°C–55°C for 5000 cycles	•	•	•	•	•	•	•
Shear bond test ISO 10477	•	•	•	•	•	•	•

Table 4.
Mean shear bond strength in MPa, standard deviation (SD), number of specimens per group (n) and confidence interval 95%

Groups	HF–BS–C (1)	HF–C (2)	HF–S–C (3)	PO–BS–C (4)	HCl–BS–C (5)	HF–BS–CS* (6)	KF·HF–BS–C (7)
Mean	19.0	13.4	13.8	6.6	0.8	24.5	18.3
SD	5.0	2.2	5.4	5.9	1.8	7.0	7.1
n	10	10	10	10	10	10	10

* Two porcelain specimens bonded with composite veneer cement.

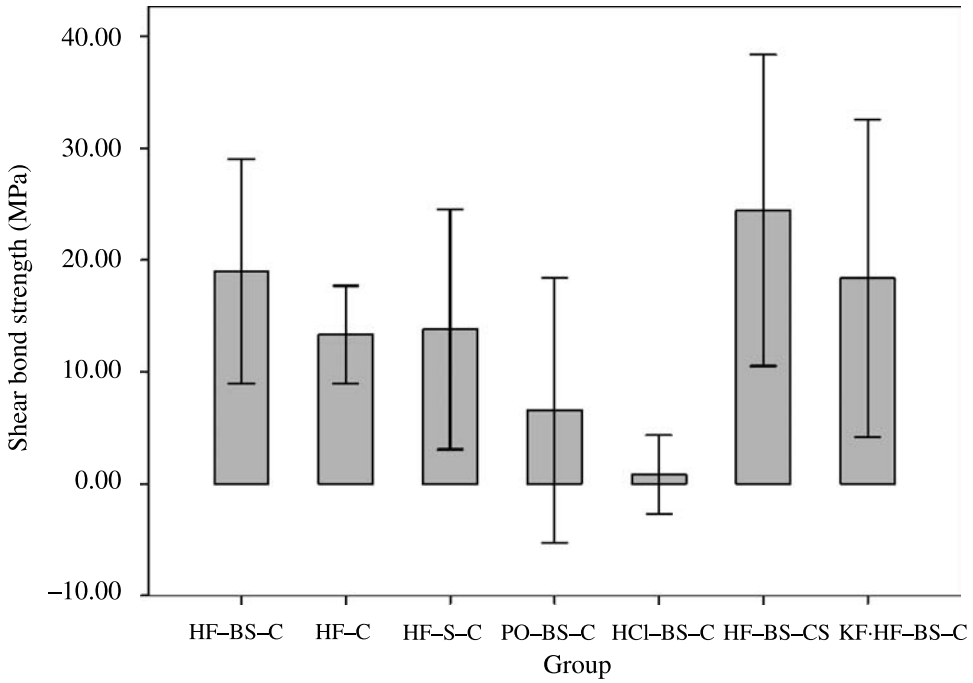


Figure 3. Results from the shear bond test for 7 experimental groups. Bars represent mean values ± 2SD.

5.9). There was no significant difference ($p = 0.424$) in shear bond strengths between group 1 and group 2 (Mean: 13.4 MPa, SD: 2.2) nor between group 1 and group 3 (Mean: 13.8 MPa, SD: 5.4). During thermocycling 8 specimens in group 5 and 3 specimens in group 4 debonded. No significant difference was obtained between the best composite groups (groups 1 and 7), using HF and KF·HF as the etching agents, respectively.

4. Discussion

In this *in vitro* study shear bond strengths were measured for different combinations of materials and methods used for porcelain repair after fracture within the porcelain.

Several studies [19–21] dealing with porcelain repair suggest etching of porcelain with hydrofluoric acid (HF) to generate the micromechanical retention necessary for the porcelain–composite bond. Chen and coworkers [22] studied the importance of the etching time of porcelain in obtaining higher bond strengths. They reported the highest shear bond strength when the porcelain surface was etched for 120 s with 5% HF. Yen and coworkers [23] reported altered surface topography, but no significant effect on flexural strength of feldspathic porcelain after etching with hydrofluoric acid up to 5 min. In the present study there was

higher shear bond strengths using two-part silane (group 1), in comparison with one-part silane (group 3), 19.0 MPa and 13.8 MPa respectively. One-part silane (group 3) showed similar bond strengths as the group without silane (group 2).

Hydrofluoric acid (HF) is widely used in the industry for etching glass. HF produces dehydration and etching of tissues, but unlike other halogen acids, hydrogen fluoride is a weak acid. However, unlike other acids, the dissociated fluoride ion, F^-, produces severe toxicity. It interferes with calcium metabolism in the underlying soft and bony tissue and the result is severe pain and cell destruction. Death has been reported from burnsinvolving concentrated acid with as little as 2.5% body surface area (BSA). Topical and parenteral calcium salts have proven effective therapy for both dermal and systemic manifestations [23]. In this study the goal was to find an alternative to HF as the etching agent for clinical use. No significant difference was obtained between the best composite groups (groups 1 and 7), using HF and KF·HF as the etching agents, respectively.

In group 7 the use of 15% KF·HF (potassium fluoride/hydrogen fluoride) as the etching agent showed almost similar results to those obtained with the hydrofluoric acid (group 1).

Biological tests on KF·HF are not available yet, but we believe it to be less toxic because the solution does not produce free hydrofluoric acid [24].

Comparison of HF with the other etching agents 15% HCl (hydrochloric acid) and 35% PO (phosphoric acid) showed significantly lower bond strengths ($p < 0.0001$).

Silane coupling agents are capable of forming chemical bonds with porcelain surfaces and bonding to the resin occurs by an addition polymerization reaction between methacrylate groups of the matrix resin and the silane molecule during curing of the composite. The bond with ceramics may occur *via* a condensation reaction between the silanol group (Si–OH) of the ceramic surface and the silanol group of the hydrolyzed silane molecule, creating a siloxane bond (Si–O–Si) and producing a water molecule (H_2O) as byproduct [15, 25]. More importantly, silanes enhance resin–porcelain bonds by promoting wetting of the ceramic surface and thus making the penetration of the resin into the microscopic porosities of the acid conditioned porcelain [17]. Hooshmand *et al.* [26] concluded that, when using an appropriate silane application technique, the effectiveness of a pre-activated silane solution based on 3-MPTS (3-methacryloyloxypropyltrimethoxysilane), acetic acid and ethanol will not deteriorate when stored for up to 1 year at room temperature. In this study we found higher bond strength using a two-part inactivated silane compared to the one-part activated silane. It is reasonable to suggest that the pre-activated silane, i.e., the one-part silane contained partly polymerized polysiloxane prior to the bonding procedure, thus preventing optimal adhesion.

Several of today's dentin–enamel bonding agents contain HEMA (2-hydroxyethyl methacrylate). HEMA has hydrophilic properties and enables the bonding agent to penetrate dentin tubules for higher bond strengths [27]. For the purpose of repairing fractured porcelain, this property is not necessary. Being hydrophilic,

HEMA will absorb water, discolor and weaken the bonding over time. In this study, a HEMA-free bonding agent was used.

One of the aims of this study was to achieve a reparation technique with a good aesthetic result. Group 6 with two porcelain specimens bonded with composite cement showed best shear bond strength in the present study (24.5 MPa).

5. Conclusions

Within the limits of this study the following conclusions are drawn.

- Pretreatment with either 9% HF or 15% KF·HF as the etching agent combined with a two-part silane gives good adhesion for porcelain reparations.
- 15% KF·HF as the etching agent gives good adhesion and may be a better alternative than 9% HF because of less toxicity.
- Porcelain fractures repaired with bonded porcelain showed in this study the best shear bond strength, and should be the first technique of choice considering aesthetic demands.

References

1. J. Coornaert, P. Adriaens and J. De Boever, *J. Prosthet. Dentistry* **51**, 338–342 (1984).
2. G. Libby, M. R. Arcuri, W. E. LaVelle and L. Hebl, *J. Prosthet. Dentistry* **78**, 127–131 (1997).
3. J. N. Walton, F. M. Gardner and J. R. Agar, *J. Prosthet. Dentistry* **56**, 416–421 (1986).
4. M. Özcan and W. Niedermeier, *Int. J. Prosthodont.* **15**, 299–302 (2002).
5. J. G. dos Santos, R. G. Fonseca, G. L. Adabo and C. A. dos Santos Cruz, *J. Prosthet. Dentistry* **96**, 165–173 (2006).
6. A. U. Güler, F. Ylimaz, M. Yenisey, E. Güler and C. Ural, *J. Adhesive Denistry* **8**, 21–25 (2006).
7. A. H. Suliman, E. J. Swift, Jr. and J. Perdigao, *J. Prosthet. Dentistry* **70**, 118–120 (1993).
8. A. Leibrock, M. Degenhart, M. Behr, M. Rosentritt and G. Handel, *J. Oral Rehabil.* **26**, 130–137 (1999).
9. A. N. Özden, F. Akaltan and G. Can, *J. Prothet. Dentistry* **72**, 85–88 (1994).
10. O. Kumbuloglu, A. User, S. Toksavul and P. K. Vallittu, *Acta Odontol. Scand.* **61**, 268–272 (2003).
11. M. Özcan, *J. Oral Rehabil.* **30**, 194–203 (2003).
12. J. H. Bailey, *J. Prosthet. Dentistry* **61**, 174–177 (1989).
13. R. Sun, N. Suansuwan, N. Kilpatrick and M. Swain, *J. Dentistry* **28**, 441–445 (2000).
14. J. P. Matinlinna, L. V. J. Lassila and P. K. Vallittu, *J. Dentistry* **34**, 721–726 (2006).
15. J. P. Matinlinna, L. V. J. Lassila, M. Özcan, A. Yli-Urpo and P. K. Vallittu, *Int. J. Prosthodont.* **17**, 155–164 (2004).
16. J. P. Matinlinna, M. Ozcan, L. V. J. Lassila and P. K. Vallitu, in: *Silanes and Other Coupling Agents*, K. L. Mittal (Ed.), Vol. 4, pp. 199–215. VSP/Brill, Leiden (2007).
17. E. P. Plueddemann, *J. Adhesion* **2**, 184–201 (1970).
18. ISO 10477, Dentistry–polymer-based crown and bridge materials (2004).
19. C. H. Pameijer, N. P. Louw and D. Fischer, *J. Am. Dental. Assoc.* **127**, 203–209 (1996).
20. H. Kato, H. Matsumura and M. Atsuta, *J. Oral Rehabil.* **27**, 103–110 (2000).
21. K. Chung and Y. Hwang, *J. Prosthet. Dentistry* **78**, 267–274 (1997).
22. J. H. Chen, H. Matsumura and M. Atsuta, *J. Dentistry* **26**, 53–58 (1998).

23. T. Y. Yen, R. B. Blackman and R. J. Baez, *J. Prosthet. Dentistry* **70**, 224–233 (1993).
24. J. C. Bertolini, *J. Emerg. Med.* **10**, 163–168 (1992).
25. K. J. Söderholm and S. W. Shang, *J. Dental Res.* **72**, 1050–1054 (1993).
26. T. Hooshmand, R. van Noort and A. Keshvad, *Dental Mater.* **20**, 635–642 (2004).
27. K. L. Van Landuyt, J. Snauwaert, J. De Munck, E. Coutinho, A. Poitevin, Y. Youshidaa, K. Suzuki, P. Lambrechts and B. van Merbeek, *J. Dental Res.* **86**, 739–744 (2007).

Evaluation of *bis*-GMA/MMA Resin Adhesion to Silica-Coated and Silanized Titanium

Mervi Puska [a,b,*], **Lippo Lassila** [a], **Pekka K. Vallittu** [a], **Jukka Seppälä** [b] **and Jukka Matinlinna** [c,d]

[a] University of Turku, Institute of Dentistry, Department of Prosthetic Dentistry and Biomaterials Science, Lemminkäisenkatu 2, FI-20520 Turku, Finland

[b] Helsinki University of Technology, Laboratory of Polymer Technology, P.O. Box 6100 FI-02015 HUT, Finland

[c] Nordic Institute of Dental Materials (NIOM), P.O. Box 70, NO-1305 Haslum, Norway

[d] University of Hong Kong, Faculty of Dentistry, Dental Materials Science, 4/F, Prince Philip Dental Hospital, 34 Hospital Road, Sai Ying Pun, Hong Kong, P.R. China

Abstract

The effects of pH value and alcohol solvent type of a silane solution on the bonding of an experimental resin to the silica-coated titanium (Ti) surface were studied. First, Ti surfaces underwent tribochemical Rocatec™ treatment followed by silanization of the surface with 3-methacryloxypropyltrimethoxysilane (MPS). Then, resin stubs based on a mixture of bisphenol-A-glycidyl dimethacrylate and methyl methacrylate were bonded and light-cured onto each silica-coated Ti surface ($n = 6$ per group). Two different solvents for MPS, namely *iso*-propanol (*i*-PrOH)/H_2O and ethanol (EtOH)/H_2O were used, at pH values of 4.5, 5.0, and 5.5, and shear bond strengths were tested both under dry storage conditions and after water sorption induced by accelerated aging (i.e. thermo-cycling). The shear bond strengths were also re-determined after the silane solutions had been stored at 4°C for 15 weeks before the silanization step. For dry samples, the shear bond strengths ranged from 7.5 to 10.6 MPa (ANOVA, $p < 0.05$) when the Ti surface had been silanized with MPS in *i*-PrOH/H_2O, and from 6.5 to 12.4 MPa (ANOVA, $p < 0.05$) when the Ti surface had been silanized with MPS in EtOH/H_2O at pH 4.5. Fifteen weeks of storage of the silane solution increased the shear bond strength of dry samples by *ca.* 1–4 MPa per test group. In contrast, thermo-cycling reduced the shear bond strength in both solvent systems. The weight of the test sample stubs increased by *ca.* 3.5 wt% after 187 days of being subjected to the water sorption test.

Keywords

Silanes, 3-methacryloxypropyltrimethoxysilane, methyl methacrylate, pH, *bis*-GMA, MMA, Ti, silica-coating

* To whom correspondence should be addresseed. Fax: +358-2-3338390; e-mail: mervi.puska@utu.fi

Adhesion Aspects in Dentistry

© Koninklijke Brill NV, Leiden, 2009

1. Introduction

Silanes are synthetic hybrid organic–inorganic compounds that are used as coupling agents across organic–inorganic interfaces for bonding dissimilar materials, e.g. paints to metal surfaces [1–3]. In the applications in dentistry and dental technology, silanes are widely used as coupling agents to bond resins to silica-coated metals, ceramics and resin composites [4–7]. When bonding an acrylic resin, the activated alkoxy groups (silanols) in silane molecules react with the metal while the organofunctional group (e.g. the vinyl bond in the methacrylate group) reacts with the monomeric resin matrix. The usefulness of silanes relies on their molecular structure, which contains easily hydrolysable alkoxy groups, such as kinetically favorable methoxy, and organofunctional groups (Fig. 1). The silane molecules first must be activated by hydrolyzing the methoxy groups to become silanol groups [4, 8]. When a hydrolyzed silane is applied onto a metal, the silanol groups will react by forming hydrogen bonds and subsequently covalently bonded siloxane structures are formed on the metal surface. The organofunctional terminal groups of silane molecules can copolymerize with the monomers of the organic matrix by a radical polymerization reaction [9]. By virtue of these chemical reactions, silanes are widely employed in dentistry as coupling agents in practically all resin composite based cements for cementing bridges, metal crowns, onlays, and inlays [4].

Nowadays, there are many commercially available silane products for dental applications [4, 10]. Typically, silane products in dentistry are based on 3-methacryloxypropyltrimethoxy (Fig. 2a), a well-known organofunctional trialkoxysilane. It is normally applied in polar aqueous aliphatic alcohol solutions (e.g. ethanol, *iso*-propanol) or in ethyl acetate, acetone, or even non-polar alkane solvents (e.g. *n*-pentane, *n*-hexane); however, the catalysts needed for activation reactions vary [11]. The concentration of 3-methacryloxypropyltrimethoxysilane (MPS) usually ranges from 1 to 5 vol% in ethanol (EtOH) or *iso*-propanol (*i*-PrOH), both diluted with 5–10% water, but lower silane concentrations are also used [4]. In fact, the low concentration of MPS in solutions is more desirable, because the autopolymerization process of silane molecules can be optimized in diluted solutions. Moreover, low silane concentrations are known to produce thin siloxane films (with a thickness of *ca.* 10–50 nm) that can promote the resin-to-metal bond [12].

In dentistry and dental technology, the biomechanical properties of restorative materials should be close to those of the tooth tissues. Dental materials based on bisphenol-A-glycidyl dimethacrylate (i.e. *bis*-GMA) and triethyleneglycol dimethacrylate (TEGDMA) prepolymers are widely exploited in tooth tissue reconstruction, because the biomechanics and clinical handling properties of *bis*-GMA/TEGDMA-based polymer systems are relatively good [13–15]. Dental resin composite cements containing *bis*-GMA/TEGDMA as the polymer matrix are often called dual-cured resin systems, because polymerization can be initiated either chemically (i.e. peroxide initiated redox polymerization reaction) or by blue light (photo-polymerization) [16, 17]. After the initiation step, the polymerization reaction occurs across the vinyl double bonds of methacrylate groups. The typical final

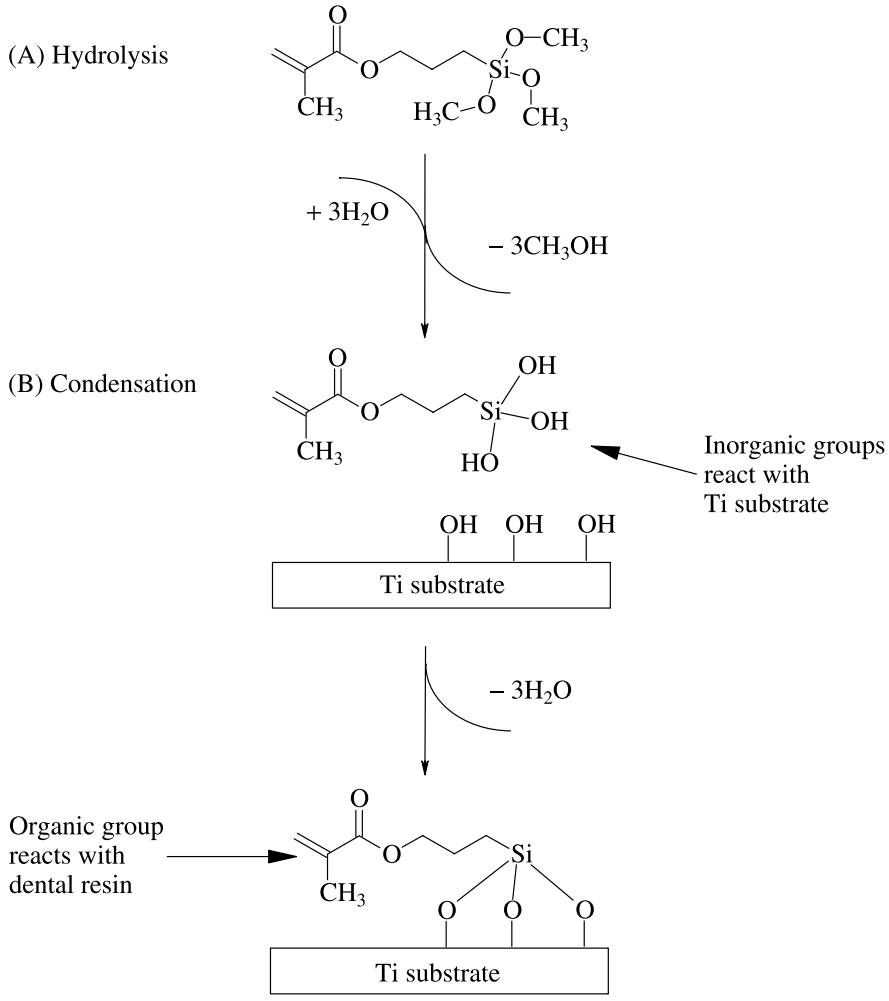


Figure 1. The illustration above shows (A) the hydrolysis reaction of MPS that activates the inorganic groups of the silane molecule and (B) the condensation reaction by which silane is adsorbed onto the surface of Ti substrate.

rate of double bond conversion in dental resin composites is *ca.* 55–75% [18, 19]. As the reaction progresses, the double bonds of methacrylate groups of *bis*-GMA and TEGDMA can also react with the methacrylate group of activated MPS. Thus, *bis*-GMA/TEGDMA resin composites offer the advantages of two relatively easy mechanisms of initiation of polymerization and the possibility of simultaneous covalent bonding of a highly cross-linked network polymer to silanized metal or glass surfaces [4].

Some studies have indicated that silane coupling agents play a key role in adhesion promotion. Several studies have demonstrated the adhesion of methacrylate-based polymers to titanium with the application of MPS [4, 20–22]. Titanium has

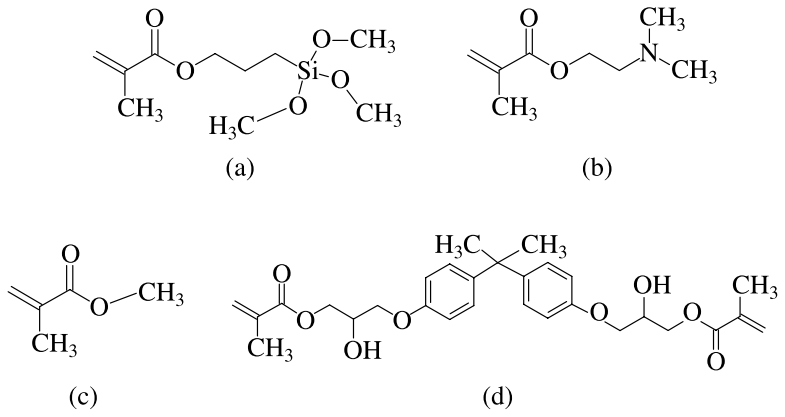


Figure 2. The molecular structures of compounds containing methacrylate group used in the experiments: (a) methacryloxypropyltrimethoxysilane, MPS, (b) *N*,*N*-dimethylaminoethyl methacrylate, DMAEMA, (c) methyl methacrylate, MMA, and (d) bisphenol-A-glycidyl dimethacrylate, *bis*-GMA.

been used as the substrate of choice because it is potentially a dental biomaterial substructure for crowns, bridges, and in particular implants. In prosthodontics, Ti crowns and bridges are cleaned prior to veneering and cementing by a controlled short-term roughening with sand-blasting and then silica-coated by the tribochemical Rocatec™ or CoJet™ (both 3M Espe) system before silanization [4, 6, 23]. The roughening method, which consist of abrasive blasting with special silica-modified aluminium oxide sand particles, provides micromechanical retention and promotes chemical adhesion, thereby improving the bond strength [21].

A well-known drawback of dental materials based on *bis*-GMA/TEGDMA is incomplete conversion of double bonds. In fact, the cured polymer network can contain up to 6 wt% residual uncured monomers [24]. The release of unreacted monomers, usually mainly methyl methacrylate (MMA), from resin composites may cause allergic reactions in some patients [25]. Another drawback is the tendency of these dental materials to absorb water (i.e. water uptake) in the oral environment. The amount of water uptake by experimental materials is normally determined in conjunction with the shear bond strength measurements, which are often done after alternating thermal stress (i.e. thermo-cycling), in order to try to simulate *in vivo* circumstances [26]. The alternating temperatures during thermo-cycling are typically +5°C for cold exposure and +55°C for hot exposure. The specimens exposed to thermal stress have mostly lower shear bond strength values than those not subjected to thermal stress (i.e. kept in dry storage conditions). It can be summarized that the clinical application of dental materials requires a good knowledge of their various biomechanical properties, such as the bond strength and water uptake in a simulated oral environment.

In this study, surface silanization with MPS was studied to determine the durability of an experimental resin bonded to a Ti substrate. We wanted to understand more about the effects of (a) pH value of the solution, (b) the aliphatic alcohol type

in the solvent, and (c) the hydrolysis time on the bond strength. These aspects have not been widely reported in the dental materials literature. We tested whether solvent and pH could significantly affect the compatibility of the silane molecule in the adhesion promotion system and hence shear bond strength. In this study, experimental silane solutions, with MPS concentrations of 0.01 vol%, were prepared in *i*-PrOH/H_2O or EtOH/H_2O solutions, the pH of which was adjusted to 4.5, 5.0, or 5.5. It has been shown that water sorption affects the long-term stability of dental polymers [27]. Therefore, the water sorption was also determined for the experimental resin employed in the shear bond strength investigation in this study. It was expected that there would be high sorption tendency for water for the experimental resin system.

2. Materials and Methods

2.1. Preparation of Experimental Resin System

The materials used in this study are listed in Table 1. In addition, Fig. 2 shows the molecular structures of compounds used in the experimental resin and silane. The laboratory-made experimental resin contained 78.43 wt% *bis*-GMA and 19.61 wt% methyl methacrylate (MMA). Thereafter, 0.98 wt% of initiator of photo-polymerisation (i.e. camphorquinone) and 0.98 wt% of activator

Table 1.
Materials used in the study

Brand	Abbr.	Manufacturer	Lot number	Type of material
Bisphenol-A-glycidyldimethacrylate	*bis*-GMA	Röhm, Germany	T0109/1	Experimental dental resin
Methyl methacrylate	MMA	Fluka, Switzerland	1119540	
Camphorquinone	CQ	Fluka, Switzerland	448343/1	
N,*N*-Dimethylaminoethyl methacrylate	DMAEMA	Aldrich, Germany	00628MU	
Ethanol (99.5%)[1]	EtOH	Primalco, Finland	160306	Experimental silane solutions (types 1–4)
2-propanol (*iso*-propanol)[2]	*i*-PrOH	Rathburn, UK	2J06MA	
Acetic acid (glacial, 99.8%)	AcOH	Merck, Germany	K22810463 610	
Methacryloxypropy-trimethoxysilane (98%)	MPS	Aldrich, Germany	S01603-022	
Titanium (c.p. grade 2)	Ti	Permascand, Sweden	ASTM B26589	Metal substrate

[1] In silane solutions of types 1 and 3, the solvent employed was a mixture of ethanol and water.
[2] In silane solutions of types 2 and 4, the solvent employed was a mixture of 2-propanol and water.

(*N*,*N*-dimethylaminoethyl methacrylate, DMAEMA) were added to the mixture of *bis*-GMA and MMA. The mixture of experimental resin (Table 1) was prepared within 15–30 min and packed in light protected polyethylene syringes. Thereafter, the resin was stored at +4°C before preparing test specimens.

2.2. Preparation of Experimental Trialkoxysilane Solutions and Their Stability Study

Two experimental 0.01 vol% solutions of MPS were prepared, in which accurate amounts of MPS were dissolved in a solvent mixture of 95 vol%/5 vol% *i*-PrOH and deionized water (Milli-RO Plus 30 water, with a resistivity of 18 MΩ cm, Millipore) or 95 vol%/5 vol% EtOH/deionized water. The MPS was purchased from Sigma-Aldrich Chemie GmbH (Steinheim, Germany, Lot S01603-022, purity 98%, unredistilled). Three silane solutions with different pH values were prepared in both alcohols, in which the pH value was adjusted to 4.5, 5.0, or 5.5 with 1 M acetic acid (Merck, Darmstadt, Germany). The carefully sealed silane solutions were allowed to undergo hydrolysis at room temperature for 1 h, before they were employed [10, 11, 21]. These silane solutions were subjected to a stability test before the bonding procedure, i.e. by storing the silane solutions in a carefully sealed container in the dark at +4°C for 15 weeks.

2.3. Grit-Blasting of the Ti Substrate

Titanium used in the studies was commercially pure grade 2 (Permascand Ltd., Ljungaverk, Sweden, Lot ASTM B26589). Titanium was cut to *ca.* 25 mm × 55 mm × 1 mm planar slides ($N = 48$). The surface was finished and polished with silicon carbide (SiC) paper (1200 grit; 0.15 μm particles). Then, the slides were cleaned for 10 min in an ultrasonic bath (Quantrex 90 WT, L&R Manufacturing, Inc., Kearny, NJ, USA) and finally rinsed with ethanol and acetone, in order to remove any grease and other impurities. A part with an area of approximately 10 mm × 55 mm of each planar Ti surface was silica-coated with a Rocatec™ Junior device (3M Espe, Seefeld, Germany), where the sand employed in Rocatec™ Plus (3M Espe), was 110 μm aluminum trioxide (Al_2O_3) abrasion particles with uniform silica (SiO_2) coating. Only the above-mentioned area was needed for the resin stubs to be light-polymerized onto surface conditioned (silicatized) and silanized Ti substrates. The silicatization was carried out using a pressure of 280 kPa, for a period of 10 s per *ca.* 1 cm^2 of the total area to be silicatized, from a perpendicular distance of 10 mm. Prior to silanization, the Ti slides were air-blasted with oil-free compressed air and kept in a desiccator.

2.4. Bonding, Shear Bond Strength Testing, and Silane Solution Stability Evaluation

Table 2 shows the classification of test groups for which the shear bond strengths of resin stubs to Ti were measured. Before the resin was bonded, the Ti slides were silanized at room temperature in the following manner: 2–3 drops of silane solution

Table 2.
Classification of test groups for measuring the shear bond strengths

Group	*N*	Silane solution	Solvent in the silane solution		pH		Time of hydrolysis
Dry[1] (60 min)	6	Type 1	EtOH/H_2O	4.5	5.0	5.5	60 min
Tc[2] (60 min)	6	Type 1	EtOH/H_2O	4.5	5.0	5.5	60 min
Dry (60 min)	6	Type 2	*i*-PrOH/H_2O	4.5	5.0	5.5	60 min
Tc (60 min)	6	Type 2	*i*-PrOH/H_2O	4.5	5.0	5.5	60 min
Dry (15 w)	6	Type 3	EtOH/H_2O	4.5	5.0	5.5	15 w
Tc (15 w)	6	Type 3	EtOH/H_2O	4.5	5.0	5.5	15 w
Dry (15 w)	6	Type 4	*i*-PrOH/H_2O	4.5	5.0	5.5	15 w
Tc (15 w)	6	Type 4	*i*-PrOH/H_2O	4.5	5.0	5.5	15 w

[1] Dry: The shear bond strengths were measured immediately after the preparation of specimens, i.e. in dry conditions.

[2] Tc: The shear bond strengths were measured after subjecting the specimens to thermal stress, i.e. after thermo-cycling.

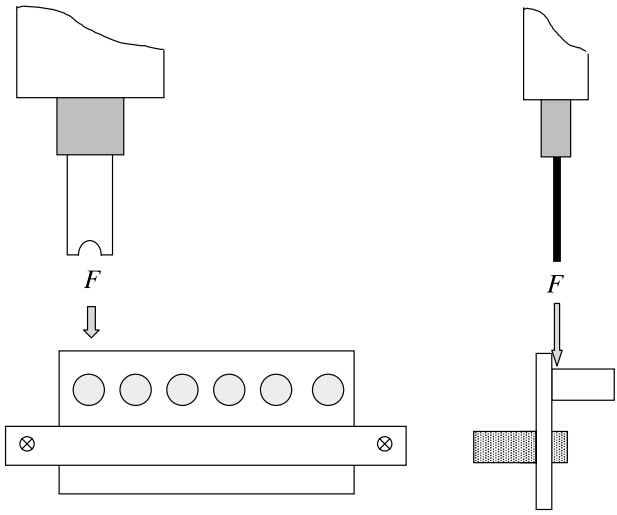


Figure 3. The illustration above shows the test setup for measuring the shear bond strengths of specimens, the system from the front (on left) and from the side (on right).

were brushed onto the substrate (one coat of silane) and allowed to react for 5 min (i.e. visually dry on the surface). Experimental resin was applied as cylindrical stubs ($n = 6$) with a diameter of 3.6 mm and height of 10 mm onto the surface-treated Ti slides. Figure 3 presents the test setup for measuring the shear bond strengths. The resin stubs were light-cured (Optolux 501, SDS Kerr, Danbury, CT, USA) for 40 s

at an average light intensity of 800 mW/cm^2. For completing the polymerization, the specimens were also cured in a light-curing oven unit (Vision Beta, 3M Espe, Seefeld, Germany) for 15 min in a vacuum. This is a custom procedure carried out at dental laboratories. The molds were then removed carefully by pressing at the same time the cured resin stub with a hand-piece instrument. The shear bond test was conducted for one half of the specimens after a dry storage in a desiccator at room temperature, i.e. in 'dry storage conditions' (labeled "Dry"). The other half (labeled "Tc") were subjected to thermal stress for 6000 cycles at temperatures alternating between +5°C and +55°C with an exposure time of 30 s and a transfer time of 2 s. In addition, after a storage period of silane solutions in the dark at +4°C for 15 weeks, the shear bond strengths were measured once again using the same test setup as described above, to carry out the stability investigation. The silane solutions were allowed to stabilize to room temperature before use. Shear bond strengths were measured with a universal material testing machine (LRX, Lloyd Instruments Ltd., Fareham, UK), using a crosshead speed of 1.0 mm/min. This machine was used according to the recommendation stated in ISO 10477 [28]. The shear bond strength was calculated using NEXYGEN 2.0 software (Nexygen, Lloyd Instruments Ltd., Fareham, UK). The following formula was used to calculate the shear bond strength (σ):

$$\sigma = F/A,$$

where F is the applied load at the failure of the bond during the shear test and A is the cross-sectional area of resin stub.

2.5. Water Sorption Study

The water sorption test was based on ISO 3696:1987 (E) and carried out accordingly [29]. The test specimens ($N = 10$) were stored in contact with 15 ml of deionized Milli-Q water (grade 2) at +37°C in sealed polypropylene flasks for the following time periods: 0, 4, 5, 6, 7, 11, 15, 22, 36, 40, 99 and 187 days. The weight increase was calculated as the weight percentage (wt%) of the original test specimen.

2.6. Statistical Analysis

The mean values for shear bond strength data were analyzed in order to determine the statistical significance of the results using ANOVA. The statistical analysis was performed using SPSS (Statistical Package for Social Science, SPSS Inc., Chicago, IL, USA) software for Windows. The dependent variable (shear bond strength) was discussed in terms of the independent variables (i.e. the pH value and hydrolysis time of silane, alcohol type, and submission of specimens to thermal stress), followed by *post-hoc* test.

3. Results

ANOVA revealed that the independent variables (see Section 2.6) had some effect on shear bond strength. However, one of the independent variables, i.e. subjecting the specimens to thermal stress, had the most significant effect. In dry storage conditions, the shear bond strengths varied between 7.6 and 10.9 MPa (ANOVA, $p < 0.05$), when the Ti-substrate was silanized using MPS in *i*-PrOH/H_2O solution. The highest shear bond strength was obtained (10.9 MPa) at pH 4.5 in *i*-PrOH/H_2O solution, whereas the lowest value was 6.5 MPa at pH 4.5 obtained using MPS in EtOH/H_2O solution. After thermo-cycling, the shear bond strengths of all test groups were reduced in both alcohol/water solution types and at all three pH levels. In the case of 1 h hydrolysis for the silane solution and after subjecting to thermal stress, the shear bond strength was least reduced at pH 4.5 from 6.5 MPa to 6.3 MPa (ANOVA, $p < 0.05$), when Ti-substrate was silanized with MPS in EtOH/H_2O. In the case of MPS in *i*-PrOH/H_2O solution, the shear bond strength least reduced at pH 5.5 (from 7.5 MPa to 5.8 MPa).

Figure 4 shows the results of shear bond strength measurements before and after the stability investigation of different silane solutions. For silane solutions aged for 15 weeks, the shear bond strengths were observed to be numerically higher in both alcohol/water solutions and at each pH level tested. The highest shear bond strength was achieved at pH 4.5 and the lowest at pH 5.5. In the case of MPS in EtOH/H_2O solution, the highest shear bond strength was 12.4 MPa in dry conditions (dry storage) at pH 4.5. In the case of MPS in *i*-PrOH/H_2O solution at pH 5.5 after dry storage, the shear bond strength was the lowest i.e. 8.5 MPa (ANOVA, $p < 0.05$).

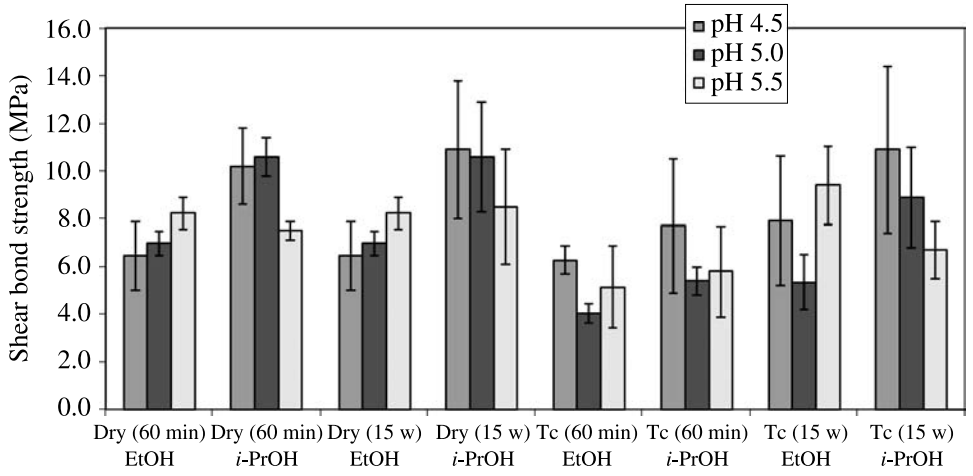


Figure 4. The shear bond strength of the specimens prepared using either 'fresh' silane solution, i.e. the hydrolysis reaction time for MPS silane in ethanol (EtOH) and *iso*-propanol (*i*-PrOH) solutions was 1 h, or silane solution after 15 weeks (w) hydrolysis reaction time. The tests were performed either after dry storage conditions ('Dry') or after subjecting to thermo-cycling ('Tc'). Different bars indicate the pH value of silane solution.

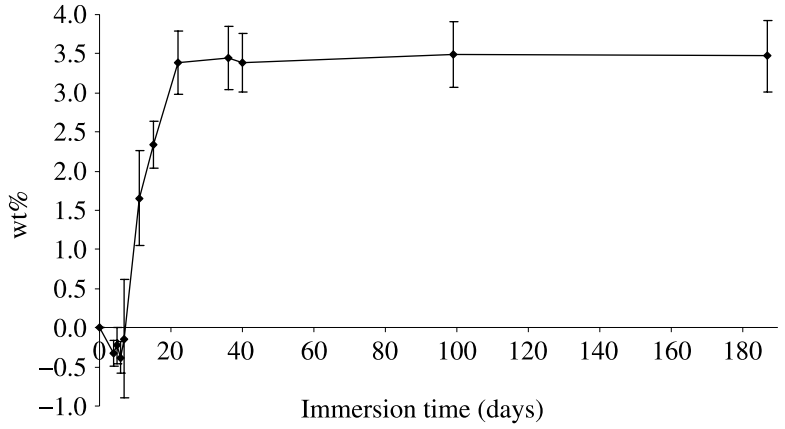


Figure 5. The curve demonstrates the weight increase during the water sorption test for the experimental dental resin.

Thermo-cycling also reduced the shear bond strengths, when 15-week-old silane solutions were employed. However, the shear bond strengths did not decrease significantly at pH 4.5 in the case of MPS in *i*-PrOH/H_2O solution.

Figure 5 shows the change in weight during the water sorption test. After 7-day immersion time, the water sorption first slightly decreased the weight of the specimens (*ca*. 0.4 wt%), because of the release of unreacted residual monomers. After 11-day immersion time, the weight of the specimens increased by *ca*. 1.7 wt%. The saturation point of water sorption was achieved in 22 days, after which the weight of specimens remained constant. At the end of water uptake capacity measurement, the weight of specimens had increased by approximately 3.5 wt%.

4. Discussion

The new information obtained in this study on adhesion promotion with MPS solutions should improve understanding and application of the silane-aided bonding concept. In addition, the ageing time study of experimental silane solutions has some scientific interest, since no inhibitors were used in the experimental solutions to inhibit the hydrolysis of MPS. Previously, it had been reported that the metal cleaning procedure as well as the concentration and pH value of silane affect the formation of silane films i.e. silane deposition time and the rate of adsorptioning onto metals, thus affecting substantially the adhesion promotion performance [3, 12]. Therefore, in this study, the effects of pH and the aliphatic alcohol solvent system used for the bonding capability of the silane molecule between *bis*-GMA/MMA resin system and silica-coated Ti surface were evaluated. Moreover, the effects of subjecting the experimental resin stubs to thermal stress (artificial aging) and the stability of silane solution after 15 weeks aging were studied based on the fact that dilute MPS solutions are known to retain their coupling properties for a long period [30]. 15 weeks correspond to a clinically relevant time period for checking the sta-

bility of experimental silane solutions. There has also been continued interest and demand in developing experimental silane-based adhesion promoters for applications in dentistry and in general in adhesion technology.

The tested silane of interest and choice was MPS (0.01 vol%) in *iso*-propanol (*i*-PrOH)/H_2O or ethanol (EtOH)/H_2O solutions, in which pH had been adjusted to 4.5, 5.0, or 5.5. For one half of the specimens, the shear bond test was conducted after storage in dry conditions at room temperature for 2 h, whereas the other half were subjected to thermal stress (thermo-cycling) to simulate the aging process in oral environment. The other tested materials, Ti and *bis*-GMA/MMA resin, were selected because of their broad utilization not only in dentistry but also in some medical devices [31]. Actually, Ti works excellently as a biomaterial and its surface is easy to modify with silanes, in principle, without [22] or with silica-coating, because of its pre-existing thin oxide layer on its outermost surface [10]. However, silicatization is often recommended prior to silanization in stead of a direct silanization [4, 20, 21]. Although, MPS has shown some preliminary signs of osteoconductive properties but still can be a relevant silane of choice in biomaterials research [32].

In dental laboratories, tribochemical Rocatec™ (3M/Espe) system as a custom pretreatment method is widely employed for metals, amalgams and ceramics [6, 23]. In this study, the Rocatec™ treatment was supposed to produce a relatively uniform and visually rough (Al_2O_3+ SiO_2) outer layer on Ti surface. Figure 3 shows the test setup for measuring the shear bond strength. In terms of tribochemical Rocatec™ treatment, the sandblasting of Ti plates created a microretentive Ti surface. This means that the adhesion of the studied resin system will increase, as Matinlinna and co-workers had previously reported [21, 22]. Therefore, in this study, the failure of the bonds during the shear test was also cohesive in the resin for all specimens. Before the application of the experimental resin onto Ti substrate, the Rocatec™ treated surface was silanized using four different silane solutions (*cf.* types 1–4, Table 2) with controlled pH levels. The pH levels used were based on of the most often used pH values in the literature with MPS. Figure 1 shows two key reactions that are supposed to occur in the silane solution during its hydrolysis [1, 2]. In the first step, the alkoxy groups are hydrolysed resulting in intermediate silanol species. The reaction is relatively fast for the kinetically labile methoxy groups. In the second step, the silanols condense to form hydrogen bonds and siloxane bonds (–Si–O–Si–) to connect the monomer resin phase chemically to the conditioned Ti substrate [4]. In fact, it has been proposed that the pH level may control both the hydrolysis and condensation reactions in dilute silane solutions [33]. In addition, these two primary reactions can also be influenced by other solution variables such as catalyst, silane concentration, and temperature, which are beyond the scope of this study but have been discussed by others [34, 35]. In fact, the hydrolysis of MPS does not require addition of any acids, because the deionized water is slightly acidic, i.e. its pH is between 6 and 7. If acid is added to the diluted MPS solutions, the kinetically controlled hydrolysis reaction will be faster and more effective. Therefore,

after 15 weeks, it is most likely that MPS would undergo hydrolysis in pure deionized water, too. This effect will be studied further.

The solvent might affect the siloxane film formation and hence adhesion promotion. Therefore, two aliphatic, "typical" alcohols were employed for comparing the obtained shear bond strengths at three pH values in two hydrolysis and ageing times. However, methanol as the simplest aliphatic alcohol was excluded from the test setup due to its obvious hazards (toxicity). According to the shear bond strength results, *i*-PrOH seems to be a more suitable solvent in conjunction with water for the MPS solution, in particular, if the hydrolysis time is relatively short. An explanation could be the very high surface energy of the Al_2O_3+ SiO_2 coated Ti surface, and lower surface tension of *i*-PrOH resulting in easier wetting as well as slightly slower evaporation of *i*-PrOH (bp. 82°C, STP) compared with ethanol (bp. 79°C, STP). Thus, the ratio between surface tension and viscosity has been reported to be higher for EtOH than *i*-PrOH [36]. Therefore, a binary mixture of *i*-PrOH and water might form a siloxane film more prone to promote adhesion on the outermost surface of the metal substrate. This effect should be investigated further in the future. This research also confirmed that 1 h time period is long enough for activating the inorganic groups in MPS molecule in *i*-PrOH/H_2O.

In dry storage conditions, the highest shear bond strength obtained was 10.6 MPa, comparable to the value obtained with MPS in EtOH/H_2O, where the highest mean shear bond strength was 8.2 MPa (ANOVA, $p < 0.05$). In addition, the lower pH value seems to activate a rapid hydrolysis reaction of MPS in *i*-PrOH/H_2O solution. When silanization was carried out using 15-week-old MPS prepared in *i*-PrOH/H_2O at pH 4.5, the shear bond strengths obtained were slightly higher, even after thermo-cycling. If the stability test storage time had been longer, the bonding capability of MPS might have decreased. We observed that MPS in *i*-PrOH/H_2O already showed some signs of ageing, i.e. initial SiO_2-gel formation. Such gel-like Si obviously makes the coupling properties inferior. To activate the alkoxy groups of MPS in EtOH/H_2O, 1 h hydrolysis time is usually enough [5, 10, 20]. Interestingly, the highest shear bond strength (12.4 MPa) in EtOH/H_2O was obtained at pH 4.5 using a silane solution that had a hydrolysis period of 15 weeks. The hydrolysis in EtOH/H_2O seems to occur at a slower rate by hindering the very rapid condensation of activated silane, which apparently occurs due to the presence of appropriate catalyst [20–22]. Therefore, the reaction activity of MPS in EtOH/H_2O solution may be increased after 15 weeks hydrolysis. This behaviour merits further investigation in the future.

It has been shown that both the shear bond strength and tensile bond strength depend highly on the materials and the geometry of the test arrangement [37]. Moreover, mechanical testing for the strength of a material is a substantially more complicated issue than it appears at first sight. The definition is easy enough: stress at failure but the ultimate question remains: does the testing simulate adequately the real clinical conditions in the oral environment [38]? It can be summarized that in dental materials science, the shear bond strength is a widely used variable for

estimating how strong the union between dissimilar dental materials would be. In this study, the number of specimens in a single test-group was relatively low, i.e. six. Nevertheless, such numbers are statistically relevant and have, in principle, successfully been used in dental materials research and testing previously [20, 39].

The silanization process was based on an aqueous silane solution at controlled pH. Typically, the pH range between 4.5 and 5.5 is commonly used for silane solutions based on published literature [1, 4, 10, 11, 20]. Some investigations have indicated that the pH of an organosilane coupling agent solution can also influence the nature of the various reactions which occur in solutions [35]. In the analysis of data between the groups, there were many independent variables (i.e. the pH and hydrolysis time of silane, alcohol type, and subjecting to thermal stress) as well as their interactions that had some effect on the shear bond strengths. Thermal stress caused the most significant difference between the shear bond strengths of various groups. In addition, the hydrolysis of MPS occurred most readily in the solution containing *iso*-propanol. This study did not find a significant relationship between pH in the range of 4.5–5.5 and shear bond strengths for the two solvent systems tested. Nevertheless, silane solutions with the lowest pH value (4.5) seemed to produce, on average, slightly higher bond strengths than those obtained with silane solutions with higher pH values, in the case of MPS dissolved in *i*-PrOH/H_2O. The tested pH range was selected on the basis of the literature [1, 4, 5] and in the future studies we may widen this range. The polarity of tested alcohol solvents did not differ enough: the polarity index for EtOH is 5.2 and that for *i*-PrOH is 4.0 [40]. Therefore, future studies could assess the effect of lower and higher pH values using other types of alcohols, e.g. 1-butanol or the highly polar, electronegative 2,2,2-trifluoroethanol.

Figure 4 presents the results of thermo-cycling and silane stability (storage) tests. As expected, thermo-cycling produced lower mean shear bond strength values with all silane solutions. According to the literature, thermo-cycling is generally known to decrease the shear bond strengths [10, 20–22, 25]. However, after 15 weeks of ageing, the shear bond strengths were found to be relatively sufficiently high, if MPS in *i*-PrOH/H_2O solution, adjusted at the lowest used pH value, was employed. Interestingly, the shear bond strengths did not decrease significantly after exposure to thermal stress. The relatively rapid hydrolysis of MPS in *i*-PrOH/H_2O solution can thus considered to occur in stable conditions, if the silane solution is stored carefully in sealed flasks in the dark at +4°C prior to the bonding procedure. In addition, the thermal stress might, to some extent, increase the condensation reaction of this kind of MPS solution. However, this needs to be investigated more precisely to obtain further evidence of this presumption. In the case of EtOH, it was recognised that the age of the silane solution played an important role and had influence on shear bond strength. After subjecting to thermal stress, the highest shear bond strength was obtained at the highest pH value in EtOH/H_2O solution. According to the results of shear bond strengths, the most suitable pH value for activating MPS in

EtOH/H_2O solution was 5.5, whereas the activation in *i*-PrOH/water solution was found to be most effective at pH 4.5.

Water sorption of polymers plays an important role in long-term stability of dental appliances in an aqueous environment [27]. Therefore, it was also relevant to study the diffusion of water molecules into the experimental polymer used in this research. According to the results of water sorption, the weight of specimens first decreased by 0.4 wt% in 7 days. The weight loss most probably indicates that unreacted residual monomers in the polymerized *bis*-GMA/MMA resin were released (this was not detected by chemical analysis, though). In the course of time, the water sorption then stabilized within 22 days, when the weight of specimens had increased by *ca.* 3.5%. After 22 days, the amount of water did not increase during the subsequent period of 165 days. According to the results of this water sorption and bond durability study, MPS in either EtOH/H_2O or *i*-PrOH/H_2O solution, is a suitable promoter in the adhesion of *bis*-GMA/MMA resin to silica-coated Ti substrate, when the pH of silane solution is between 4.5 and 5.5. Moreover, the water sorption of the experimental dental resin was relatively low.

5. Conclusions

Within the limited scope of this pilot study, the following conclusions can be drawn:

(1) The pH range of 4.5 to 5.5 is relevant to activate MPS in the studied two solvent systems, based on EtOH and *i*-PrOH, and with a final hydrolysis time of 15 weeks.

(2) In the case of *i*-PrOH/H_2O at pH 4.5, the highest adhesion promotion capacity for MPS was obtained within 1 h. The thermal stress (i.e. aging by thermocycling) did not reduce the shear bond strength values significantly, i.e. from 10.2 MPa to 7.7 MPa (ANOVA, $p < 0.05$). In addition, if 15-weeks-old silane solutions were used for adhesion promotion, the shear bond strength values did not decrease dramatically, i.e. ∼1–4 MPa/test group.

(3) The water uptake of the experimental *bis*-GMA/MMA-based non-filled polymer was *ca.* 3.5 wt% in 187 days.

Acknowledgements

The research was conducted as a part of the Bio- and Nanopolymers Research Group activity of the Center of Excellence (CoE), which is jointly funded by the Academy of Finland and TEKES (Finnish Funding Agency for Technology and Innovation). It was also part of the NIOM (Nordic Institute of Dental Materials, Oslo, Norway) Biomaterials Network in the Nordic Countries. Ms. Hanna Mark, B.Sc. (University of Turku) and Mr. Torbjørn Knarvang, B.Sc. (Nordic Institute of Dental Materials, NIOM) are thanked for their skillful technical assistance. Dr. Trevor Lane (University of Hong Kong) is thanked for the language proofreading of this article.

References

1. E. Plueddemann, *J. Adhesion* **2**, 184 (1970).
2. E. Plueddemann and G. Stark, *Mod. Plast.* **54**, 102 (1977).
3. T. Child and W. van Ooij, *Trans. Inst. Metal Finish.* **77**, 64 (1999).
4. J. Matinlinna, L. Lassila, M. Özcan, A. Yli-Urpo and P. Vallittu, *Int. J. Prosthodont.* **17**, 155 (2004).
5. T. Hooshmand, R. Daw, R. van Noort and R. Short, *Dental Mater.* **17**, 1 (2001).
6. M. Özcan, *J. Prosthet. Dentistry* **87**, 469 (2002).
7. J. P. Matinlinna, M. Ozcan, L. P. J. Lassila and P. K. Vallittu, in: *Silanes and Other Coupling Agents*, Vol. 4, K. L. Mittal (Ed.), pp. 199–215. VSP/Brill, Leiden, The Netherlands (2007).
8. E. Plueddemann, H. Clark, L. Nelson and K. Hoffman, *Mod. Plast.* **39**, 135 (1962).
9. J. Marsden, in: *Handbook of Adhesives*, I. Skeist (Ed.), pp. 536–548. Van Nostrand Reinhold, New York (1990).
10. J. Matinlinna, L. Lassila and P. Vallittu, *J. Dentistry* **34**, 721 (2006).
11. T. Chen and G. Brauer, *J. Dental Res.* **61**, 1439 (1982).
12. W. van Ooij, D. Zhu, G. Prasad, S. Jayaseelan, Y. Fu and N. Teredesai, *Surface Eng.* **16**, 386 (2000).
13. N. Lin, P. Drzal and S. Lin-Gibson, *Dental Mater.* **23**, 1211 (2007).
14. E. Asmussen and A. Peutzfeldt, *Dental Mater.* **14**, 51 (1998).
15. Y. Finer and J. Santerre, *J. Biomed. Mater. Res.* **81A**, 75 (2007).
16. Y. Chen, J. Ferracane and S. Prahl, *Dental Mater.* **23**, 655 (2007).
17. W. Schroeder and C. Vallo, *Dental Mater.* **23**, 1313 (2007).
18. B. Kalipcilar, L. Karaagaclioglu and U. Hasanreisoglu, *J. Oral Rehabil.* **18**, 399 (1991).
19. E. Viljanen, M. Skrifvars and P. Vallittu, *J. Appl. Polym. Sci.* **93**, 1908 (2004).
20. J. Matinlinna, L. Lassila, I. Kangasniemi and P. Vallittu, *J. Dental Res.* **84**, 360 (2005).
21. J. Matinlinna, L. Lassila, I. Kangasniemi, A. Yli-Urpo and P. Vallittu, *Dental Mater.* **21**, 287 (2005).
22. J. Matinlinna, M. Özcan, L. Lassila and P. Vallittu, *Dental Mater.* **20**, 804 (2004).
23. M. Özcan, *J. Prosthodont.* **15**, 47 (2006).
24. M. Taira, A. Khan, K. Ohmoto, N. Satou, H. Shintani, K. Wakasa and M. Yamaki, *J. Mater. Sci. Lett.* **13**, 1229 (1994).
25. H. Schweikl, G. Spagnuolo and G. Schmalz, *J. Dental Res.* **85**, 870 (2006).
26. M. Gale and B. Darvell, *J. Dentistry* **27**, 89 (1999).
27. V. Miettinen, K. Narva and P. Vallittu, *Biomaterials* **20**, 1187 (1999).
28. ISO 10477:2004, Dentistry — Polymer-based crown and bridge materials.
29. ISO 3696:1987 (E), Water for analytical laboratory use — Specification and test methods.
30. T. Hooshmand, R. van Noort and A. Keshwad, *Dental Mater.* **20**, 635 (2004).
31. E. Erbe, T. Clineff and G. Gualtieri, *Eur. Spine J.* **10**, S147 (2001).
32. S. Shinzato, T. Nakamura, T. Kokubo and Y. Kitamura, *J. Biomed. Mater. Res.* **55**, 277 (2001).
33. B. Arkles, *Chemtech* **7**, 766 (1977).
34. M.-L. Abel, R. Allington, R. Digby, N. Porritt, S. Shaw and J. Watts, *Int. J. Adhesion Adhesives* **26**, 2 (2006).
35. G. Tesoro and Y. Wu, *J. Adhesion Sci. Technol.* **5**, 771 (1991).
36. A. Han, G. Mondin, N. Hegelbach, N. De Rooij and U. Staufer, *J. Colloid Interface Sci.* **293**, 151 (2006).
37. R. van Noort, S. Noroozi, I. Howard and G. Cardew, *J. Dentistry* **17**, 61 (1989).

38. B. Darvell, *J. Mater. Sci.* **25**, 757 (1990).
39. M. Dündar, M. Özcan, B. Gokce, E. Comlekoglu, F. Leite and L. Valandro, *Dental Mater.* **23**, 630 (2007).
40. P. Di Martino, R. Censi, L. Malaj, D. Capsoni, V. Massarotti and S. Martelli, *Cryst. Res. Technol.* **42**, 800 (2007).

XPS Analysis of Silane Films on the Surface of a Dental Ceramic

Tabassom Hooshmand [a,*], **Alireza Keshvad** [b] **and Richard van Noort** [c]

[a] Department of Dental Materials, School of Dentistry/Research Center for Science and Technology in Medicine, Tehran University of Medical Sciences, Ghods Street, Tehran 14174, Iran
[b] Department of Prosthodontics, School of Dentistry, University of Shahed, Italia Street, Tehran 14317, Iran
[c] Department of Adult Dental Care, School of Clinical Dentistry, University of Sheffield, Claremont Crescent, Sheffield S10 2TA, UK

Abstract
This study was designed to investigate the surface properties and the thickness of organofunctional silane films formed on leucite-reinforced feldspathic (LRF) ceramic surfaces after different methods of silane application using X-ray photoelectron spectroscopy (XPS). Six LRF ceramic discs (Mirage®, Myron Intl., Kansas City, KS, USA) were produced according to the manufacturer's instructions and polished to a 1 μm finish. A silane coupling agent was applied to five ceramic discs using different application methods: (A) immersion in silane solution for 60 s and dried with compressed air spray for 15 s; (B) as method A but heat treated with hot air at 50 ± 5°C for 15 s; (C) silane was applied with a brush for 60 s and dried with compressed air spray for 15 s; (D) as method C but heat treated with hot air at 50 ± 5°C for 15 s; (E) as method C followed by rinsing the specimens with hot water (15 s) and drying with hot air for 30 s. The ceramic surfaces were then analyzed by XPS at 15°–60° take-off angles. The results showed the highest and the lowest increase of C_{1s} (C in the structure of silane) for treatments A and E, respectively. Signals of COO or C–COO in the high resolution spectra of C_{1s} were observed for all silane-treated ceramic surfaces. The proportion of C–Si groups on the silane-treated surfaces compared with the untreated surface was significantly increased. XPS analysis indicates that the thickness of the silane film on a leucite-reinforced feldspathic ceramic surface is a function of the mode of application. The lowest film thickness of silane was found for treatment E, which more closely matches that of a monolayer.

Keywords
Silane, X-ray photoelectron spectroscopy, ceramic surface, treatment method

1. Introduction

Dental ceramics as a highly esthetic material are being used extensively in today's dentistry. The major desirable properties of ceramics are their durability,

* To whom correspondence should be addressed. Tel.: 0098-21-88212484; Fax: 0098-21-88081699; e-mail: hoshmand@sina.tums.ac.ir

Adhesion Aspects in Dentistry
© Koninklijke Brill NV, Leiden, 2009

biocompatibility, and resistance to abrasion and chemical degradation. Ceramic restorations such as ceramic inlays/onlays, laminate veneers, crowns, and fixed partial dentures are usually cemented onto the tooth substructure with resin composite luting agents. In addition, resin composites are used to repair fractured ceramic restorations in repair systems. The adhesive bond between ceramic surface and resin composite is usually created *via* two mechanisms, micro-mechanical attachment by hydrofluoric acid (HF) etching and/or gritblasting, and chemical bonding using a silane coupling agent. Studies on evaluating bond strengths between ceramic and resin composite have arrived at different conclusions about the effect of surface treatments. Several studies have reported that optimum bond strengths were obtained using a combination of an etched ceramic surface with silane treatment [1–3]. However, a major concern exists on the hazardous effects of HF as an etchant for dental ceramics [4]. In addition, new glass-ceramics are being developed that have such a fine crystalline phase that the etching process might have no further effect in improving the micromechanical retention over what can be achieved simply by grit blasting.

The use of silane coupling agents in enhancing the bond of resin composites to silica-based ceramics is well accepted in the dental literature [5–8]. A silane coupling agent with the general formula R–Si–$(OR')_3$ is an organosilicon compound with a 'coupling' action. The organo-functional group (R) is chosen for reactivity with the organic matrix, while the hydrolyzable groups (R′) are precursors in the formation of silanol groups (Si–OH) for bonding to mineral (e.g., ceramic) surfaces. The most commonly used silane in dental applications is γ-methacryloxypropyltrimethoxysilane (γ-MPTS). The choice is based on the compatibility of the methacrylate group with the dimethacrylates used in composite technology. An excellent overview on silanes and their clinical applications in dentistry has been provided elsewhere [9].

In a previous study by Hooshmand *et al.* [10], a rod-to-rod tensile bond strength test arrangement was used to show that using silane the resin bond to a leucite-reinforced feldspathic ceramic could be improved to such a degree that cohesive failure occurred within the luting resin rather than at the resin–ceramic interface. A freshly prepared silane solution was used, which had been left for 2 h for hydrolysis. It was concluded that a durable resin–ceramic bond could be obtained by using an appropriate silane application without the need for HF acid etching the ceramic surface. The silane treatment method consisted of brush application for 60 s, hot air drying at 50 ± 5°C for 15 s followed by rinsing with hot water for 15 s and drying again with hot air for 30 s.

In addition, the interfacial fracture toughness of smooth and roughened leucite-reinforced feldspathic ceramic surfaces bonded with a luting resin was investigated in another work [11]. These results also showed a reliable bond between resin and ceramic without HF acid etching when using the optimized silane treatment method, confirming the earlier observation [10]. A possible explanation for these

observations was that the silane application procedure used resulted in the formation of an monolayer of the silane coupling agent by washing away any unreacted silane primer components, rather than the formation of an interphase layer as described by Ishida and Koenig [12].

X-ray photoelectron spectroscopy (XPS) is widely used as a direct surface analytical technique and involves the detection and analysis of electrons over a range of binding energies. The purpose of this study was to investigate using XPS the surface properties of organofunctional silane films formed on leucite-reinforced feldspathic ceramic surfaces after different methods of silane application. The intention was to correlate the thickness of silane film on ceramic surfaces with the results of the bond strength and fracture toughness of resin–ceramic interface from earlier observations [10, 11]. Such work has not previously been reported in the dental literature.

2. Experimental

2.1. Materials and Methods

Six leucite-reinforced feldspathic ceramic discs (Mirage®, Myron Intl., Kansas City, KS, USA; batch no. J2715K, Body D_4) with approximately 10 mm in diameter and 2 mm in thickness were condensed into discs and fired in a vacuum oven (Vacumat 200, Vita Zahnfabrike, Germany) according to the manufacturer's instructions. The ceramic discs were polished to a 1 μm finish with diamond pastes (Buehler Ltd, Coventry, UK) in order to ensure high-quality signal from the surface for analysis. The specimens were then cleaned ultrasonically in acetone for 15 min. To prevent water vapor contamination in the high-vacuum chamber of the spectrometer arising from the absorbed water in the bulk of ceramic, the ceramic discs were kept in a vacuum oven at 110°C for 48 h and then transferred to a vacuum desiccator at room temperature on the day before analysis. Adsorption of water from the atmosphere during transportation from the oven to the spectrometer was found not to be a problem.

A silane solution, consisting of 2.5% γ-methacryloxypropyltrimethoxysilane (γ-MPTS; from Sigma Aldrich, St Louis, MO, USA) in a solvent of 2.5% acetic acid and 95% ethanol by volume (BDH Ltd, Poole, UK) was prepared. The silane solution was left for 2 h to hydrolyze before being used. Five ceramic disc specimens were treated each with one of silane application methods as follows:

(A) Ceramic disc was immersed in the silane solution for 60 s and then dried with compressed air spray at room temperature for 15 s.

(B) Ceramic disc was immersed in silane solution for 60 s and heat treated with hot air at 50 ± 5°C for 15 s.

(C) Silane solution was applied with a brush for 60 s and then dried with compressed air spray at room temperature for 15 s.

(D) As method C but heat treated with hot air at 50 ± 5°C for 15 s.

(E) As method C followed by rinsing the specimens with hot water at 80°C (15 s) and drying with hot air for 30 s.

The remaining disc was kept untreated as a control.

2.2. XPS Analysis

The XPS analysis of the ceramic discs was carried out on a VG CLAM 2 (Vacuum Generators, East Grinstead, UK) with the Mg K_α X-ray source run at 100 W, 10 kV and 10 mA. Survey scans with a range corresponding to binding energies of 0–1100 eV were used for quantification at a pass energy of 100 eV. To obtain high resolution scans (narrow scans) for determination of chemical states, a pass energy of 20 eV was selected. All samples were analyzed at 15°, 30°, 45° and 60° take-off angles.

The binding energies for all spectra were calibrated assuming the major component of the C_{1s} peak to result from hydrocarbon contamination at a binding energy of 285.0 eV [13]. In addition to elemental composition, high resolution narrow scans of C_{1s} for all groups at 15° take-off angle were also analyzed in order to obtain information on the chemical states. These were analyzed using a computer curve-fitting program, assuming the peak envelope to consist of the following components found in the structure of γ-MPTS: carbon singly bonded to oxygen (C–O), carbonyl (C=O), carboxyl (COO) or bonded carboxyl (C–COO), and C–Si at binding energies of +1.5, +2.7–3, +4, +0.7, and −0.7 eV, respectively, relative to the hydrocarbon peak (C–H). Voigt peak shapes were assumed. In the routine, peak width and energy were fixed and only peak heights varied for each component to obtain optimum fit between the experimental and reference spectra.

Atomic concentrations were calculated using Scienta software (Scienta Instruments, Upsala, Sweden) and relevant sensitivity factors for the elements [14].

The thickness of the silane films on the ceramic surfaces following the five treatment methods was estimated from photoelectron signal intensities by the following equation [15]:

$$\frac{I}{I_\mathrm{o}} = \exp\left(-\frac{d}{\lambda \sin\theta}\right),$$

where d is the overlayer thickness, I is the ratio of photoelectron signal intensities from the overlayer to the substrate of a particular element, I_o is the photoelectron intensity from the same element at the depth d, θ is the take-off angle, and λ is the inelastic mean free path of the element.

Since aluminium was present only in the ceramic substrate, photoelectron signal intensities of Al_{2p} (I) from the wide scans of silane-treated ceramic surfaces at 30° take-off angle (θ) and that of untreated surface at 60° take-off angle (I_o) were used in the above equation. At 15° take-off angle, signals were assumed not to be strong enough to be yielded from the overall of silane film because the X-ray surface flux

density decreases as the sample is tilted to lower angles. The value chosen for the inelastic mean free path of Al_{2p} was ~2.4 nm [16, 17].

3. Results

The surface composition (in atomic %) of the major elements for the untreated (control) and silane-treated ceramic surfaces at different take-off angles are presented in Table 1. A significant increase of atomic percent for C_{1s} (C in the structure of silane) on silane-coated ceramic surfaces, except for treatment E, at 15° take-off angle was found when compared with untreated control. Atomic concentrations (in %) of C_{1s} for different silane treatment methods at 15° take-off angle are shown graphically in Fig. 1. The most and the least increases of C_{1s} were found for treatments A and E, respectively. An absence or decrease of atomic percent for K_{2p} and Na_{1s} and also decrease of Al_{2p}, Mg_{1s}, Si_{2p} (elements present in the bulk of ceramic) at 15° take-off angle were also observed. This suggests the presence of silane films on all silane-treated ceramic surfaces.

For the untreated ceramic surface, the concentrations of Al_{2p}, Mg_{1s}, Si_{2p}, O_{1s}, K_{2p} and Na_{1s} (atomic %) increased at 60° take-off angle, approaching the ceramic surface. There was also a decrease of atomic percent for C_{1s} from 15 to 60° take-off angle, assuming hydrocarbon contamination at the lower take-off angles.

Treatments B and D were heat treated versions of treatments A and C, respectively. Significant decreases of C_{1s} (atomic %) for treatments B and D were found compared with those of treatments A and C, respectively.

There was also a significant decrease of Al_{2p} (atomic %) for treatment A, followed by treatments B and C when compared with the untreated ceramic disc at 15° take-off angle. The least reduction of Al_{2p} was found for treatments D and E.

Results for the chemical states of elements obtained from narrow scans of C_{1s} signals at 15° take-off angle for the untreated and silane-treated ceramic surfaces are presented in Table 2. The carbon peaks had complex peak envelopes due to the presence of multiple carbon–oxygen functional groups. Signals of COO or C–COO in the high resolution spectra of C_{1s} were observed for all silane-treated ceramic surfaces. No signals of COO or C–COO were detected for control ceramic disc. The proportion of C–Si groups on the silane-treated surfaces compared with the untreated surface was significantly increased. The proportion of hydrocarbons (C–H) as a whole in the signal was reduced in all silane-treated ceramic surfaces. The concentration of C=O groups also increased further upon heating in treatments B, D and E.

The calculated values for the thickness of the silane coatings are shown in Table 3. Treatment A gave the highest film thickness (1.02 nm), which was found to reduce after heat treatment (0.84 nm) in treatment B. A thinner silane film resulted from treatment C (0.96 nm) when compared with treatment A, followed by a further reduction in silane film thickness for treatments D and E. The lowest film thickness of silane was found for treatment E (0.6 nm).

Table 1.
XPS surface composition (at%) of untreated and silane-treated ceramics with five silane treatment methods at different take-off angles (15°, 30°, 45° and 60°)

	Control				Treatment A				Treatment B				Treatment C				Treatment D				Treatment E			
	15°	30°	45°	60°	15°	30°	45°	60°	15°	30°	45°	60°	15°	30°	45°	60°	15°	30°	45°	60°	15°	30°	45°	60°
Al	5.5	5.9	6.4	6.6	2.9	4.0	4.6	3.9	3.4	4.7	5.0	4.3	3.7	4.7	4.4	4.4	4.6	5.3	5.0	4.7	4.7	5.1	5.0	5.9
Mg	5.6	5.8	4.9	5.4	3.5	4.6	4.8	4.5	3.6	4.3	4.5	4.3	5.9	6.0	7.3	7.1	4.9	5.5	5.5	5.3	5.2	6.1	5.6	5.1
Si	20.9	21.7	22.5	23.2	17.0	20.6	21.0	19.8	18.7	20.2	20.9	20.3	21.0	23.8	22.4	22.7	22.5	22.4	22.5	22.2	20.5	22.1	23.3	23.5
C	25.8	22.5	20.4	17.6	42.0	35.5	32.2	29.7	34.0	28.3	23.8	23.1	41.8	34.7	29.4	26.6	33.4	29.6	24.7	23.4	24.8	20.0	16.6	16.2
O	39.3	40.9	42.8	43.5	34.5	35.3	37.0	41.0	40.3	41.8	44.8	46.7	27.6	30.3	35.7	38.2	34.0	36.2	41.0	43.0	43.9	46.1	48.6	48.1
K	1.7	1.8	1.8	1.9	–	–	0.3	0.8	–	0.7	0.9	1.0	–	0.5	0.7	0.9	0.4	0.9	1.0	1.2	–	0.3	0.7	0.8
Na	0.5	0.7	0.6	0.8	–	0.2	0.2	0.3	–	0.3	0.4	0.5	–	0.2	0.3	0.4	0.2	0.3	0.4	0.5	0.1	0.3	0.4	0.5

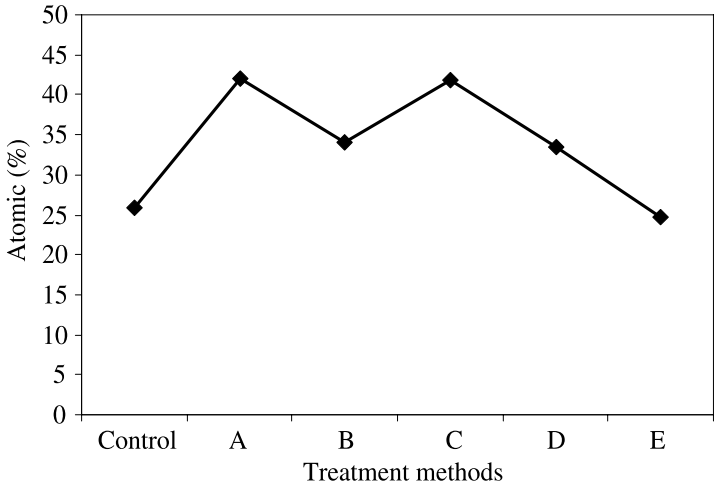


Figure 1. XPS atomic % of C_{1s} for different silane treatment methods at 15° take-off angle.

Table 2.
XPS area % of functional groups in the C_{1s} signals at 15° take-off angle for different silane treatment methods and untreated control

	Control	A	B	C	D	E
C–H	84.8	57.9	50.8	60.9	63.4	47.7
C–O	6.6	15.1	10.4	7.8	8.3	13.4
C=O	2.9	2.5	6.1	2.5	3.7	5.0
	–	6.3	5.2	2.8	2.0	8.0
	–	6.3	5.2	2.8	2.0	8.0
C–Si	6.0	12.5	22.1	20.0	20.8	17.9

Table 3.
Estimated thicknesses of silane films on ceramic surfaces for different silane treatment methods

	Treatment A	Treatment B	Treatment C	Treatment D	Treatment E
Thickness (nm)	1.02	0.84	0.96	0.72	0.6

4. Discussion

It has been suggested that the optimum time for adsorption from a silane solution is after hydrolysis and before oligomerization of silanols since the silane coupling agents are most effective when adsorbed as monomers [18]. In this study, simi-

lar to previous works, a freshly prepared silane solution based on γ-MPTS, acetic acid and ethanol was used, despite this silane solution having been reported to be effective for coupling ceramic surfaces even over 1-year storage period [19].

XPS analysis showed the presence of silane films on ceramic surfaces. This was revealed by (1) reduction of major elements present on the uncoated ceramic surface (Al_{2p}, Mg_{1s}, Si_{2p}), (2) increase of C_{1s} (C present in the structure of silane), and (3) absence or significant decrease of K_{2p} and Na_{1s} after silanization at 15° take-off angle (Table 1). However, the major elements present on untreated ceramic surface were detectable in all silane treatment methods even at 15° take-off angle. This may be due to the migration of these elements into the silane film as has been observed in other studies [20]. The other explanation for this finding is that these elemental signals of ceramic surface through a very thin layer of silane film (less than 1 nm) may be unavoidable.

The concentration of Al_{2p}, Si_{2p}, and O_{1s} increased after heat treatment at 15° take-off angle (treatment B compared with treatment A, and treatment D compared with treatment C). Further, this might have occurred because of diffusion of above elements from the ceramic surface into the silane film as a result of an attack of the substrate, and/or a reduction of film thickness due to oxidation [21].

From the narrow scan data (Table 2), signals of COO or C–COO were detected in the high resolution spectra of C_{1s} for all silane treatment groups, again confirming the presence of silane coatings on the treated ceramic surfaces. The proportion of C–Si groups on the silanized surfaces compared with uncoated control surface was also significantly increased. The proportion of hydrocarbons (C–H) as a whole in the signal was reduced in all silane-treated surfaces compared with control. It was assumed that hydrocarbon contamination had been replaced by silane during treatment. However, the hydrocarbon concentrations (above 40%) for all treatments are too large to be attributed solely to the carbon present in the silane. It may partially be due residual contamination not displaced by the silane [22].

The concentration of C=O groups also increased further upon heating for treatments B, D, and E. This is in agreement with the observation of another study by van Ooij and Sabata [21].

If it is assumed that the organosilanes uniformly cover the mineral surfaces, the thickness of the adsorbed film can be determined from the XPS data [23]. Thus, the thickness of the silane coatings on the ceramic surfaces following the five silane treatments was estimated. It was found that the ceramic surface immersed in the silane solution (treatment A) gave the highest film thickness. Application of the silane on the ceramic surface by a brushing technique (treatment C) as opposed to immersion (treatment A) resulted in a thinner silane layer. The thickness of silane film was again reduced after heat treatment in both treatment methods. Heat treatment eliminates water, alcohol and other by-products and helps the silane–silica condensation reaction [24]. A further reduction of silane film thickness for treatment E (0.6 nm), the optimized method for silane application from previous studies on bond strength and interfacial fracture toughness of resin to ceramic, was also

observed. However, it should be noted that a possible disadvantage of XPS study of silanes could be the instability of silane compounds in high vacuum [25]. If volatilization of parts of coatings has occurred, the values in Table 3 represent the remaining and most stable part of the coatings which in reality might be considerably thicker. With this proviso, the thickness of silane coating for treatment E (rinsed by hot water) can be assumed to be equivalent to a monolayer (up to 1 nm). It has been pointed out that optimum bond strength and, consequently, greater adhesion between polymer and a hydrated mineral substrate could be achieved when a monolayer of silane was used [26].

Silanes form essentially three different structures in the interphase [12, 27]. The outermost layers consist of small oligomers which are physisorbed to the glass so that they can readily be washed away by organic solvents or water at room temperature. Nearer the glass surface there is a second region, which consists of oligomers similar to the outer layers except for a few siloxane bonds connecting the oligomers and is hydrolyzable by hot water. In the region near the glass, uniformity and extent of crosslinking of the layers increases and a regular three-dimensional network is formed which is hydrolytically quite stable. Only this last layer of coupling agent on the surface is necessary for improved bonding. The major portion of the silane is, therefore, of no value in bonding, and may even be detrimental [28, 29]. Hence, improvement may be possible by removing the outermost layer of the silane film and leaving the most stable and chemisorbed layer on the ceramic surface. The remaining silane layer is composed of more firmly held polysiloxane networks. This very thin layer of chemisorbed polysiloxanes is considered sufficient to chemically bond the polymer to the mineral substrate and is not too thick to weaken the properties of the interface [25]. In order to ensure a monolayer of the silane, early removal of the excess loosely bound oligomers is preferred since there is an increasing resistance to desorption of these oligomers due to the homopolymerization of the organofunctional groups [12].

The adsorption of silanes on E-glass fibers has been investigated by several analytical techniques [30]. The strength of the silane–glass interaction has been related to the extent of removal of the adsorbed species by washing with a range of solvents.

Other studies have also used X-ray photoelectron spectroscopy to measure the thickness of silane films on other mineral substrates [23, 25, 31]. The overlayer thickness of five different types of silanes on E-glass fibers was determined [23]. The thickness of the adsorbed silane layer was in the range of 1.5–3.0 nm (2.6 nm for γ-MPTS). In another study by Dupraz *et al.* [25], the thickness of different silane coatings on hydroxyapatite powders (filler in composite biomaterials) has been estimated. Attenuation in the Ca_{2p} and P_{2p} signal intensities due to the silane coating was not total, indicating that the substrate contributed to the analysis and that the coating was thinner than the scan depth. They assumed that the scan depth was limited to 10 nm and the thickness of the silane film could be estimated using the decrease of the Ca or P (at%), elements present in the substrate, and not in the silane, at the surface. The estimated thickness of γ-MPTS coating was reported to

be approximately 1.9 nm. It should be noted that differences in types of substrates, silane solutions, methods of application, type of XPS instrument, and way of data analysis from one study to another would affect the reported results. Thus, comparison of the results of this study with others must be treated with due caution.

The formation of a thin chemisorbed layer of γ-MPTS on the ceramic surface as a consequence of removal of the loosely bound outermost layers of the silane coupling agent when using this particular silane treatment method is consistent with the strength and durability of the resin to ceramic bond previously reported [10, 11].

It should be noted that one specimen per treatment method was analyzed by XPS in this study and further work with a larger sample size is recommended in future studies. Furthermore, the interaction between the silane and the ceramic is certainly governed by surface phenomena and, therefore, influenced by the composition and chemical environment of the ceramic surface. The extent to which the results from this study can be transferred to other leucite-reinforced feldspathic ceramics has already been discussed elsewhere [32].

5. Conclusion

Within the limitations of this study, XPS analysis indicated that the thickness of the silane film on a leucite-reinforced feldspathic ceramic surface is a function of the mode of application. From the results, there is strong indication that monolayer coverage of organosilane on the surface of a leucite-reinforced feldspathic ceramic was obtained by the method of silane application consisting of brush application, followed by hot air drying and rinsing with hot water.

References

1. M. F. Ayad, N. Z. Fahmy and S. F. Rosenstiel, *J. Prosthet. Dentistry* **99**, 123–130 (2008).
2. G. P. Stewart, P. Jain and J. Hodges, *J. Prosthet. Dentistry* **88**, 277–284 (2002).
3. A. M. Spohr, L. C. Sobrinho, S. Consani, M. A. Sinhoreti and J. C. Knowles, *Int. J. Prosthodont.* **16**, 277–282 (2003).
4. M. Meldrum, *Regul. Toxicol. Pharmacol.* **30**, 110–116 (1999).
5. T. Hayakawa, K. Horie, M. Aida, H. Kanaya, T. Kobayashi and Y. Murata, *Dental Mater.* **8**, 238–240 (1992).
6. A. S. Brentel, M. Ozcan, L. F. Valandro, L. G. Alarça, R. Amaral and M. A. Bottino, *Dental Mater.* **23**, 1323–1331 (2007).
7. Y. Shimakura, Y. Hotta, A. Fujishima, J. Kunii, T. Miyazaki and T. Kawawa, *Dental Mater. J.* **26**, 713–721 (2007).
8. T. Nagai, Y. Kawamoto, Y. Kakehashi and H. Matsumura, *J. Oral Rehabil.* **32**, 598–605 (2005).
9. J. P. Matinlinna, M. Özcan, L. V. J. Lassila and P. K. Vallittu, in: *Silanes and Other Coupling Agents*, K. L. Mittal (Ed.), Vol. 4, pp. 199–215. VSP/Brill, Leiden (2007).
10. T. Hooshmand, R. van Noort and A. Keshvad, *Dental Mater.* **18**, 179–188 (2002).
11. K. Moharamzadeh, T. Hooshmand, A. Keshvad and R. van Noort, *Dental Mater.* **24**, 172–177 (2008).
12. H. Ishida and J. L. Koenig, *J. Polym. Sci. Polym. Phys.* **18**, 1931–1943 (1980).

13. D. Briggs and M. P. Seah, *Practical Surface Analysis, Vol. 1. Auger and X-ray Photoelectron Spectroscopy*, 2nd ed. Wiley, Chichester (1990).
14. R. J. Ward and B. J. Wood, *Surface Interface Anal.* **18**, 679–684 (1992).
15. M. Pijolat and G. Hollinger, *Surface Sci.* **105**, 114–128 (1981).
16. S. Tanuma, C. J. Powell and D. R. Penn, *Surface Interface Anal.* **11**, 577–589 (1988).
17. B. R. Strohmeier, *Surface Interface Anal.* **15**, 51–56 (1990).
18. F. D. Blum, W. Meesiri, H. Kang and J. E. Gambogi, *J. Adhesion Sci. Technol.* **5**, 479–496 (1991).
19. T. Hooshmand, R. van Noort and A. Keshvad, *Dental Mater.* **20**, 635–642 (2004).
20. D. Wang, F. R. Jones and P. Denison, *J. Adhesion Sci. Technol.* **6**, 79–98 (1992).
21. W. J. van Ooij and A. Sabata, *J. Adhesion Sci. Technol.* **5**, 843–863 (1991).
22. R. A. Cayless and D. L. Perry, *J. Adhesion* **26**, 113–130 (1988).
23. C. G. Pantano and T. N. Wittberg, *Surface Interface Anal.* **15**, 498–501 (1990).
24. E. P. Plueddemann, *Silane Coupling Agents*, 2nd ed. Plenum Press, New York, NY (1991).
25. A. M. P. Dupraz, J. R. de Wijn, S. A. T. vd Meer and K. de Groot, *J. Biomed. Mater. Res.* **30**, 231–238 (1996).
26. J. Comyn, in: *Structural Adhesives: Development in Resins and Primers*, A. J. Kinloch (Ed.), p. 269. Elsevier Science, London (1986).
27. M. E. Schrader, I. Lerner and F. G. D'Oria, *Modern Plastics* **45**, 195–282 (1967).
28. J. L. Koenig and H. Emadipour, *Polym. Composites* **6**, 142–150 (1985).
29. J. Berg and F. R. Jones, *Composites* **29A**, 1261–1272 (1998).
30. A. E. E. Jokinen, P. J. Mikkola, J. G. Matisons and J. B. Rosenholm, *J. Colloid Interface Sci.* **196**, 207–214 (1997).
31. A. K. Wong and U. J. Krull, *Anal. Bioanal. Chem.* **383**, 187–200 (2005).
32. T. Hooshmand, R. Daw, R. van Noort and R. D. Short, *Dental Mater.* **17**, 1–6 (2001).

Part 2
Mechanics and Durability Aspects

Numerical Analysis of Biomechanical Response of a Dental Prosthesis with Regard to Bone–Implant Adhesion Phenomena

Arturo N. Natali *, **Emanuele L. Carniel and Piero G. Pavan**

Centre of Mechanics of Biological Materials, University of Padova, Via F. Marzolo 9, I-35131 Padova, Italy

Abstract

Bone–implant interaction of endosseus oral implants is investigated by means of numerical models to describe their mechanical behaviour. The constitutive models of bone tissue include the definition of anisotropy, visco-elasticity and plasticity and are implemented in a finite element code for the analysis of phenomena induced by a non-passive connection between oral implants and framework. This condition induces relevant stress/strain fields that also depend on bone–implant adhesion process, as term capable of affecting the osteo-integration and the consequent stability of the implant. In particular, a fixed prosthesis placed in the premolar region of a mandible is modelled, made up of two implants connected by a framework. The mechanical state arising from the misfit is considered for its effects in dependence on the properties of peri-implant bone tissue and bone–implant interface configuration. Continuity or detachment with or without adhesion between implant and bone are considered and the consequent response of mandible-prosthesis system is evaluated. The investigation offers the possibility to evaluate the influence of interaction phenomena between implant and bone on the biomechanical behaviour of the prosthetic system in condition of misfit and for different bone–implant adhesion configurations.

Keywords

Oral implants, bone–implant interaction, constitutive models, inelastic behaviour, finite element analysis

1. Introduction

The use of endosseus implants [1, 2] has become quite common in dentistry because it ensures the replacement of oral functionality in totally or partially edentulous patients. The fixity of the prosthesis and its reliability over time depends on biological, bio-chemical and mechanical factors. The functional behaviour of the prosthesis from a biomechanical point of view is related to the way in which an implant is connected to adjacent bone. Bone–implant interaction phenomena and the quality

* To whom correspondence should be addressed. Tel.: +39 049 827 5598; Fax: +39 049 827 5604; e-mail: arturo.natali@unipd.it

Adhesion Aspects in Dentistry
© Koninklijke Brill NV, Leiden, 2009

of bone tissue in the jaw region of implant placement are direct factors affecting the prosthesis fixity. It is important to underline that the conformation of the peri-implant bone tissue and its mechanical properties, such as anisotropy, stiffness and strength, undergo changes from the initial stage of implant insertion to the desired final stage of implant osseointegration [3, 4]. These changes are functions of different factors and are also influenced by the surgical technique adopted, for example the press fit induced by self-tapping implants in the peri-implant region. The change in structural conformation of bone tissue over time entails a variation of the stress paths in the peri-implant region. Also for this reason, the attempt to investigate the mechanics of bone–implant interaction by experimental techniques is usually very difficult. A growing interest has been shown for an analysis of these problems by means of numerical methods, which makes it possible to define sophisticated models of anatomical regions and prostheses and carry out several predictive investigations of the mechanical response of such a system. The comparative analysis of the mechanical behaviour of a fixed prosthesis as a function of different factors, such as bone strength and stiffness, provides interesting data to evaluate the whole biological scenario that can be experienced.

In particular, the aim of this work is to analyse by a numerical approach the effects of a misfit [5–7] between implants and connecting framework for the typical configuration of a two-implant prosthesis placed in a premolar region. This condition is quite frequent because the accuracy of bar manufacturing process is not always adequate for determining a perfect passive coupling between framework and implants. The consequence for screw-retained restorations, which are the objects of the investigation, is a co-action that must be investigated considering, in particular, the behaviour of peri-implant bone tissue at the bone–implant interface [8]. Attention is paid to define a suitable constitutive model [9] for the bone tissue, capable of describing inelastic effects caused by the misfit. The material model allows for anisotropy characterising bone tissue and the visco-elasto-plastic behaviour [10–14] to be evaluated during the co-action induced. It must be pointed out that stress relaxation phenomena take place in the peri-implant region, contributing to the biomechanical compatibility of the implant [15]. The mechanical interaction between implants and bone is affected by the adhesion, especially in those regions of bone where tensile stresses arise because of the loading conditions applied. The contact condition at the bone–implant interface can be characterised by null strength for tensile normal stress or by the presence of cohesive forces between implant and bone, which ensure a strength of the bone–implant interface also in the case of interface stresses. In particular, the values of these cohesive forces are set on the basis of experimental data already present in the literature [16–21].

The mechanical effects of the interaction between bone and implant are considered in terms of stress states, accounting, in particular, for the reduction of the level of stress due to relaxation phenomena, evaluated by performing a quasi-static analysis.

2. Materials and Methods

The material behaviour of both cortical and trabecular bones is described by adopting an orthotropic visco-elastic-plastic constitutive model. While the general formulation of the constitutive model is the same regardless of the tissue region, different sets of constitutive parameters are adopted.

The elastic behaviour of bone is described by an orthotropic linear constitutive model, defining a set of nine basic parameters and providing a distribution of properties that assures a very accurate and continuous representation.

Time-dependent behaviour of bone tissue is described by using a visco-elastic constitutive model [22], based on the definition of specific viscous internal variables, represented by the instantaneous and time-dependent terms:

$$\boldsymbol{\sigma}(\boldsymbol{\varepsilon}, t) = \boldsymbol{\sigma}^0(\boldsymbol{\varepsilon}) \sum_{i=1}^{n} \mathbf{q}^i(\boldsymbol{\varepsilon}, t). \tag{1}$$

The symbols $\boldsymbol{\sigma}$ and $\boldsymbol{\varepsilon}$ are the Cauchy stress tensor and the small strain tensor, respectively. The term $\boldsymbol{\sigma}^0$ represents the instantaneous stress, while the terms $\mathbf{q}^i$ are the viscous internal variables defining the so-called non-equilibrated stresses, referred to each visco-elastic branch adopted to define the rheological model, which depend on time t. The evolution law of the viscous internal variables is given by equations of the type:

$$\dot{\mathbf{q}}^i + \frac{1}{\tau^i}\mathbf{q}^i = \frac{\gamma^i}{\tau^i}\boldsymbol{\sigma}^0, \tag{2}$$

being τ^i the relaxation times and γ^i the relative stiffness of the ith viscous branch.

The relative stiffness parameters satisfy the condition:

$$\gamma^\infty + \sum_{i=1}^{n} \gamma^i = 1, \tag{3}$$

where γ^∞ is the relative stiffness modulus of the elastic branch.

Inelastic phenomena induced in the bone tissue are described by including plastic behaviour. The constitutive model developed accounts for two important aspects shows by experimental data, i.e., yield stress in bone is affected by strain rate, while yield strain is not [23] and is independent of the loading direction [24–26].

The stress–strain law of the elasto-plastic behaviour is expressed by:

$$\boldsymbol{\sigma}^0[\boldsymbol{\varepsilon}(t)] = \mathbf{D}^{\mathrm{e}} : [\boldsymbol{\varepsilon}(t) - \boldsymbol{\varepsilon}^{\mathrm{p}}(t)], \tag{4}$$

with $\mathbf{D}^{\mathrm{e}}$ the fourth-rank elasticity tensor and $\boldsymbol{\varepsilon}^{\mathrm{p}}$ the permanent strain that evolves according to an associative strain-driven flow rule:

$$\dot{\boldsymbol{\varepsilon}}^{\mathrm{p}} = \dot{\lambda}\frac{\partial \phi}{\partial \boldsymbol{\varepsilon}}. \tag{5}$$

The symbol λ is the plastic flow and ϕ the yield potential [27], which is written as:

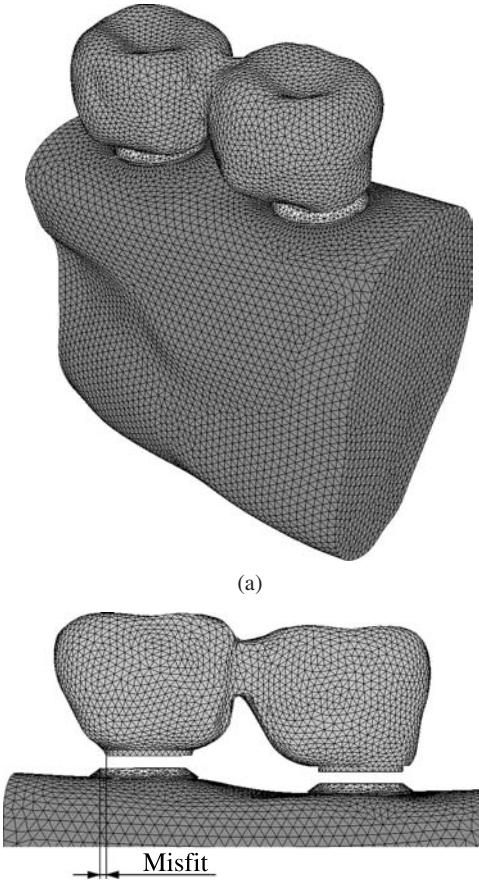
$$\phi[\boldsymbol{\varepsilon}(t), \lambda(t)] = \bar{\varepsilon}(t) - \varepsilon_y[\lambda(t)] = 0, \tag{6}$$

where $\bar{\varepsilon}$ is the equivalent Von Mises strain, while ε_y is the yield strain. It should be noted that ε_y depends on the plastic flow, therefore it accounts for the hardening behaviour shown by bone tissue over the elastic range. The hardening behaviour of bone is described as a linear relationship between yield strain and plastic field:

$$\varepsilon_y(\lambda) = \varepsilon_y^{\mathrm{I}} + \beta\lambda, \tag{7}$$

where $\varepsilon_y^{\mathrm{I}}$ is the initial yield strain and β the hardening parameter.

The three-dimensional finite element model of the implanted portion of mandible is obtained by meshing (Patran, MSC.Software Corporation, Santa Ana, CA, USA) the geometrical model with the use of four-noded linear solid elements (Fig. 1(a)). The numerical model adopted is specifically developed for the present analysis, with attention to the number and the characteristics of the elements adopted, also aiming at limiting the computational effort. The relevance of this aspect is also due



(a)

(b)

Figure 1. Finite element model of the portion of mandible and prosthetic system (a) with a detail of the misfit between bar and implant (b).

to the non-linear characteristics of the analysis, with regard to both the post-elastic and time-dependent behaviours of the bone tissue and the contact interaction at the bone–implant interface. Implants, connecting framework and portion of mandible consist of 1 014 158 elements and 188 635 nodes. The geometric model of the anatomical region is developed starting from Computerised Tomography (CT) survey. Bitmapped images have been segmented to identify the boundary between the main regions of bone, namely cortical and alveolar bone. The segmentation procedure is based on the use of spline curves, which are imported in a virtual solid modeller (UGS NX3, Siemens PLM Software, Munich, Germany) to create the solids. Geometric reconstruction of implants and other components is achieved in the solid modeller on the basis of a direct measurement of their dimensions.

Misfit conditions are defined as relative displacements imposed between implants and framework [28], corresponding from a mechanical point of view to a non-passive coupling of the different components. A misfit of 0.1 mm is considered along the distal-mesial direction, as depicted in Fig. 1(b), showing the initial configuration before the coupling of framework and implants. The numerical analysis (ABAQUS 6.3, Dassault Systèmes Simulia Corp., Providence, RI, USA) is quasi-static and mimics a surgical procedure. The non-passive coupling is applied in a time interval of 25 s and the effects on the system are analyzed for the following 1000 min, from initial step that is conventionally considered as the time step of application of the total misfit. This time interval allows for a complete development of relaxation process.

The elastic mechanical properties of the cortical region are specified for each finite element allowing for a spatial distribution that is related to the mesh refinement adopted. The typical spatial distribution of the Young's modulus in mesial-distal direction (E_3) is depicted for a transversal section in Fig. 2(a), while Fig. 2(b) shows the variation along a longitudinal section of the mandible. Direction 2 is along the cortical thickness of the mandible, while direction 1 completes the local orthogonal system of coordinates. As a reference, the set of constants with the maximum value of the Young's modulus is given by: $E_3 = 19\,750$ MPa, $E_2 = 12\,510$ MPa, $E_1 = 10\,630$ MPa, $G_{32} = 5840$ MPa, $G_{21} = 4850$ MPa and $G_{13} = 3890$ MPa. The independent Poisson ratios are: $\nu_{32} = 0.313$, $\nu_{31} = 0.246$, $\nu_{21} = 0.226$.

The values of the constitutive parameters related to viscosity are calculated on the basis of experimental data from creep tests performed according to different values of imposed uni-axial stress [11, 29]. The use of three viscous branches allows for a good fit between numerical results and experimental data, with viscous parameters set as follow: $\gamma^1 = 0.272$, $\gamma^2 = 0.194$, $\gamma^3 = 0.022$, $\tau^1 = 0.67$ min, $\tau^2 = 450$ min and $\tau^3 = 6400$ min.

From experimental tests of static loading on samples of cortical and trabecular tissue [23, 30, 31] the constitutive parameters defining the plastic behaviour are found to be $\boldsymbol{\varepsilon}_y^{\mathrm{I}} = 0.8\%$ and $\beta = 0.6$ in accordance with the results obtained in previous investigations [32]. Both viscous and plastic parameters are assumed to be constant within the cortical region.

The elastic properties of the trabecular region are assumed to be homogeneous with Young's moduli $E_3 = 907$ MPa, $E_2 = 575$ MPa, $E_1 = 488$ MPa, shear moduli $G_{32} = 268$ MPa, $G_{21} = 223$ MPa and $G_{13} = 179$ MPa and Poisson's ratios $\nu_{32} = 0.226$, $\nu_{31} = 0.246$, $\nu_{21} = 0.222$. The local coordinate system is defined as for the cortical region. Viscous and plastic parameters are also assumed to be constant in the trabecular region and set as $\gamma^1 = 0.091$, $\gamma^2 = 0.220$, $\gamma^3 = 0.435$, $\tau^1 = 44$ min, $\tau^2 = 175$ min, $\tau^3 = 680$ min for the viscosity and $\boldsymbol{\varepsilon}_y^{\mathrm{I}} = 0.8\%$, $\beta = 0.6$ for the plasticity. In the transition zone between trabecular and cortical regions the elastic properties vary with continuity, as shown in Fig. 2.

The mechanical properties of each peri-implant region have been considered with orthotropic axes disposed according to a cylindrical coordinate system placed on the

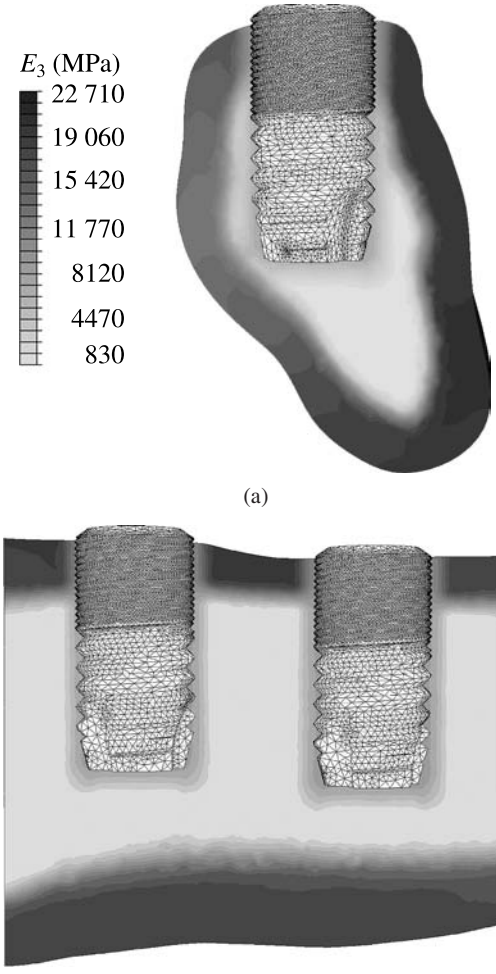


Figure 2. Spatial distribution of the Young's modulus E_3 on a transversal (a) and a longitudinal (b) section of the mandible.

axis of the implant. The direction of maximum Young's modulus is radial. Considering the change in morphology of the bone immediately around the implant and its tendency to a corticalisation during the healing phase, the definition of the mechanical properties for this bone region makes the assumption that the conformation of the tissue already shows distinct orthotropic characteristics, while the values of the elastic moduli are assumed to be lower than the values that are typical of a complete corticalisation process.

The contact configuration between the implant and bone is investigated by means of three different models of the cohesive forces. These forces are defined by the limit values of the tensile and shear stresses. When the tensile or shear stress at the bone–implant interface are below these limits a continuity between bone and implant is assumed while, on the contrary, a detachment or a sliding between implant and bone occur. In the first model the values of $\sigma_{\text{lim}} = 4$ MPa, $\tau_{\text{lim}} = 20$ MPa have been adopted for tensile and shear strengths, respectively. This model of contact condition between implant and bone will be shortly indicated with the term 'cohesive contact'. This model is compared with other two numerical models, one with sliding contact between implant and bone and the other with a full continuity between implant and bone, i.e., with no detachment or sliding irrespective of whether tensile or shear stress are present at the bone–implant interface. These other two models of contact will be shortly indicated as 'sliding contact' and 'full continuity', respectively.

3. Results

The results presented refer to the time step of misfit application and the time step of 1000 min after the coupling of framework and implants. The deformed configuration of the system as resulting from the non-passive coupling is depicted in Fig. 3, where the magnitude displacements (Fig. 3(a)) are reported by using a magnification factor to show the effective configuration of the system. The two implants

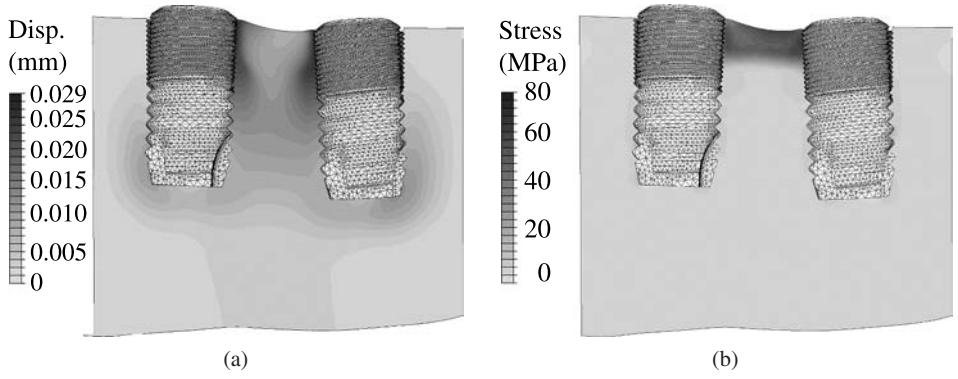


Figure 3. Magnitude displacement field (a) and maximum compressive stress field (b) on a longitudinal section of the mandible at the final time step of application of the misfit.

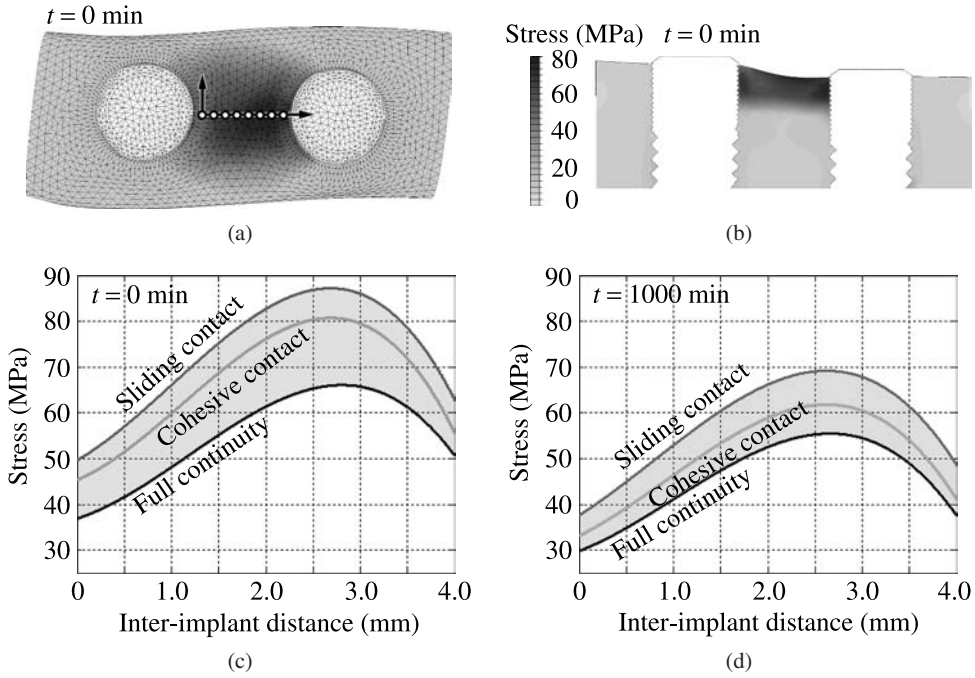


Figure 4. Upper view (a) and longitudinal section (b) of the maximum compressive stress on the mandible at the application of the misfit, for the case of cohesive contact. The values of the same variable for the physical path indicated in (a) are reported for the three cases analysed at the application of the misfit (c) and at the end of the relaxation process (d).

are subjected to a combined translation–rotation, determining the maximum compression in the cortical region of the bone in between the implants. The maximum compressive stress is reported as a contour in the longitudinal section of Fig. 3(b), with a maximum value located in the coronal region. Both figures show the case of sliding contact between implants and bone. This condition causes a partial detachment of bone and implant, which is highlighted by the magnification used in the representation.

Figure 4 represents the distribution of stress levels in the region between the two implants. Figure 4(a) and 4(c) represent the maximum compressive stress of the mandible at the time of application of the misfit for an upper view and a longitudinal section, respectively. The results refer to the case of cohesive contact. Figure 4(c) and 4(d) shows the variation of the maximum compressive stress along the physical path shown in Fig. 4(a) for the time steps 0 and 1000 min, respectively. The charts report a comparison of the compressive stress in the case of sliding contact (upper curve), cohesive contact (intermediate curve) and full continuity between implant surface and bone (lower curve), which are the three conditions for bone–implant interface properties analysed.

The strain states are reported in Fig. 5 with the same way of representation as in Fig. 4. The distribution of maximum compressive strain in the upper surface of the

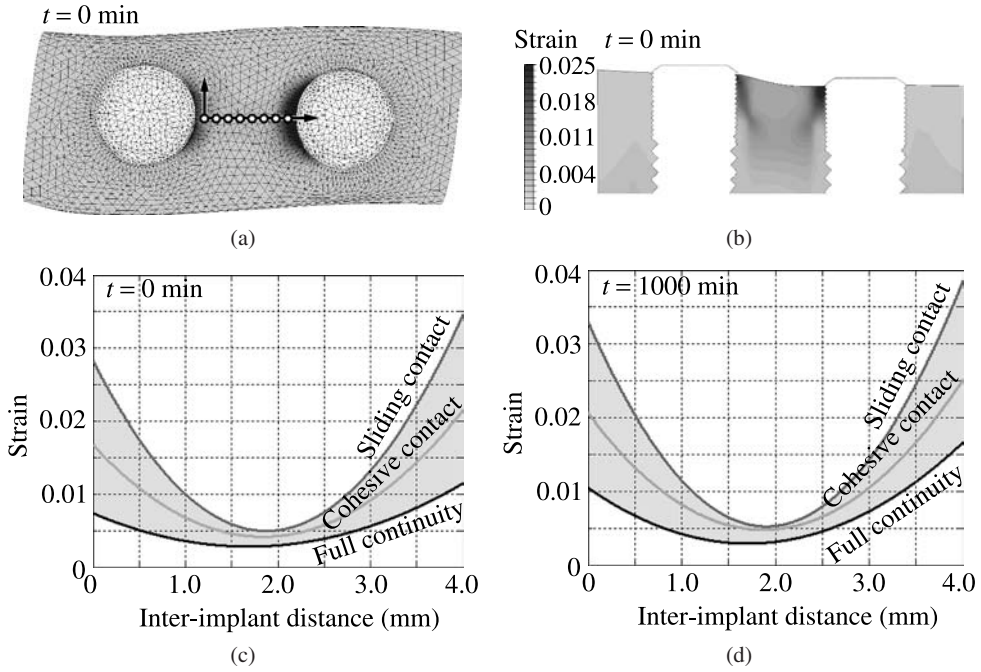


Figure 5. Upper view (a) and longitudinal section (b) of the maximum compressive strain on the mandible at the application of the misfit, for the case of cohesive contact. The values of the same variable for the physical path indicated in (a) are reported for the three cases analysed at the application of the misfit (c) and at the end of the relaxation process (d).

mandible and for a longitudinal section is reported for the time step 0 (application of the misfit). Also in this case the Fig. 5(a) and 5(b) refers to the cohesive contact condition. The variation of the maximum compressive strain along the physical path of Fig. 5(a) is represented at the application of the misfit (Fig. 5(c)) and at the end of the relaxation process (Fig. 5(d)), for the three cases of bone–implant contact conditions considered: cohesive contact, sliding contact, and full continuity.

Finally, Fig. 6 shows the distribution of the plastic flow in the same region of the mandible. The plastic flow makes it possible to evaluate the region in which the strain exceeds the elastic limit so that the tissue undergoes plastic strain. The plastic flow is represented as upper view (Fig. 6(a)) and as longitudinal section (Fig. 6(b)) at the time step 0. A comparison of the different values of plastic flow along the physical path represented in Fig. 6(a) is reported for the three cases considered at time 0 (Fig. 6(c)) and at the end of the relaxation process (Fig. 6(d)).

4. Discussion

The results reported allow for a definition of the characteristic behaviour of bone–implant interaction phenomena under misfit condition and are reported with specific attention to the adhesion level occurring between the implant and the trabecular and

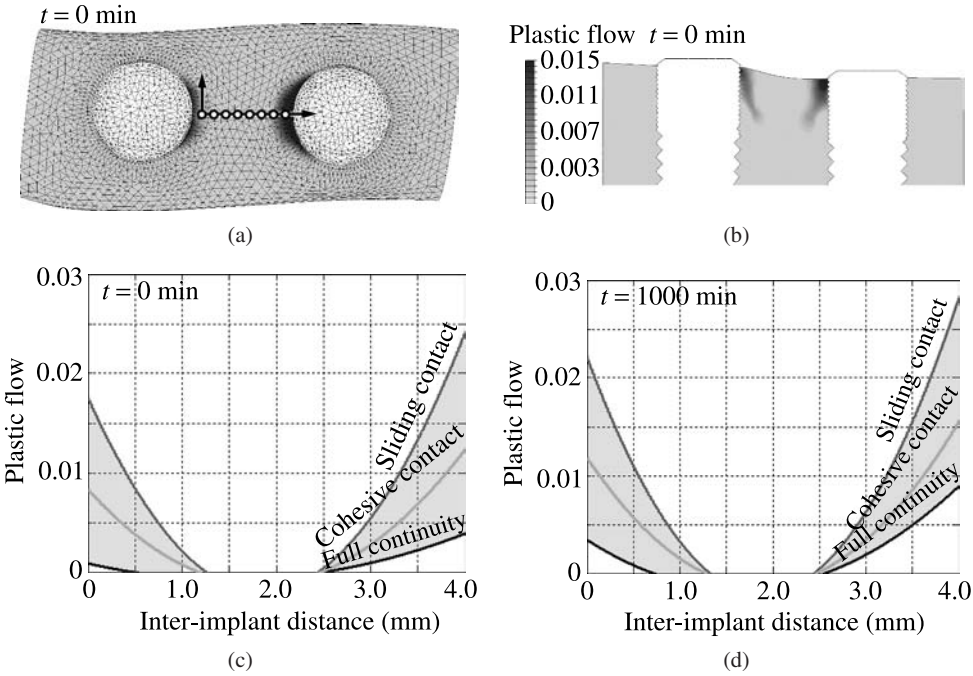


Figure 6. Upper view (a) and longitudinal section (b) of the plastic flow on the mandible at the application of the misfit, for the case of cohesive contact. The values of the same variable for the physical path indicated in (a) are reported for the three cases analysed at the application of the misfit (c) and at the end of the relaxation process (d).

cortical bone tissues at the interface. These aspects of the problem are evaluated considering the time dependent phenomena of stress relaxation and also considering the plastic behaviour of bone tissue caused by the effects induced by the misfit. The misfit causes a maximum strain in the upper region of the mandible and a yielding in the bone, even if only in limited regions around the implants. The level of initial stress is afterwards reduced because of the viscous phenomena.

The adhesion problems appear to have a significant relevance as the magnitudes of stress and strain in the bone vary considerably, being higher in the case of sliding contact, as cohesive contact produces an additional force to withstand the misfit action and causes force transmission to the bone through a much larger region.

The difficulty in the definition of real cohesive forces at bone–implant interface with regard to a direct correlation with osseointegration level still represents a relevant problem. The mechanical properties of the bone–implant interface depend on the level of osseointegration, being function of several factors such as time of healing after implantation, quality of bone, age and general conditions of the patient, showing a large variability over time [4]. From a mechanical point of view, the behaviour of the bone–implant interaction has been modelled by using different contact strategies and considering shear strength and cohesive forces in traction.

The possibility of a detachment has been assumed in the case of tensile and/or shear forces being greater than the strength limits assumed.

The ultimate shear strengths obtained by experimental tests show a large range [16, 17]. Also cohesive forces, which make it possible the existence of a tensile strength of the bone–implant interface, vary from very low values [19–21] to much larger values [18]. The present analysis proves to be capable of giving refined results in the specific conditions considered, namely, sliding contact, specific cohesive forces, and full continuity between implant surface and bone. The comparison of these conditions amongst the possible configurations at the bone–implant interface makes it possible to identifies the worst operational condition for the prosthesis. Therefore, the problem of the variability in the mechanical properties of the peri-implant tissue is overcome.

The level of stress/strain induced in the peri-implant bone tissue is related also to the stiffness of the framework connecting the system, in addition to the magnitude and type of misfit. A lower stiffness of the framework favours the limiting of stress/strain in the bone, thus reducing the risk of plastic phenomena of the tissue adjacent to the implant. An extension of these preliminary analyses should include a parametric investigation of the geometric properties of the framework to evaluate the effects of the variation in its stiffness on the mechanical state of the bone.

In the clinical practice, it is possible that the initial misfit between the implant and framework is not completely eliminated. In fact, the development of plastic phenomena in the coupling of different components (implant, abutment, etc.) could result in a partial elimination of the misfit. Since, these conditions cause lower strains on the peri-implant tissue, the total elimination of the initial misfit between implant and bone is analysed as the worst condition for the bone.

The excess of the stress/strain in the peri-implant tissue can be correlated to possible bone loss phenomena that need to be clinically evaluated in the follow-up of the patients. These phenomena must be taken into account to evaluate the biomechanical reliability of the prosthesis over time, since its fixity is completely dependent on the way in which the bone represents an effective boundary for the implants. Since the experimental evaluation of the behaviour of a prosthesis following a non-passive coupling through the framework is extremely difficult, the possibility of a preliminary investigation of the mechanical behaviour by means of numerical methods is important. In fact, by using this procedure it is possible to estimate the effective risk related to the certain defectiveness that may be present in the surgical practice, evaluated from the survey of the morphometric characteristics of the patient, through the manufacturing of the prosthetic components, to the actual placement of the prosthesis.

The evaluation of the risk of failure due to the microstrain induced in the peri-implant bone entails the assumption of specific strength criteria that can change over time according to the morphological change of the peri-implant bone due to its biological adaptation capability. This important issue, which is not part of the

present work, requires extensive additional experimental data and a specific formulation of the biomechanical response of the bone tissue over time.

5. Conclusions

The numerical analysis of the misfit phenomena presented shows that this kind of approach is capable of giving interesting results concerning the biomechanical behaviour of oral implants, including the post-elastic behaviour of bone and non-linear contact conditions between bone and implant. These results pertain, in particular, to the mechanical behaviour of the bone–implant interface and the correlation that exists between osteo-integration level, adhesion phenomena and stability of the implant over time.

The development of reliable numerical models needs the acquisition of extended experimental data about the mechanical properties of bone tissue and bone–implant interface and, in particular, to obtain information about the change of these properties over time. However, if well supported by experimental data, the numerical approach proves to be a useful tool in the design process of oral fixed prostheses, making it possible to thoroughly investigate important physical phenomena that are directly correlated to the clinical practice and the attempt to continuously improve clinical techniques and their success rate.

References

1. J. Feine, R. Jacobs, F. Lobbezoo, B. J. Sessle, D. Van Steenberghe, M. Trulsson, O. Fejerskov and P. Svensson, *J. Oral Rehabil.* **33**, 309 (2006).
2. A. Eliasson, T. Eriksson, A. Johansson and A. Wennerberg, *Int. J. Oral Maxillofac Implants* **21**, 567 (2006).
3. R. Branemark, L.-O. Ohrnell, P. Nilsson and P. Thomsen, *Biomaterials* **18**, 969 (1997).
4. J. B. Brunski, *Adv. Dental Res.* **13**, 99–119 (1999).
5. T. Jemt and K. Book, *Int. J. Oral Maxillofac Implants* **11**, 620 (1996).
6. J. Y. Kan, K. Rungcharassaeng, K. Bohsali, C. J. Goodacre and B. R. Lang, *J. Prosthet. Dentistry* **81**, 7 (1999).
7. A. B. Carr, D. A. Gerard and P. E. Larsen, *J. Prosthet. Dentistry* **76**, 500 (1996).
8. A. N. Natali, P. G. Pavan and A. L. Ruggero, *Dental Mater.* **22**, 388 (2006).
9. S. C. Cowin (Ed.), *Bone Mechanics Handbook*. CRC Press, Boca Raton, FL (2001).
10. S. C. Cowin and Q.-C. He, *J. Biomech.* **38**, 141 (2005).
11. A. É. Melnis, I. V. Knets and P. A. Moorlat, *Mech. Composite Mater.* **15**, 574 (1980).
12. C. U. Brown, T. L. Norman, V. L. Kish, T. A. Gruen and J. D. Blaha, *J. Biomech. Eng.* **124**, 456 (2002).
13. C. Mercer, M. Y. He, R. Wang and A. G. Evans, *Acta Biomater.* **2**, 59 (2006).
14. T. Iyo, Y. Maki, N. Sasaki and M. Nakata, *J. Biomech.* **37**, 1433 (2004).
15. T. Jemt and U. Lekholm, *Clin. Oral Implants Res.* **9**, 272 (1998).
16. M. Müller, F. F. Hennig, T. Hothorn and R. Stangl, *J. Biomech.* **39**, 2123 (2006).
17. C. Chu, X. Xue, J. Zhu and Z. Yin, *Mater. Sci. Eng. A* **429**, 18 (2006).

18. S. G. Steinemann, J. Eulenberger, P.-A. Maeusli and A. Schroeder, in: *Biological and Biomechanical Performance of Biomaterials*, P. Christel, A. Meunier and A. J. C. Lee (Eds), pp. 409–414. Elsevier, Amsterdam (2000).
19. J. L. Taylor, J. B. Brunski, S. J. Hoshaw, G. V. B. Cochran and K. W. Higuchi, in: *Tissue Integration in Oral, Orthopedic and Maxillofacial Reconstruction*, W. R. Laney and D. E. Tolman (Eds), pp. 125–132. Quintessence, Chicago (1992).
20. J. T. Edwards, J. B. Brunski and K. W. Higuchi, *J. Biomed. Mater. Res.* **36**, 454 (1997).
21. P. Aspenberg and R. Skripitz, *Transactions of the 44th Orthopaedic Research Society*, p. 220. New Orleans, LA (1998).
22. J. C. Simo and T. J. R. Hughes, *Computational Inelasticity*. Springer, New York, NY (1998).
23. A. É. Melnis and I. V. Knets, *Mech. Composite Mater.* **18**, 358 (1982).
24. W. C. W. Chang, T. M. Christensen, T. R. Pinilla and T. M. Keaveny, *J. Orthopaedics Res.* **17**, 582 (1999).
25. T. M. Keaveny, in: *Bone Mechanics Handbook*, S. C. Cowin (Ed.), pp. 1–42. CRC Press, Boca Raton, FL (2001).
26. J. Currey, *J. Biomech.* **37**, 549 (2004).
27. T. Belytschko, W. K. Liu and B. Moran, *Nonlinear Finite Elements for Continua and Structures*. John Wiley, New York, NY (2000).
28. A. N. Natali, A. Gasparetto, E. L. Carniel, P. G. Pavan and S. Fabbro, *J. Biomed. Mater. Res. B* **83**, 332 (2007).
29. E. Yamamoto, R. P. Crawford, D. D. Chan and T. M. Keaveny, *J. Biomech.* **39**, 1812 (2006).
30. D. L. Kopperdahl and T. M. Keaveny, *J. Biomech.* **31**, 601 (1988).
31. E. F. Morgan and T. M. Keaveny, *J. Biomech.* **34**, 569 (2001).
32. A. N. Natali, E. L. Carniel and P. G. Pavan, *Med. Eng. Phys.* **30**, 905 (2008).

Bond-Disruptive Stresses Generated by Resin Composite Polymerization in Dental Cavities

David C. Watts [a,*], **Luis Felipe J. Schneider** [a,b] **and Hanadi Y. Marghalani** [a,c]

[a] Biomaterials Science Research Group, School of Dentistry and Photon Science Institute, The University of Manchester, Higher Cambridge Street, Manchester M15 6FH, UK

[b] The University of Passo Fundo, Dental School, Área de Materiais Dentários Campus I — Bairro São José — BR 285 — Km 171 — Passo Fundo, RS 99001-970, Brazil

[c] Conservative Dental Science Department, Faculty of Dentistry, King Abdulaziz University, Jeddah, Kingdom of Saudi Arabia

Abstract

Though many advances have been made in the development of dental adhesives, the immediate, or short-term, disruption created by stress — due to polymerization of resin composite restorative materials within dental cavities — is still a challenge yet to be completely solved in restorative dentistry. Therefore, the aim of this paper is to present a general overview of the subject, concerning resin composite formulations, origins of stress, clinical consequences of stress development, *in vitro* methods used for its measurement and methods used to reduce stress magnitudes and rates of development.

Keywords

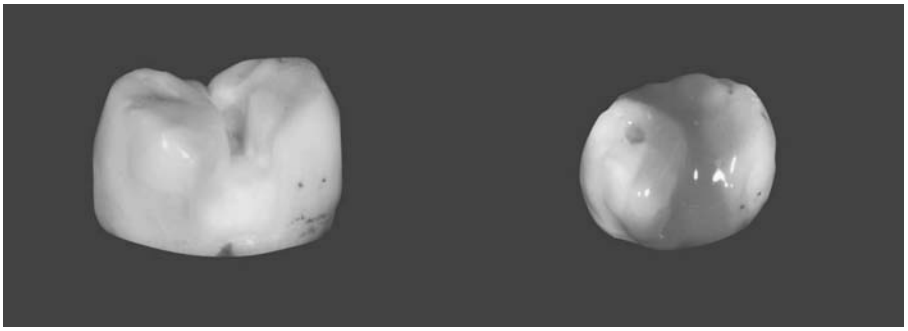
Dental materials, resin composite, resin monomer, polymerization shrinkage, stress, shrinkage measurement

1. Introduction

Dental resin composites were developed and became commercially available in the late 1950s [1, 2]. Besides their acceptable appearance, these materials can be directly bonded to tooth structure without removing healthy tissues to promote macromechanical retention. This is possible due to advances in resin composite system adhesives. The sequence of events is that: (a) an acid treatment promotes demineralization of inorganic components from the dental structures (Fig. 1); (b) the remaining structure is conditioned by a primer solution; (c) fluid resin monomers are applied to infiltrate the spaces created by demineralization; (d), the resin is photoactivated, creating an interlocking layer between the polymerized material and the remaining tooth structure (Fig. 2). Additionally, since the infiltrated material is

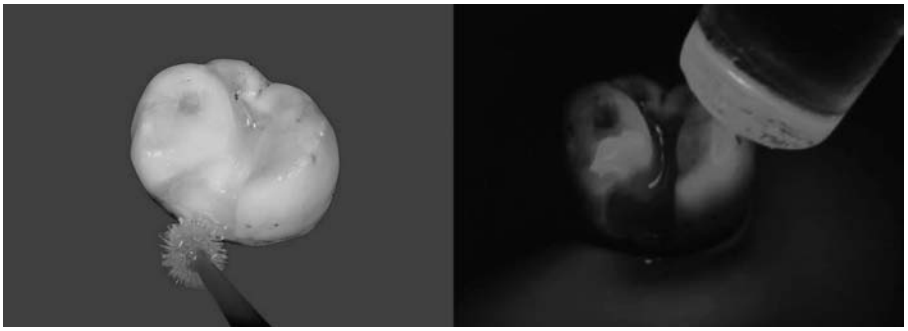
* To whom correspondence should be addressed. Tel.: +44 (0)161 275 6749; e-mail: david.watts@manchester.ac.uk

Adhesion Aspects in Dentistry
© Koninklijke Brill NV, Leiden, 2009



(a) (b)

Figure 1. (a) Dental cavity to be restored with resin composite. (b) Acid gel applied over the tooth structure to promote demineralization.



(a) (b)

Figure 2. (a) Primer and adhesive combination applied over the conditioned structure. (b) Blue light application to activate initiators that start the polymerization process.

based on dimethacrylates, the adhesion of further resinous materials, such as the resin composites, is possible. The use of resin bonding agents is a very complex subject and many investigations have been carried out to understand the mechanisms of adhesion, material improvements and long term stability. The literature is extensive [3].

Though many advances have been made in the development of dental adhesives, two major factors can still affect the stability of the bonding layer:

(a) disruption created by the resin composite stress due to polymerization [4] and

(b) biochemical deterioration over time (long-term process) [5]. The present review will be focused on the first problem, which mainly arises when resin composites are polymerized within some type of cavity, as is the usual clinical condition.

Therefore, the objectives of this overview are to address the following questions:

1. What are resin composite restoratives?
2. How are they constructed in dental cavities?

3. How do interfacial stresses arise?
4. What are the clinical consequences of stress?
5. How do the stresses vary in magnitude with time and location?
6. How can such stresses be measured *in vitro*?
7. How can stresses be offset in clinical placement?
8. How can intrinsic stresses be reduced by re-design of materials?

2. What Are Resin Composite Restoratives?

The term "composite", in materials science, is defined as a multiphase material that exhibits properties of the constituent materials so as to produce a material with better properties than could be achieved by each constituent material alone. For dental applications, resin composites are a combination of particles, coated by a coupling agent, dispersed in an organic resinous matrix. Figure 3 shows a schematic representation of a dental resin composite. There is a related class of fiber-reinforced composite materials, now also used in dentistry, but their consideration is beyond the scope of this review.

Particulate inorganic fillers are used in dental resin composites to provide material strengthening and reinforcement [6]. Many types, shapes, sizes, volume fractions and distributions of filler particles have been used to provide a wide range of products with respect to diverse clinical applications. For example, a material used for aesthetic restorations might exhibit higher polishability, whereas for posterior restorations it might possess high strength to resist the occlusal forces. Thus, the filler content plays an essential role in composite properties and many investigations have established the relationship between the filler content and the resultant properties, such as: abrasion resistance and hardness [7, 8]; thermal stability [9, 10]; radio-opacity [11]; gloss retention and roughness [12]; water sorption; material

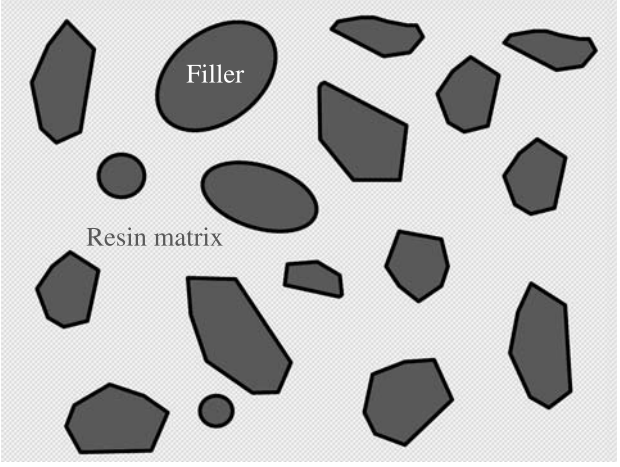


Figure 3. Schematic representation of a dental resin composite.

shrinkage [13]; visco-elastic creep and recovery [14]; elastic moduli [15]; fracture toughness [16]; and fracture behaviour [17, 18].

Initially, ground quartz fillers, with a mean particle size of 10–20 μm, were incorporated into the methacrylate-based restorative materials. Unfortunately, these materials were very difficult to polish and the end result was an unacceptable appearance. Consequently, the filler phase was changed to extremely small particles of colloidal silica with a mean size of 0.02 μm. However, the large total surface area of all these small particles made their incorporation in the resinous matrix difficult. To provide a material with both acceptable aesthetics and strength, hybrid materials with a mean particle size of 1 μm were commercialized and variations have been used up to the present time [19]. Very recently, "nanofillers" have been applied in resin composite formulations and it has been claimed that these materials could provide strength and aesthetic properties that allow the clinicians to use them for both anterior and posterior restorations [20].

The resin matrix is formulated with organic monomers, in the fluid state, that are converted into rigid polymers through the radical addition polymerization process. 2,2 bis[4-2(2-hydroxy-3-methacryloyloxypropoxy)-phenyl] propane, know as Bis-GMA or Bowen's resin, has been widely used since the introduction of dental composites. This high-molecular-mass monomer is extremely viscous due to hydrogen bonding caused by the presence of hydroxyl groups. This hinders the addition of fillers. Consequently, diluent monomers, such as the triethyleneglycol dimethacrylate (TEGDMA), have to be used to make the resin more fluid. Some other monomers can also be used as the resinous matrix, for example, urethane dimethacrylate (UDMA), 2,2 bis[4-(2 methacryloyloxyethoxy)-phenyl]propane (Bis-EMA), ethyleneglycol dimethacrylate (EGDMA) and others. Additionally, an initiator: co-initiator system that start the polymerization process, an inhibitor to allow long term storage, and pigments that provide a wide range of tooth-matching colour-shades [21] are required.

A coupling agent is used to bond the inorganic phase (filler particles) with the organic phase (resinous matrix) [22]. The most common agent is γ-methacryloxypropyl-triethoxysilane (γ-MPTS); and its use increases the mechanical properties of the material. The silane agent has the important function of enabling stress-transfer between the resin and the particulate phase, during loading applications, and reducing the possibility of crack initiation sites. Furthermore, this coupling agent reduces the water sorption/solubility phenomena and increases the material's wear resistance [19].

Until recently, all dental resin composite matrices were polymerized by free-radical addition (FRA) polymerization mechanisms, activated by light irradiation or *via* chemical mixing. The general FRA polymerization mechanism for light-activated dental composites has discrete stages: activation/initiation, propagation and termination. Resin composites for direct restorative procedures typically employ camphoroquinone (CQ) as the molecule responsible for the photo-initiation reaction [23–25]. Consequently, visible light centered in the blue region of the

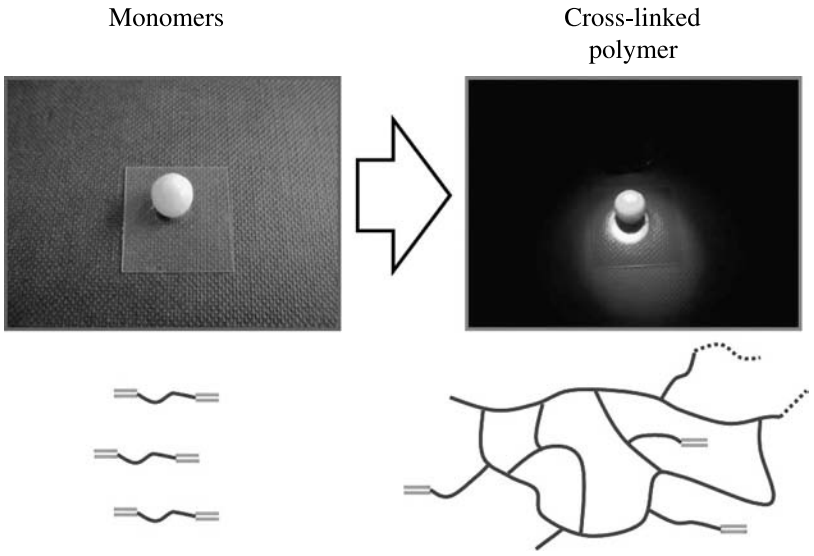


Figure 4. Resin composite paste to be polymerized and schematic representation of the polymerization and crosslinking process.

spectrum (400–550 nm), usually emitted from a quartz–tungsten–halogen bulb or light-emitting diode (LED) sources, is required to activate this molecule and convert it to an excited triplet state. The excited CQ then reacts with a co-initiator to form free radicals, which are molecules with unpaired electrons, starting the polymerization process (activation and initiation stages) [26] (Fig. 4).

When a free radical reacts with a monomer molecule, an active centre is created. Thus, propagation involves growth of each polymer chain by rapid sequential addition of monomer to the active centers *via* covalent bonds until the maximum degree of conversion (DC) of C=C double-bonds, to C–C bonds, is reached. Individual polymer chains, with free radical chain-ends, may become de-activated by several possible mechanisms so that they cannot grow anymore (termination). Moreover, active radical-ended chain units become trapped in the increasingly viscous matrix and thus are sterically and thermally hindered from further reaction at the ambient temperature, especially after the vitrification point (glassy condition) is reached.

It is important to highlight that volumetric shrinkage occurs during the overall process of polymeric growth as a result of the fact that the distance between the two groups of atoms resulting from the van der Waals forces is reduced to establish the covalent bond. The magnitude of composite volumetric shrinkage is dictated by the filler volume fraction, monomer composition and the final degree of conversion of the resin matrix [27]. Resin composites applied in restorative dentistry exhibit volumetric shrinkage values from less than 1% up to 6%, depending on the formulation and curing conditions [28, 29].

The rate of monomer disappearance (conversion into polymers) as a function of time is known as the rate of polymerization (R_p) (Fig. 5). For dimethacrylates,

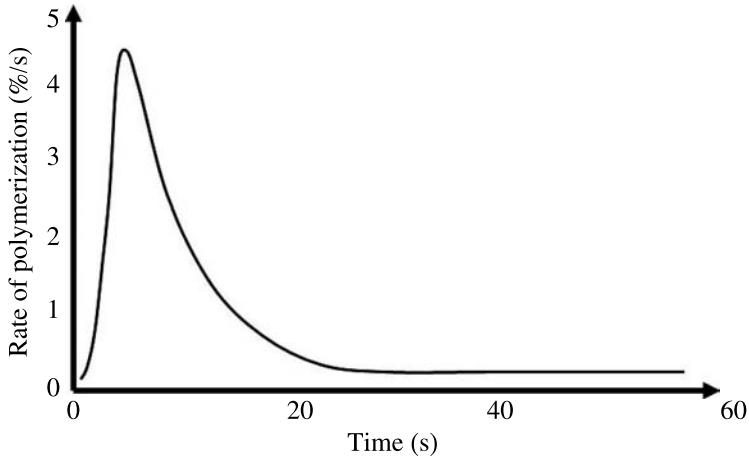


Figure 5. Typical shape of kinetic curve of polymerization rate as a function of irradiation time for the polymerization of dimethacrylates.

there is sharp increase in (R_p) (auto-acceleration) as the conversion of monomer increases. Thus, R_p achieves a maximum value (R_p^{max}) and then suddenly decreases (auto-deceleration). This happens because, as indicated above, while the polymer chains grow, the viscosity of the medium also increases, restricting the propagation and diffusion of the polymer chains. The reaction kinetics has been detailed by Andrzejewska [30] and Watts [31].

3. How Are Resin Composite Restorations Constructed in Dental Cavities?

Resin composites can be used for a wide range of purposes such as: (i) for replacement of natural tissues injured or diseased by the caries process, (ii) for occlusion adjustments, and (iii) for reasons of appearance. The use of visible-light activation makes the clinical procedures easy and fast, since the clinician does not have to wait for a slow chemical reaction to occur, holding the material in the correct place until complete cure. After the aforementioned dental adhesive application, dentists can build up restorations by the application of resin composite layers followed by light irradiation, hardening the material almost immediately.

4. How Do Interfacial Stresses Arise?

Polymerization stress development is a complex phenomenon and will differ according to the composite formulation [32]. Stresses can be developed within the resin composite mass *per se* and there are several causes. Firstly, the free-radical addition polymerization mechanism is an exothermic process and, since resin matrix and filler particles have different thermal expansion coefficients, stresses may develop at the resin–filler interfaces. Secondly, "hoop stresses" may arise since the resin matrix is bonded to fillers by the coupling agent, which restricts molecular

segmental motions during the molecular rearrangement and free shrinking of the material [33, 34].

Since the use of resin composites is primarily for space-filling purposes, such as restorative or cementation procedures, the polymerization reaction normally happens within constricted areas. As the resin composite is bonded to the cavity walls while shrinking and becoming stiffer, there is a very short-time period where the material can deform and flow to relax any developing stress. Consequently, the magnitude of stress within a cavity is much greater than in a situation where the material can freely shrink [35]. It is important to keep in mind that the tooth cavity configuration varies according to the clinical conditions and the spatial stress-distribution varies according to the constriction situation [36].

In summary, polymerization stress arises from multiple factors. The polymerization reaction, the material's formulation and the boundary conditions all play essential roles in stress development and/or transmission to tooth structures [31, 35, 37–42].

5. What Are the Clinical Consequences of Stress?

When a material is cured without bonding to cavity walls, the material is able to shrink and to flow, developing very low values of stress. However, in common clinical situations the material has to be placed inside a cavity and should be bonded to the surrounding walls, i.e. material deformation is restricted — thereby developing stresses which are also transferred to the bonding region as tensile forces. Consequently, the rapid increase of stress can create two major undesired situations:

(a) Disruption of the bonding area at localized points when the local contraction stress overcomes the adhesive layer bond strength. This situation creates spaces that might allow penetration of residual food and micro-organisms facilitating the occurrence of secondary caries [43, 44], and aesthetic problems due the marginal discoloration (Fig. 6).

(b) Cusp displacement. This may result in patient hyper-sensitivity or fracture and crack formation at the surrounding walls (Fig. 7) [45–48].

The typical time-scale of a failure event can be limited to the short term, after or during the polymerization reaction, or it can arise in the long term. In the latter case, the failure might be associated with fatigue-loading due to mechanical forces and also due to thermal expansion, since tooth, adhesive layer and the restorative composite have different thermal expansion coefficients.

6. How Do the Stresses Vary in Magnitude with Time and Location?

Many factors affect the magnitude of stress developed. They will be considered under the headings of clinical variables and material formulation and properties.

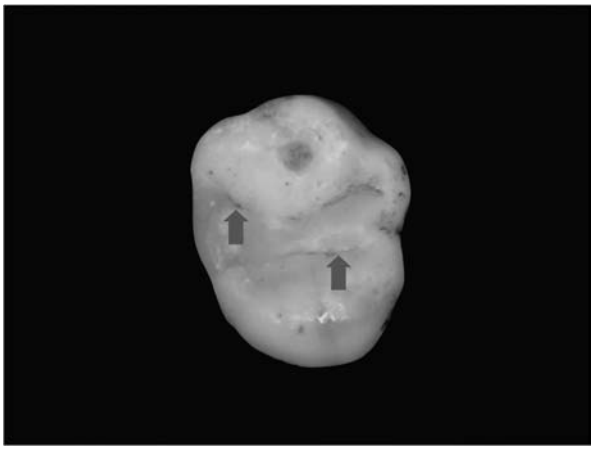


Figure 6. After the restoration procedure, the tooth was immersed in 'caries reveal' solution to mark possible marginal leakage. It is possible to see gap formed between the restoration and the tooth structure (arrows) almost all around restoration.

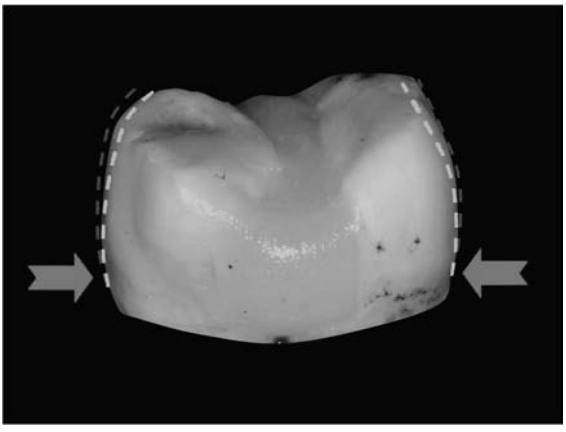


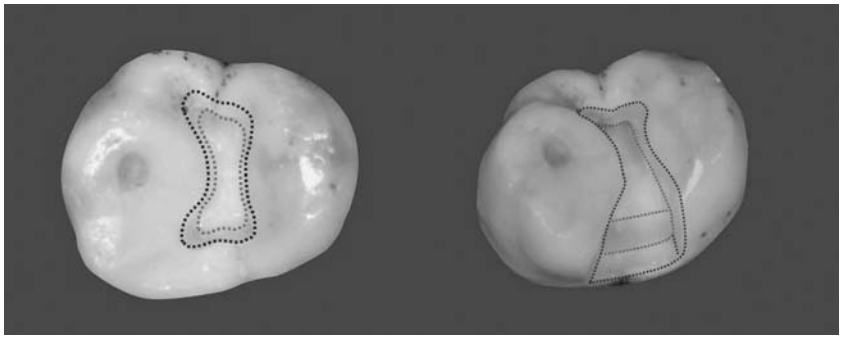
Figure 7. Hypothetical cusp displacement (dotted lines) that may result in formation of enamel cracks and, as a worse case scenario, in cusp fracture. This kind of fracture is commonly observed at the base of the cusp (arrows).

6.1. Clinical Factors Related to Stress Development

6.1.1. C-factor

As mentioned above, the restriction imposed by the surrounding walls affects the magnitude of stress development. However, the tooth cavity design varies since each clinical situation imposes very different design conditions. These include: the extent of caries removed, the amount of remaining healthy tissue, the tooth-region and the tooth location (anterior, posterior) and type (Fig. 8).

The expected stress magnitude due to the restriction imposed by the cavity walls might be estimated through the "configuration factor" (abbreviated as the



(a) (b)

Figure 8. The same tooth in different conditions due to different amounts of remaining tissues after preparation of different designs of cavity. The dotted lines are inserted to more easily identify the cavity walls.

"C-factor"). This is the ratio of the bonded to the unbonded area [35]:

$$\text{C-factor} = \text{Bonded area}/\text{Unbonded area}.$$

Using a constriction measurement system, Feilzer *et al.* [35] observed that the higher this C-factor, the higher was the corresponding stress. These authors suggested that composite flow would occur at the unbonded surface areas of the restoration. Thus, a higher proportion of unbonded composite surface would result in less restriction to bulk shrinkage and consequently stress would be reduced. At that time, in 1987, many resin composites available were still chemically-cured, where setting processes were relatively slow. Figure 8 shows different situations that exemplify this rationale. To restore a tooth in case a, the composite must fill a cavity that has approximately 5 walls to be bonded whereas only one is non-bonded (occlusal). Thus, the C-factor would be approximately 5/1. On the other hand, in case b the C-factor would be lower than in a since the proportion of surrounding walls is reduced, which also increases the possibility of tooth deformation by cusp bending due to the reduced mutual support of the surrounding walls.

6.1.2. Mass or Volume of Material Undergoing Shrinkage

It is evident that the cavity configuration plays an important role in stress development, other things being equal. However, it has been suggested recently that the C-factor approach in isolation may overestimate the effect of the degree of constriction [38] since it underestimates or neglects the effect of the mass [49] or, equivalently, volume [50] of resin composite applied. For example, one study verified that shrinkage stress and microleakage were higher in restorations with larger diameters and depths and the authors concluded that microleakage seemed to be related to a restoration's volume, but not to its 'C' factor [50].

The intrinsic shrinkage strain — and thus stress — magnitudes arise directly from the mass of material undergoing polymerization. When narrower cavities are encountered, especially the thin gaps between inlays and tooth tissues, it is normally

the case that the mass of material required to fill the gap is greatly reduced. Hence the C-factor and the mass are opposing factors in such a case.

6.2. Factors Involving the Material Formulation and Resultant Properties

6.2.1. Resin Matrix/Filler Ratio

According to Hooke's law, as an approximate constitutive relationship for pure solids, stress is the product of elastic modulus and strain. Although polymerized resin composites cannot be considered pure solids, because they also present a viscous component, it is considered that the stress developed is the product of two main factors: the volumetric shrinkage strain and the elastic modulus, both of which are time dependent during the setting process.

As mentioned before, resin composites are a combination of inorganic particles, coated by a coupling agent, dispersed in an organic polymer matrix. Since inorganic fillers are stiff, the higher the proportion of filler the greater is the composite elastic modulus [15] and the resultant or developed stress [51]. On the other hand, the polymer matrix has a lower elastic modulus than the inorganic phase but shrinks when polymerized. For example, Braga *et al.* [52] found similar stress values among materials with different viscosities, suggesting that shrinkage also plays an important role [52]. Therefore, the polymer matrix/filler ratio has a dominant effect upon strain and stress developed. High values of shrinkage, combined with an increasing elastic modulus, produce increased stress within the composite structure [53].

6.2.2. Resin Matrix Composition

The resin matrix chemical composition is the primary determinant of both the magnitude and kinetics of shrinkage phenomenon and the elastic modulus development. The principal chemical structural factors are the monomer functionalities, molecular architecture — including hydrogen-bonding groups — and molecular mass or size. These have major influences upon monomer viscosity, which also affects the maximum volume-fraction of filler that can be incorporated into the monomers. Hence, rheological parameters are valuable in assessment of candidate monomer mixtures [54, 55].

6.2.3. Photoinitiator System and Inhibitor of Polymerization

In theory, more time would be available for viscous flow and chain relaxation to occur in a polymer cured at slower rates [56]. Consequently, the concentration, ratio and type of photoinitiator system can affect the rate of polymerization and degree of conversion [57–59]. Since these two factors also affect the rate and final values of stress developed, thereby polymerization stress is also affected by the photoinitiator system and the polymerization inhibitor used in the monomer mixture [58, 60]. Braga and Ferracane [58] examined experimental materials with different concentrations of inhibitor (2,6-Di-tert-butyl-4-methyl-phenol = BHT), and showed that increased inhibitor concentration reduced the rate of polymerization and the shrinkage stress without significantly compromising the final degree of conversion of monomer to polymer. Furthermore, it was recently demonstrated that the use of

phenyl-propanedione, an alternative photoinitiator, combined with CQ may reduce the rate of stress development without decreasing the final material performance properties [59, 60].

6.2.4. Interrelationship of Properties

Shrinkage stress is a complex phenomenon since the underlying properties are interrelated. The greater the C=C bond conversion of the monomers, the greater the number of units combining to form the polymeric matrix; consequently, stiffness (elastic modulus) and volumetric shrinkage both increase [51, 61]. Thus, degree of C=C conversion and stress developed are directly related [42, 58, 62]. Furthermore, the polymerization rate dictates the shrinkage rate and the rate of increase of elastic modulus, which restricts the material's ability to undergo relaxation. Consequently, the polymerization rate directly affects the stress development rate.

It is hard to identify the weighted contribution of each individual factor (or determinant). But some very recent outcomes help to understand such contributions [63, 64]. Gonçalves *et al.* [63] used model composites and verified by regression analyses the relationship between stress developed and degree-of-conversion, shrinkage, and elastic modulus and verified that the coefficient of determination between stress and conversion ($r^2 = 0.905$) was higher than those between stress and shrinkage ($r^2 = 0.825$) and stress and elastic modulus ($r^2 = 0.623$). The authors suggest that this behavior may follow from the combined dependence of shrinkage and modulus upon conversion. Additionally, stress developed was more strongly related to shrinkage than to modulus, which is a different conclusion from the previous work of Kleverlaan and Feilzer [28]. Differences may relate to the different measurement geometries and other experimental conditions.

7. How Can Such Stresses Be Measured *In Vitro*?

Since polymerization stress is considered one of the major drawbacks of resin composite applications, extensive efforts have been made to understand the phenomenon and to devise means for its reduction. Suitable measurement methods are essential to determine magnitudes and their changes with proposed minimization protocols (to be discussed in Sections 8 and 9). Five methods of varying complexity, cost and measurement principle can be identified: force transducers [4, 27, 35, 39, 40, 49, 65–73], bonded strain-gauges [74], a ring slitting method [75, 76], photoelastic analysis [77–79] and finite element analysis [36, 39, 71, 80, 81].

Force transducers are the most widely used and versatile methods. By variations in cylinder/disk size and aspect ratio, it is possible to analyze C-factor and mass dependence. This method is based on measurements of axial stress developed as a function of time within a composite sample. Although the basic principle is the same, different measurement approaches exist. The most significant variation concerns the inevitable instrument compliance — the deformation per unit stress of all measuring system (sample and instrument) parts. Ferracane [53] reviewed data obtained with different materials and a variety of measurement systems and

concluded that outcomes depend upon system compliance, which varies among different studies. However, unlike measurements of shrinkage strain, which is a material property, shrinkage stress is not a material property. Hence, there is no such thing as a 'correct' magnitude. What is required is one (or more) 'level playing field(s)' to compare different materials and treatments (such as cure temperature, photon dose) on the same basis.

Universal testing machines with extensometers connected to a computer servo-control unit are considered the most rigid systems [4]. The extensometers can identify, with variable precision, movement of extension caused by the polymerization shrinkage and, as a feedback response, in theory the system compensates deformations to produce minimal compliance. Thus, these assemblies have very low compliance and, consequently, the registered values of stress tend to be higher than by more compliant methods [71]. Some variations may exist within this method, and a significant one is the kind of substrate to which the resin composite sample is attached. Gonçalves *et al.* [73] evaluated the effect of system compliance on polymerization stress for a wide range of resin composites when using poly(methyl methacrylate), or glass rods. As expected, the authors verified that stress determined with poly(methyl methacrylate) rods was lower (by 53–68%) than with glass rods so that composite ranking varied slightly due to differences in the substrate longitudinal and transverse deformations.

Force transducers adapted to systems with unknown or calculated compliance have also been used [38, 40, 66, 70]. However, besides variations in the final stress magnitude (that can be 15× lower in magnitude than when compared with a "highly-rigid methods"), the comparisons among different materials [53] and also the interpretation of some phenomena may also change. For example, while previous outcomes with rigid systems have reported a direct relationship between maximum stress developed and the stress development rate [58], Schneider *et al.* [60] and Pfeifer *et al.* [64] recently found an inverse correlation between final stress and maximum polymerization rate and maximum stress development rate. Thus, it is reasonable to state that care should be taken when analyzing data and that the compliance should be considered. To generate shrinkage stress data that might reflect the clinical situations, instrument compliance should be similar to that of the prepared tooth, as Watts and Satterthwaite [49] and Lee *et al.* [82] note.

As mentioned above, there are some other ways to determine polymerization stress. Strain-gauges are used to directly evaluate stress at specific locations [74] and can also be used to determine cuspal displacement [48, 83]. The use of the "ring-slitting method" is a simple and inexpensive way to evaluate residual stress in ring-shape resin composite specimens [75, 76]. Researchers have also employed photoelastic or finite element analyses (FEA) to better understand the spatial distribution of stress, since it is non-uniform within the restoration. Photoelastic analysis determines stress distribution through optical fringes [77–79], whereas FEA evaluates stress distributions by computer models (Fig. 9). This method requires not only an anatomically-accurate geometry but other input data, especially elastic moduli,

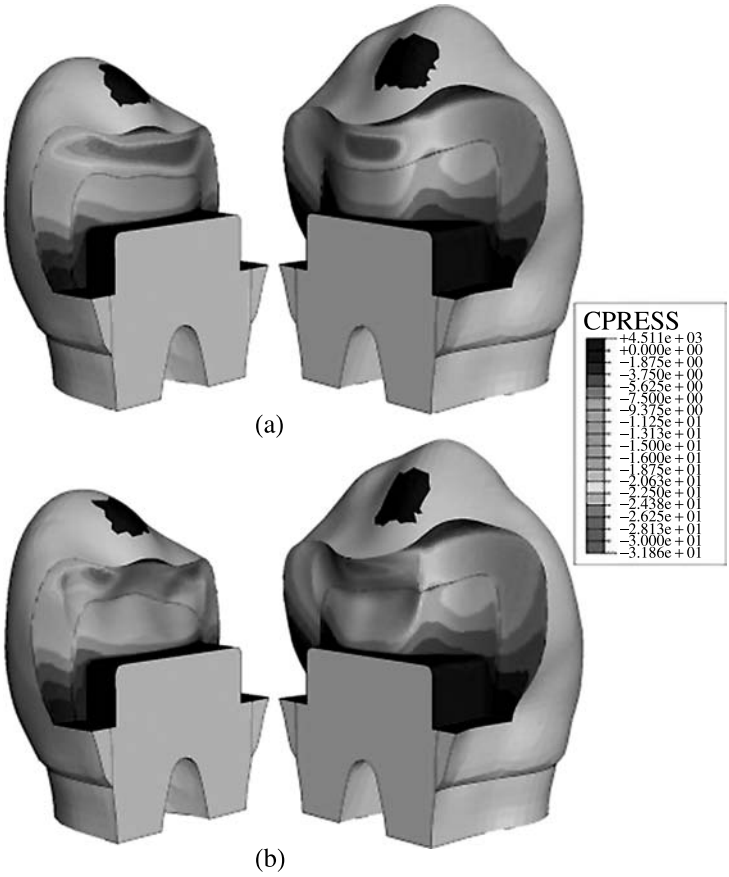


Figure 9. 3D images, computed by finite element analysis, of a restored tooth with (a) conventional and (b) optimized cavity designs. The tooth, with its restoration removed for clarity, is split mesio-distally into two approximately equal halves to reveal stress distributions on the cavity surfaces at the tooth–composite interface. Very high tensile stresses exist in case (a) in the enamel region on the buccal and lingual surfaces of the cavity. Reproduced with permission [104].

Poisson's ratios, shrinkage strain [36, 39, 71, 80, 81, 105] and, preferably, material 'solid viscosity' [106].

8. How Can Stresses Be Offset in Clinical Placement?

8.1. Restoration Placement Techniques

Since difficulties imposed by the cavity configuration play an important role in stress development, the use of "incremental techniques" has been proposed to minimize these clinical problems [84, 85]. Shrinkage may be less detrimental when there are fewer bonded cavity walls involved at each stage of the restoration procedures.

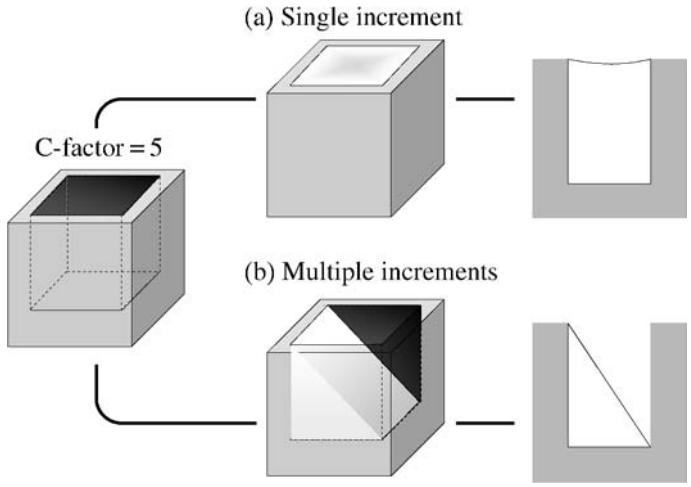


Figure 10. A dental cavity is here represented by a highly idealized cubic geometry, with four walls, one 'floor' and one open surface. When filled by a single increment (a) of a resin composite material, this gives a 'ratio of bonded to non-bonded surfaces' (C-factor) of 5. Higher stress is expected to result in comparison with case b, where the cavity is restored with multiple increments of resin composite, allowing a larger surface area for stress relief between successive increments.

Figure 10 shows a cavity with C-factor equal to five. Using a single increment (A), the resin composite would polymerize within five bonding surfaces (one base and four surrounding walls) while free-shrinkage would only occur at the upper surface, producing a very high level of stress between the bonded surfaces. However, using an incremental technique, the bonded/unbonded ratio would be reduced and, consequently, the stress level within the cavity might be lower, preserving the bonded area.

8.2. Stress Absorbing Layers with Low Elastic Modulus Liners

The use of (polymeric) materials with low elastic modulus has been suggested as a means of overcoming polymerization shrinkage stress [52, 86, 87]. An applied liner could create surrounding walls with increased compliance and thus stress development would be lower than in a very rigid cavity. However, actual implementation of such a "stress absorbing" material is problematic. Restorative materials encompass a wide variety of shrinkage and elastic modulus values. Consequently, some combinations might give reduced performance compared with the common restorative material applied alone.

8.3. Light Curing Procedures

Diverse photoactivation protocols have been advocated to reduce the polymerization stress [61, 88–90]. More rapid polymerization might result in increased shrinkage stress, while reduced initial irradiance may result in a slower development of stiffness of resin composite and prolong the time-window for material flow and stress release [91, 92].

The most common irradiation techniques are:

– Conventional: light irradiance is constant during the illumination period (20–40 s);
– Soft-start: initial exposure with reduced light irradiance for 10 s, followed by full irradiance.
– Pulse-delay: initial exposure with reduced light irradiance for 3 s, followed by a waiting period without irradiance (seconds or minutes); and full irradiance afterwards.

Figure 11 shows the stress increase with time when standard (40 s at 350 mW/cm^2) and pulse-delay methods were applied (5 s at 350 mW/cm^2 + 1 min without light exposure + 35 s at 450 mW/cm^2).

Alternative light-curing protocols may not significantly affect final properties of the hardened material. However, the following considerations should be noted:

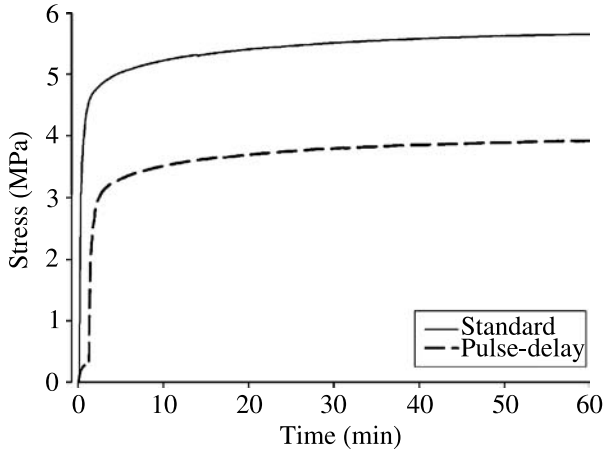
(i) The flowability of a material, during an extended pre-set stage, may have minimal consequences, because most shrinkage stress is developed during and after the vitrification stage. Therefore, opportunities for polymer relaxation would be restricted during the short period of light-activation [41]. (ii) Concurrent experiments on degree of C=C conversion (DC) and stress development show that soft-start irradiation procedures give somewhat lower DC levels, associated with reduced stress, [93]. (iii) A reduced polymerization rate is associated with decreased cross-link density (CLD), manifest as greater solvent-softening [94] and/or lower final elastic modulus [95].

9. How Can Intrinsic Stresses Be Reduced by Re-design of Materials?

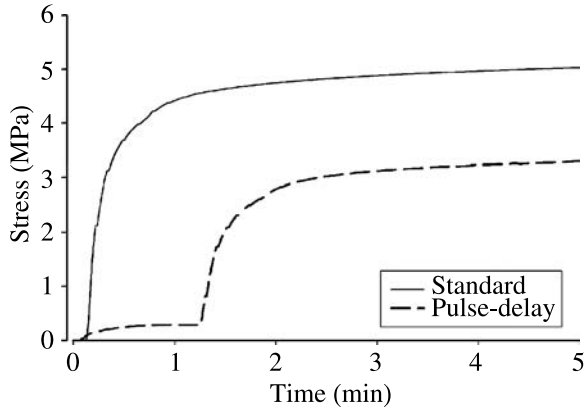
Many monomer combinations and alterations of the resin composite formulation have been developed and evaluated with the goal of decreasing polymerization shrinkage stress. 'Cyclic' monomers, such as the vinylcyclopropanes and siloranes have provided particularly interesting and commercially-viable results [96–101]. Such monomers 'open' their molecular structures with local volumetric expansion and this may partly or totally compensate for volumetric shrinkage from C=C or similar polymerization.

As already detailed, changes in the photoinitiator systems and polymerization inhibitors have also been evaluated. Braga and Ferracane [58] found that increase of inhibitor (BHT) concentration was associated with reductions in stress-rate and final stress. Schneider *et al.* [60] found that phenyl-propanedione, substituting for part of the camphorquinone content, reduced the stress development rate without compromising the final degree-of-conversion and degradation resistance of the composite.

Besides change in the resin matrix composition, studies have demonstrated reduced shrinkage stress through alterations in filler content. Condon and Ferracane [67] suggested that addition of non-bonded 40 nm colloidal silica might act as stress-relieving sites through plastic deformation. Condon and Ferracane [102] also verified that composites with nanofiller particles treated with a non-functional silane



(a)



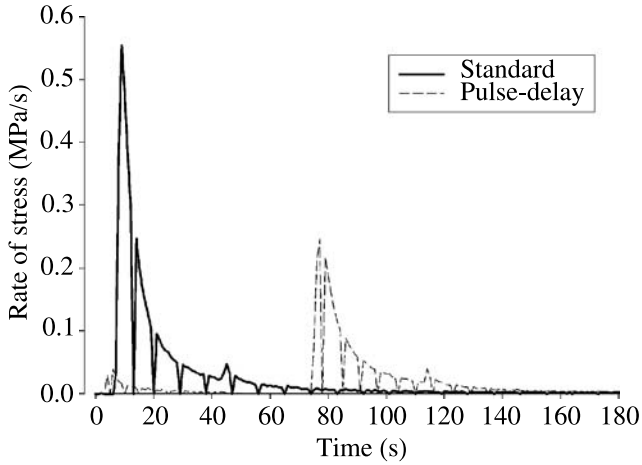
(b)

Figure 11. (a) Stress development over 60 min using standard and pulse-delay methods. (b) Expanded view for 0–5 min. (c) Stress development rate. Data from a commercial resin composite, Filtek Supreme™.

developed 50 percent less stress than composites fully treated with the functional coupling agent. Another possible approach is inclusion of a component readily allowing plastic deformation during stress development, such as UHMWPE (ultra-high molecular weight polyethylene) fibres [103].

10. Conclusions

The functional performance of restoratives cannot be considered apart from their host environment. In addition to mechanical chewing stresses imposed during intra-oral function, there is the further challenge of additional stresses from bulk shrinkage of the resin composite during the polymerisation process in the tooth cavity environment. These stresses are distributed spatially and temporally. Methods of



(c)

Figure 11. (Continued.)

characterising these stress distributions experimentally and by computational modelling are now becoming fruitful. These approaches are being applied to candidate formulations, sometimes involving novel chemistry, so that a definite amelioration of this problem is now feasible. These same physico-chemical and mechanical considerations may also apply to non-dental and non-biological contexts of adhesive bonding of materials in constrained cavity environments. Hence this subject is of wider interest to the adhesion science community.

Acknowledgements

Authors are thankful to Ataís Bacchi, undergraduate student from The University of Passo Fundo, and Dr. Larissa M. A. Cavalcante, Professor of Restorative Dentistry at The University of Passo Fundo, for help with the illustrations.

References

1. R. L. Bowen, *J. Dental Res.* **35**, 60–69 (1956).
2. R. L. Bowen, *J. Am. Dental Assoc.* **66**, 51–64 (1963).
3. G. Eliades, D. C. Watts and T. Eliades, *Dental Hard Tissues and Bonding.* Springer-Verlag, Berlin (2005).
4. C. L. Davidson, A. J. de Gee and A. Feilzer, *J. Dental Res.* **63**, 1396–1399 (1984).
5. L. Breschi, A. Mazzoni, A. Ruggeri, M. Cadenaro, R. Di Lenarda and E. De Stefano Dorigo, *Dental Mater.* **24**, 90–101 (2008).
6. J. L. Ferracane, R. C. Antonio and H. Matsumoto, *J. Dental Res*. **66**, 1140–1145 (1987).
7. M. Braem, W. Finger, V. E. Van Doren, P. Lambrechts and G. Vanherle, *Dental Mater.* **5**, 346–348 (1989).
8. K. H. Kim, J. H. Park, Y. Imai and T. Kishi, *J. Dental Res*. **73**, 499–504 (1994).

9. K. J. Söderholm, *J. Dental Res*. **63**, 1321–1326 (1984).
10. R. Yamaguchi, J. M. Powers and J. B. Dennison, *Oper. Dentistry* **14**, 64–67 (1989).
11. J. W. van Dijken, K. R. Wing and I. E. Ruyter, *Acta Odontol. Scand.* **47**, 401–407 (1989).
12. L. M. Cavalcante, K. Massouras, D. C. Watts, N. Silikas and L. A. F. Pimenta, *Am. J. Dentistry* **22**, 60–64 (2009).
13. L. A. Linden and J. Jakubiak, *Polimery* **46**, 590–595 (2001).
14. K. Baroudi, N. Silikas and D. C. Watts, *Eur. J. Oral Sci.* **115**, 517–521 (2007).
15. K. Masouras, N. Silikas and D. C. Watts, *Dental Mater.* **24**, 932–939 (2008).
16. K. H. Kim, J. L. Ong and O. Okuno, *J. Prosthet. Dentistry* **87**, 642–649 (2002).
17. S. A. Rodrigues Jr, J. L. Ferracane and A. Della Bona, *Dental Mater.* **24**, 426–431 (2008).
18. S. A. Rodrigues Jr, S. S. Scherrer, J. L. Ferracane and A. Della Bona, *Dental Mater.* **24**, 1281–1288 (2008).
19. R. van Noort, *Introduction to Dental Materials*. Elsevier, London, UK (2007).
20. S. B. Mitra, D. Wu and B. N. Holmes, *J. Am. Dental Assoc.* **134**, 1382–1390 (2003).
21. A. Peutzfeldt, *Eur. J. Oral Sci*. **105**, 97–116 (1997).
22. N. M. Mohsen and R. G. Craig, *J. Oral Rehabil.* **22**, 183–189 (1995).
23. E. Dart and J. Nemcek, British Patent number 1 408 265 (1975).
24. M. Taira, H. Urabe, T. Hirose, K. Wakasa and M. Yamaki, *J. Dental Res.* **67**, 24–28 (1988).
25. H. H. Alvim, A. C. Alecio, W. A. Vasconcellos, M. Furlan, J. E. de Oliveira and J. R. Saad, *Dental Mater.* **23**, 1245–1249. (2007).
26. J. W. Stansbury, *J. Esthet. Dentistry* **12**, 300–308 (2000).
27. R. R. Braga, R. Y. Ballester and J. L. Ferracane, *Dental Mater.* **21**, 962–970 (2005).
28. C. J. Kleverlaan and A. J. Feilzer, *Dental Mater.* **21**, 1150–1157 (2005).
29. W. Weinmann, C. Thalacker and R. Guggenberger, *Dental Mater.* **21**, 68–74 (2005).
30. E. Andrezejewska, *Prog. Polym. Sci.* **26**, 605–665 (2001).
31. D. C. Watts, *Dental Mater.* **21**, 27–35 (2005).
32. R. L. Sakaguchi, N. C. Shah, B. S. Lim, J. L. Ferracane and S. E. Borgersen, *Dental Mater.* **18**, 197–202 (2002).
33. J. L. Ferracane, *Dental Mater.* **21**, 36–42 (2005).
34. K. J. Söderholm, M. Zigan, M. Ragan, W. Fischlschweiger and M. Bergman, *J. Dental Res.* **63**, 1248–1254 (1984).
35. A. Feilzer, A. J. De Gee and C. L. Davidson, *J. Dental Res.* **66**, 1636–1639 (1987).
36. A. Versluis, D. Tantbirojn and W. H. Douglas, *J. Dental Res.* **77**, 1435–1445 (1998).
37. C. L. Davidson and A. J. de Gee, *J. Dental Res.* **63**, 146–149 (1984).
38. A. Miguel and J. C. de la Macorra, *Dental Mater.* **17**, 241–246 (2001).
39. G. A. Laughlin, J. L. Williams and J. D. Eick, *J. Biomed. Mater. Res.* **63**, 671–678 (2002).
40. D. C. Watts, A. S. Marouf and A. M. Al-Hindi, *Dental Mater.* **19**, 1–11 (2003).
41. H. Lu, J. W. Stansbury and C. N. Bowman, *Dental Mater.* **20**, 979–986 (2004).
42. J. W. Stansbury, M. Trujillo-Lemon, H. Lu, X. Ding, Y. Lin and J. Ge, *Dental Mater.* **21**, 56–67 (2005).
43. T. J. Hilton, *Am. J. Dentistry* **15**, 198–210 (2002).
44. J. L. Ferracane and J. C. Mitchem, *Am. J. Dentistry* **16**, 239–243 (2003).
45. B. E. Causton, B. Miller and J. Sefton, *Br. Dental J.* **159**, 397–400 (1985).
46. A. J. McCullock and B. G. Smith, *Br. Dental J.* **161**, 405–409 (1986).
47. G. J. Pearson and S. M. Hegarty, *Biomaterials* **8**, 473–476 (1987).
48. N. Meredith and D. J. Setchell, *J. Dentistry* **25**, 331–337 (1997).
49. D. C. Watts and J. D. Satterthwaite, *Dental Mater.* **24**, 1–8 (2008).

50. R. R. Braga, L. C. Boaro, T. Kuroe, C. L. Azevedo and J. M. Singer, *Dental Mater.* **22**, 818–823 (2006).
51. J. R. Condon and J. L. Ferracane, *J. Am. Dental Assoc.* **131**, 497–503 (2000).
52. R. R. Braga, J. L. Ferracane and T. J. Hilton, *J. Am. Dental Assoc.* **134**, 721–728 (2003).
53. J. L. Ferracane, *Oper. Dentistry* **33**, 247–257 (2008).
54. A. J. Feilzer and B. S. Dauvillier, *J. Dental Res.* **82**, 824–828 (2003).
55. A. Charton, V. Falk, P. Marchal, F. Pla and P. Colon, *Dental Mater.* **23**, 1447–1459 (2007).
56. R. L. Sakaguchi, B. D. Wiltbank and C. F. Murchison, *Dental Mater.* **20**, 402–407 (2004).
57. Venhoven, A. J. de Gee and C. L. Davidson, *Biomaterials* **17**, 2313–2318 (1996).
58. R. R. Braga and J. L. Ferracane, *J. Dental Res.* **81**, 114–118 (2002).
59. L. F. Schneider, C. S. Pfeifer, S. Consani, S. A. Prahl and J. L. Ferracane, *Dental Mater.* **24**, 1169–1177 (2008).
60. L. F. Schneider, S. Consani, R. L. Sakaguchi and J. L. Ferracane, *Dental Mater.* **25**, 566–572 (2009).
61. N. Silikas, G. Eliades and D. C. Watts, *Dental Mater.* **16**, 292–296 (2000).
62. F. C. Calheiros, R. R. Braga, Y. Kawano, R. Y. Ballester, *Dental Mater.* **20**, 939–946 (2004).
63. F. Gonçalves, C. S. Pfeifer, J. L. Ferracane and R. R. Braga, *J. Dental Res.* **87**, 367–371 (2008).
64. C. S. Pfeifer, J. L. Ferracane, R. L. Sakaguchi and R. R. Braga, *J. Dental Res.* **87**, 1043–1047 (2008).
65. R. L. Bowen, *J. Am. Dental Assoc.* **74**, 439–445 (1967).
66. M. R. Bouschlicher, M. A. Vargas and D. B. Boyer, *Am. J. Dentistry* **10**, 88–96 (1997).
67. J. R. Condon and J. L. Ferracane, *Dental Mater.* **14**, 256–260 (1998).
68. F. C. Calheiros, F. T. Sadek, R. R. Braga and P. E. Cardoso, *J. Dentistry* **32**, 407–412 (2004).
69. H. Lu, J. W. Stansbury, S. H. Dickens, F. C. Eichmiller and C. N. Bowman, *J. Mater. Sci. Mater. Med.* **15**, 1097–1103 (2004).
70. R. L. Sakaguchi, B. D. Wiltbank and C. F. Murchison, *Dental Mater.* **20**, 388–396 (2004).
71. M. F. Witzel, R. Y. Ballester, J. B. Meira, R. G. Lima and R. R. Braga, *Dental Mater.* **23**, 204–210 (2007).
72. S. H. Lee, J. Chang, J. L. Ferracane and I. B. Lee, *Dental Mater.* **23**, 1093–1100 (2007).
73. F. Gonçalves, C. S. Pfeifer, J. B. Meira, R. Y. Ballester, R. G. Lima and R. R. Braga, *Dental Mater.* **24**, 645–652 (2008).
74. R. L. Sakaguchi and J. L. Ferracane, *Dental Mater.* **14**, 106–111 (1998).
75. J. W. Park and J. L. Ferracane, *Dental Mater.* **21**, 882–889 (2005).
76. J. W. Park and J. L. Ferracane, *J. Dental Res.* **85**, 945–949 (2006).
77. Y. Kinomoto and M. Torii, *J. Dentistry* **26**, 165–171 (1998).
78. Y. Kinomoto, M. Torii, F. Takeshige and S. Ebisu, *J. Dent.* **27**, 383–389 (1999).
79. C. P. Ernst, G. R. Meyer, K. Klöcker and B. Willershausen, *Dental Mater.* **20**, 313–321 (2004).
80. A. Versluis, W. H. Douglas, M. Cross and R. L. Sakaguchi, *J. Dental Res.* **75**, 871–878 (1996).
81. P. Ausiello, A. Apicella, C. L. Davidson and S. Rengo, *J. Biomechanics* **34**, 1269–1277 (2001).
82. S. H. Lee, J. Chang, J. L. Ferracane and I. B. Lee, *Dental Mater.* **23**, 1093–1100 (2007).
83. W. M. Palin, G. J. Fleming, H. Nathwani, F. J. Burke and R. C. Randall, *Dental Mater.* **21**, 324–335 (2005).
84. F. Lutz, I. Krejci and T. R. Oldenburg, *Quintessence Int.* **17**, 777–784 (1986).
85. A. A. Suliman, D. B. Boyer and R. S. Lakes, *Dental Mater.* **9**, 6–10 (1993).
86. C. M. Kemp-Scholte and C. L. Davidson, *J. Dental Res.* **69**, 1240–1243 (1990).
87. K. K. Choi, J. R. Condon and J. L. Ferracane, *J. Dental Res.* **79**, 812–817 (2000).
88. R. L. Sakaguchi and H. X. Berge, *J. Dentistry* **26**, 695–700 (1998).

89. C. S. Pfeifer, R. R. Braga and J. L. Ferracane, *Oper. Dentistry* **31**, 610–615 (2006).
90. L. G. Cunha, R. C. Alonso, C. S. Pfeifer, L. Correr-Sobrinho, J. L. Ferracane and M. A. Sinhoreti, *Dental Mater.* **24**, 392–398 (2008).
91. S. Uno and E. Asmussen, *Scand. J. Dental Res.* **99**, 440–444 (1991).
92. B. S. Lim, J. L. Ferracane, R. L. Sakaguchi and J. R. Condon, *Dental Mater.* **18**, 436–444 (2002).
93. H. Lu, J. W. Stansbury and C. N. Bowman, *J. Dental Res.* **84**, 822–826 (2005).
94. E. Asmussen and A. Peutzfeldt, *J. Dental Res.* **80**, 1570–1573 (2001).
95. L. Feng and B. I. Suh, *J. Biomed. Mater. Res. Part B Appl. Biomater.* **78B**, 63–69 (2006).
96. N. Moszner and U. Salz, *Prog. Polym. Sci.* **26**, 535–576 (2001).
97. N. Moszner, T. Volkel, F. Zeuner and V. Rheinberger, *Polymer Preprints* **38**, 86–87 (1997).
98. N. Moszner and U. Salz, *Macromol. Mater. Eng.* **292**, 245–271 (2007).
99. R. Guggenberger and W. Weinmann, *Am. J. Dentistry* **13**, 82D–84D (2000).
100. J. D. Eick, E. L. Kostoryz, S. M. Rozzi, D. W. Jacobs, J. D. Oxmann, C. C. Chappelow, A. G. Glaros and D. M. Yourtee, *Dental Mater.* **18**, 413–421 (2002).
101. J. D. Eick, S. P. Kotha, C. C. Chappelow, K. V. Kilway, G. J. Giese, A. G. Glaros and C. S. Pinzino, *Dental Mater.* **23**, 1011–1017 (2007).
102. J. R. Condon and J. L. Ferracane, *Biomaterials* **23**, 3807–3815 (2002).
103. J. L. Ferracane, L. L. Ferracane and R. R. Braga, *J. Biomed. Mater. Res. B Appl. Biomater.* **66**, 318–323 (2003).
104. L. Shi, A. S. L. Fok and A. Qualtrough, *Dental Mater.* **24**, 1444–1453 (2008).
105. F. P. Rodrigues, J. Li, N. Silikas, R. Y. Ballester and D. C. Watts, *Dental Mater.* **25**, e47–e55 (2009).
106. J. Li, H. Li, A. S. L. Fok and D. C. Watts, *Dental Mater.* **25**, 829–836 (2009).

Fatigue Resistance of Resin-Bonded Post–Core–Crown Treated Teeth with Flared Root Canal

Qiufie Xie [a,*], **Wei Wu** [a], **Peng Liu** [a] **and Pekka K. Vallittu** [b]

[a] Department of Prosthodontics, Peking University School and Hospital of Stomatology, Zhongguancun Southern Avenue 22, Haidian District, Beijing 100081, China

[b] Department of Prosthetic Dentistry and Biomaterials Science, Institute of Dentistry, Faculty of Medicine, University of Turku, Turku, Finland

Abstract

Here the objective was to evaluate fatigue resistance of anterior teeth with flared root canal restored using resin-bonded individualized fiber-reinforced composite (FRC) posts, prefabricated FRC posts, or prefabricated stainless-steel posts.

Twenty-four maxillary central incisors were endodontically treated and prepared as flared root canals. They were divided into three groups of 8 each. In Group 1, individual posts were made of FRC material. Prefabricated FRC posts were used for Group 2 and prefabricated stainless-steel posts used in Group 3. All posts were cemented with a self-adhesive resin into canals. The composite core and porcelain fused to metal crown were made for each. The specimens underwent thermocycling and dynamic mechanical loading and survived specimens were loaded to fracture. The data were statistically analyzed using ANOVA and independent sample *t*-test.

In the fatigue test, Group 1 had no failure; all Group 2 specimens failed; and 7 specimens of Group 3 survived. There were significant differences in numbers of cyclically mechanical loading times between Groups 1 and 2, and Groups 2 and 3 ($p < 0.01$, $p < 0.05$). The average of residual load-bearing capacity was 317.5 ($\pm$90.2) N for Group 1 and 403.8 ($\pm$138.2) N for Group 3 and there was no significant difference between these two groups. The fracture mode of specimens was cervical root fracture with or without vertical crack in both Groups 1 and 3. In Group 2 the debonding mostly occurred at the cement–post interface.

This *in vitro* study indicates that the flared canal teeth restored with individually formed FRC posts and prefabricated serrated stainless-steel posts provide good resistance against cyclic loading. The teeth restored with conventional prefabricated FRC posts may not be strong enough to resist masticatory forces without a ferrule.

Keywords

Fatigue resistance, fiber reinforced composite, flared root canal, load-bearing capacity, post and core, resin bonded

* To whom correspondence should be addressed. Tel.: +86 10 62179977-2552; Fax: +86 10 62173402; e-mail: xieqiuf@163.com

Adhesion Aspects in Dentistry

© Koninklijke Brill NV, Leiden, 2009

1. Introduction

The restoration of endodontically treated teeth still is an important topic in restorative dentistry. The teeth with extensive structural defects due to decay, trauma, and prior restoration often require post–core–crown restoration. Cast metal posts are traditionally used, but their rigid nature may pose a risk for root fracture [1, 2]. Fiber-reinforced composite (FRC) root canal posts have been introduced as an alternative to support weak coronal dentine for crown restoration, since their elastic modulus is close to that of dentine [3]. Recently, various types of prefabricated FRC root canal posts have been used because of their certain advantages, such as ready to use, reduced risk of fracture, and esthetic quality. Clinical durability of teeth restored with a combination of fiber post and resin core has been reported [4, 5].

In clinical situation, root canal treatment may remove decayed dentine to great extent, resulting in thin wall and flared root canal. It is a challenging endeavor to restore such kind of teeth. Insertion of prefabricated FRC or metal root canal posts into flared root canals only fills the canal space partly and the rest space is frequently filled with a low fracture strength composite resin luting cement. On the other hand, the teeth with a thin dentine wall render preparation of ferrule difficult [6]. It is known that high stresses caused by biting force concentrate on the cervical part of the crown-restored teeth. Optimization of the strength and structural stiffness of the cervical part of the restored teeth is, therefore, needed. This can be reached by increasing the volume of the FRC material of the post in the flared root canal opening. This kind of FRC post is referred to individually formed FRC post. Besides commonly used glass fibers, polyethylene fibers as customized post and core systems have been fabricated and luted directly into the root canal [7, 8]. However, polyethylene fibers as reinforcing fibers for resins still suffer from poor adhesion, which hinders their long term clinical use [9]. Individually formed FRC posts with high volume of FRC material provide stiffness which supports the crown against marginal breakdown. In metal posts, the stiffness is obtained from the rigidity of the material itself rather than from design of the post construction. Compared with metal posts, the FRC posts caused more often repairable fractures to the roots [10].

Strengthening of restoration for an endodontically treated tooth depends on its load-bearing capacity and distribution of the bite force in the tooth. In order to obtain load transfer from crown to core and post, and finally to dentine, adhesive interfaces play an important role. In the case of FRC root canal posts which are made of reinforcing fibers and semi-IPN (semi-interpenetrating polymer network) polymer matrix, the adhesion of the composite resin luting cement is shown to be better than that in the fiber post containing cross-linked polymer matrix only, as in all currently available prefabricated FRC posts [11, 12]. A few studies have been conducted in dynamic loading tests to examine whether there is any difference between different post types [13]. Therefore, the hypothesis of this study is that individually formed FRC posts containing semi-IPN matrix have no different performance from other prefabricated posts in the fatigue test.

The purposes of this *in vitro* study were to evaluate fatigue resistance of resin-bonded post–core–crown treated anterior teeth with flared root canals, to compare performance of three kinds of posts — individually formed FRC post containing semi-IPN matrix, prefabricated FRC post, and prefabricated metal post — and to evaluate modes of failure.

2. Materials and Methods

2.1. Preparation of Teeth

A total of 24 human maxillary central incisors with similar sizes were selected for this study. Teeth with root caries, restorations, and observable cracks were not included. The selected teeth were stored in 0.01% Chloramine T at 4°C and used within 6 months.

All the teeth were horizontally cut 1–2 mm above the cementoenamel junction and coronal portion was removed with thin tapered diamond burs (Mani Inc., Japan) using a high-speed handpiece under air–water spray, and then finely cut leaving 12 mm root portion. The root canals were prepared using K-files (Mani Inc., Tochigi-Ken, Japan) finished to No. 40 file, and the prepared canals were coated with zinc oxide–eugenol (Cortisomol; Pierre Rolland, Merignac Cedex, France) and filled with laterally condensed gutta-percha points (Gapadent JIAFA, Co. Ltd., Korea). After preparation, all teeth were restored in 0.09% NaCl at 4°C.

One week after root canal treatment, the gutta-percha points of 9 mm were removed from all root canals with a Pesso Reamer (Mani Inc., Japan) using a slow-speed handpiece, leaving a 3 mm apical fill. The root canals were subsequently enlarged using round-end tapered diamond burs (Mani Inc., Japan) under air–water spray to simulate flared root canals. The root canal walls were measured at labial, mesial, lingual, and distal aspects from root canal opening using a digital caliper (Beijing Liangju Renju Chang, Beijing, China) and further prepared to thin walls of 1 mm. The labiolingual and mesiodistal dimensions of each root were recorded at the level of canal opening and the length of the root was measured from apex to the transection. The prepared roots were assigned to three groups of 8 specimens each. There were no significant differences among groups in terms of length and labiolingual and mesiodistal dimensions ($p > 0.05$, ANOVA). All roots were reconstructed with one of three post systems: individually formed FRC post containing semi-IPN matrix (Group 1), prefabricated FRC post (Group 2), and prefabricated stainless-steel post (Group 3), as well as with porcelain fused to metal (PFM) crowns (Table 1 and Fig. 1).

2.2. Post and Core Fabrication

In Group 1, individually formed FRC posts were handled according to the manufacturer's instructions and fabricated with semi-translucent flexible FRC material (experimental package, everStick, Stick Tech Ltd., Finland). The FRC material was made of continuous silanized glass fibers impregnated with resin consisting

Table 1.
Description of experimental groups and materials used

Group ($n = 8$)	Post system	Core material	Luting agent	Porcelain-fused-to-metal crown
1	Glass fiber-reinforced composite material (everStick, Stick Tech Ltd., Finland) Experimental package	LuxaCore (DMG, Germany) Lot 568579	Rely X Unicem (3M Espe, Seefeld, Germany) Lot 154417	Ni–Cr alloy (metal coping), Vita porcelain-fused-to-metal powder (VMK95, VITA, Germany)
2	Prefabricated fiber posts (fibio, anthogyr, France) Lot 06012408	Same as above	Same as above	Same as above
3 (controls)	Prefabricated stainless-steel posts (ParaPost, Coltène/Whaledent Inc., Mahwah, NJ, USA) Lot MT-25775	Same as above	Same as above	Same as above

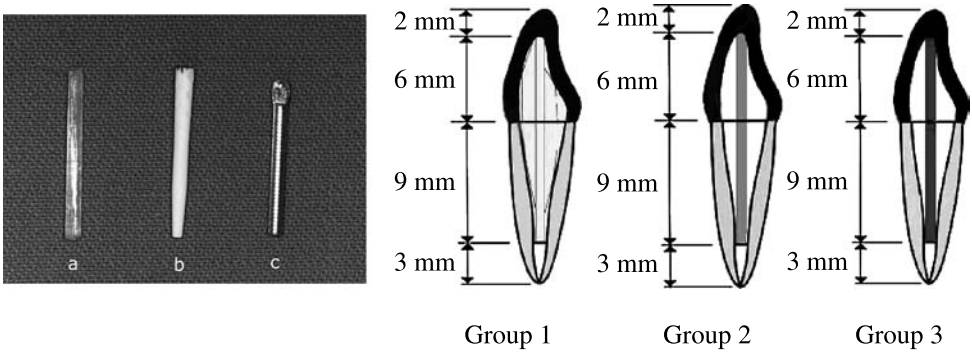


Figure 1. Root canal posts and scheme of post–core–crown restored teeth of three groups. (a) FRC root canal post material (everStick, Stick Tech Ltd., Finland); (b) Prefabricated FRC post (fibio, anthogyr, France); (c) Prefabricated stainless-steel post (ParaPost, Coltène/Whaledent Inc., Mahwah, NJ, USA). Group 1: tooth restored with individually-formed FRC post and crown; Group 2: tooth restored with prefabricated FRC post and crown; Group 3: tooth restored with prefabricated stainless-steel post and crown.

of bis-GMA and PMMA which during polymerization formed a semi-IPN matrix. A bundle of 15 mm long glass fiber-reinforced composite (GFRC) was first inserted into the canal and was compressed to the canal wall with a spreader and then one or two bundles of GFRC were filled in the rest space of the canal. The individually formed post was initially light cured for 10 s in the canal (Optilux 501; SDS Kerr, Danbury, CT, USA, 660 mW cm^{-2}) and followed by light curing for 40 s after it was removed from the canal. In Group 2, prefabricated FRC posts of 1.5 mm diam-

eter (fibio, anthogyr, France) were used. In Group 3, as the control, prefabricated stainless-steel posts of 1.5 mm diameter (ParaPost, Whledent/Coltene, USA) were used.

The flared canals were cleaned with a water spray and dried only with air blow for 3 s (not overdried). The prepared dual-cured self-adhesive resin (Rely X Unicem, 3M Espe, Seefeld, Germany) was first injected into the flared root canals, the surface of post was also coated with the self-adhesive resin, and then the post was inserted into the flared canal. All the posts were cemented using the same self-adhesive resin into canals under finger pressure for 5 min. After removal of excess cement, the resin cement was cured by irradiation for 40 s. The coronal core portion was made from light polymerized core build-up composite resin (LuxaCore®-Dual, DMG, Germany). First, the Contax primer and bond (DMG, Germany) were applied in succession to the coronal portions of the posts and exposed luting cement around posts and then were light cured for 20 s. The cores were subsequently built up with core composite using clear plastic molds and light cured for 40 s in labial and lingual aspects. The clear plastic molds were used in this study to construct the same size cores for all specimens. A flat-end tapered diamond bur was used to achieve a uniform shoulder of 1 mm width and no ferrule was prepared. The shape and size of three groups of specimens are depicted in Fig. 1.

2.3. Preparation of Porcelain-Fused to Metal (PFM) Crowns

Impressions of prepared specimens were made with polyether impression material (Impregum™, 3M Espe, Grefeld, Germany) and were poured using a die stone. PFM crowns were fabricated using Ni–Cr alloy (Heraeus-Kulzer Corporation, Germany) and VITA VMK95 porcelain (VITA, Germany) by a skilled technician, who was uninformed of the group allocation. The form of the final PFM crown was measured and corrected with a digital caliper for the same size for all. The crown was luted using a glass ionomer cement (Ketac™ Cem, 3M Espe, Seefeld, Germany), as in a clinical process.

2.4. Fatigue Resistance and Residual Load-Bearing Capacity Tests

To simulate the periodontal ligament, the roots of specimens were covered with three layers of Teflon tape (0.08 thick and 10 mm wide) (Shuanghuan, Ningbo, China) with a total thickness of approximately 0.24 mm. Finally, the specimens were vertically embedded in an acrylic resin (Shanghai Dental Material, Shanghai, China) at a depth of 2 mm below the margins of PFM crowns in metal tubes.

Each specimen in the tube was positioned in a special mounting jig and was aligned at a 135 degree angle with respect to the long axis of the tooth. The specimens underwent thermocycling and dynamic mechanical loading (TCML) at the lingual fossa with a hemispherical head with a diameter of 6 mm for simulating 5-year use (12 000 × 5/55°C; $1.2 \times 10^7 \times 30$ N, 1.7 Hz) [13, 14] in a TCML chewing simulator (Peking University, Medical Center, Beijing, China). The number of cyclically mechanical loading times was recorded. The survived specimens were

further loaded to fracture with a crosshead speed of 0.5 mm/min in a universal testing machine (DCS5000, Shimadzu, Japan). Failure threshold was defined as the point at which the loading force reached a maximum value by fracturing the root, bending the post, or debonding the post or cement [6]. The fracture loads were recorded and the mode of fracture was observed by visual inspection (using a microscope at a magnification $\times 20$). Crack propagation and canal wall fracture were classified into three categories: root cervical fracture: crack only in cervical portion, or cervical fracture of root; root middle fracture: crack from cervical to middle portion, or cervical and middle fracture of root; root vertical fracture: crack from cervical to apical portion, or cervical, middle, and apical fracture of root. Two tested specimens from each group were processed and transections of roots and debonded post areas were examined by SEM (S-4800, HITACHI Japan).

2.5. Statistical Analysis

Statistical analyses of the results were performed using the SPSS 10.0 for Windows (SPSS Inc., Chicago, IL, USA). The numbers of cyclic loading times of all three groups were analyzed with ANOVA. Because none of specimens in Group 2 survived in the fatigue test, comparison of fracture load values was made between Groups 1 and 3 with independent sample t-test. The statistical significance level was $\alpha = 0.05$.

3. Results

3.1. Fatigue and Fracture Tests

In simulating 5-year service, the specimens of Group 1 (individually formed FRC posts) sustained cyclic loads and no one failed; all the specimens of Group 2 (prefabricated FRC posts) failed with one post fractured and 7 posts dislocated in about 3 year service; 7 specimens of Group 3 (prefabricated stainless-steel posts) survived, only one post fractured (Table 2). There were significant differences in the numbers of cyclical loading times among the three groups. Groups 1 and 3 had greater numbers of cyclical loading times than Group 2 ($p < 0.01$, $p < 0.05$) and there was no significant difference between Groups 1 and 3.

In the test for residual load-bearing capacity, the mean load value was 317.5 ($\pm$90.2) N for Group 1 and 403.8 ($\pm$138.2) N for the 7 specimens of Group 3 (Table 2). There was no significant difference between the two groups ($p > 0.05$).

3.2. Microscopic Observation

The fracture was observed at the root cervical portion in 5 out of 8 specimens of Group 1 and in 4 out of 7 specimens of Group 3 (Table 3). The vertical crack from the cervical to apical portion of the root was found in 3 specimens of Group 1. The vertical crack from the cervical to middle portion of the root occurred in 3 specimens of Group 3 (Table 3).

Table 2.
Fatigue resistance of Group 1 (individually formed FRC posts), Group 2 (prefabricated FRC posts), and Group 3 (prefabricated stainless-steel posts) in number of cyclically mechanical loading times (in 10 thousands) and residual load-bearing capacity (in Newton)

Specimen	Cyclical loading			Residual load-bearing capacity	
	Group 1	Group 2	Group 3	Group 1	Group 3
1	120.0	88.7 (PD)	120.0	382.20	311.64
2	120.0	93.1 (PD)	120.0	252.84	516.46
3	120.0	84.4 (PD)	120.0	375.34	310.66
4	120.0	78.9 (PF)	120.0	219.52	502.74
5	120.0	85.2 (PD)	120.0	490.00	240.10
6	120.0	86.5 (PD)	120.0	281.26	613.48
7	120.0	96.5 (PD)	120.0	272.44	334.18
8	120.0	75.9 (PD)	30.9 (PF)	266.56	–
Mean ± SD	120.0 ± 0.0	86.2 ± 6.8**#	108.7 ± 31.5	317.52 ± 90.16	403.76 ± 138.18

PD: post dislodgement; PF: post fracture.
**: $p < 0.01$, compared between Groups 1 and 2, #: $p < 0.05$, compared between Groups 2 and 3 with ANOVA and multiple comparisons.

Table 3.
Fracture modes of specimens of Group 1 and Group 3 under maximum load

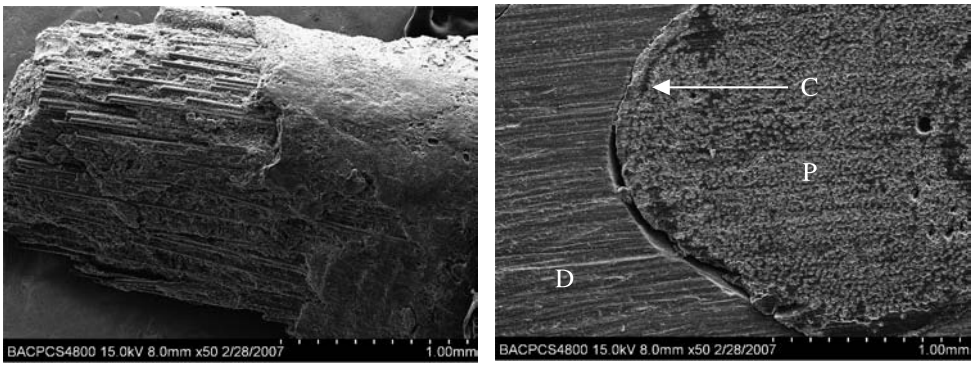
Fracture mode	Group 1	Group 3
Crown or post fracture	0	0
Root cervical fracture	5 (62.5%)	4 (57.1%)
Root middle fracture	0	3 (42.9%)
Root vertical fracture	3 (37.5%)	0

Root cervical fracture: crack only in cervical portion, or cervical fracture of root.
Root middle fracture: crack from cervical to middle portion, or cervical and middle fracture of root.
Root vertical fracture: crack from cervical to apical portion, or cervical, middle, and apical fracture of root.

Examination of the specimens in Group 2 showed that all dislocated prefabricated FRC posts exposed their smooth surfaces in apical and middle portions without resin cement remaining and only cervical portion was covered by resin cement. One individually formed FRC post of Group 1 completely dislocated from the canal under maximum loading and was mostly covered by resin cement.

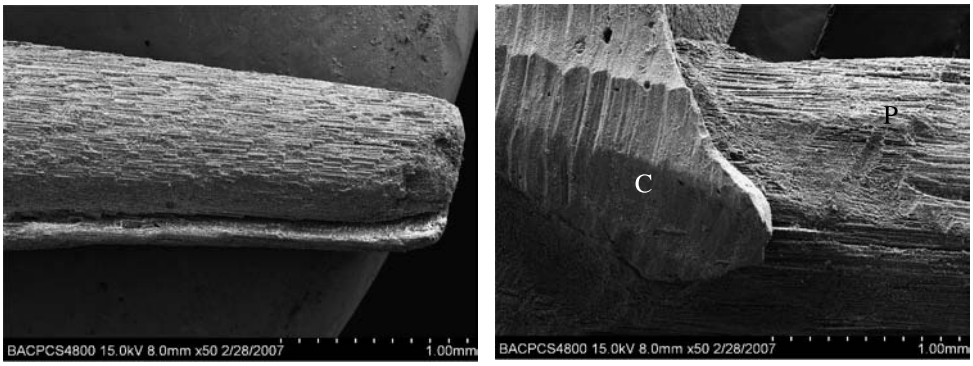
3.3. SEM Observation at Bonded Interfaces

Two specimens from each group were observed with SEM. The specimens' images of Group 1 were different from those of Group 2 and 'debonding' of posts mainly



(a) (b)

Figure 2. SEM images of individually formed semi-IPN FRC post of Group 1 failure specimen. Resin cement covered partially apical third and middle third of the post (a). Some air bubbles can be observed in the post and a thin cement layer around the post (b). C: cement; P: post; D: dentine.



(a) (b)

Figure 3. SEM images of prefabricated FRC post of Group 2 failure specimen. The apical third of post splits and is not covered by cement (a), and in coronal third of the post, a thick cement resin layer can be observed around the post (b). C: cement; P: post.

occurred at the dentine–cement interface. The middle and cervical portions of individually formed GFRC posts were covered with a thin resin cement layer, except the part of apical portion without cement layer where debonding occurred at the cement–post interface (Fig. 2). Several small bubbles were observed in individually formed GFRC post.

In Group 2 the debonding mostly occurred at the cement–post interface. There was no cement layer around the apical and middle portions of debonded prefabricated FRC post, but a thick layer of resin cement was observed around cervical portion of the post (Figs 3 and 4). Voids were observed in the prefabricated fiber post.

In the failed specimens of Group 3, fracture occurred at the cement–post interface and within resin cement (Fig. 5). Fragments of resin cement were left in the notches

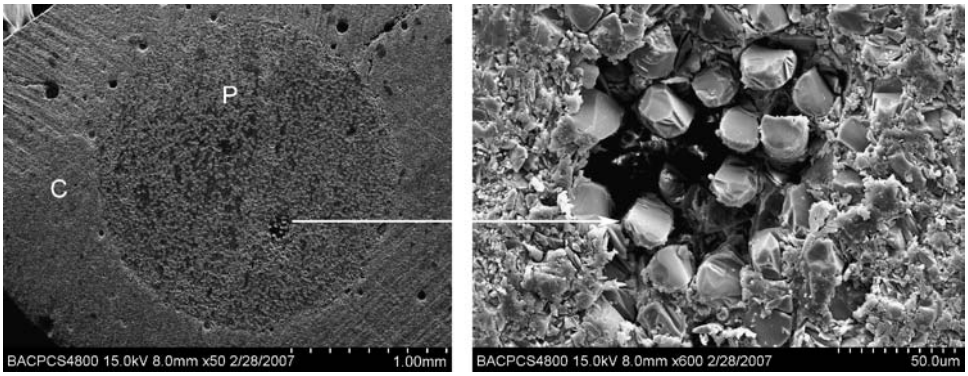


Figure 4. SEM images of the cross section of the prefabricated FRC post of Group 2 failure specimen, showing unimpregnated fibers. A thick cement resin layer can be observed around the post with some bubbles. C: cement; P: post.



Figure 5. SEM image of prefabricated stainless-steel post of Group 3 failure specimen. Fragments of resin cement can be observed in notches and certain surface of the post.

of serrated stainless-steel post. The mode of bond failure was a combination of interfacial and cohesive bond failures.

4. Discussion

The extracted central incisors were employed to simulate endodontically treated teeth in previous studies [15–17] and they were also used to make flared canal teeth for this study. Even though the anatomic size of the central incisors is not exactly same, the incisors were selected for similar size and assigned to three groups. No statistical difference was found in dimensions. Moreover, the specimens were prepared by measuring with a digital caliper to reduce the variation in specimen dimension. The necessity to simulate the periodontal ligament for examining mechanical properties of the restorations was explained by Sirimai *et al.* [17]. It is complicated to coat root surface with a constant thin layer of poly(vinyl siloxane),

so a Teflon tape was therefore used in this study. This resilient tape was 0.08 mm thick and easy to wrap the root for simulating periodontal ligament.

The uncured flexible, surface-sticky, and light polymerizable characteristics of the FRC post material (everStick) allowed to construct an individual FRC post conforming to the shape of the flared root canal. This kind of individually formed FRC posts can be first light cured in the root canal and further polymerized by the chair side with a curing unit. This method ensures proper polymerization of the resin matrix of the FRC post and diminishes polymerization shrinkage of the resin in the root canal. Thus, the chair-side polymerization of the FRC post can be considered a better approach than *in situ* polymerization of the FRC post directly in contact with root canal dentine [6]. The individually cast metal posts and cores have the ability to carry a higher load and might perform better than those used in this study. However, the cast metal posts and cores were not included, because they were reported to pose a risk and cause unfavorable root fracture [1, 2].

The surface configurations of these three kinds of posts were not consistent, which might affect debonding force values at the post–cement interface. In Group 3, the prefabricated stainless-steel posts had mechanically interlocked serrated surface, which provided high pull-out force [11]. Regarding the FRC posts, it is known that smooth-surface semi-IPN posts adhere better to the resin composite luting cement than a serrated prefabricated FRC post [11]. In that study, conventional dimethacrylate monomer based dual-curing luting cement (Variolink II, Ivoclar Vivadent AG, Schann, Liechtenstein) was used. In the present study, the Rely X Unicem cement is a novel acidic monomer composite cement that has not previously been tested in terms of adhesion to the semi-IPN FRC post. The SEM examination in the present study revealed that the adhesion of Rely X Unicem cement to any of the studied posts, including semi-IPN post, was not optimal. Despite this, the fatigue test on restored teeth with the individually formed semi-IPN posts in the present study showed good performance.

Brandall *et al.* [18] indicated that when a post-restored tooth undergoes stress, the most rigid element of the tooth shifts the mechanical stress to the most flexible one. Based on this finding, restorative materials for teeth should have the elastic modulus same as or close to that of dentine for even distribution of force. The fiber posts having the elastic modulus closer to that of dentine are often used in a clinic for restoration of endodontically treated teeth. The presence of coronal dentine can not only increase the retention of the crown but also improve resistance to dynamic occlusal load with ferrule effect [15, 16, 19]. In the case of teeth with flared root canals, occlusal force must be resisted by posts due to absence of the ferrule. In Group 2, the prefabricated FRC posts with low volume of load-bearing FRC material and thus low design-based stiffness might have deformed the restored teeth under cyclically mechanical load, finally breaking the bond between the post and resin cement. The SEM showed that the most portions of the dislocated prefabricated fiber posts in the specimens of Group 2 were exposed without residual resin cement, indicating debonding at the interface between post and dentine.

Based on the results of this study, the specimens of Group 1, the individually formed semi-IPN FRC posts, provided good fatigue resistance since all of them sustained 5-year simulated service and none failed. The Group 3, prefabricated stainless-steel posts, sustained 5-year simulated service as well, but one specimen failed due to the post broken in the simulated service, which might be just a coincidence due to an inherent flaw. The values of residual load-bearing capacity of both Groups 1 and 3 were higher than the maximum bite force of the central incisor [20, 21] which is not encountered in daily mastication, except for men with severe dental attrition [22] and accident. The results of this study might indicate that a more rigid post sustains more force without deforming and decreases the flexibility of the root dentine by stiffening it. By doing so, less shear stress is introduced at the dentine–adhesive–post interface, decreasing risks for bond failure and post dislodging. When a rigid post becomes debonded, it acts as a lever arm, and it may cause root fracture. However, when a fiber post with low elastic modulus is dislodged it may not be as effective a lever arm as a more rigid post. Thus, it could decrease the risk for root fractures after post dislodgement. Further study is needed to test the microleakage at the crown margin after thermocycling and dynamic mechanical loading.

5. Conclusions

In this study, the anterior teeth with flared root canals restored using three kinds of root canal posts and PFM crowns were examined for fatigue resistance and residual load-bearing capacity. Within the limitation of this *in vitro* study, the teeth restored with individually formed semi-IPN FRC posts and serrated stainless-steel posts provided good resistance against cyclic loading. The specimens of these two groups show high residual load-bearing capacity. The teeth restored with conventional prefabricated FRC posts may not be strong enough to resist masticatory forces during long-term use without existence of ferrule.

References

1. A. Torbjömer, S. Karlsson, M. Syverud and A. Hensten-Pettersen, *Eur. J. Oral Sci.* **104**, 605–611 (1996).
2. E. Asmussen, A. Peutzfeldt and T. Heitmann, *J. Dentistry* **27**, 275–278 (1999).
3. F. Isidor, P. Odman and K. Brondum, *Int. J. Prosthet.* **9**, 131–136 (1996).
4. P. A. King, D. J. Setchell and J. S. Rees, *J. Oral Rehabil.* **30**, 785–789 (2003).
5. M. Ferrari, A. Vichi and F. García-Godoy, *Am. J. Dentistry* **13**, 15B–18B (2000).
6. M. P. Newman, P. Yaman, J. Dennison, M. Rafter and E. Billy, *J. Prosthet. Dentistry* **89**, 360–367 (2003).
7. D. S. Hornbrook and J. H. Hastings, *Proc. Periodontics Aesthet. Dentistry* **7**, 33–42 (1995).
8. S. S. Kimmel, *Gen. Dentistry* **48**, 7000–7006 (2000).
9. K. Takagi, H. Fujimatsu, H. Usami and S. Ogasawara, *J. Adhesion Sci. Technol.* **9**, 869–882 (1996).
10. W. A. Fokkinga, A. M. LeBell, C. M. Kreulen, L. V. J. Lassila, P. K. Vallittu and N. H. J. Creugers, *Int. Endodont. J.* **38**, 230–237 (2005).

11. A. M. LeBell, J. Tanner, L. V. J. Lassila, I. Kangasniemi and P. K. Vallittu, *J. Adhesive Dentistry* **6**, 319–325 (2004).
12. F. Mannocci, M. Sheriff, T. F. Watson and P. K. Vallittu, *Int. Endodont. J.* **38**, 46–51 (2005).
13. S. Hu, T. Osada, T. Shimizu, K. Warita and T. Kawawa, *Dental Mater. J.* **24**, 225–231 (2005).
14. M. Kern, W. H. Douglas, T. Fechtig, J. R. Strub and R. DeLong, *J. Dentistry* **21**, 117–121 (1993).
15. A. Martinez-Insua, L. da Silva, B. Rilo and U. Santana, *J. Prosthet. Dentistry* **80**, 527–532 (1998).
16. P. A. King and D. J. Setchell, *J. Oral Rehabil.* **17**, 599–609 (1990).
17. S. Sirimai, D. N. Riis and S. M. Morgano, *J. Prosthet. Dentistry* **81**, 262–269 (1999).
18. J. I. Brandall, J. I. Nicholls and G. W. Harrington, *J. Prothet. Dentistry* **58**, 161–165 (1987).
19. J. A. Sorensen and J. T. Martinoff, *J. Prosthet. Dentistry* **51**, 780–784 (1984).
20. E. Helkimo, G. E. Carlsson and M. Helkimo, *Acta Odontol. Scand.* **35**, 287–303 (1977).
21. S. Kiliaridis, H. Kjellberg, B. Wenneberg and C. Engström, *Acta Odontol. Scand.* **51**, 323–331 (1993).
22. A. Waltimo, M. Nyström and M. Könönen, *Scand. J. Dental Res.* **102**, 92–96 (1994).

Thermocycling Effects on Resin Bond to Silicatized and Silanized Zirconia

Timo T. Heikkinen [a,*], **Lippo V. J. Lassila** [a], **Jukka P. Matinlinna** [a,b] **and Pekka K. Vallittu** [a]

[a] Department of Prosthetic Dentistry and Biomaterials Science, Institute of Dentistry, University of Turku, Lemminkäisenkatu 2, FI-20520, Turku, Finland

[b] University of Hong Kong, Faculty of Dentistry, 4/F Dental Materials Science, The Prince Philip Dental Hospital, 34 Hospital Road, Sai Ying Pun, Hong Kong, P.R. China

Abstract

Various techniques have been introduced to create a durable resin composite bond to sintered zirconia (Y-TZP). Shear bond strength values achieved through tribochemical treatment have been investigated in numerous studies, but less is reported about long-term durability.

The objective here was to evaluate the effects of thermocycling and silane on shear bond strength of a composite luting cement to silicatized Y-TZP. Two groups of Y-TZP (Procera Zirconia, Nobel Biocare), both consisting of 40 specimens were prepared. The specimen surfaces were air particle abraded with silica-coated aluminum trioxide particles (particle size 110 μm, duration 15 s, air pressure 300 kPa, nozzle distance 10 mm). The silica-coated surfaces in group ZA were silanized with an acrylate-functional silane (Experimental laboratory-made acrylate silane, Toray Dow Corning Silicone) and in the other group ZM with a pre-activated methacrylate silane (ESPE Sil, 3M ESPE). The surfaces were coated with adhesive system (Scotchbond 1, 3M ESPE) and photo-polymerized for 10 s. Resin composite luting cement (RelyX ARC, 3M ESPE) stubs were bonded to substrates and photo-polymerized for 40 s. The test specimens were thermocycled for 0, 1000, 3000, 8000 or 15 000 times (temperature 5–55°C, exposure time 20 s). The shear bond strengths of luting cement to ceramics were measured with a crosshead speed of 1.0 mm/min. ANOVA was used for statistical analysis. ANOVA revealed that both silane and thermocycling affected significantly ($p < 0.001$) the shear bond strength. Short term hydrolytic stability of acrylate silane was superior. It was concluded that evaluation of bonding requires extended thermocycling.

Keywords

Zirconia, Y-TZP, silicatization, silane, resin composite, luting cement, shear bond strength

1. Introduction

Oxide ceramics, e.g. yttria stabilized zirconium dioxide (Y-TZP), have established their position as one possible substitute for metal alloys in restorative and prosthetic

* To whom correspondence should be addressed. Tel.: +358 17 2827050; e-mail: timppa.heikkinen@dnainternet.net

Adhesion Aspects in Dentistry

© Koninklijke Brill NV, Leiden, 2009

dentistry. Their usability is mainly based on their superior aesthetic properties and a wide variety of clinical applications, such as root canal posts, crowns, veneers, fixed partial dentures, implants, and implant abutments [1], are possible. Their excellent strength and lack of potentially allergenic and toxic metallic compounds [2] have been other arguments for their increasing use in prosthodontics as well. Resin composite luting cements are commonly used to attach these structures to enamel and dentin.

In order to create a clinically stable resin composite bond to sintered, non-etchable ceramics, many bonding techniques have been studied, tested and introduced [3]. The shear bond strengths achieved by one of these, namely tribochemical treatment, have been investigated in numerous studies. The procedure requires initial conditioning by silicatization [4–6] followed by silanization with a silane coupling agent [7] in order to form a reactive surface for consequent bonding with adhesive resins. Tribochemistry in essence involves creating chemical bonds by applying kinetic energy [8], e.g. in the form of airborne particle abrasion, without any application of additional heat or light.

Tribochemical silica coating using CoJet™ system (3M ESPE, Seefeld, Germany) at the dentist's office is a widely used method for the initial preparation of ceramic or metal alloy structure prior to reparation or cementing [9, 10]. The system is a so-called tribochemical silicatization method because the energy needed for silicatization is transferred to the substrate material in the form of kinetic energy, which generates frictional heat. However, silicatization takes place macroscopically without any change in temperature [4]. The CoJet™ system is based on airborne micro-blasting with silica-modified aluminum trioxide. The outcome is that the system provides the ceramics with a fresh reactive silica-rich outer surface prone to the silanization reactions. Silane monomers react spontaneously with silica and glass [11]. The system also provides the following resin composite adhesion for suitable luting cements. However, less attention has been paid to long term durability of tribochemically achieved shear bond strength values.

There are also available several luting cements based on, e.g. modern organophosphate resin composites, that, unlike the products and methods dealt with in the present study, do not necessarily require silicatization nor silanization in order to be reactive and effective. Moreover, alternative conditioning methods for silicatization, such as selective infiltration of zirconia, have recently been introduced [12]. Still, the present study focuses on the tribochemical bonding because of the bright future of this method and its variants.

In numerous studies thermocycling and varying times of water storage have been used as an artificial ageing method [5, 12–16]. It is a well known fact that thermocycling is a controversial method and other methods have been suggested [17]. However, thermocycling is in accordance with the ISO 10477 standard concerning the ageing of a bond [18]. It is to be noted that there is no concrete evidence that failures in practice occur because of thermal stresses, notwithstanding the theoretical expectation. However, the distinction must be made between the equivalent

static stress test and fatigue failure, where repeated loading to a stress below the static strength occurs. Also, it has never been determined whether it is the time at temperature, i.e. cumulative duration under stress, as opposed to true fatigue, that is relevant factor. In other words, whether failure occurs due to flow, i.e. deformation, in one or other of the layers in the bonded structure, is unknown. This must be dependent on the glass transition temperatures (T_g) of these bonded components, which apparently have not been determined. Such flow would lead to collapse in a truly static test at a stress below the ordinary static strength. Cycling testing as such cannot discriminate these issues, and ignoring this might account, in part, for the inconsistency in test results so far reported. The test outcome depends on the stress generated and the failure mechanism [19].

The aim of the present study was to evaluate the effect of thermocycling on the shear bond strength and to compare the effect of using two chemically different types of silanes on the shear bond strength of resin composite luting cement to tribochemically conditioned and silanized Y-TZP.

2. Materials and Methods

All the materials used in the present study are presented in Table 1. Two groups of Y-TZP (Procera Zirconia, Nobel Biocare, Göteborg, Sweden), consisting of 40 specimens each were prepared. Square shaped pieces (2 mm × 10 mm × 10 mm) of ceramic material were embedded into plastic cylinders (diameter 20 mm, height 10 mm) and filled with acrylic resin to form the specimen and bonding substrate for the resin composite stubs. The surfaces of the specimens were air particle abraded for 15 s with silica-coated aluminium trioxide particles (Rocatec™ Plus, 3M ESPE, Seefeld, Germany) 110 μm in diameter. Air pressure of 300 kPa was used to condition the surfaces. A distance of 10 mm between the tip of the blasting device and the substrate surface was maintained by securing the blasting device in a mounting jig above the substrate.

A 95.0 vol.-% ethanol and 5.0 vol.-% de-ionized water (milli-Q water) mixture was prepared. Its pH was adjusted with 1 M acetic acid to 4.5 and then this solvent system was allowed to stabilize for 24 h at room temperature. 1.0 vol.-% solution of 3-acryloxypropyltrimethoxysilane monomer was prepared in the acidified ethanol–water solution, in 50 ml polyethylene bottles. The silane was allowed to hydrolyze for 1 h at room temperature as described in literature [13, 14]. A fresh ESPE Sil which contains pre-activated 3-methacryloxypropyltrimethoxysilane was used as a control. Next, the silica-coated surfaces of zirconia group ZA were silanized with the acrylate silane. The other group ZM was silanized with a methacrylate silane (ESPE Sil, 3M ESPE, Seefeld, Germany). One coat of silane was applied with a fine brush and a new brush tip was used each time.

Next all surfaces were coated with an adhesive resin (Scotchbond 1, 3M ESPE, Seefeld, Germany) and photo-polymerized for 10 s (Optilux 501, Kerr, Orange, CA, USA). Resin composite luting cement (RelyX ARC, 3M ESPE, Seefeld, Ger-

Table 1.
Materials used in this study

Material	Manufacturer	Chemical composition	Batch number
Procera Zirconia	Nobel Biocare, Göteborg, Sweden	Yttria stabilized zirconium dioxide (Y-TZP)	N/A
Rocatec™ Plus	3M ESPE, Seefeld, Germany	Silica-coated aluminium trioxide, particle Ø 110 micrometer (µm)	305
Experimental laboratory-made acrylate silane	Toray Dow Corning Silicone, Tokyo, Japan	3-Acryloxypropyltri-methoxysilane, 1.0 vol.-%	THJM010206
ESPE Sil	3M ESPE, Seefeld, Germany	3-Methacryloxypropyl-trimethoxysilane, ca. 1.0-2.0 vol.-%	142104
Scotchbond 1	3M ESPE, Seefeld, Germany	Water, ethanol, 2-HEMA, *bis*-GMA, dimethacrylates, methacrylate functional copolymer of polyacrylic and polyitaconic acids, photoinitiator	3JK
RelyX ARC	3M ESPE, Seefeld, Germany	Water, ethanol 2-HEMA, *bis*-GMA, TEGDMA, 2-HEMA, TMDI, copolymer of acrylic & itaconic acids, DDMA, photoinitiator, amine, peroxide, silica, zirconia	20040130

many) stubs (diameter 3.5 mm, height 5.0 mm) were formed by means of a plastic mold and a plunger inside the mold onto substrates and photo-polymerized for 40 s (Optilux 501, Kerr, Orange, CA, USA). The distance between the tip of the photo-polymerizer and the stub was controlled by pressing the tip on the plastic mold (height 10 mm).

The specimens of both groups ZA and ZM were randomly divided into five subgroups. The test specimens ($n = 8$/group) were thermocycled 0, 1000, 3000, 8000 or 15 000 times between $55 \pm 1°C$ and $5 \pm 1°C$ (Thermocycling unit 81, custom-made, Biomechanical Testing Laboratory, University of Turku, Finland). Duration of exposure to both temperatures was 20 s at a time.

The shear bond strengths of the luting cement to the ceramics were measured with a crosshead speed of 1.0 mm/min using a universal materials testing device (Model LRX, Lloyd Instruments Ltd, Fareham, England) as shown in Fig. 1 and the data were recorded using a PC software (Nexygen 4.0, Lloyd Instruments Ltd, Fareham, England). The specimens were secured in a mounting jig (Bencor Multi-T



Figure 1. The shear bond strength test jig in the universal testing machine.

shear assembly, Danville Engineering Inc., San Ramon, CA, USA) and the stress was applied to the stubs with a half circle shearing rod against and parallel to the resin composite and ceramic interface. The shear bond strength data were analysed with analysis of variance (two-way ANOVA) using silane and thermocycling as independent factors. Tukey's *post hoc* test was carried out at a significance level ($p < 0.05$) with SPSS 10.0 (Statistical Package for Social Science, SPSS Inc., Chicago, IL, USA).

3. Results

Mean values of shear bond strengths are presented in Table 2. Additionally, the shear bond strength values have been presented as a function of thermocycling in Fig. 2. ANOVA revealed that both factors, silane and thermocycling, affected significantly the shear bond strength.

Table 2.
Mean values of shear bond strengths with standard deviations as a function of thermal cycles

Group	Thermal cycles (+5 ± 1°C and +55 ± 1°C)				
	0	1000	3000	8000	15 000
ZA	23.0 ± 6.7^{a}	20.8 ± 5.5^{ab}	13.5 ± 7.0^{b}	4.7 ± 1.4^{c}	4.7 ± 2.7^{c}
ZM	16.8 ± 4.2^{a}	10.2 ± 5.1^{bc}	6.9 ± 4.0^{bc}	4.4 ± 1.8^{c}	2.7 ± 1.2^{c}
p (within cycles)	0.058	0.002	0.056	0.723	0.105

Same superscript letter within row indicates homogeneous subset (Tukey [$p < 0.05$]).

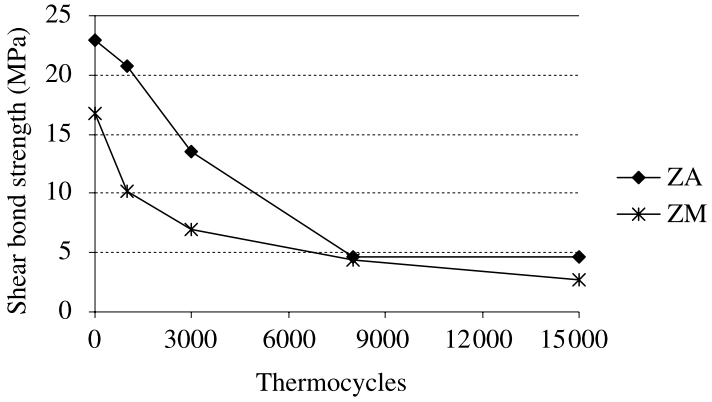


Figure 2. Mean values of shear bond strength as a function of thermocycling.

There were considerable differences between bond strengths after extended thermal cycles between the two groups. The shear bond strength values in dry condition were considerably higher for both materials than after aging at 1000, 3000, 8000 or 15 000 times between 55 ± 1°C and 5 ± 1°C in the thermocycler. Group ZA (acrylate silane) revealed superior results compared to group ZM (methacrylate silane) prior to 8000 cycles. However, after that the bond values for group ZA rapidly decreased towards values for group ZM showing similar values after 8000 and 15 000 cycles. Group ZM revealed statistically ($p < 0.05$) lower shear bond strength values prior to 8000 cycles compared to group ZA ($p < 0.05$) (Table 2).

4. Discussion

This study suggested that thermocycling considerably diminished the shear bond strength values measured between resin composite luting cement and tribochemically conditioned Y-TZP. Post-curing due to increased temperature during thermocycling has been reported to have an influence on bond strength values, but this study did not demonstrate any enhanced bonding. Higher degree of conversion of resin composite also increases the glass transition of the polymer by restricting

molecular motions of the chains [16]. Thus, the thermoset-based composites used as luting cements are well cross-linked after light-curing and hence in practice are more insensitive to post-curing by heat.

Furthermore, acrylate silane monomer (ZA) is more reactive, since it does not have the protecting methyl group, as methacrylate silane monomer (ZM) does. Acrylate silane was selected for this study, since it has been reported to produce higher shear bond strength values than methacrylate silane [13] and it was of great interest to evaluate long term stability of ZA in this test set-up. As silanes react, they form a branched, 3D polysiloxane film between ceramic surface and resin composite. The film consists of siloxane, Si–O–Si–, bonds and acrylate/methacrylate groups [11].

The experimental laboratory-made acrylate silane group ZA showed superior shear bond strength values in the initial condition compared with the methacrylate silane group ZM. After 1000 and 3000 rounds in thermocycler the same behaviour was observed. However, after 8000 rounds both groups showed considerable decline in shear bond strength values, indicating that thermocycling strongly affects the bond between ceramic material and luting cement. Hence, the long-term durability of bond achieved by tribochemical treatment is arguable and needs further investigation.

Conventional shear bond test is a typical test for evaluation of adhesion, but it produces a non-uniform interfacial stress at cement–ceramic interface. The specific fracture pattern may cause cohesive failure within the cement or the ceramic, which may lead to erroneous conclusions [3]. The difference in linear coefficient of thermal expansion (LCTE) of resin composite and ceramic may have an effect on the mechanism of failure at the ceramic–resin composite interface. LCTEs of resin composite luting cements are approximately 40–60 microstrain/°C (μ-strain/°C), whereas LCTEs of ceramic materials are typically less than 10 microstrain/°C (μ-strain/°C). This difference causes thermal stresses at the cement–ceramic interface, probably leading to unequal changes in dimensions, and eventually to failure of the bond. The difference between LCTEs is particularly high between ceramics and initially flowable luting cements, which have lower filler content than conventional restorative filling resin composites in order to improve the flow of the cement and to facilitate the fit of the prosthetic structure [20, 21]. Moreover, hygroscopic expansion of luting cements presumably causes extra stresses at the interface of zirconia and cement as the water sorption of the resin composite increases [22].

According to the present study the effect of different silanes should also be taken into consideration when studying variables of tribochemical treatment. It may be possible to find new chemical combinations more favourable for use as a durable substitute for methacrylate-functional silane as some recent reports suggest [14, 15]. It might also be useful to continue testing using longer water-storage periods to evaluate the stability of the bonding silane layer to hydrolytic effects. Silane bonds are known to rearrange and re-form. Water is always present at a molecular level in the siloxane film and there is not much published information on

the hydrolytic stability of the siloxane bonding between the materials used in the study [7, 11].

Kern and Wegner [23] used short term water storage and compared it to long time water storage combined with 37 500 thermocycles, which in case of certain materials led to spontaneous dissolution of the bond even without shear bond strength testing. On the basis of their results the number of thermocycles seems to play an important role when considering the durability of the bond. Different materials seem to behave differently during cycling as well. Thus, within the limitations of this study, it seems important to emphasize that extended cycles, along with long-term water storage at 37°C, should be used when evaluating long term stability of the bond.

As previously mentioned, thermocycling has been criticized as to what extent it mimics the clinical situation. ISO 10477 prescribes 6000 cycles, which may be insufficient for evaluating the long term stability. The temperatures and dwelling times used in the several studies have been questioned as well as the meaning of rest time and the frequency of cycling. While there is no concrete evidence that failures occur because of thermal stresses, every thermocycling test remains arbitrary. Cycling tests cannot by themselves discriminate the type of the failure that causes the collapse of bond to ceramic. One possibility might be a less severe test which would improve discrimination of the failure point as long as the stresses remain below those causing immediate collapse. However, the mechanism of the failure caused by cycling testing needs further investigation [19].

5. Conclusions

Within the limitations of this *in vitro* study, the following conclusions can be drawn:

1. Short term hydrolytic stability of acrylate silane is superior to methacrylate silane.
2. Extended aging by thermocycling and water storage is needed in order to evaluate the true benefit of different silanes for enhancement of bonding capacity of resin composite luting cement.

Acknowledgements

The authors wish to thank Nobel Biocare and 3M ESPE for their generous supply of test materials. This investigation was financially supported by grants from The Finnish Dental Society Apollonia and Turku University Foundation. The research was also a part of the NIOM Biomaterials Network Cooperation in the Nordic countries.

References

1. B. Ardlin, *Dental Mater.* **18**, 590–595 (2002).
2. J. C. Wataha, *J. Prosthet. Dentistry* **83**, 223–234 (2000).

3. M. B. Blatz, A. Sadan and M. Kern, *J. Prosthet. Dentistry* **89**, 268–274 (2003).
4. R. Guggenberger, *Dtsch. Zahnarztl. Z.* **44**, 874–876 (1989).
5. M. Özcan and P. K. Vallittu, *Dental Mater.* **19**, 725–731 (2003).
6. M. Kern and V. P. Thompson*, J. Dentistry* **22**, 300–306 (1994).
7. J. P. Matinlinna, L. V. Lassila, M. Özcan, A. Yli-Urpo and P. K. Vallittu, *Int. J. Prosthodont.* **17**, 155–164 (2004).
8. C. K. Kajdas, *Tribology Int.* **38**, 337–353 (2005).
9. T. T. Heikkinen, L. V. J. Lassila, J. P. Matinlinna and P. K. Vallittu, *Acta Odontol. Scand.* **65**, 241–248 (2007).
10. R. Amaral, M. Özcan, L. F. Valandro, I. Balducci and M. A. Bottino, *J. Biomed. Mater. Res.* **85B**, 1–9 (2007).
11. E. P. Plueddemann, *Mod. Plast.* **3**, 92–98 (1970).
12. M. N. Aboushelib, C. J. Kleverlaan and A. J. Feilzer, *J. Prosthet. Dentistry* **98**, 379–388 (2007).
13. J. P. Matinlinna, L. V. J. Lassila and P. K. Vallittu, *J. Dentistry* **34**, 740–746 (2006).
14. J. P. Matinlinna, L. V. J. Lassila and P. K. Vallittu, *Dental Mater.* **23**, 1173–1180 (2007).
15. J. P. Matinlinna, L. V. J. Lassila and P. K. Vallittu, *Acta Odontol. Scand.* **65**, 44–51 (2007).
16. G. Meric and I. E. Ruyter, *Dental Mater.* **23**, 1157–1163 (2007).
17. R. van Noort, S. Noroozi, I. C. Howard and G. Cardew, *J. Dentistry* **17**, 61–67 (1989).
18. ISO 10477 Dentistry — Polymer-Based Crown and Bridge Materials, Amendment (1996).
19. M. S. Gale and B. W. Darvell, *J. Dentistry* **27**, 89–99 (1999).
20. A. Tezvergil, L. V. J. Lassila and P. K. Vallittu, *Dental Mater.* **19**, 471–477 (2003).
21. G. Meric and I. E. Ruyter, *Dental Mater.* **24**, 1050–1057 (2008).
22. I. D. Sideridou, M. M. Karabela and E. C. Vouvoudi, *Dental Mater.* **24**, 1131–1136 (2008).
23. M. Kern and S. M. Wegner, *Dental Mater.* **14**, 64–71 (1998).

Part 3
Adhesion Testing

Adhesion Strength Testing — Time to Fail or a Waste of Time?

Brian W. Darvell *

Dental Materials Science, Faculty of Dentistry, The University of Hong Kong, Prince Philip Dental Hospital, 34 Hospital Rd, Hong Kong

Abstract

The simplistic approach to mechanical testing routinely employed in dental research does not recognize the many factors that influence the outcome, not least the non-existence of strength as a true material property. The roles of test time-scale, environmental interaction, and internal changes need evaluation. However, service conditions also involve multiple loading cycles which interact with other processes, while 'episodic' challenges are altogether outside the normal frame of testing. The case is made for testing that allows for dynamic damage-accumulation through a survival-curve approach.

Keywords

Strength, toughness, test design, shear, bond strength, environmental variables, time-scale

1. Introduction

The strength of a material and the strength of the union of dissimilar materials are central to a great deal of work reported for dentistry. It seems to be self-evident what is meant, and likewise without doubt important, but equally it is not welcomed when that meaning is questioned and the importance challenged. However, many things need to be considered before embarking on a strength test of any kind, for any purpose. I should like here to discuss some of the issues.

2. Broken Concepts

First of all, there are only two real 'strengths': tensile and shear. These arise from pure loading modes, although shear can be in-plane (Mode II) or out-of-plane (Mode III) (Fig. 1), referring to the distortion with respect to the plane of the specimen. Tension is Mode I. All other test systems are combinations, as it were, in more or less complicated ways, of such stresses such that the mode of failure (as opposed to the mode of loading) needs careful consideration. For example,

* Tel.: +852 2859 0303; Fax: +852 2548 9464; e-mail: b.w.darvell@hku.hk

Adhesion Aspects in Dentistry
© Koninklijke Brill NV, Leiden, 2009

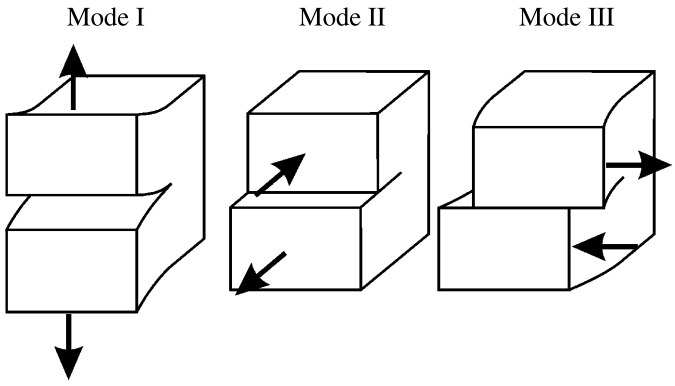


Figure 1. The modes of failure. I — tensile (opening), II — in-plane shear (sliding) and III — out-of-plane shear (tearing).

there is no such thing as 'compressive strength' [1], since failure in compression is physically not meaningful; whatever happens is 'sideways', not in the loading direction.

The concept of strength is that a fundamental material property is to be determined. The definition is easy enough: stress at failure. This implies that strength is scale-free, that correcting for the cross-sectional area is enough. This, in turn, is predicated on the proportionality of the failure stress to the number of molecular, intermolecular or interatomic bonds that need to be broken. However, the inability to approach theoretical strengths for materials, based on otherwise known bond strengths at the atomic and molecular level, led to the development of the understanding of the role of flaws and the Griffith criterion [2]. Effectively, flaws alter the local stress, and no material can be flaw-free. We must draw a very clear distinction, therefore, between the material and the substance(s) from which it is built. A material has structure, and this includes the defects, of whatever kind. It then follows that strength cannot be scale-free, an invariant material property, because the size of flaws that can exist in a specimen depends on the size of the specimen — a contradiction of the concept of a fundamental property.

There is a further violation of this concept. Part of the Griffith formulation is the strain-energy density, the amount of energy stored elastically at a given stress. If this stored energy is equal to or greater than that required to create a fracture surface then that failure must occur. The system is unstable with respect to the overall lower energy state of the broken piece. But so far this failure has, implicitly, been in tension, and it has been assumed that there is no other energy-dissipation mechanism. However, shear must still be considered. Shear is the essence of flow, or plastic deformation. If the shear strength is exceeded, then this mode of deformation must follow. Thus it is a matter of considering which comes first: the critical stress for failure in tension or shear? Now, stored energy increases as the volume of the piece, stress as the cross-section. A small enough body simply cannot store enough energy elastically to pay the energy cost of the creation of the surface of a tensile

crack. Put simply, all materials are plastic on a small enough scale, and all materials are brittle on a large enough scale [3].

This second breaking of scale invariance means, for example, that alumina — classically brittle — is plastic on a micrometre scale. The problem is our perception and operational scale for the execution of a mechanical test. Generally, we can only work over a scale range of a tenth of millimeter or so up to some tens of centimetres. It follows that we normally fail to see these effects, yet both Griffith flaws and the plastic-brittle scale transition are defining aspects of what we test.

We must never forget, therefore, that what we are testing are objects, not abstracted, idealized, disembodied materials. We are thus obliged to take a more pragmatic, operational definition of strength — in the context of the scale of actual usage, and in the context of all of the conditions that pertain to it. There is then a further scale issue: time.

3. Testing Time

What is unstated when we discuss strength is that it is understood to be the stress that will just cause failure, collapse in some sense, when it is applied instantaneously. That is to say, it is the 'static' strength which is of concern. Yet it is obvious that there is no such test. All testing, whether under displacement- or load-control, involves a steady increase in stress and thus a particular time to failure for each test. Remembering that if a pathway exists, it will be taken: any stress-relaxation process that is available will contribute to the outcome (the principle of least work). Again, this has to be viewed in the context of our usual operating range — a few tenths of a second to a few minutes — out of the possible range of (say) nanoseconds to megayears, which gives us a fairly narrow view without making a special effort.

In the case of organic chain polymeric systems, strain-rate sensitivity is part and parcel of our understanding of properties through such behaviour as chain segment diffusion. But it must not be forgotten that active chemistry may be involved as well. Bond-exchange mechanisms provide a significant means of stress-relaxation in many systems, and these must also be subject to kinetic considerations and so be under diffusion control, as well as be dependent on the concentration of active and reactable species. All such diffusion-limited processes have an activation energy and so are temperature-dependent, which is primarily manifest in this kind of material as the glass-transition temperature. Still, we must bear in mind that this arises from a second-order behaviour and thus has a spread, not a precise value. In consequence, it is hard to be categorical about test temperature in relation to it, and especially so when the system has more than one such temperature. Should phase-separation occur, or domains of differing composition be present (silane layer against the rest of the matrix?), each region will have its own characteristics. The strain-rate — temperature (near!) equivalence adds a further layer of complication for the design of a test and the interpretation of results.

Metals, too, are temperature and strain-rate dependent in their mechanical behaviour, although this is not commonly seen because of our narrow operational perception window. Creep is at root a diffusion-based phenomenon, albeit stress-directed, and so has a temperature dependence. Failure through creep at loads appreciably below 'static' (sc. 'short term') test values is well known. Strength, however, is fundamentally a function of temperature because it is ultimately a matter of (chemical) bond strength, and it falls to zero at the melting point and some other transitions. This is clearly seen in dental silver amalgam, where a peritectic melting occurs close enough to 'normal' temperatures that its influence is marked. The homologous temperature of a test is therefore important. Creep that occurs during the course of a test influences the outcome and cannot be separated from it. Consider this: strong specimens have been under load for longer than the weaker members of its group — is like being compared with like, geometrically, structurally?

It is easy to draw idealized test designs, with force vectors and stress fields doing exactly what one would like. The physical realization is another matter. A simple case: in an axial compressive test, the parallelism of the platens — and of the specimen ends — is critical for the uniformity of the cross-sectional stress. The stiffer the test material, the worse this sensitivity gets, and obviously (!) premature failures predominate. The misguided ruse often employed is to insert padding, a thin layer of compliant material to accommodate the faults, ignoring the fact that the mechanical behaviour of this extra material now controls the failure. Parasitic stresses, arising from the interplay of friction and the deformation of the padding, can change the pattern of fracture substantially. This abuse has been taken to extremes in the 'diametral compression' or so-called indirect tensile test, in which effectively any strength value one wishes can be obtained by suitable modification of the test arrangements [1]. Parasitic stresses from the non-alignment of grips for tensile tests, irregularities in the specimen, or the design tolerances in the geometry of the test machine itself can all influence the outcome. Indeed, deformation of platens and grips is normally ignored (and perhaps can be for low modulus of elasticity test materials), but it is there nonetheless.

Whilst flaws in the Griffith sense are strength-limiting for brittle failures, it must be recognized that these include surface defects. A grain boundary or exposed pore may provide a sufficient crack-nucleation site, but more often than not it is the extrinsic topography that is crucial, but underappreciated. In other words, the texture from the mould wall or separating agent, or the machining marks (remembering that these can be below the limit for our best visual acuity of $\sim$70 μm) may be the limiting factor. In this sense, 'polishing' with 600-grit abrasive paper ($\sim$15 μm particles), as is commonly reported as a final step in specimen preparation, is seen to be an overstatement: invisibility is not the same as non-existence. Since hydrolytic corrosion of the surface of glass fibres dramatically reduces their strength, it is difficult to see how deliberate damage on a larger scale can be accepted unblushingly.

The more brittle the behaviour, the less forgiving a system will be because flaw blunting through plastic deformation will not occur.

4. Reaction Time

In polymer systems, plastic deformation is markedly affected by plasticizers, substances that facilitate chain segment diffusion. These are typically rather small molecules, the most common — indeed, unavoidable in the dental context — being water. Thus, any polymer that goes into the mouth for any length of time is going to be exposed to a high water activity, and water must therefore dissolve in the polymer, changing its properties, most obviously the glass-transition temperature, but also stiffness, strength, work to failure and so on. Obviously, the time required for equilibration (diffusion is time- and temperature-, as well as non-Fickian concentration-dependent), in relation to the time of test, matters. However, it is little appreciated that, for example, filled restorative resin materials contain some water as supplied, because the factory preparation conditions were not anhydrous, that they quickly absorb water from the air during handling and specimen preparation (especially if the user is breathing over them), and will equilibrate with whatever laboratory air they are left to stand in, even in an incubator at 37°C. Desiccation is not relevant (the material is not then as-supplied), but temperature changes the equilibrium uptake as this affects polymer free volume, as does the water itself — swelling.

Equilibration means identical water activity everywhere, but activity is dependent on solutes. Air saturated with water (100% RH) has the same activity as water at the same temperature — it does not require liquid to be present, but any solute decreases the activity. Thus, 100% RH has a greater water activity, and would lead to greater water uptake, than saliva.

The water is important in many systems for another reason: hydrolysis. If a reaction is possible, it will occur, at a rate dependent on the availability of reactants and temperature (there is an inevitability to this because it is all thermodynamically-driven). Breakdowns occur at the filler–matrix interface, at hydrolysable bonds anywhere, in fact. Polymers and ceramics are vulnerable. Such chemistry is also pH-dependent, primarily in rate but sometimes in the nature of the bonds that can be attacked. But even in the absence of hydrolysis flaws can develop. The stress-relaxation that occurs in polymers on absorbing water may lead to a phase-separation such that distinct water-rich domains may form, if not actual ‘pools’. Such zero-strength structures are flaws in the Griffith sense. They may be deduced as occurring when the uptake curve does not flatten off, and commonly occur at weak, hydrolysable interfaces. Clearly, the time at which a test is conducted in the face of all of these changes is of some concern [4].

Water has yet a further role to play. In the Griffith expression for critical failure stress is a term for the surface energy of the material. This arises because it is the energy cost of the crack which forms that provides the criterion, i.e., the total surface

energy of the newly-formed interface between fractured material and environment. This surface energy is not a material property, but the result of the interaction of material and the substances in that environment. These interactions may be of various kinds, but all must be accounted for. The complete composition of, say, saliva matters, including its pH and CO_2-content: all ions, all proteins, all polar species, all polarizable species. Whilst it is undoubtedly true that some may have negligible effect (which remains a relative matter and subjective), whether through chemistry or concentration, in the absence of data it is very difficult to argue for neglect.

Since a crack must grow through an object in the course of failure, all aspects of the structure and constitution of the object are relevant as the path that the crack takes is the one of least work at each successive step. Weak interfaces, flaw populations, weak phases and so on are all relevant, as are all crack-blunting mechanisms such as flow and stress-induced phase changes. Because all of this depends on preparation details — such as mixing ratio, time of mixing, extent of reaction at the point of moulding, thermal history — as well as the development of stresses within the material due to polymerization shrinkage, molar volume changes, and temperature changes during setting or machining, the upshot is that everything must be finely controlled for a consistent outcome. In a nutshell, a change in any condition almost inevitably results in a change in the material.

A common mistake is to think that a 'set' material is now chemically inert. Unfortunately, there is hardly a material that is formed by reaction (as opposed to casting from the melt) that can be considered to have stopped changing in a time one might consider reasonable. Glass ionomer cement, filled resins, silver amalgam, for just three examples, all have continuing reactions that change properties measurably over long periods of time. On top of this, stress-related processes also proceed. Cast materials of whatever kind have residual stresses, and these may relax with time at sufficiently high temperature (as well as modifying the stress at failure anyway as a pre-stress). Test results are time-dependent in many ways.

5. The Road to Tolerance

One curious aspect of the entire field, despite the well-promoted improvements that have occurred in nearly all materials used in dentistry, at least from the point of view of static strength, is that failure rates in practice have not changed very much, if at all. The clearest example of this is in the ceramics: a 200-fold improvement in strength has not led to an equivalent improvement in longevity, even allowing for a proportion of preparation faults. This has been attributed to what is called 'episodic' loading. In effect, most materials are perfectly adequate for function under 'normal' conditions — normal presumably in the sense of typical or averaged peak loads — and may well be good to the 99th percentile. But, we all may experience the one-in-a-thousand event of a piece of grit in our bread, a misjudged bite, or a jaw-numbing collision with some object that results in a rapidly-applied load several hundred times 'normal'. In the face of this, nothing can survive if it is in the right place to

suffer the impact. One might ask whether designing for strength is relevant. After all, if all of the improvement is as demonstrated by laboratory tests, and this is not matched by service observations, it is a rather self-serving occupation. The circular argument does not touch the real world.

The problem in testing may, however, be more subtle still. Loading in practice is always intermittent, typically of very short duration, but with very high numbers of events: this is fatigue. Although a static test result is supposed to indicate a survivable load, even with the added sophistication of allowing a tolerance on an acceptable upper bound by reference to some arbitrary (and unjustifiable — there is no universal law) static failure load distribution, this is not to say that damage has not occurred during that event. Perhaps damage is too strong a term? Let us say 'change' instead. We need only cite dislocation creep in metals, or chain segment stress relaxation in polymers, to realize that these changes are cumulative. Generally, there is no microscopic reversibility, and the path is one-way: downhill. At some point we are obliged to recognize that the changes have in fact been detrimental: cracks nucleate, and we have fatigue failure. Each chewing cycle offers such a loading; no matter that the loading mode, the direction, and the magnitude vary, each cycle is a step towards failure. How many steps are required can only be determined by a long, expensive trial that has to be accelerated artificially to obtain any results in a time shorter than normal service, which acceleration often has to be assumed to have no deleterious overtones of its own. Needless to say, there are few such dynamic fatigue tests in the relevant literature. But, given such cumulative damage, and the role of flaws in determining failure in static testing anyway, episodic failures do not seem so outlandish a proposition. All materials in service have been compromised by that service. Survival curves may be more relevant than we have hitherto been prepared to accept.

This brings us to damage tolerance. Essentially, this means insensitivity to accumulating defects acquired in service, because mechanisms such as crack tip blunting or path deviation prevent or at least delay catastrophic failure, like Oliver Wendell Holmes' 'One-Hoss Shay'. Here, then, we need to consider the work to failure, or more fundamentally (because it is linked to the structure of the Griffith criterion), fracture toughness. Brittle materials have no capacity for absorbing energy beyond that needed to create the 'least work' crack; tough materials have diversionary mechanisms. Indeed, there is a school of thought that says fracture toughness is the only thing that should be considered, that strength (as perhaps should be clear from the above) is less than fully informative. Even so, fracture toughness testing (which is an order of magnitude more demanding than simple strength testing) remains 'static'. It may involve controlled (stable) crack growth, as opposed to the uncontrolled, unstable cracking of typical strength tests, but it is only a one-shot event. There is no sense of dynamic testing, no sense of ascertaining the consequences of service-acquired damage. Nevertheless, it is much more informative about the process of cracking, and the process should guide materials design.

6. Adhesive Principles

Overall, then, mechanical testing for the strength of a material is a substantially more complicated business than at first appears. However, our focus is adhesion — the strength of the union between two materials, where the differences in properties affect several key issues. But before going on it might be worth emphasizing that the term adhesion is presumptive in that for many it implies a chemical interaction beyond van der Waals forces. Thus, 'bond' means a specific chemistry rather than the more general concept of resistance to separation. This is not to say that covalent bonds may not be formed, but in practice mechanical interference, 'key', plays a larger role than is often recognized. As an extreme example, the solvent-based 'gluing' of polymers involves no chemical bonds except those of the original chains, which are now entangled. This is not adhesion, yet the word is implied by the third body, the adhesive. What then of infiltrated 'hybrid layers'? Broadly, care has to be taken in using the words so as not to be prejudicial, biassing the thinking and interpretation. Thus, a luting agent, with admittedly no specific chemical interaction with tooth or crown, still provides resistance to displacement. Is this or is this not functionally retentive?

A principal difficulty with adhesion testing follows from the general test design problems mentioned above. Purity of stress field is very hard to attain because the geometrical requirements for the specimen and specimen grips or platens are more severe than is generally recognized, and the Saint-Venant principle [5] rarely capable of being relied upon. Ensuring that the applied load remains perfectly aligned with respect to the test interface is hard when the specimen is non-uniform, harder when working on a semi-micro or micro scale because machining tolerances (grips, specimen, mould) become proportionately larger, and even harder when handling forces can approach or exceed those involved in the test itself. The number of specimens that do not make it to test is an important statistic, and very rarely reported.

Adhesion testing is focussed on the interface, and often special tricks have to be employed to ensure that failure starts there. Logically, of course, there is no reason why it necessarily should in the face of Griffith theory: critical flaws can occur in substrate or adhesive as well as at the interface itself. The path the crack takes is then governed by the least-work principle and may wander back and forth across that boundary. There is much agonizing over the interpretation of such behaviour and the inability to assign a value to the interfacial strength when failure does not occur there. The systems approach, allowing for the existence of crack-controlling defects everywhere, seems to be overlooked.

7. Shear Optimism

Much of the above has been implicitly in terms of the tensile failure, for which it is fairly easy to set up tests. However, shear is a different story. The concept may be simple, but the embodiment is not. The literature is full of half-baked ideas for sup-

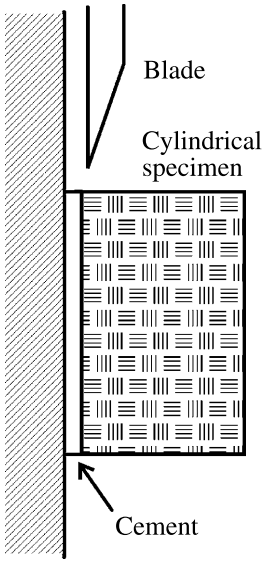


Figure 2. A typical 'shear' test as used in dentistry. Despite many variations and attempts at refinement, Mode II failure cannot be made to occur.

posed shear tests that clearly are no such thing, as has been amply demonstrated (but almost completely ignored). Indeed, it is so obvious where the defects are: 'stress concentration' and 'levering' covers them all (Fig. 2). Inevitably, mismatch of modulus of elasticity across an interface means that a uniform stress cannot be obtained under simplistic designs — gradients nearly always exist. But such is the enthusiasm for shear testing that naïve wishful thinking overrides all other considerations. Many of the same considerations as apply to simpler mechanical tests (mentioned above) apply here, but with much greater import. Exact alignments are harder, and point contacts frequently unavoidable, as are fillets or notches in the adhesive layer. In fact, an 'ideal' right-angle adhesive–substrate (cylinder on plane) arrangement is a Griffith 'flaw' as it is itself a stress-concentrating design. The analysis of such systems is not difficult, but one needs to recognize that it needs to be done for it to be effective.

It should now be clear that one cannot determine the strength of an object as a material property as such, and that of an interface is trickier still. But the question has to be: are we missing the point? After all, in practice, loading systems are never pure and the concept of service-condition mimicry may be more applicable than an idealized abstraction. This means that the test system should be set up to reproduce the actual failure pattern of the material in service. It is only recently that a start has been made on observing and analysing real failures, with fracture mechanics becoming more widely recognized as an essential discipline and foundation for materials design [6], but there are as yet very few useful data on modes and frequencies.

To take the specific example of an adhesive interface: it is extremely unlikely that one could fail in pure shear in a catastrophic 'static' manner, let alone in pure tension. Micro-tensile testing may be popular [7], but this popularity does not of itself validate the results as interpretable, relevant measures of the goodness of a union. Thus, one can envisage fatigue-driven, peeling-mode separation, affected by hydrolysis and stress-relaxing plastic deformation, progressively opening a crack in the fracture-toughness sense, as being a first approximation to an operational definition of the test that is required. Here we have all of the issues of scale, temperature, environment, strain rate and intrinsic flaws playing their part in a dynamic context. In this approach we begin to recognize the damage-accumulation of actual service, the gradual rather than catastrophic failure of most such systems, and the inevitability of the survival-curve, probabilistic domain in which materials function.

8. Coda

This has been a personal overview of the context, one which has attempted to draw attention to many factors that are often unrecognized as being essential as controlling test outcomes. It is not meant to be like a textbook on testing; much is simply nodded at in passing, much is omitted. However, I hope that it provides a (possibly provocative) stimulus for further study, some careful thinking, painstaking experimental design, and critical interpretation. One good experiment is worth a thousand potboilers.

References

1. B. W. Darvell, *J. Mater. Sci.* **25**, 757 (1990).
2. A. A. Griffith, *Phil. Trans. Roy. Soc. Lond. Series A* **221**, 163 (1921).
3. J. Glucklich, Strain-energy size effect, Technical Report 32-1438, Jet Propulsion Laboratory (1970).
4. L. Musanje, M. Shu and B. W. Darvell, *Dental Mater.* **17**, 394 (2001).
5. S. P. Timoshenko and J. N. Goodier, *Theory of Elasticity*, 3rd ed. McGraw-Hill, New York, NY (1934).
6. I. Ichim, Q. Li, W. Li, M. V. Swain and J. Keiser, *Biomaterials* **28**, 1317 (2007).
7. D. H. Pashley, R. M. Carvalho, H. Sano, M. Nakajima, M. Yoshiyamae, Y. Shono, C. A. Fernandes and F. Tay, *J. Adhesive Dentistry* **1**, 299 (1999).

Navigating the Dentin Bond Strength Testing Highway: Lessons and Recommendations

Jack L. Ferracane *, **Jon M. Dossett**, **Fernanda Pelogia**, **Manoel R. P. Macedo and Thomas J. Hilton**

Division of Biomaterials and Biomechanics, Department of Restorative Dentistry, Oregon Health & Science University, School of Dentistry, 611 S.W. Campus Drive, Portland, Oregon 97239, USA

Abstract

Dentin bond strength testing remains a subject of high interest based on the prevalence of studies reported in the dental literature. But making general conclusions about materials or methods by comparing results from different studies can be a dubious proposition due to the many variables involved in testing. Though guidelines exist for bond testing, they unfortunately are not always followed by all researchers. This three-part manuscript was written to help navigate the prolific literature in this field of study. In the first part, the most popular testing modes are described by providing an analysis of their loading mechanics and stress distributions. In the second part, a review of the test variables that may influence outcomes of bond strength testing are presented for the different test methods, and the extent to which each affects the results is discussed. Data collected from thirty studies published within the past five years for one specific adhesive are used to emphasize the nature and extent of these effects. In the third part, studies that included specific brands of resin dentin bonding agents that represent the current most popular types are reviewed in an attempt to make general statements about how the brands compare to one another within the different test methods. While it is difficult at this time to provide a simple consensus opinion about how bond strength testing should be conducted, this paper attempts to clarify some of the important issues in this popular, but complex, field.

Keywords

Dentin, adhesion, bonding, test methods, mechanics, bond strength, adhesive

1. Introduction

How popular is dentin bond strength testing? A quick search of the PubMed database using the following search string, 'dentin adhesive bond strength' returned nearly 1300 entries for the past 20 years. This represents a phenomenal effort by a truly staggering number of investigators. These articles represent studies of a multitude of variables associated with a clinically very important topic. However, the

* To whom correspondence should be addressed. Tel.: 1-503-494-4327; Fax: 1-503-494-8260; e-mail: ferracan@ohsu.edu

Adhesion Aspects in Dentistry
© Koninklijke Brill NV, Leiden, 2009

frustrating aspect of reviewing this literature, aside from its sheer magnitude, is the variability in the results presented for the same materials from study to study. This variability often makes it impossible to draw useful conclusions, because results must always be qualified by a presentation of the many important factors that could affect them. Perhaps the variable with the most influence is the test method itself. Although there are many other variables associated with each test, the literature suggests that certain ones may affect outcomes significantly while the others may have minimal overall influence. In any case, it is still very important to be very clear in presenting the specifics of the testing situation in any article. However, as one examines the literature, it is somewhat surprising how often critical information is not specified.

This paper will not attempt a critical assessment of the vast body of literature in the area of bonding to dentin with resin-based adhesives. There are several articles that have presented reviews or summaries of much of this literature [1–4]. Rather, the goal is to present an overview of the field in three parts. The first part will include a review of the common bond strength test methods in terms of their mechanics and stress analysis. The second part will involve a review of the test variables that may affect outcomes of bond strength testing, highlighting specific issues pertaining to the different test methods when applicable, and identifying those variables that have been determined to have the most significant effect on bond strength results. Throughout this second part, data collected from 30 studies published within the past five years on one specific adhesive, Clearfil SE Bond (SEB) from Kuraray (see detailed explanation in Part 3) will be used to validate the conclusions. In the third part, studies that included several specific brands of resin dentin bonding agents are reviewed to make general statements about how the brands compare to one another and across the different test methods.

2. Part 1: Review of Test Methods

Numerous test methods exist for the determination of bond strength values in an attempt to characterize and quantify the potential for successful clinical performance of dentin bonding adhesives. To date no single *in vitro* test method has been validated as the gold standard for clinical adhesive performance and clinical trials are still the only valid method for evaluating the performance and efficacy of dental adhesives. It is recommended that clinicians should critically assess the literature for specific trends that may indicate a durable adhesive [5]. This is difficult, however, when laboratory results are so varied; sometimes even showing ranking inversions when comparing the same combinations of materials [6]. Most important, though, is communication of the specific test design parameters and material microstructure that are critical to the interpretation of strength data [7]. There are, however, certain test procedures (tensile, shear, microtensile and microshear) based on common mechanical principles that are frequently employed to measure bond strengths. This analysis will review the mechanics of these test methods, discuss the common

parameters and significant differences in these methods, and compare the stress distributions generated across the bonded adhesive interface.

2.1. Shear and Tensile Test Methods

Static dental adhesive bond strength tests typically involve the application of a load causing a distributed stress to develop at the bonded interface or within the substrate or tooth sections leading ultimately to fracture of the specimen. One of the simplest ways to accomplish this is through the use of the traditional planar shear bond strength test. Although multiple test designs are used to apply a shear load to the adhesive interface, the traditional method applies the load to a cylindrical resin composite material bonded to a tooth substrate. Load application is either concentrated at or some distance from the interface (through a blade contacting the bonded specimen and running in parallel with the bonded interface), distributed axially along the composite cylinder (sliding cylinder model), or cosine distributed along the interface (simulating a wire loop) (Fig. 1). The wire loop method is thought to reduce the stress concentration along the load application area, but underestimation of the shear bond strengths due to high local stress concentrations near the interface still

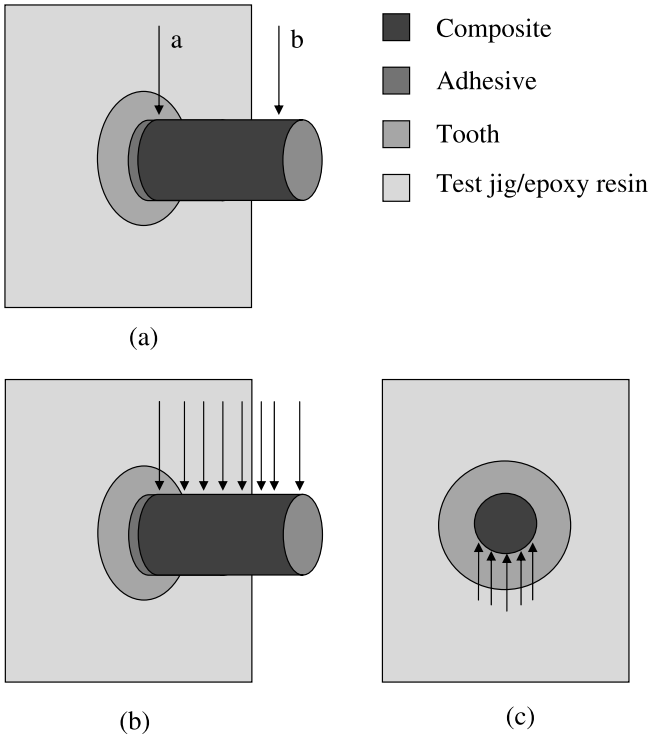


Figure 1. Schematic diagrams of different shear bond strength test designs. (a) Point load application a near and b far from the adhesive interface. (b) Loading along the entire length of the composite. (c) End-on view showing uniformly distributed stress when a wire loop is in contact with the composite cylinder.

result [8]. Another significant concern related to the shear test is the development of a bending moment causing concentrated areas of tension and compression to occur along the interface. Failure at the interface occurs as a consequence of the tensile stresses induced by this bending moment [9]. The stress distribution along the interface is influenced by the geometric configuration of the test arrangement (load and specimen design) and the stiffness of the materials used [10]. As the loading point increases in distance from the bonded interface, bending moments are set up which create high tensile stresses at the interface on the side where the load is applied, and compressive stresses on the underside of the loading cylinder. The higher the elastic modulus of the composite cylinder, the higher the interfacial stresses. Also, FEA analysis demonstrates a non-uniform stress distribution along the interface bringing into question the validity of nominal bond strength accuracy relative to the measurement of true maximum shear forces [8, 10, 11].

Tensile bond strength test applies a tensile load uniaxially along the specimen and, ideally, perpendicular to the adhesive interface. Alignment of specimens is difficult to control and, due to combination of elastic and plastic deformations, asymmetric load application and stress concentration lead to variations in results [12–14]. Non-uniform stress distributions are also noted across the adhesive interface when assessed using FEA modeling and are influenced by the height of the composite cylinder and stiffness of the materials used [10]. Again, composites with higher elastic modulus lead to higher stresses at the bonded interface, predisposing failure to initiate here. Stresses also are concentrated at the interface when the composite cylinder is 3 mm or taller, but move away from the interface and at unpredictable locations when the cylinder height is less than 3 mm. Thus, loading should be accomplished through composite cylinders at least 3 mm tall for tensile tests.

2.2. Microshear and Microtensile Test Methods

The microshear (microbond) bond strength test uses cylindrical composite specimens with a cross-sectional area of approximately 1 mm^2. This design allows multiple specimens to be bonded to the same substrate, requires no trimming of specimens, and provides the potential for regional mapping of bond strength across the substrate. Optimized load configurations make it possible to control the mode of failure by maximizing the shear stress at the interface relative to the tensile stresses and reducing the potential for cohesive failure noted frequently with shear testing [15–17]. However, because the relative adhesive layer thickness remains constant in both shear and microshear tests, the potential for this lower modulus material to affect the overall stress distribution is thought to be greater in microshear due to locally induced stress concentration gradients at the interface. As the specimen size decreases and when the load application is directed very close to the interface in combination with low modulus resin composites, an area of relative stress intensification is created rendering true stress measurements difficult and less accurate [18].

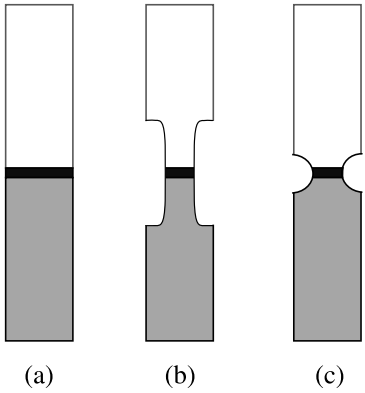


Figure 2. Shapes used in microtensile bond strength testing: (a) stick, (b) dumbbell and (c) hourglass.

The microtensile bond strength test seems to be the most popular bond testing method currently employed [19]. Tensile loads are applied to specimens with adhesive cross-sectional areas of approximately 1 mm^2. Typically three specimen designs (stick, dumbbell and hourglass) fixed with a testing jig allow measurement of ultimate fracture strengths (Fig. 2). Stress distributions for the dumbbell and stick shapes are similar; however, the hourglass shape, due to increased bulk of material and the process of grinding or cutting to produce the narrow dimension of the dumbbell at the interface with a high speed rotary instrument, exhibits increased risk of failure. Factors affecting overall bond strength results include [20] adhesive thickness, evenness of the adhesive interface, misalignment of loading axis, presence of flaws, selection of test fixture, and others discussed later in this paper. Of particular importance is the increased risk of flaw induction due to the mechanical shaping of the specimens. While the use of smaller adhesive surface areas should reduce the potential for critical size defects at and near the interface, this benefit may be negated by the creation of defects during cutting with the high speed bur. In any case, bond strength values from microtensile and microshear tests are typically higher than from their respective macro-scale counterparts [13, 21].

Differences in variability among test methods continue to be a significant issue. Knowledge of stress distributions based on test design and specimen geometry, supported by experimental and FEA results, are key in critically interpreting bond strength values. It is recommended that researchers understand the limitations of the test methods employed, carefully and cautiously assess results within studies, and strive for standardization of test methodologies.

3. Part 2: Review of Important Variables in Bond Strength Testing

There are numerous factors that can affect the results obtained from bond strength testing to dentin. Among others, these include the species of the bonding substrate, the roughness of the prepared substrate, the moisture content of the substrate, the

storage conditions for the prepared specimen, the use of any preloading treatments (e.g., thermal cycling), the mode of load application, the area of the bonded surface, the geometry of the specimen, the method for fixing the specimen for testing, and the rate of load application. The importance of each of these factors, or lack thereof, will be briefly reviewed.

3.1. Bonding Substrate

Due to the large number of studies and the limited availability and access to human teeth, alternative substrates, such as bovine teeth, often have been used in bond strength tests [3]. It has been suggested that bovine teeth may provide an adequate substitute for human teeth in studies of caries lesions due to sufficient similarities in structure and composition [5]. More recent studies with current restorative systems have demonstrated no differences in shear bond strengths between human permanent dentin and bovine coronal dentin [22]. Others have suggested that bovine dentin can be considered as a suitable alternative to human teeth in bond strength tests involving primary dentition [23]. The results from the nine shear bond strength studies involving SEB from Part 3 were equivalent for bovine (22.7 MPa; $n = 2$ studies) and human dentin (24.0 MPa; $n = 7$ studies). However, previous reviews of the literature demonstrated that while typically there was no significant difference between the bond strengths obtained with bovine dentin compared to human dentin, there were enough differences in the results between the two substrates that one might come to different conclusions concerning relative outcomes for different adhesives based on the choice of substrate [24, 25]. Therefore, because it is not clear that data from studies employing human and bovine dentin may be directly comparable, it is still important to state the nature of the substrate used in the test.

3.2. Surface Roughness of Substrate

As adhesion is a surface phenomenon, it seems intuitive that bonding to dentin would be affected by substrate surface properties, such as surface roughness. Preparing dentin with different procedures (SiC, diamond or carbide bur, air abrasion, ultrasonically driven burs and lasers) creates quantitatively and qualitatively different smear layers, surface roughness, and surface topography, all of which have been shown to affect resin–dentin bond strength [26, 27]. This is likely to be due to differences in the density of the smear layer more than its thickness, as very dense smear layers have been shown to compromise bonding efficacy, especially for the self-etch systems, which typically contain mild acids [28, 29]. In one study, a coarse diamond bur operated at high speeds lowered the bond strength of two-step self-etching bonding systems due to inadequate infiltration of the acidic self-etching primers into dentin surfaces covered with a thick smear layer [30]. Therefore, selection of the type of bur used to prepare the substrate has the potential to enhance or reduce the bond strength, at least for certain self-etching adhesive systems [31].

The recent literature suggests that the most common surface preparation method for shear bond strength tests is treatment with 600-grit abrasive paper followed by

1000-grit paper. A 600-grit paper would be the equivalent of an abrasive with a particle size of approximately 15 μm, or an extra-fine grit diamond. A 1000-grit paper would have approximately 4–5 μm abrasive particles. For microtensile testing, 600-grit paper is most often used, but rougher papers, such as 180-grit (approximately 75 μm particles) and medium burs (up to 100 μm particles) are also popular. Results for SEB show no substantial difference in shear bond strengths when using dentin surfaces prepared with 600-grit (23.1 MPa; $n = 5$ studies) *vs*. 1000-grit (27.0 MPa; $n = 3$ studies) abrasive papers, and slightly higher values in microtensile tests when using 600-grit paper (53.9 MPa; $n = 7$ studies) *vs*. medium diamond burs (48.0 MPa; $n = 4$ studies) or 180-grit paper (42.8 MPa; $n = 5$ studies). Based on the potential to have a subtle influence on bond strength, the surface finishing method should always be specified in order to make meaningful comparisons among studies.

3.3. Dentin Moisture Conditions

Dentin bonding agents are known to be technique-sensitive, in part due to variations in the moisture content on the dentin substrate. In recent years, self-etching adhesives have been promoted as a better alternative to etch-and-rinse systems in terms of reduced post-operative sensitivity. One of the reasons proposed for improvement in this area was a better control of the dentin moisture. Eliminating the requirement for a rinsing step to be followed by some degree of drying minimizes the potential variability in the final moisture content on the surface prior to bonding. Studies to evaluate the bond strength of moist, dehydrated, and rehydrated dentin have shown that bond strength to dried dentin surfaces was reduced when using etch-and-rinse adhesives, but that the application of a re-wetting solution significantly increased mean shear bond strengths to pre-dried dentin [32, 33]. Thus, it is important to maintain the specimen in a hydrated state, and to explain how this was accomplished during the test. This may be especially important for etch-and-rinse adhesives, but due to the potential for dentin cracking and other drying effects, it is likely to be important for self-etch adhesives as well.

3.4. Specimen Storage Conditions

Adhesive systems are generally hydrophilic in nature, because water miscibility is desirable for bonding to moist substrates, such as dentin. However, subsequent water sorption within the bonded interface may contribute to degradation of the bond during storage [19]. The sorption and solubility behavior of the bonding materials is related to their hydrophilicity and have been suggested to influence the long-term performance of resin-based composite restorations [34]. Water is typically the medium of choice for storing specimens prior to debonding, but disinfecting agents and artificial salivas also have been used. Several studies have showed that extended water-storage time decreased the bond strength for most dentin bonding agents [35–37]. Microtensile bond strength studies with SEB show similar results when the specimens are aged in water (44.6 MPa; $n = 17$ studies) *vs*. artificial

saliva or chloramine (46.3 MPa; $n = 3$ studies), and the same was true for shear bond tests (water — 20.4 MPa; $n = 3$ studies *vs*. chloramine — 22.1 MPa; $n = 4$ studies). Therefore, there may be only little effect of storage conditions when aqueous media are used, but the time of storage is likely to have an effect and should be reported in order to permit comparison of results between studies.

The storage temperature in most bond strength tests is typically 37°C, though in some studies this is never mentioned. In any case, the effect of storage temperature on bond strength has not been delineated.

3.5. Thermal Cycling

There has been much discussion about the mismatch in thermal expansion coefficient between the tooth structure and restorative materials, and the effect this may have on maintaining the integrity of the interface of the restoration. Similarly, mechanical loading of the interface could also produce interfacial stresses that affect bond strength. Some authors have used different methods to apply stress to simulate the aging of a restoration. Frequently, thermal cycling is used in laboratory studies for this purpose. However, thermal cycling has not shown a significant difference in bond strength up to 100 000 cycles compared with non-cycled controls [38–41]. Thus, it appears that thermal cycling does not have a definable effect on dentin bond strength and there seems to be little rationale for including it in dentin bonding studies with resin adhesives.

3.6. Test Method

The numerous test methods used for measuring bond strength to dentin were reviewed in the first part of this paper. There are arguments for each design, and no standardized method exists. What is clear is that data generated from the various test methods cannot be directly compared in absolute value terms, which is likely due to the differences in stress distribution and other experimental conditions [42]. In general, as will be shown in the next part, it is generally true that dentin bond strengths obtained in microtensile mode are greater than those obtained in shear mode. One may conclude that this is simply a function of specimen size, but the results from microshear tests do not seem to differ greatly from those obtained in conventional shear bond tests [43, 44]. Further complicating factors include the type of jig used to support the specimen, the method for applying the load, and other factors reviewed below. For the studies on SEB tested in the microtensile manner, at least six different devices were identified in the literature for supporting the specimen during the test, and there are not enough data available to discriminate between them. For shear tests, many studies did not even describe the method for applying the load. However, the results from studies in which the load application mode was not reported for SEB (22.7 MPa; $n = 5$ studies) did not differ from those of studies that used a knife edge or blade (25.0 MPa; $n = 4$ studies). Thus, the importance of the test fixture method for load application does not seem to be as critical as the test method itself (i.e., shear *vs*. microtensile). Regardless of the test method, the

variation (scatter) in the data obtained from shear and microtensile test methods is typically in the same range, and this is typically between 20 and 25%.

3.7. Area of Bonded Interface

The discussion in Part 1 about the stress distributions in the various bond strength tests suggests that bonding area may significantly influence test results. The microtensile bond strength has been shown to be inversely related to the bonded surface area [13]. Typically, the cross-sectional area adopted is 0.8–1.2 mm^2 at the bonded interface [45, 46]. Trimming is often accomplished to produce the defined bonding area, but this may induce additional stresses at the interface and produce flaws, which may result ultimately in weaker bonds and a higher proportion of pretest failures [47]. Because of this, others recommend specimens with larger bonding areas, such as 1.5 mm^2 with a cylindrical design, which are easier to produce and test [48]. Results from microtensile bond tests on SEB did not show a considerable difference in value for cross-sectional areas of 0.5 mm^2 (45.5 MPa; $n = 2$), 0.7–0.9 mm^2 (50.1 MPa; $n = 6$), or 1.0 mm^2 (47.0 MPa), but did show a reduced bond strength in one study when tested at 1.4 mm^2 (20.4 MPa).

Based on the results from microtensile testing, the bonding area also can be predicted to affect the bond strength in shear bond tests, with greater values being expected with smaller surface areas. However, with limited data for SEB, this difference was not apparent. Bond strengths were actually somewhat lower for bonding diameters of approximately 2 mm (20.9 MPa; $n = 3$ studies) *vs*. 3 mm (27.7 MPa; $n = 2$ studies) or 3.6 mm (26.8 MPa; $n = 2$ studies). In a recent evaluation in our laboratory, the bond strength of SEB in shear mode at 3 mm diameter (33.0 MPa) was larger than at 5 mm diameter (17.0 MPa). Therefore, it may not be possible to directly compare results from studies when there are large differences in bonding areas.

3.8. Specimen Geometry

When conducting shear tests, it is common and desirable to use cylindrically-shaped specimens and the literature does not show alternative geometries. However, several options have been reported for the microtensile test method, including sticks, dumbbells and hourglass shapes. The stick configuration was the first shape designed for the microtensile test described by Sano *et al.* [13]. The bond strengths obtained from sticks have been shown to be higher than those obtained with the hourglass or dumbbell design [20, 47]. However, others have reported that the specimen geometry did not influence the results of the microtensile bond test [48, 49]. In recent microtensile studies involving SEB, no difference has been shown between dumbbell (43.4 MPa; $n = 1$ study), hourglass (45.5 MPa; $n = 6$ studies) and stick designs (47.1 MPa; $n = 13$ studies). In any case, the stick seems to be the preferred design by many researchers because it is easy to prepare and produces values that are at least as high as the dumbbell and hourglass designs.

3.9. Specimen Fixation Method

Finite element studies suggest that the fixation method can significantly influence the microtensile bond strength test results [42]. The specimen can either be glued to the jig, or gripped in some manner. Gripping is most common for dumbbell and hourglass-shaped specimens. Gluing is by far the most common technique reported in the literature. Of the studies on testing SEB, all but one study fixed the specimens without glue, and this was because dumbbell-shaped specimens were being tested and they could be held in place with grips.

The stress distributions in each technique vary and are likely to influence the results obtained. The most common method with stick specimens is gluing to a flat faced jig. An alternative approach is to use a flat jig with a narrow channel within which the specimen can be positioned. The narrow channel enables the specimen to be more easily and accurately aligned perpendicular to the interface, thereby better concentrating the tensile stress at the actual interface [42]. Results with this design were favorable, showing failure more often occurring closer to the dentin–composite interface and with a lower coefficient of variation for the strength values [2, 47]. To emphasize the importance of the alignment, Silva *et al.* [50] showed that applying loads to the adhesive junctions oriented at 10, 20 and 30° to the usual perpendicular interface produced reduced bond strengths as the angle increased for at least some of the adhesives tested. Another study showed that the method of applying the cyanoacrylate glue did not significantly affect the results, but suggested that a precise and uniform technique should be followed [47]. Thus, it would seem that the most critical aspect to specimen fixation for microtensile testing is ensuring that the specimen is perpendicular to the test interface for uniaxial loading.

3.10. Loading Rate

The loading rate, or crosshead speed, may also affect the results of the test since the materials being examined are somewhat viscoelastic in nature. This would suggest that faster test rates may produce higher bond strengths. According to Oshida and Miyazaki [51], crosshead speed has varied widely between investigators from 0.1 to 10 mm/min, although 0.5, 1.0, 2.0 and 5.0 mm/min were most commonly employed in dentin bond strength testing for both tensile and shear modes. While many loading rates have been used, it is noteworthy that few, if any, of the reports provide a rationale for selecting these crosshead speeds. In their study, Oshida and Miyazaki reported that speed did not affect outcomes as long as it was below 1.0 mm/min [51]. Above 1.0 mm/min, the bond strengths increased showing strain rate sensitivity of the bonded interface. Their study implied that crosshead speeds of 0.5 to 1.0 mm/min should be preferred for shear bond strength testing. In a more recent study in which a large range of crosshead speeds were tested, Yamaguchi *et al.* [52] showed that the influence of the crosshead speed was essentially negligible when measuring microtensile bond strengths. The microtensile bond strength studies with SEB showed greater bond strength when tested at 1.0 mm/min

(48.8 MPa; $n = 14$) than when tested at 0.5 mm/min (39.5 MPa; $n = 5$). The shear bond strengths were also somewhat higher in one study when tested at 5.0 mm/min (26.4 MPa) as compared with 1.0 mm/min (22.5 MPa; $n = 6$) and 0.5 mm/min (17.7 MPa; $n = 2$). Thus, it appears that loading rate may have an effect on bond strength results and, therefore, it is important to report this test variable.

3.11. Handling of Pre-test Failures

Another consideration when using the microtensile test method is how one handles the specimens that fail before ever being tested. Due to the small size and fragility of the specimens, this may not be an uncommon occurrence when using this method. Some studies do not describe how they treat these pre-test failures. Others include the failures with a value of zero. Others delete the failures and consider them as missing data. The studies examining SEB that included pre-test failures as zeros showed slightly higher bond strength (54.1 MPa; $n = 5$ studies) compared to those that considered the failures as missing data (44.3 MPa; $n = 4$ studies). Perhaps of greater interest is the coefficient of variation for the two conditions. Studies that included the pre-test failures as zeros had an average variation of 29.6%, while the studies that considered these specimens as missing data had a much lower average variation of 10.5%. Thus, while there is no generally accepted approach for treating these pre-test failures in microtensile bond strength tests, one can expect that lower variation in the data set will be obtained if one omits these specimens from the analysis. However, when a significant proportion of the specimens undergo pre-test failure, deleting these data does not seem to be prudent and likely gives one a false sense of security in terms of the adhesion of the particular material, or the quality of the preparation and handling.

3.12. Additional Factors of Interest

An additional variable in bond strength studies is the type of material and the dimensions of the composite 'button' that is bonded to the dentin substrate with the adhesive system. A survey of studies involving SEB show that a variety of dental resin composites are used in shear and microtensile tests, with no particular one seemingly preferred. More than likely the choice is one of convenience. However, it should be noted that in almost all cases, the composite is a hybrid or microhybrid type and not a microfill. This is important since it means that the elastic modulus of the composite 'button' material, which could affect bond strength as discussed in Part 1, is not likely to vary as much from study to study as it would if microfills were used.

Other issues related to the composite are the height of the button, and the total energy used for light-curing. One could imagine that an undercured button could affect the results of the study. In shear bond strength studies on SEB, more often than not the height of the button was not specified. When the height was discussed, it was almost always set at 2 mm tall. For the microtensile test studies, the height is nearly always specified and varies between 4 mm (44.0 MPa; $n = 2$ studies),

5 mm (47.3 MPa; $n = 6$ studies) and 6 mm (48.9 MPa; $n = 9$ studies), with little difference between the results. The total energy used to cure the composite, which is typically performed in increments, varies from 12 to 30 kJ/cm^2. There appears to be no correlation between the amount of energy used to cure each increment made to build up the button and the bond strength, suggesting that in these studies, sufficient curing energy was always used to provide adequate curing of the composite.

4. Part 3: Review of Outcomes of Studies Including Common Materials

It is always tempting to review literature generated with disparate test protocols and arrive at consensus statements regarding comparing materials or other factors. This approach may be ill-advised, as the first two parts of this manuscript point out, unless a detailed examination of the individual reports is undertaken. Based on the vast amount of literature in this field, this is a very daunting task. An attempt is made here to demonstrate the extent to which general statements can be made by focusing only on a portion of the literature. The literature was searched in PubMed for studies published between 2003 and 2008 on evaluating the dentin bond strengths of four specific adhesives. The four adhesives represented a three-part etch and rinse system (Optibond FL [OBFL], Kerr, Orange, CA, USA), a two-part etch and rinse system (Prime and Bond NT [PBNT], Caulk/Dentsply, Milford, DE, USA), a two-part self-etch system (Clearfil SE Bond [SEB], Kuraray, Tokyo, Japan), and a one-part self-etch system (Prompt [PLP], 3M ESPE, Seefeld, Germany). These adhesives were chosen based primarily on their frequency of appearance in the literature. For a study to be included, it had to include Clearfil SE Bond and at least one of the other three adhesives. Studies of shear and microtensile bond strengths were included, as these were by far the most popular test methods. Separate spreadsheets containing study results and entries for the important variables identified in Part 2, as well as others, were assembled for microtensile and shear tests. Twenty-one articles reported using the microtensile test to evaluate the bond to human dentin [27, 28, 37, 62–79], and nine reported the shear test to evaluate the bond to human or bovine dentin [53–61]. Bovine dentin was included based on the expected equivalency of the two substrates and because there were fewer overall reports employing shear tests.

A comparison of the four adhesives based on the results from the multiple studies shows that the mean microtensile bond strengths ranged from 22.5 to 53.75, with the one-component self-etch system (PLP) having the lowest bond strength, followed by a nearly 50% greater bond strength for the two-component etch and rinse system (PBNT), and then the two-component self-etch system (SEB), and finally the three-part etch and rinse system (OPFL) had the highest bond strength (Fig. 3). This result is similar to that reported by DeMunck *et al.* [19] for a variety of adhesives in these categories when tested in their laboratory. The results from the shear bond strength tests on these same four adhesives show the same relative order (Fig. 4), but the calculated average values are typically about twice as high

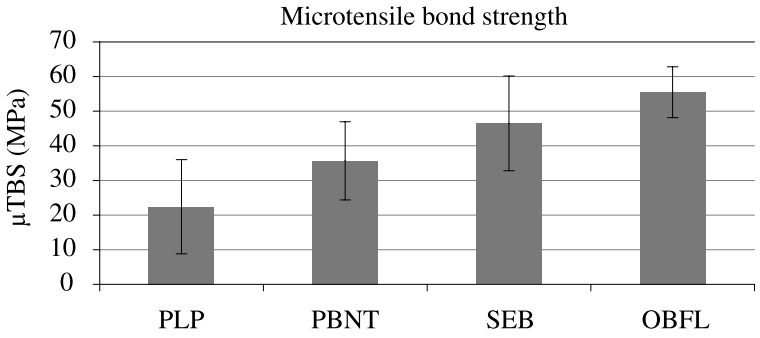


Figure 3. Microtensile bond strength (MPa, ±1 s.d.) of four dental adhesives to human dentin obtained by simply averaging results from multiple studies: SEB (range from 21 studies was 20.4–74.9 MPa), PLP (range from 13 studies was 6.2–51.6 MPa), PBNT (range from 9 studies was 20.5–56.3 MPa), OBFL (range from 7 studies was 43.4–63.0 MPa).

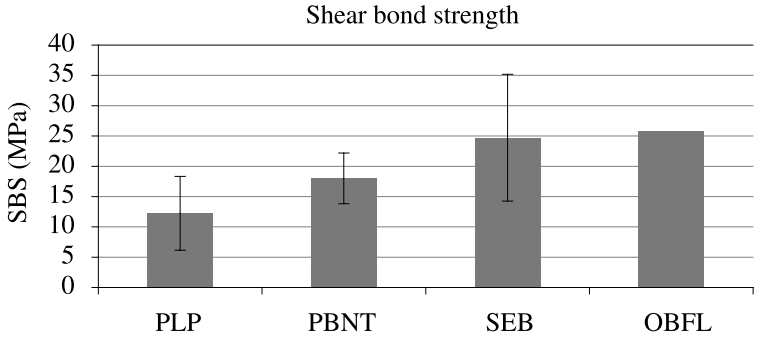


Figure 4. Shear bond strength (MPa, ±1 s.d.) of four dental adhesives to human or bovine dentin obtained by simply averaging results from multiple studies: SEB (range from 9 studies was 15.9–39.0 MPa), PLP (range from 8 studies was 6.2–20.1 MPa), PBNT (range from 3 studies was 15.1–22.8 MPa), OBFL (1 study, thus no s.d.).

when tested in the microtensile mode. This difference was anticipated based on the smaller cross-sectional area typically used in the microtensile test, as well as the more homogeneous stress distribution and lower stress. Both of these factors would contribute to the observed results, because smaller samples imply smaller flaw sizes, and a more homogeneous stress distribution would make it less likely to experience premature failures.

5. Conclusion

Both shear and tensile tests, as well as so-called ‘micro’ versions of these tests using smaller specimen bonding areas, are popular for testing adhesive strengths of materials to tooth surfaces. In general, values obtained from the ‘micro’ tests are typically higher than those from the ‘standard’ shear and tensile tests. It is noted that there is no ideal test method, and it is recognized that researchers will choose

a specific test protocol based on their expertise, available facilities, as well as their specific needs in terms of the type of data required. This paper has identified many of the important issues in bond strength testing to teeth and has emphasized the importance of explaining and describing the test variables that may affect the outcomes, such as the surface preparation and moisture condition of the substrate, the specimen storage conditions, the area of the bonded interface, the specific nature of the test fixtures, the specimen fixation method, the loading rate, and the method for handling pre-test failures. It is important that regardless of the method chosen, the researcher should be familiar with its strengths and limitations.

References

1. K. J. Söderholm, *J. Adhesive Dentistry* **9** (Suppl. 2), 227 (2007).
2. A. Poitevin, J. De Munck, K. Van Landuyt, E. Coutinho, M. Peumans, P. Lambrechts and B. Van Meerbeek, *Dental Mater. J.* **26**, 694 (2007).
3. F. A. Rueggeberg, *Dental Mater.* **7**, 2 (1991).
4. D. H. Pashley, *Dentistry Today* **22**, 112, 116, 118 (2003).
5. International Standardization Organization: guidance on testing of adhesion to tooth structure, ISO/TR 11405 (2003).
6. G. LeLoup, W. D'Hoore, D. Bouter, M. Degrange and J. Vreven, *J. Dental Res.* **80**, 1606 (2001).
7. J. Kelly, *Dental Mater.* **11**, 103 (1995).
8. P. DeHoff, K. Anusavice and Z. Wang, *Dental Mater.* **11**, 126 (1995).
9. S. Rasmussen, *Int. J. Adhesion Adhesives* **16**, 147 (1996).
10. R. Van Noort, S. Noroozi, I. Howard and G. Cardew, *J. Dentistry* **17**, 61 (1989).
11. J. Drummond, R. Sakaguchi, D. Racean, J. Wozny and A. Steinberg, *J. Biomed. Mater. Res.* **32**, 533 (1996).
12. R. Van Noort, G. Cardew, I. Howard and S. Noroozi, *J. Dental Res.* **70**, 889 (1991).
13. H. Sano, T. Shono, H. Sonoda, T. Takatsu, B. Ciucchi, R. M. Carvalho and D. Pashley, *Dental Mater.* **10**, 236 (1994).
14. D. Pashley, H. Sano, B. Ciucchi, M. Yoshiyama and R. M. Carvalho, *Dental Mater.* **11**, 117 (1995).
15. Y. Shimada, S. Yamaguchi and J. Tagami, *Dental Mater.* **18**, 380 (2002).
16. W. McDonough, J. Antonucci, J. He, Y. Shimada, M. Chiang, G. Schumacher and C. Schultheisz, *Biomaterials* **23**, 3603 (2002).
17. D. Banomyong, J. Palamara, M. Burrow and H. Messer, *Eur. J. Oral Sci.* **115**, 502 (2007).
18. E. Placido, J. Meira, R. Lima, A. Muench, R. de Souza and R. Ballester, *Dental Mater.* **23**, 1086 (2007).
19. J. De Munck, K. Van Landuyt, M. Peumans, A. Poitevin, P. Lambrechts, M. Braem and B. Van Meerbeek, *J. Dental Res.* **84**, 118 (2005).
20. E. Ghassemieh, *Dental Mater.* **24**, 536 (2008).
21. P. Cardoso, R. Braga and M. Carriho, *Dental Mater.* **14**, 394 (1998).
22. R. Schilke, O. Bauss, J. A. Lisson, M. Schuckar and W. Geurtsen, *Am. J. Dentistry* **12**, 92 (1999).
23. S. Krifka, A. Börzsönyi, A. Koch, K. A. Hiller, G. Schmalz and K. H. Friedl, *Dental Mater.* **24**, 888 (2008).
24. T. J. Hilton, *Am. J. Dentistry* **15**, 198 (2002).
25. T. J. Hilton, *Am. J. Dentistry* **15**, 279 (2002).
26. W. R. L. Dias, P. N. R. Pereira and E. J. Swift Jr., *J. Adhesive Dentistry* **6**, 195 (2004).

27. V. Sattabanasuk, V. Vachiramon, F. Qian and S. R. Armstrong, *J. Dentistry* **35**, 467 (2007).
28. S. Semeraro, D. Mezzanzanica, D. Spreafico, M. Gagliani, D. Re, T. Tanaka, S. K. Sidhu and H. Sano, *Oper. Dentistry* **31**, 317 (2006).
29. M. Ogata, N. Harada, S. Yamaguchi, M. Nakajima, P. N. Pereira and J. Tagami, *Oper. Dentistry* **26**, 375 (2001).
30. K. Koase, S. Inoue, M. Noda, T. Tanaka, C. Kawamoto, A. Takahashi, Y. Nakaoki and H. Sano, *J. Adhesive Dentistry* **6**, 97 (2004).
31. J. De Munck, B. Van Meerbeek, S. Inoue, M. Vargas, Y. Yoshida, S. Armstrong, P. Lambrechts and G. Vanherle, *Am. J. Dentistry* **16**, 414 (2003).
32. J. Perdigão, E. J. Swift Jr., H. O. Heymann and M. A. Malek, *Am. J. Dentistry* **11**, 207 (1998).
33. A. V. Ritter, H. O. Heymann, E. J. Swift Jr., J. Perdigão and B. T. Rosa, *J. Esthet. Dentistry* **12**, 85 (2000).
34. A. F. Reis, M. Giannini and P. N. Pereira, *Oper. Dentistry* **32**, 53 (2007).
35. A. I. Abdalla, M. El Eraki and A. J. Feilzer, *Am. J. Dentistry* **20**, 370 (2007).
36. R. N. Garcia, M. F. de Goes and M. Giannini, *J. Contemp. Dental Pract.* **8**, 46 (2007).
37. J. De Munck, K. Shirai, Y. Yoshida, S. Inoue, K. Van Landuyt, P. Lambrechts, K. Suzuki, H. Shintani and B. Van Meerbeek, *Oper. Dentistry* **31**, 456 (2006).
38. K. M. Burger, R. L. Cooley and F. Garcia-Godoy, *J. Esthet. Dentistry* **4**, 197 (1992).
39. S. Amano, A. Yamamoto, K. Tsubota, A. Rikuta, M. Miyazaki, J. A. Platt and B. K. Moore, *Oper. Dentistry* **31**, 616 (2006).
40. F. H. Mitsui, A. R. Peris, A. N. Cavalcanti, G. M. Marchi and L. A. Pimenta, *Oper. Dentistry* **31**, 240 (2006).
41. Y. Asaka, S. Amano, A. Rikuta, H. Kurokawa, M. Miyazaki, J. A. Platt and B. K. Moore, *Oper. Dentistry* **32**, 73 (2007).
42. C. J. Soares, P. V. Soares, P. C. Santos-Filho and S. R. Armstrong, *J. Dental Res.* **87**, 89 (2008).
43. W. G. McDonough, J. M. Antonucci, J. He, Y. Shimada, M. Y. M. Chiang, G. E. Schumacher and C. R. Schultheisz, *Biomaterials* **32**, 3603 (2002).
44. J. Foong, K. Lee, C. Nguyen, G. Tang, D. Austin, C. Ch'ng, M. F. Burrow and D. L. Thomas, *Austr. Dental J.* **51**, 252 (2006).
45. H. Omar, W. El-Badrawy, O. El-Mowafy, O. Atta and B. Saleem, *Oper. Dentistry* **32**, 24 (2007).
46. W. W. Brackett, F. R. Tay, S. W. Looney, S. Ito, L. D. Haisch and D. H. Pashley, *Oper. Dentistry* **33**, 89 (2008).
47. A. Poitevin, J. De Munck, K. Van Landuyt, E. Coutinho, M. Peumans, P. Lambrechts and B. Van Meerbeek, *J. Adhesive Dentistry* **10**, 7 (2008).
48. S. Phrukkanon, M. F. Burrow and M. J. Tyas, *Dental Mater.* **14**, 212 (1998).
49. N. Betamar, G. Cardew and R. Van Noort, *J. Adhesive Dentistry* **9**, 159 (2007).
50. N. R. Silva, C. S. Calamia, M. Harsono, R. M. Carvalho, L. F. Pegoraro, C. A. Fernandes, A. C. Vieira and V. P. Thompson, *Dental Mater.* **22**, 314 (2006).
51. Y. Oshida and M. Miyazaki, *Biomed. Mater. Eng.* **6**, 87 (1996).
52. K. Yamaguchi, M. Miyazaki, T. Takamizawa, K. Tsubota and A. Rikuta, *Dental Mater.* **22**, 420 (2006).
53. F. Courson, D. Bouter, N. D. Ruse and M. Degrange, *J. Oral Rehabil.* **32**, 296 (2005).
54. R. Atash and A. Van den Abbeele, *Int. J. Pediatr. Dentistry* **15**, 264 (2005).
55. U. Salz, J. Zimmermann, F. Zeuner and N. Moszner, *J. Adhesive Dentistry* **7**, 107 (2005).
56. W. T. Naughton and M. A. Latta, *Quintessence Int.* **36**, 259 (2005).
57. A. Peutzfeldt and E. Asmussen, *Eur. J. Oral Sci.* **107**, 65 (1999).
58. S. Y. Kim, I. B. Lee, B. H. Cho, H. H. Son and C. M. Um, *J. Biomed. Mater. Res. B* **77**, 164 (2006).

59. B. Bulucu, C. Yesilyurt, S. Cakir and A. D. Meydan, *J. Adhesive Dentistry* **8**, 217 (2006).
60. K. B. Thomsen and A. Peutzfeldt, *Clin. Oral Investig.* **11**, 45 (2007).
61. J. L. Chapman, J. O. Burgess, S. Holst, A. Sadan and M. B. Blatz, *Quintessence Int.* **38**, 637 (2007).
62. R. B. Ermis, J. De Munck, M. V. Cardoso, E. Coutinho, K. L. Van Landuyt, A. Poitevin, P. Lambrechts and B. Van Meerbeek, *Dental Mater.* **23**, 1250 (2007).
63. A. L. de Silva, D. A. Lima, G. M. de Souza, C. T. dos Santos and L. A. Paulillo, *Oper. Dentistry* **31**, 562 (2006).
64. M. V. Cardoso, E. Coutinho, R. B. Ermis, A. Poitevin, K. Van Landuyt, J. De Munck, R. C. R. Carvalho and B. Van Meerbeek, *Dental Mater.* **24**, 492 (2008).
65. F. L. de Castro, M. F. de Andrade, S. L. Duarte Júnior, L. G. Vaz and F. J. Ahid, *J. Adhesive Dentistry* **5**, 129 (2003).
66. L. Ceballos, D. G. Camejo, M. Victoria Fuentes, R. Osorio, M. Toledano, R. M. Carvalho and D. H. Pashley, *J. Dentistry* **31**, 469 (2003).
67. S. R. Armstrong, M. A. Vargas, Q. Fang and J. E. Laffoon, *J. Adhesive Dentistry* **5**, 47 (2003).
68. C. Yesilyurt and B. Bulucu, *J. Contemp. Dental Pract.* **1**, 26 (2006).
69. R. Osorio, J. Pisani-Proenca, M. C. Erhardt, E. Osorio, F. S. Aguilera, F. R. Tay and M. Toledano, *J. Dentistry* **36**, 163 (2008).
70. J. P. Proença, M. Polido, E. Osorio, M. C. Erhardt, F. S. Aguilera, F. García-Godoy, R. Osorio and M. Toledano, *Dental Mater.* **23**, 1542 (2007).
71. J. Perdigão, G. Gomes, R. Gondo and J. W. Fundingsland, *J. Adhesive Dentistry* **8**, 367 (2006).
72. F. T. Sadek, A. H. Cury, F. Monticelli, M. Ferrari and P. E. Cardoso, *Dental Mater.* **21**, 1144 (2005).
73. K. Shirai, J. De Munck, Y. Yoshida, S. Inoue, P. Lambrechts, K. Suzuki, H. Shintani and B. Van Meerbeek, *Dental Mater.* **21**, 110 (2005).
74. D. Spreafico, S. Semeraro, D. Mezzanzanica, D. Re, M. Gagliani, T. Tanaka, H. Sano and S. K. Sidhu, *J. Dentistry* **34**, 237 (2006).
75. A. F. Reis, M. Giannini and P. N. Pereira, *J. Biomed. Mater. Res. B* **85**, 10 (2008).
76. L. A. Knobloch, D. Gailey, S. Azer, W. M. Johnston, N. Clelland and R. E. Kerby, *J. Prosthet. Dentistry* **97**, 216 (2007).
77. P. Magne, W. S. So and D. Cascione, *J. Prosthet. Dentistry* **98**, 166 (2007).
78. M. Toledano, R. Osorio, A. Albaladejo, F. S. Aguilera and E. Osorio, *J. Biomed. Mater. Res. A* **77**, 128 (2006).
79. M. Toledano, R. Osorio, A. Albaladejo, F. S. Aguilera, F. R. Tay and M. Ferrari, *Oper. Dentistry* **31**, 25 (2006).

Critical Evaluation of Adhesive Test Methods Used in Dentistry

Karl-Johan M. Söderholm *

Department of Dental Biomaterials, Box J-0446, College of Dentistry, University of Florida, Gainesville, FL 32610-0446, USA

Abstract

Through the years, numerous articles dealing with dental adhesives have been published in the dental literature. A critical comparison of such articles reveals large differences in measured values, differences that not only seem to be between products, but also between different research groups. Because of these differences, the objective of this paper was to critically review some fundamental aspects of adhesion, and relate those aspects to dental adhesive studies. The outcome of that review was not very encouraging, because research, particularly in fields such as mechanical engineering and physics, does not support the notion of an overall adhesive strength value as we usually define in dentistry. Instead, adhesive studies should approach the problem from a fracture mechanics point of view rather than from an overall strength point of view. This review reveals that it is time to abandon traditional strength testing and move toward an increased use of fracture toughness tests and fatigue tests. Having said that, it is also important to realize and accept that as long as we do not have strong evidences correlating clinical success with any particular adhesive test method, *in vitro* tests should not be used as predictors of clinical performance. Only when we have reliable correlations between *in vitro* test results and clinical performance such methods will have any practical meaning.

Keywords

Fracture mechanics, failure modes, fracture energy, surface energy, work of adhesion

1. Introduction

The need to attach different materials to tooth structures is as old as man's ability to make dental reconstructions. One of the first known dental adhesives was invented by the Maya Indians in pre-Columbian time and used for attaching semi-precious stones to cavities drilled on labial surfaces of anterior teeth [1]. That cement consisted of a mixture of bone powder and acidic fruit juices. Before setting, the acidic cement etched both tooth and stone in contact with the cement, and during setting, cement crystals grew into the etched surface irregularities and provided micromechanical retention for the inlay.

* Tel.: +(352) 392 0575; e-mail: ksoderholm@dental.ufl.edu

Adhesion Aspects in Dentistry
© Koninklijke Brill NV, Leiden, 2009

Zinc phosphate cement, first introduced around 1850 and still commonly used, consists of a mixture of zinc oxide and phosphoric acid. Also this cement, like the one invented by the Maya Indians, etches the surfaces in contact with the acidic cement and forms zinc phosphate crystals, contributing to micromechanical retention. However, whether the retention is purely micromechanical can be questioned. Calcium ions from the tooth are likely to diffuse into the acid and react with phosphate ions and precipitate as calcium phosphate. Some phosphate ions from the acid and zinc ions from the zinc oxide powder should also be able to diffuse into the tooth surface and react with calcium and phosphate ions present on the tooth surface. Consequently, some form of chemical bonding should also be present in addition to the mechanical bond. The assumption that we are dealing with a mechanical bond only is more likely related to the brittle nature of the zinc phosphate cement. If a crack starts growing in a brittle material such as zinc phosphate cement, it easily propagates through the brittle cement and the brittle interface causing debonding of the restoration, and gives the impression that the bond is not of chemical nature.

As time passed, more sophisticated dental cements and dental adhesives evolved. Today, the most popular adhesives consist of different resins capable of bonding to tooth surfaces and restorative materials. Some of these adhesive resins are not acidic and require that the tooth surface is pre-etched, while acidic monomer systems can etch the tooth surface by themselves [2]. Even though major improvements in adhesive resin systems have occurred during the past 10–20 years, these adhesives may still debond when subjected to clinical loads.

Debonding can result in clinical problems such as restoration loss, which results in loss, inhalation or swallowing of the dislodged restoration. To avoid such problems, there is a need to determine the reliability of an adhesive before it is introduced on the market. Such determinations are usually done *in vitro* with different adhesive tests. According to some of these laboratory tests, the adhesive strength can be quite high. In fact, in some cases the test failures occur in the dentin or the composite rather than in the adhesive [3]. Despite these claims, the adhesion *in vivo* between restoration and dentin is generally insufficient when compared to the strength of the dentin and the composite material. If clinical bonding was as good as some *in vitro* results imply, dentin adhering to the restoration after clinical failures would be relatively common. However, such findings are very rare if they exist.

1.1. In Vitro vs *Clinical Performance*

During the past 20 years, questions have been raised whether test methods used have any clinical relevance and if they even measure true adhesive strength [4]. Most adhesive tests used in dentistry determine tensile or shear strength values. During such tests a bonded composite specimen is dislodged at a certain force, and the strength is determined by dividing the dislodging force with the size of the initially bonded area. A shortcoming with such tests is that the failure is initiated locally, and that a localized stress level is introduced in the failing region. The localized stress level is often several times higher than the overall stress level determined

by dividing the force at failure by the surface on which the force has acted. Thus, the failure occurs at a stress level significantly higher than the overall stress levels usually reported in the literature.

Another explanation for poor correlations between test results and clinical performance is that *in vitro* testing usually neglects important clinical realities [5]. For example, the substrate used during *in vitro* testing may not represent the substrate used clinically [6]. Both enamel and dentin are anisotropic biological materials and have different properties at different locations. Differences in orientations of enamel rods and dentinal tubules, including their variation in branching of the tubules at different locations explain some of these variations [7, 8]. The mineralization level among teeth differs too, depending on the age of the tooth and where the tooth was mineralized [9]. Besides, bond tests are usually performed on intact caries-free, young teeth, while clinical bonding is usually performed on teeth that have been exposed to caries or excessive erosion or tooth brushing before the bonding procedure is performed.

Furthermore, dentists performing clinical bonding procedures *in situ* may not do the bonding procedure in the same ways as *in vitro* bonding. For example, in clinical situations, the risk for saliva contamination is a real concern, while in most *in vitro* situations, saliva is not present. Also, the geometry of cavities treated clinically may differ from the geometry used during *in vitro* testing.

In vitro testing procedures can be standardized, at least to some degree, and data generated between different testing sites can be used for comparison. Unfortunately, even though significant attempts have been made to standardize *in vitro* testing, it is well known that large variations still exist among different laboratories [10–12]. These variations can be related to differences in testing protocols, selection of teeth (tooth location, patient age, structure and composition of tested tooth), tooth preparation and in bonding technique. In other words, results presented from bond tests should not be regarded as true, reproducible values. They should only be regarded as a rough estimate of a property we need to understand better.

1.2. The Adhesive Joint

The complex nature of a dentin adhesive joint is shown in Fig. 1. Dentin is a tissue through which dentin tubules extend from the pulp to the dentin. Depending on the direction in which the dentin surface has been cut, the orientation of the tubules in relation to the cut surface may differ from perpendicular to parallel orientation. In clinical situations, these tubules in newly erupted teeth are filled by water and organic components, dentinal fluids and protoplasmic extensions from the odontoblasts. As a consequence, a cut dentin surface will contain a certain amount of moisture and will require that a hydrophilic resin system is used to wet the moist dentin surface. The process is more complex than just wetting the dentin surface *in vitro*. The dentin surface also needs to be cleaned before the adhesive is placed on the dentin surface. During dentin cutting, a so-called ‘smear layer’ is formed and it covers the entire cut surface. The smear layer consists of a mixture of hydrox-

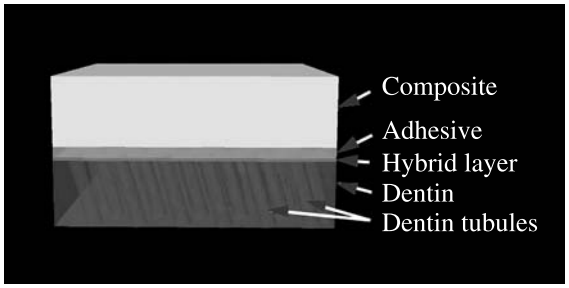


Figure 1. Schematic drawing of a dentin bonded composite. During bonding, hydrophilic monomers can enter the tubules and migrate into side branches of the tubules, and thereby form good mechanical interlocking. The hydrophilic monomer also infiltrates the exposed collagen layer where it forms mechanical retention.

yapatite crystals embedded in a fluid/organic layer consisting of water, saliva and dentin liquor, and collagen. The smear layer may partly seal the dentinal tubules and decrease the moisture flow through the tubules, which could be an advantage. However, because the smear layer is weak and poorly attached to the dentin surface, it is not capable of forming a stable support for the adhesive. Therefore, to avoid the negative effects of the smear layer, it is removed by etching the dentin surface with either an inorganic acid, usually 30–40% phosphoric acid, or an acidic resin primer. During this step, the dentin surface is demineralized, leaving an exposed collagen network attached to the remaining mineralized dentin. The thickness of the collagen layer will vary depending on the degree of demineralization of the dentin. By leaving the exposed collagen film moist after the etching procedure, the collagen fibers can be prevented from collapsing, thereby making it easier for the hydrophilic primer to infiltrate the collagen network and some of the tubules. On the other hand, desiccation may result in a collapse and gelling of the collagen, which, in turn, significantly limits the diffusion of the primer into the collagen web and reaching the mineralized dentin surface.

The infiltrated collagen/tooth surface is referred to as the hybrid layer [13–15]. After the collagen layer has been infiltrated with the primer, solvent and water are removed from the hybrid layer by air drying. The priming and air drying steps are crucial steps, because the moisture/solvent level of the hybrid layer affects both the polymerization of the hybrid layer as well as the usually hydrophobic adhesive resin placed on top of the hybrid layer [16]. The adhesive layer and the hybrid layer are cured after the adhesive resin has been placed on the primed surface. The composite restorative material is then placed and cured.

1.3. Objective of the Paper

Dentin bonding is no doubt a challenge in dentistry. Research data vary considerably between researchers. Because of these variations in adhesive test results, the objective of this paper is to critically look at different adhesive test methods and identify advantages and drawbacks of different methods. Prior to a discussion of

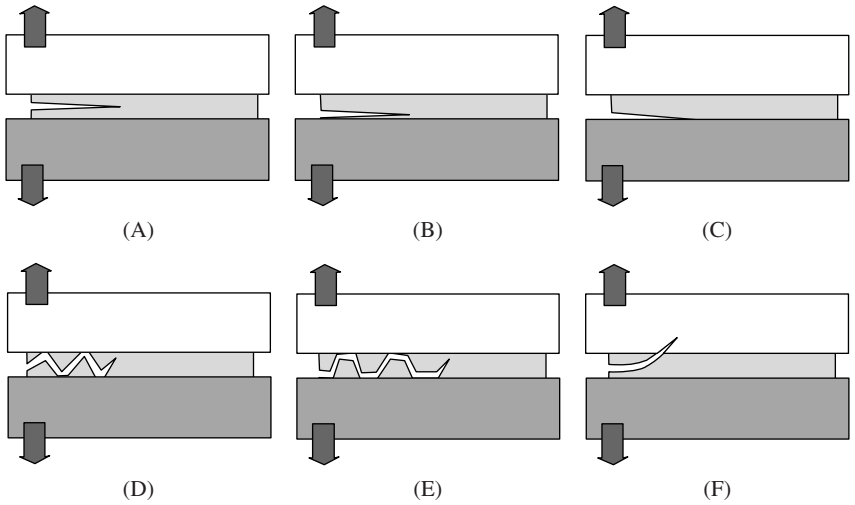


Figure 2. Drawings of possible failures of the adhesive joint. Failures (A) and (B) represent cohesive failures in the adhesive, failure (C) an interfacial failure, failures (D) and (E) mixed failures, while failure (F) represents a combined cohesive failure of the adhesive and the adherend. Of these failures, failures like failure (F) should not be considered in analysis of adhesive joints.

test methods, the different types of failures of an adhesive joint identified during adhesive testing will be discussed (Fig. 2), and these failures will be related to the failure mechanism of an adhesive joint.

2. Failure of the Adhesive Joint

An adhesive joint can fail at different locations. Researchers define failure in the adhesive region differently but use often similar terms, which causes some confusion. To avoid confusion, we first need to define the term *adhesive joint* (Fig. 2).

An adhesive joint consists of an adhesive and the adherend(s) to which the adhesive is bonded. When a failure occurs, it occurs either in the adhesive, at the adherend/adhesive interface, or in the adherend. Of these locations, failure in the adherend is not true adhesion failure. It is just failure of the adherend. Numerous dental adhesive studies include failure in the adherend and define it as cohesive failure. Rather than including such failures in the results, the results for such specimens should have been reported but excluded from the adhesive test results before data analysis.

So-called cohesive/adhesion failures are more complicated than pure adherend failure. In order to include such failures in the analysis of results, the fracture should only be located in the adhesive material or at the adhesive/adherend interface, thus making the inclusion of such failures questionable when it comes to data analysis.

The complexity of determining failure mode during dentin bond testing can be illustrated by a failure through the hybrid layer. In this case, a cohesive failure occurs through the collagen fibers as the crack propagates through the hybrid layer.

The initiation of the failure has not been determined. If the failure is caused by weak collagen fibers, then the failure in the hybrid layer is more a matter of material failure of the collagen rather than of the adhesive. Such effect can be decreased by increasing the cohesive strength of the adhesive rather than improving its adhesive strength.

True adhesion failures should ideally be restricted to interfaces between adhesives and adherends, while in reality they often include all the material(s) and adhesive/adherend interfaces. It is sometimes difficult to precisely identify the failure location, but adhesion failures should be limited to the regions located between interfaces of the adherends. Based on such a restriction, the failures that should be included in adhesive testing are listed below.

Cohesive fracture: A true cohesive failure of an adhesive causes the failure to propagate through the bulk polymer of the adhesive or the hybrid layer. In this case, the surfaces of the two adherends will be covered with a film of the adhesive. The location of the crack may be either in the center of the adhesive, between the adhesive and the hybrid layer, or within the hybrid layer. The fracture should not expose the adherend surface. A good adhesive is an adhesive that fails cohesively during fracture. In such a case the weakness of the adhesive is the strength of the adhesive rather than its ability to form a strong bond to the adherend.

Interfacial fracture: A fracture between the adhesive and the adherend is called interfacial fracture. The occurrence of interfacial fracture for a given adhesive is usually associated with low fracture toughness. Usually, interfacial fractures are detected by visual inspection, but advanced surface characterization techniques makes it possible to identify the precise location of the crack path at the interface.

Other types of fracture: Fracture modes may include the mixed fracture type and the alternating crack path. A ‘mixed’ fracture type occurs if the crack propagates at some locations in a ‘cohesive’ and in others in an ‘interfacial’ failure mode. The ‘alternating crack path’ fracture type occurs if the crack occurs at one interface and then moves over to the other adhesive/adherend interface. This type of fracture appears in the presence of tensile pre-stresses in the adhesive layer.

In addition to the above modes, fracture can occur in the adherend provided the adhesive is tougher than the adherend. In such a case the adhesive remains intact and bonded to one substrate and with some remnants on the other substrate. Another type of failure that should not be called adhesion failure is when the crack propagates from the adhesive region into one of the adherends. Under these conditions, the fracture has found a path that provides less resistance than the adhesive or the adhesive/adherend interfaces.

3. What is Adhesion?

A cohesive failure is by definition a failure within a material, while an adhesion failure is a failure between different materials at their interface. It is important to

make this distinction. This distinction helps us to focus on improving the cohesive strength or the adhesion strength of an adhesive.

Materials placed in molecular contact develop bonds as a result of van der Waals force interactions between molecules [17, 18]. By separating van der Waals bonded surfaces, or by introducing a contamination between the two surfaces, van der Waals force interactions drop off rapidly. This could very well be one of many explanations for the poor correlation between *in vitro* results and *in vivo* performance of dentin adhesives [5].

One way of improving adhesion may be to roughen the surface of the adherend and increase the interaction between the molecules of the adhesive and the adherend. The micromechanical retention also improves as a result of surface roughening. By avoiding shrinkage of the adhesive during setting, the risk of adhesive/adherend separation will decrease and thereby adhesion will be promoted. Other possible approaches to enhance adhesion is to increase the shock absorbing ability of the adhesive joint, or perform some surface treatment of the involved surfaces to decrease environmental degradation of these surfaces.

Assume that enamel and dentin adhesives form relatively thin films (<100 μm) between cusps and composite restorations, and that the bonded cusps are exposed to forces trying to separate the cusps from the composite restorations. The general assumption is that composite restorations are retained to the surrounding tooth tissue through micromechanical retention to either acid etched enamel or to resin infiltrated hybrid layers of dentin. More neglected are the van der Waals forces acting between the adhesive and the enamel and between the adhesive and the dentin surface. Thus, the adhesion relies on both mechanical interlocking and weak molecular interactions.

Based on dipole interactions, Hamaker [19] could determine the level of attractive forces at surfaces of different geometries. From these relationships it became clear that adhesion forces are always connected with an adhesion energy. Hamaker's calculations revealed that this energy decreases very quickly as the adhering surfaces are separated. His calculations can also explain why a tensile test on an adhesive joint is not very reliable. During such a test, due to Poisson's ratio, the cross-sectional area of the joint becomes smaller than the adherends when the modulus of elasticity of the adhesive film is smaller than that of the adherends. As a consequence, the localized stress level in the periphery of the adhesive increases drastically and cracks start forming at the periphery of the adhesive joint. These cracks propagate from their initiation sites and increase the distance between the two surfaces located in the peripheral regions. The increased distance between these two surfaces results in a significant decrease in van der Waals force interaction in this region, and in an increased stress concentration at the formed crack tips, which triggers a failure. Since the stress level becomes substantially higher at the crack tips than the value determined by dividing the force at failure with the total cross-sectional area, the stress level causing the failure becomes significantly higher than such a strength value shows. As a consequence, traditional strength test becomes

rather meaningless, at least when it comes to determining the true strength value [20, 21].

The true fracture strength value determined from the fracture mechanics can be expressed as:

$$\sigma_f = \left(2E\gamma/(\pi c_0)\right)^{1/2}, \quad (1)$$

where σ_f is the fracture strength in uniform tension, E the plain strain elastic modulus, γ the surface energy per unit area, and c_0 the starter crack size [21, 22]. This expression reveals that both high elastic modulus and high surface energy of formed surfaces increase fracture strength, while larger flaw sizes decrease the strength. This expression explains in a nutshell why traditional strength values are difficult to reproduce. For example, differences in primer/adhesive/solvent concentrations would affect E and γ, while differences in techniques may affect flaw size, c_0, introduced during the bonding procedure.

The true fracture strength is difficult to determine if we do not know all the terms in equation (1). This problem, though, can be handled by considering energy rather than strength. A fracture energetic approach determines the 'work of adhesion' rather than the strength. Work of adhesion is the energy required to fracture a unit area of adhesive/adherend interface and is expressed as Joules per square meter. From theory we know that typical work of adhesion due to van der Waals forces is 0.07 J/m^2, and that even the strongest chemical bonds would increase this value to only 5–10 J/m^2 [23]. The important concept with the energy approach is that it shows the energy needed to cause fracture is not very high when a flaw exceeding a critical size has been introduced, which also explains the observed brittleness of adhesive joints.

When failure between a deflecting cusp and the composite occurs, it usually occurs in a brittle way through crack growth. A brittle failure suggests that the amount of energy needed to drive the fracture process is low. Brittleness implies that the material does not have the ability to plastically deform and redistribute localized stresses at the propagating crack tip. The localized stress level at the crack tip can become rather high and drives the propagating crack even though the overall force level on the cusp may not be high. The only restricting force preventing the crack to grow is the increased surface energy generated when a new surface forms as a result of crack growth. As long as the new surface energy is higher than the increased mechanical energy of the stressed joint, the crack will not propagate. It is only when the mechanical energy level of the stressed joint exceeds the surface energy of newly formed fracture surfaces, the crack will grow. Only when an energy balance occurs between the mechanical energy of the stressed joint and the increased surface energy of the growing crack, the crack growth will stop.

For a very small flaw, i.e., the first formed flaw, the surface energy level is often higher than the mechanical energy, preventing the crack from propagating. In order to propagate, the flaw needs to exceed a critical flaw size, which happens when the localized stress level at the crack tip reaches such a high mechanical energy

level that the only way to balance energy is to increase the surface area of the flaw and thereby decrease the mechanical energy of the adhesive joint. Thus, the energy balance between mechanical energy and surface energy of a propagating crack in the adhesive joint explains why the force acting on the deflecting cusp may cause debonding. Such failure may be triggered by defects existing in the adhesive joint initially, introduced during the bonding process. In addition, molecules present in the oral environment may also interact with the existing and growing flaw surfaces, thereby decreasing the surface energy level of the flaws and facilitate crack propagation.

Probably the easiest way of determining the work of adhesion is to use a peel test. Unfortunately, because of the properties of dental adhesives, peel tests are not easily used in dentistry because of the relatively brittle nature of dental adhesives. Therefore, other fracture mechanics approaches have to be used, approaches that will be discussed in the following section. However, before we proceed to that section, it is important to conclude that the key reason the regular strength tests are not reliable is simply that flaws exist or develop during an early step of the test. These flaws induce local stress concentrations, and when such local stress concentrations develop, the concept of an overall strength determination becomes difficult to support. Instead, the science of fracture mechanics seems to be the right way to proceed, because this science has evolved to a level where we now can understand reasons for crack initiation and crack propagation in materials and predict the consequences [24].

4. Strength or Toughness of the Adhesive Joint?

According to a recent review by Heintze [5], the most common tests used to study the strength of dental adhesives are the shear bond test, followed by tensile and microtensile bond tests. According to his review of 1465 adhesive related articles identified on MEDLINE as of November 2006, 857 articles included shear bond testing, 324 included tensile bond testing, 197 microtensile bond testing, 55 fracture toughness testing, and 32 'push-out' testing. Of these tests, the microtensile bond test had gained most in popularity during the past 5 years. Results generated from primarily shear and microtensile tests are commonly used when different products are being marketed, giving the reader the impression that a higher bond strength results in better clinical performance.

Today, no agreement has been reached favoring a particular strength test method regarding its clinical correlation. Too many variables are involved in bond testing, and because of interactions between these variables, it is difficult or impossible to compare results from different studies. According to Leloup *et al.* [25], expressed in descending order, the variables affecting bond testing include dentin depth, crosshead speed, sample storage time, maximum storage time, bonding area, tooth storage temperature, sample storage temperature, and composite stiffness. Difference among operators is also important to consider [26]. To illustrate how

difficult it is to interpret the bond strength of a particular product, a comparison of shear strength values revealed that in one study the shear bond strength of a specific product after 24 h was 18.1 MPa [27], in another study the value was 6.6 MPa [28], and in a third the value was 2.9 MPa [29].

The microtensile test is well known for its pretest failures occurring during sample preparation. These failures are most likely due to flaws introduced during sample cutting. By comparing different studies we find that these pretest failures can range from 0% [30] to 23% [31], but in some cases even as high as 89% [32].

Even when the same batches and seemingly the same experimental conditions are used, significant variations still exist among researchers within the same group [26]. Considering all these variations it seems fair to state that bond strength data generated by different groups and individuals are far from reproducible [25, 33, 34]. The reason is that bond strength values neglect the true stress distribution [4] and that the results are highly affected by defects introduced during sample preparation [26]. There are also evidences suggesting that intra-tooth variability is greater than inter-tooth variability, at least when it comes to microtensile bond testing [35]. Therefore, and in order to obtain enough statistical reliability with microtensile bond strength testing, 6 extracted teeth have to be used, from which at least 7 beams per tooth can be measured [36]. Unfortunately, many of the published results from microtensile tests are flawed because the authors had not replicated the same bonding procedures on different teeth.

Comparing *in vivo* bond strength results with *in vitro* bond strength values, it has been shown that microtensile bond strength of samples from Class II restorations placed *in vivo* is lower than if the restoration had been placed *in vitro* [37]. This finding is in contrast to the results obtained on composite cylinders bonded to molars *in vivo* and evaluated in shear after extraction. These *in vivo* bonded cylinders showed to have higher shear bond strength than cylinders bonded *in vitro* [38]. Whether these differences in findings are due to operator variability, defects introduced during extraction, defects introduced during final sample preparation, the structure of the substrate, or just reflect differences in testing methods are not known at the present time.

Two concepts must be considered when evaluating dental adhesives. The first one is that traditional strength testing does not report the actual strength value at the propagating crack tip. This is important to realize, because it is the localized stress that drives the crack growth. The second one is that strength testing of dental adhesives does not generate reproducible results, because of large variations in dentin structure, modulus of elasticity, surface energies of generated fracture surfaces, and the introduction of flaws of different sizes during sample preparation and bonding. Thus, one should not expect that isolated strength testing results can be reliable predictions of the clinical performance of dental adhesives.

Rather than using strength testing approaches, it seems reasonable to suggest that fracture mechanics approaches should be used instead and and by use of fracture mechanics the impact of crack formation and crack propagation on the clinical

behavior should be investigated. Neither micro-tensile nor shear bond testing use fracture mechanics to address the adhesive testing problem. However, when tensile and shear tests are compared, there is a distinct difference between these two methods. This difference relates to how the force affects the opening mode of the joint. Even though it might seem that the failure occurs instantaneously over the entire bond area when the adhesive joint fails, the crack starts propagating from an edge and quickly propagates over the surface. Factors such as stress concentration at the crack tip and the speed with which energy stored in the stressed system recovers become the main factors of interest. Fracture mechanics tests, in contrast to strength tests, consider localized stress concentration factor, K, and the energy release rate, G. The benefit with such models is that the behavior of the adhesive layer itself can be neglected and only the adherends need to be considered.

During a fracture mechanics analysis, the load is ideally kept constant during the testing procedure. To achieve a constant load condition for such a test, one will need to use an adhesive joint design that can produce a constant load condition. Such condition is achievable by combining proper material and geometric variables. Unfortunately, this requirement often tends to result in samples that are more complex than those used for a regular strength test. In adhesively bonded structures, the global geometry and the loading conditions are kept constant by structural considerations, while the design procedure focuses on the 'material properties' of the adhesive, i.e., select a 'good' adhesive, and on local changes in the geometry. Increased joint resistance is usually obtained by designing its geometry so that:

(a) the bonded zone is large,

(b) it is mainly loaded in mode II,

(c) stable crack propagation will follow the appearance of a local failure.

5. Testing the Fracture Resistance of the Adhesive

A wide range of testing devices have been developed to determine the fracture resistance of bonded structures in pure mode I, pure mode II or in mixed mode III (Fig. 3). Most of these devices use beam type specimens. Some of the popular fracture resistance tests are briefly described below.

The general clinical experience is that the adhesive properties of different adhesives may seem to be good initially, but over time some adhesives have retentive properties better than other products. From fracture mechanics it is known that adhesion energy varies with crack speed, temperature, shrinkage, and other experimental parameters. Crack speed is the dominant variable. It has been found that at slow rates of separating a crack, the work of adhesion corresponds to the van der Waals force level for a joint between polymer and glass, but as separation speed is increased the force at the crack tip increases considerably. Shrinkage of the adhesive is also important to consider, because fracture mechanics reveals that shrinkage always decreases the adhesion. From a practical point of view, a larger restoration

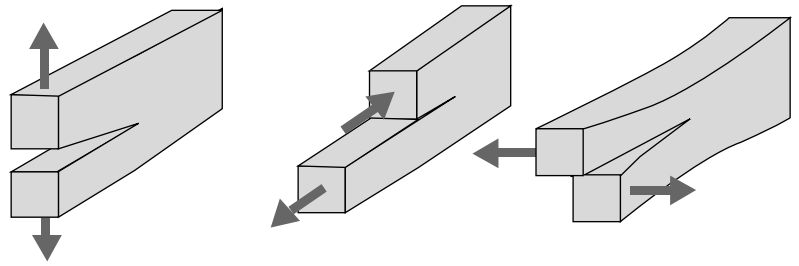


Figure 3. Modes of failure. Mode I (left drawing) is an opening or tensile mode where the loading is normal to the crack. This is what we expect when micro tensile bond testing is used. The drawing implies that as the initial flaw starts propagating, the cross-sectional area, where separation occurs, decreases. Mode II (central drawing) is a sliding or in-plane shear mode where the crack surfaces slide over one another in direction perpendicular to the leading edge of the crack. This is typically the mode for which the adhesive exhibits the higher resistance to fracture, and this is the typical failure mode when shear testing is used. Mode III (right drawing) is a tearing or antiplane shear mode. This mode can occur during both microtensile and shear bond testing, where usually it is unintentionally introduced.

that shrinks more during polymerization than smaller restorations should therefore be associated with more devastating shrinkage effects than smaller restorations. Another parameter that can differ considerably is surface roughening. The impact of surface roughening is less predictable, though, because roughening can have both positive and negative effects.

It is very rare to find dentin adhering to a restoration that has come loose. When this happens, it is mainly connected with the fracture of a cusp. Since dentin fractures without an associated cusp fracture are rare clinically, one can assume that the adhesive bond to dentin is, in general, insufficient to cause dentin fracture. Thus, dentists should not rely on the adhesive material alone when it comes to retaining restorations.

For a better understanding of dentin adhesion, more K_{IC} (plain strain fracture toughness) determinations should be performed (Fig. 4(a)–4(j)), because the K_{IC} parameter represents an intrinsic material property that characterizes a material's resistance to fracture. With a linear elastic fracture toughness test, both bond strength and inherent defects across the interface will be considered. The advantage with determining the plain strain fracture toughness of the interface is that the material's ability to tolerate defects under known load conditions can be determined. However, it should be emphasized that with fracture toughness evaluations, there will still be relatively high coefficients of variation [39]. The advantage of using fracture toughness values is that these values are more related to unstable crack propagation originating from a local flaw as opposed to generalized failure of a broad area which may contain regions of different bond integrity as is the case with a tensile bond strength test. However, even with fracture toughness measurements the coefficient of variation is still sufficiently high to raise questions about reproducibility. The variability in fracture toughness values is higher with dentin than with enamel,

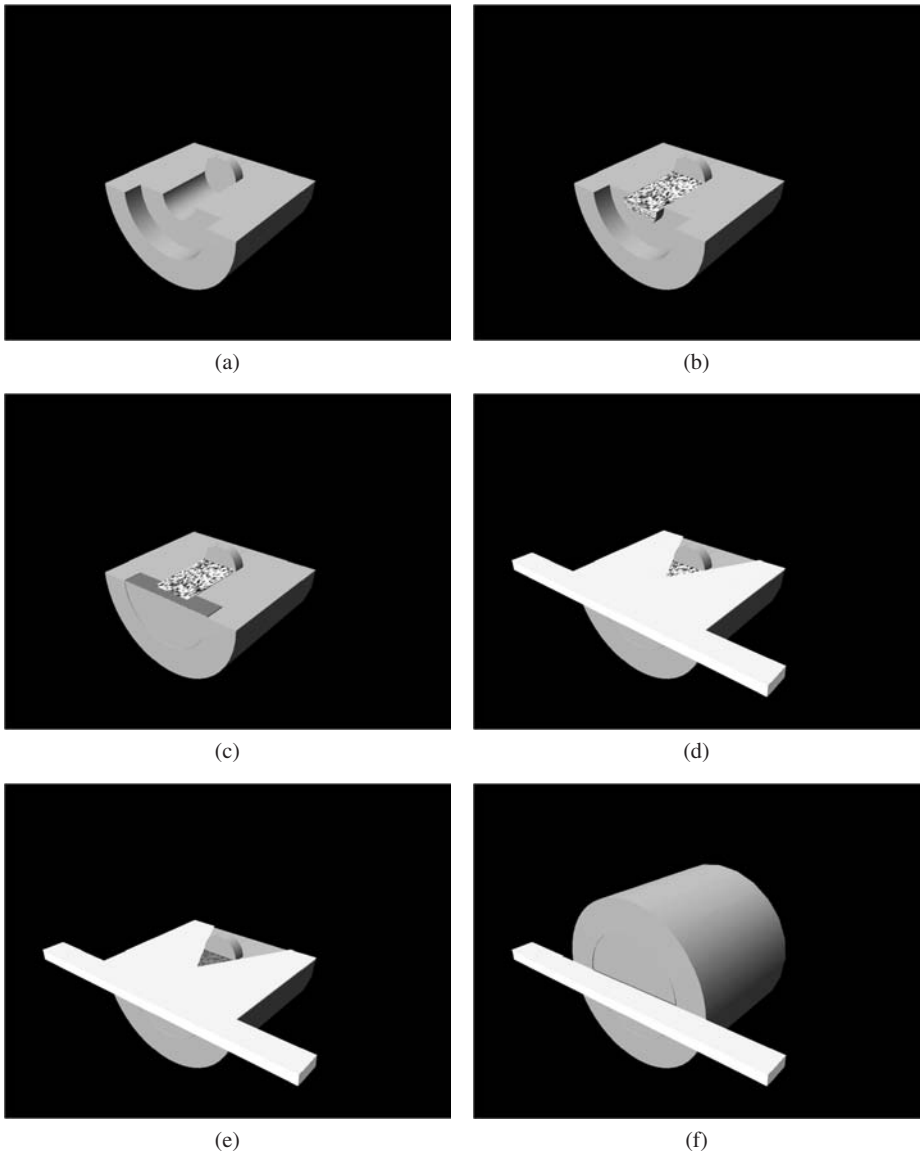


Figure 4. (a) Polyethylene mold. A polyethylene disk is placed at the bottom of the smaller cylindrical shape to make it easier to remove the final specimen. (b) A dentin disk, 4 × 7 × 1.0 mm is bonded to a split mold and polished flat. (c) Composite is inserted into the space under the dentin disk and into the larger half-cylindrical space at the outer edge of the dentin disk. (d) A stainless steel sheet, 0.1 mm thick and with a 60° angle is placed to expose an equal sided triangle of the dentin surface. (e) The exposed triangular dentin surface is coated with adhesive and cured. (f) The other half of the polyethylene mold is placed over the stainless steel sheet resting against the dentin disk. The mold is then filled with composite and cured.

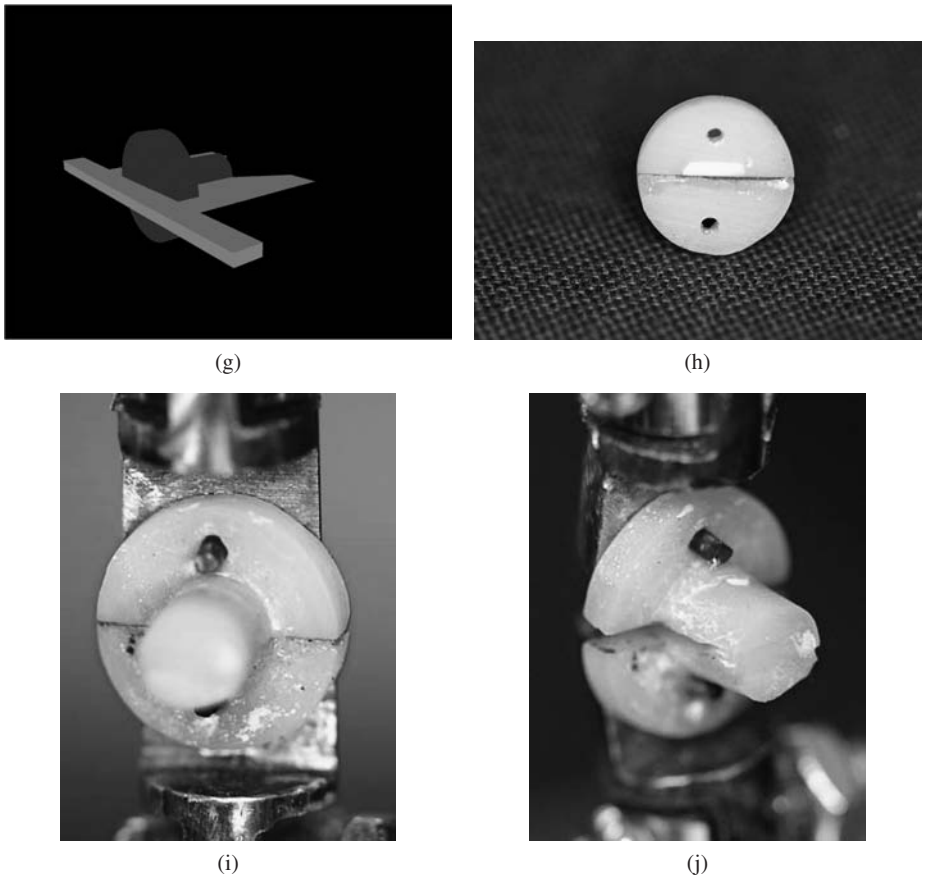


Figure 4. (g) The two polyethylene mold parts are removed leaving a composite/dentin specimen with the stainless steel sheet. (h) After the stainless steel sheet has been removed, two holes are drilled through the specimen collar. (i) The specimen is attached to a tensile testing device and slowly loaded in tension. (j) At a certain load level, a crack starts propagating from the triangular edge located closest to the collar. The K_{IC} value can then be determined from: $K_{IC} = P_c Y_m^* / \{D(w)^{1/2}\}$, where P_c = peak load at time of fracture, D = specimen diameter (in our case 4 mm), $w =$ specimen length from end to load (in our case 7 mm), Y_m^* = minimum stress intensity factor.

which may be related to larger differences in dentin composition. Thus, differences in dentin age and mineralization level play most likely significant roles in the final results.

Provided flaws play a major role in the fracture process of the adhesive joint, a good correlation between defects around the margins of restorations and low clinical retention rate should be expected, but little proof exists in dentistry when it comes to such correlations. Heintze [5] tried to correlate bond strength with microleakage, and bond strength with results from marginal gap analyses. Of all studies he reviewed, 80% revealed no correlation between marginal quality and bond strength. In this study, he also compared marginal quality with clinical out-

come, and found only 18% correlation. The conclusion that can be drawn is that gap studies do not correlate well with bond strength data. Fracture toughness values were not included, and the question remains whether there is any better correlation between clinical success and fracture toughness.

The primary goal with dentin adhesive testing must be to predict clinical performance. Thus, such a test should consider flaws within the material and failure at the interface, while the impact of a geometric factor should be minimized [40]. If the goal is just to screen new adhesive systems or rank material performance against various parameters, a traditional strength test may be appropriate as long as one accepts that the strength value is a ranking value within a group of tests performed rather than a true strength value. However, if the goal is to determine an interfacial material property, such as crack growth resistance, linear elastic fracture mechanics is more appropriate. Armstrong *et al.* [41] have used plane-strain (chevron-notch) fracture toughness (ASTM E1304-89) to study the effect of removing collagen. The plain-strain fracture toughness for All-Bond 2 (Bisco Inc., Schaumburg, IL, USA) was 0.88 ± 0.24 MPa·m$^{1/2}$ while for dentin pretreated with NaOCl it was 0.73 ± 0.24 MPa·m$^{1/2}$. These results are similar to those published by Tam and Pilliar [42].

It is well documented that microtensile bond strength samples often fail in the adhering substrates [42], suggesting that a fracture toughness approach should be more appropriate for adhesion determination. In fracture toughness studies, Tam and Pilliar [43] showed that failures occurred within; (a) the smear layer, (b) a resin modified layer between the interdiffusion zone and the adhesive, (c) a well-infiltrated hybrid inter-diffusion zone, and (d) a non-infiltrated unsupported collagen layer. Smear layer failures (a-failures) occurred in areas without etching, while b-failures occurred for desiccated teeth. The c-failures occurred when a weaker acid was used, while d-failures occurred as a result of a too extensive etch followed by incomplete resin diffusion.

Fracture toughness determinations of dental adhesives have advantages and drawbacks. The drawbacks relate primarily to the use of biological materials and the fact that properties differ among such specimens. Another limitation is that teeth are relatively small and not always that easy to get hold of. These limitations make it difficult to make samples with proper shapes and evaluate a sufficiently large number of specimens.

A goal when it comes to adhesion testing is to identify methods that can predict the lifetime of a structure. These methods have been reviewed by Ritter [44, 45]. Such lifetime predictions rely on calculations involving Weibull strength parameters and the crack-growth exponent. The reliability of such predictions is very dependent on the number of test specimens, and at least 50 specimens are recommended [46]. It becomes even more complicated when one considers that dentin (and bone) samples usually are too small to meet the requirements of linear elastic fracture mechanics and more complex non-linear methods are, therefore, required. By considering these aspects, fracture toughness tests may not be the ideal screening tests for small samples such as teeth.

Rather than considering traditional fracture mechanics approaches only, fatigue testing should also be considered. Materials used in the oral environment are subjected to fatigue and may, therefore, fail [47]. Fatigue is a process involving nucleation, propagation, and coalescence of cracks. During cycling, one can plot the rate of crack growth per cycle (da/dN) where da represents a change in crack length per cycle (N) as a function of ΔK (change in stress intensity factor). By plotting such curves, three regions can be identified. The first region is relatively steep and represents rapid crack growth due to crack nucleation. The second region is less steep and represents cracks growing slower than initially, referred to as the subcritical crack growth region. The third region is the steepest region and represents rapid crack propagation and coalescence just before failure.

A fatigue testing approach was used when De Munck *et al.* [48] determined how the thickness of the adhesive layer affected adhesion. The reason they investigated this topic can be traced to a paper by Lloyd *et al.* [49] who claimed that the interface should be rigid rather than easy to deflect. Lloyd *et al.*'s [49] claims have also been supported in fracture toughness determinations conducted by Tam and Pilliar [50]. However, a weakness with Tam and Pilliar's [50] claims is that they did not really target the thickness of the adhesive resin. They rather targeted the rigidity of the interfacial region in general. In a later study, Tam *et al.* [51] showed that a more filled resin improved the fracture toughness values. The fracture toughness parameter represents an intrinsic material property which is not dependent on specimen geometry, in contrast to conventional shear and tensile bond tests. Fracture tougness failures generally occur along the bonded interface. Thicker layers increase the failure probability [52]. Thinner layers may be more associated with complete oxygen inhibition. Independent of thickness, failures seem to occur between infiltrated layer and the adhesive layer [53].

In De Munck *et al.*'s study [48], specimens were evaluated regarding microtensile strength and microfatigue tests. The microtensile strength was not affected by adding an additional intermediate elastic layer, while such an addition significantly decreased the microrotary fatigue resistance. Whether this method is a more reliable predictor of clinical success than traditional strength testing or fracture mechanics approaches cannot be judged at the present time. Even though fatigue testing may not be better than fracture mechanics approaches, sample preparation and testing seems less complicated, suggesting that the method De Munck *et al.* [48] proposed may have the potential of being a test method that could replace the traditional strength test methods.

6. Conclusion

By critically reviewing the literature dealing with adhesive strength testing of dental, particularly dentin, adhesives, most tests have focused on strength determination, despite the fact that these methods do not really measure what they claim to measure. Instead, the author finds it is better to perform fracture toughness de-

terminations. However, compared to strength determinations, fracture toughness determinations often require larger sample sizes and are also more complicated when it comes to sample preparation and testing. Since fatigue testing has the potential of being able to simulate fatigue processes occurring clinically, they should be evaluated more frequently.

This review suggests that the time has come to abandon traditional strength tests that have until now dominated adhesive testing in dentistry, and move toward an increased use of fracture toughness tests as well as fatigue tests. At the same time, it is important to realize and accept that as long as we do not have strong evidences correlating clinical success with any particular adhesive test method, *in vitro* tests should not be used as predictors of clinical performance. Only when we have such correlations, the *in vitro* test methods will have a practical meaning.

References

1. S. Fastlicht, *Tooth Mutilation and Dentistry in Pre-Columbian Mexico*. Quintessence, Chicago, IL (1976).
2. K.-J. M. Söderholm, *J. Adhesive Dentistry* **9**, 227 (2007).
3. T. Jacobsen, K. J. Söderholm, I. Garcea and E. Mondragon, *Eur. J. Oral Sci.* **108**, 247 (2000).
4. R. Van Noort, S. Noroozi, I. C. Howard and G. Cardew, *J. Denistry* **17**, 61 (1989).
5. S. D. Heintze, *J. Adhesive Dentistry* **9**, 77 (2007).
6. K.-J. Söderholm, *Dental Mater.* **7**, 74 (1991).
7. I. A. Mjör and I. Nordahl, *Arch. Oral Biol.* **41**, 401 (1996).
8. A. Nanci (Ed.), *Ten Cate's Oral Histology: Development, Structure and Function*, 6th ed. Mosby, St Louis, MO (2003).
9. W. H. Arnold and P. Gaengler, *Annals Anatomy* **189**, 183 (2007).
10. C. L. Davidson, A. I. Abdalla and A. J. De Gee, *J. Oral Rehabil.* **20**, 291 (1993).
11. R. P. Chappell and J. D. Eick, *Quintessence Int.* **25**, 359 (1994).
12. J. R. Holtan, G. P. Nystrom, P. S. Olin, R. A. Phelps 2nd, J. J. Phillips and W. H. Douglas, *J. Dentistry* **22**, 96 (1994).
13. N. Nakabayashi, K. Kojima and E. Masuhara, *J. Biomed. Mater. Res.* **16**, 265 (1982).
14. B. Van Meerbeck, Dentine adhesion: morphological, physico-chemical and clinical aspects, *PhD Thesis*, Department of Operative Dentistry and Dental Materials, College of Dentistry, Catholic University of Leuven, Belgium (1993).
15. J. Perdigao, An ultra-morphological study of human dentine exposed to adhesive systems, *PhD Thesis*, Department of Operative Dentistry and Dental Materials, College of Dentistry Catholic University of Leuven, Belgium (1995).
16. T. Jacobsen and K.-J. Söderholm, *Dental Mater.* **11**, 132 (1995).
17. D. Tabor, in: *Colloid Dispersions*, J. W. Goodwin (Ed.), Chapter 2, Special Publication, No 43. Royal Soc. Chem., London (1981).
18. J. Israelachvilli, *Intermolecular and Surface Forces*, Chapter 1. Academic Press, London (1985).
19. H. C. Hamaker, *Rec. Trav. Chim.* **57**, 61 (1938).
20. C. E. Inglis, *Trans. Inst. Naval Architec.* **55**, 219 (1913).
21. A. A. Griffith, *Phil. Trans. Roy. Soc. A* **221**, 163 (1920).
22. J. R. Kelly, *Dental Mater.* **11**, 103 (1995).

23. K. Kendall, in: *Adhesion: Its Theory and Practice in Restorative Dentistry*, Proc. of the International Symposium held under the auspices of the IADR Dental Materials Group in collaboration with ICI Dental, Chicago, IL, pp. 3–7 (1987).
24. R. W. Hertzberg, *Deformation and Fracture Mechanics of Engineering Materials*, 2nd ed. Wiley, New York, NY (1983).
25. G. Leloup, W. D'Hoore, D. Bouter, M. Degrange and J. Vreven, *J. Dental Res.* **80**, 1605 (2001).
26. K.-J. Söderholm, M. Guelmann and E. Bimstein, *J. Adhesive Dentistry* **7**, 57 (2005).
27. T. J. Hilton, K. S. Vandewalle, A. Egge and J. L. Ferracane, *J. Dental Res.* **82** (Special Issue A, abstract 23) (2003).
28. M. J. Bell, J. O. Burgess and D. Mercante, *J. Dental Res.* **82** (Special Issue A, abstract 1632) (2003).
29. W. Ziecina, W. C. Wagner, A.-M. L. Neme and B. B. Maxson, *J. Dental Res.* **82** (Special Issue A, abstract 572) (2003).
30. R. Frankenberger, J. Perdigao, B. T. Rosa and M. Lopes, *Dental Mater.* **17**, 373 (2001).
31. S. Inoue, M. A. Vargas, Y. Abe, Y. Yoshida, P. Lambrechts, G. Vanherle, H. Sano and B. Van Meerbeek, *J. Adhesive Dentistry* **3**, 237 (2001).
32. S. R. Armstrong, M. A. Vargas, Q. Fang and J. E. Laffoon, *J. Adhesive Dentistry* **5**, 47 (2003).
33. S. K. Al-Salehi and F. J. Burke, *Quintessence Int.* **28**, 717 (1997).
34. F. J. T. Burke, A. Hussain and G. Fleming, *J. Dental Res.* **82** (Special Issue B, abstract 715) (2003).
35. A. D. Loguerico, L. P. Barroso, R. H. Grande and A. Reis, *J. Adhesive Dentistry* **7**, 151 (2005).
36. V. G. Arias, G. M. B. Ambrosano and L. A. F. Pimenta, *J. Dental Res.* **85** (Special Issue C, abstract 818) (2006).
37. J. H. Purk, V. Dusevich, A. Glaros, P. Spencer and J. D. Eick, *J. Am. Dental Assoc.* **135**, 185 (2004).
38. P. N. Mason, M. Ferrari, M. C. Cagidiaco and C. L. Davidson, *J. Dentistry* **24**, 217 (1996).
39. R. M. Pilliar, D. C. Smith and B. Maric, *J. Dental Res.* **65**, 1308 (1986).
40. A. J. Kinloch, *Adhesion and Adhesives: Science and Technology*, pp. 264–338. Chapman and Hall, London (1987).
41. S. R. Armstrong, D. B. Boyer, J. C. Keller and J. B. Park, *Dental Mater.* **14**, 91 (1998).
42. L. E. Tam and R. M. Pilliar, *J. Dental Res.* **72**, 953 (1993).
43. L. E. Tam and R. M. Pilliar, *J. Dental Res.* **73**, 607 (1994).
44. J. E. Ritter, *Dental Mater.* **11**, 142 (1995).
45. J. E. Ritter, *Dental Mater.* **11**, 147 (1995).
46. J. E. Ritter, N. Bandyopadhyay and K. Jakus, *Ceram. Bull.* **60**, 798 (1981).
47. H. W. A. Wiskott, J. I. Nicholls and U. C. Belser, *Int. J. Prosthodont.* **8**, 105 (1995).
48. J. De Munck, K. Van Landuyt, M. Peumans, A. Poitevin, P. Lambrechts, M. Braem and B. Van Meerbeek, *J. Dental Res.* **84**, 118 (2005).
49. C. H. Lloyd, S. N. Scrimgeour, D. Brown, R. L. Clarke, R. V. Curtis, P. V. Hatton, A. J. Ireland, J. F. McCabe, J. W. Nicholson, J. C. Setcos, M. Sherriff, R. van Noort, D. C. Watts, C. J. Whitters, D. Wood, *J. Dentistry* **25**, 173 (1997).
50. L. E. Tam and R. M. Pilliar, *J. Dentistry* **28**, 487 (2000).
51. L. E. Tam, S. Khoshand and M. Pilliar, *J. Dentistry* **29**, 217 (2001).
52. S. G. Croll, in: *Adhesion Aspects of Polymeric Coatings*, K. L. Mittal (Ed.), pp. 107–129. Plenum Press, New York, NY (1983).
53. G. T. Knight and N. Barghi, *J. Dental Res.* **76** (Special issue A, abstract 2134) (1997).

Shear Bond Strength of Cement to Zirconia

M. Rosentritt [a,*], **M. Behr** [a], **J. M. van der Zel** [b] **and A. J. Feilzer** [b]

[a] Department of Prosthetic Dentistry, Regensburg University Medical Center, D-93042 Regensburg, Germany

[b] Department of Dental Materials Science, Academic Centre for Dentistry, Universiteit van Amsterdam and Vrije Universiteit, NL 1066 EA Amsterdam, The Netherlands

Abstract

This study investigated the shear bond strength (SBS) of various cements to zirconia ceramic.

CoCr-cylinders were bonded to zirconia plates (20 mm × 10 mm × 2 mm; $n = 8$ per group) using four self-adhesive resin cements (one capsule, three hand-mixed) and four resin cements, partly in combination with a tribochemical/silane treatment. All cements were auto-polymerizing. The bonding areas were sand-blasted using 110 µm Al_2O_3. The shear bond strength was determined after 24 h, 30 days, 90 days of water storage (37°C) and after 12 000 thermal cycles. Statistical analysis was performed using one-way analysis of variance (ANOVA) and Bonferroni *post hoc* test ($\alpha = 0.05$).

After 24 h and after thermal cycling (TC) the lowest value of shear bond strength was found for the control Variolink without bonding pre-treatment (9.5 MPa/3.1 MPa) and the highest results were determined for Calibra with bonding pre-treatment (37.3 MPa/31.9 MPa). After 30 days and 90 days of storage in water the highest SBS values were found for RelyX (33.3 MPa/28.6 MPa), and again lowest values were determined for Variolink (8.8 MPa/9.1 MPa). After 90 days storage all samples of Maxcem failed. The groupwise comparison revealed significantly different SBS results between 90 days storage and the initial results after 24 h ($p = 0.003$). No significant differences were found between the other storage conditions ($p > 0.057$). The systems without bonding pre-treatment provided significantly lower SBS in comparison to the self-adhesive systems and the systems with bonding pre-treatment ($p = 0.000$).

Within the limitations of this study, three of four self-adhesive bonding systems provided bond strengths to zirconia, comparable to systems with additional bonding pre-treatment. The durability of the bonding resin and zirconia can only be judged after long-term water storage.

Keywords

Zirconia, bonding, self-adhesive, resin

1. Introduction

During the 1950s, standards for crown retention were described on the basis of taper, height and surface area [1]. Decreasing taper and increasing both the height and the surface area of the prepared tooth increased the retention of convention-

* To whom correspondence should be addressed. Tel.: +49-941-944-6054; Fax: +49-941-944-6171; e-mail: Martin.Rosentritt@klinik.uni-regensburg.de

© Koninklijke Brill NV, Leiden, 2009

ally cemented crowns. Investigations from Palacios *et al*. [2] and Ernst *et al*. [3] evaluated the axial retention stress of low tapered (10° Palacios, 5° Ernst) abutments. The authors found that resin-modified glass ionomers retained experimental crowns as well as adhesive resin cements. It has been reported that the retentive values of adhesive resins at 24° taper were 20% higher than the retention values of conventional cements at 6°-taper [4]. The retention standards of tapers less than 10° cannot be fulfilled in all clinical cases and, therefore, adhesive bonding is promoted to safely lute a restoration if the mechanical retention is insufficient. In contrast to cast dentures, CAD/CAM restorations have a rough surface due to the manufacturing process [5], which promotes additional micromechanical interlocking of the luting agent. Nevertheless, for the restoration of ceramic implant abutments, the standards of crown retention are often not optimized: the height of an abutment is often low, the surface area is small due to screw channels or small diameters and — depending on the implant insertion path — the angles of taper are high. Additionally, contamination during try-in may reduce the bond strength [6]. Therefore, the cementation of zirconia restorations on tooth, and especially on zirconia abutments/implants, may require special bonding techniques. In these cases, the chair-side treatment is more acceptable if the dentist abstains from expensive ceramic pre-treatments.

Hydrofluoric acid etching does not work with zirconia surfaces because of lack of a glass phase. Some investigations describe roughening with sandblasting to achieve a resin-to-zirconia bond [5]. Good bonding qualities are described with these treatments [7, 8], but their application may also alter the state and phase of the zirconia surface and may damage the ceramic in the long term [9, 10]. Sandblasting may damage thinly designed crown margins and if it is applied *in vivo*, it may harm the gingival tissue or the implant body.

It was demonstrated that silane can strengthen the bond between silica-based ceramic and resin cement [11, 12]. However, silanes in general fail to link the resin to oxide-ceramic like zirconia [13]. A sufficient bond between these components was demonstrated only for special silane coupling agents and after short-term water storage [12], but this bond failed with increasing storage time due to hydrolysis [8, 13, 14]. Other pre-treatment methods are plasma spray treatment, addition of low fusing porcelain layers [15], tribochemical silica coating (Rocatec, 3M Espe, Seefeld, Germany) [5, 13], or the use of phosphate acid ester monomers [8, 16]. The last was described to successfully bond resin to zirconia [13, 16]. However, Kern and Wegner emphasized that all these procedures can only be judged following prolonged water storage in excess of 30 days [13]. Unfortunately, many investigations [8, 12, 14–16] only take thermal cycling and storage less than a week into consideration. Therefore, they were not able to show the impact of hydrolysis on the resin-to-zirconia bond.

This study investigated different resin-to-zirconia bonding concepts after different storage conditions. The aim was to find methods which are easy to use. Self-adhesive composite cements were compared with systems using silica coat-

ing pre-treatment or phosphate ester monomer pre-treatment. The hypothesis of this study was that there is a difference between the SBS values of sophisticated multi-step bonding systems and self-adhesive systems.

2. Material and Methods

2.1. Specimen Preparation

320 plates were cut from a zirconia ceramic (Cercon Base, white colour; 93 wt% zirconium dioxide, 5 wt% yttrium oxide, >2 wt% hafnium dioxide, >1 wt% aluminium trioxide and silicon oxide, DeguDent, Hanau, Germany). The specimens were ground flat using a trimming device (diamond 'fine' wheel; Reco GMT 5330, Ritter, Karlsruhe, Germany) without any lubricant and sintered for 6 h (1350°C) to their final dimensions (thickness 2 mm, length 20 mm, width 10 mm). The peak-to-valley surface roughness (R_a) of all materials was determined for each sample using a profilometric contact surface measurement device (Perthometer S6P, Feinprüf-Perthen, Göttingen, Germany). The resulting surface roughness R_a was 0.9 μm, which is comparable to the surface roughness after milling.

A total of 320 cobalt–chromium (Dentitan; 69.5 wt% Co, 24 wt% Cr, 4.5 wt% Mo and 2 wt% Ti; Krupp, Essen, Germany) cylindrical specimens were cast (using Globocast HF3, Krupp, Essen, Germany). The specimens had a diameter of 5 mm and a height of 3 mm. The front sides of the cylinders were ground flat under water cooling using a grinding machine (Motopol, Buehler, Schaan, Liechtestein, Al_2O_3-grinding paper; grit: 800). The surface roughness R_a after treatment was 1.2 μm.

The zirconia specimens and the front sides of the CoCr cylinders were all airborne particle abraded with 110 μm Al_2O_3 for 10 s at 0.28 MPa. A punched tape was used to coat the zirconia specimens in order to restrict the working area to a diameter of 5 mm (bonding area: 19.6 mm^2). The CoCr surface was treated with a thiophosphoric methacrylate resin (Metal Primer, GC, Tokyo, Japan). After airborne particle treatment the surface roughness reduced to 1.1 μm (CoCr) and 0.76 μm (zirconia).

2.2. Application of the Luting Agents

All resin cements (Table 1) were mixed and applied at room temperature under orange room light for preventing light polymerisation and for guaranteeing auto-polymerization. A thin cement layer was placed onto the front side of the CoCr cylinder and then pressed onto the bonding area of the zirconia specimens. The cement was allowed to set under a constant weight of 1 kg for 5 min, the excess cement was removed and the specimens were randomly assigned into four subgroups. A total of eight specimens per cement/group were investigated. Group 1 was stored for 24 h in distilled water at 37°C and group 2 underwent 12 000 thermal cycles in distilled water alternating between water baths maintained at 5°C and 55°C. The holding time in each bath was 2 min. The entire thermal cycling process lasted 17 days. Group 3 and group 4 were stored for 30 and 90 days, respectively, in distilled water maintained at 37°C.

Table 1.
Resin cements and their application procedure on zirconia

Resin cements	Manufacturer	Primer/no primer on zirconia	Mixing procedure	Linking agent
Maxcem	Kerr, Orange, CA, USA	No primer	Self-mixing	Phosphate-groups
Multilink Sprint	Ivoclar-Vivadent, Schaan, Liechtenstein			
RelyX Unicem hand-mixed	3M Espe, Seefeld, Germany	No primer	Hand-mixing for 15 s	
RelyX Unicem		No primer	Automatic mixing 15 s	
RelyX Unicem		Rocatec 13 s; Silane: Espe Sil		Silica coating
Multilink	Ivoclar-Vivadent, Schaan, Liechtenstein	Adhesive agent (SR Link[1]) allowed to dry	Self-mixing	Organophosphate groups
Variolink II low viscosity		Rocatec 13 s; Silane: Espe Sil	Hand-mixing for 20 s	Silica coating
Variolink II low viscosity		No primer (CONTROL)		–
Calibra	Dentsply, Konstanz, Germany	Repeated application (2 × 40 s) of a mixture of Prime & Bond XP[2] and self-cure activator (SCA)[2]		Silane coupling agent
Panavia F	Kuraray, Osaka, Japan	No primer		MDP

[1] Ivoclar-Vivadent, Schaan, Liechtenstein.
[2] Dentsply, Konstanz, Germany.

2.3. Shear Bond Strength Test

Shear bond strength (SBS) was determined following ISO TR 11405. The specimens were fixed in a shear bond device, which allowed the loading die to strike the CoCr cylinder. The distance between chisel and alloy panel was 0.1 mm, for avoiding the cantilever effect on the adhesive surface. The universal testing machine Zwick 1446 (Zwick, Ulm, Germany) pushed the die down at a crosshead speed of 1 mm/min. SBS was calculated using the formula:

$$\text{shear bond strength (MPa)} = \frac{\text{maximum force (N)}}{\text{bonding area (mm}^2\text{)}}.$$

The fracture mode was analysed using a reflected-light microscope (Stereoscan, Zeiss, Jena, Germany). A fracture was denoted ‘adhesional’ if more than 75% of the

zirconia surface (of the restricted area) was visible. A 'cohesive' fracture showed more than 75% of the surface covered with resin. All other cases were classified as 'mixed fractures'. The means and standard errors of means were calculated, and statistical differences were determined using one-way analysis of variance (ANOVA/Bonferroni *post hoc*) at a level of significance of $\alpha = 0.05$.

3. Results

After 24 h, the lowest values of shear bond strength were found for the control Variolink without bonding pre-treatment (9.5 MPa) and Variolink/Rocatec treatment (13.2 MPa). Highest results were determined for Calibra with bonding pre-treatment (37.3 MPa). Significant differences were found for the following combinations: RelyX/Rocatec, Multilink, RelyX hand-mixed and Calibra in comparison to Variolink ($p < 0.028$) and Calibra with Variolink/Rocatec ($p = 0.000$).

After thermal cycling (TC), a similar ranking of SBS was found: Calibra (31.9 MPa) provided highest result and lowest results were found for Variolink without bonding pre-treatment (3.1 MPa) and Variolink/Rocatec treatment (14.1 MPa). Variolink provided significantly ($p < 0.023$) lower results in comparison to Maxcem, RelyX, RelyX hand-mixed, RelyX/Rocatec and Calibra.

After 30 days of storage in water the highest SBS values were found for RelyX (33.3 MPa) and Calibra (28.2 MPa). Lowest value was obtained for Variolink (8.8 MPa). RelyX showed statistically significantly higher ($p < 0.032$) results than Panavia, Variolink and Mulitlink. For Calibra significantly higher ($p = 0.020$) results were found in comparison to Variolink.

After 90 days storage, the different systems provided SBS values between 28.6 MPa (RelyX) and 9.1 MPa (Variolink), and no significant differences were found between Maxcem and Variolink ($p = 0.031$). All samples of Maxcem failed after 90 days storage. Detailed information about the SBS results is provided in Fig. 1.

The groupwise comparison revealed significant SBS results only between 90 days storage and the initial results after 24 h ($p = 0.003$). No significant differences were found between the other storage conditions ($p > 0.057$). The systems without bonding pre-treatment provided significantly lower SBS values in comparison to the self-adhesive systems and the systems with bonding pre-treatment ($p = 0.000$).

With the exception of encapsulated RelyX, all samples failed at the ceramic but not on the alloy side. Cohesive fractures were only observed for RelyX. All other systems showed adhesional or mixed failure modes.

4. Discussion

The hypothesis of this study that there is a difference between the SBS values of sophisticated multi-step bonding systems and self-adhesive systems was found not

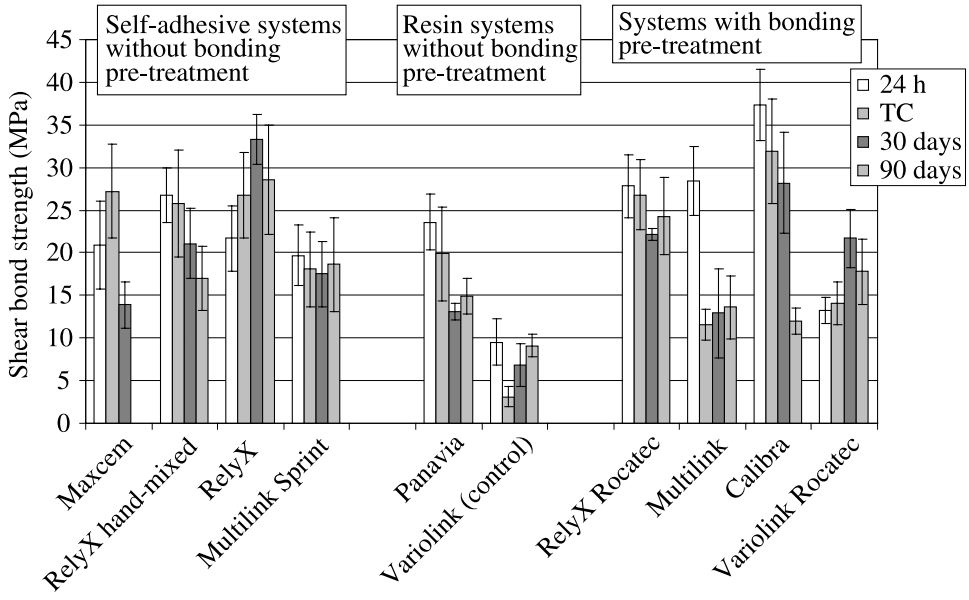


Figure 1. Shear bond strength (means, standard error of means, *: complete failure; Roc = Rocatec; cont = control; TC = thermal cycling).

to be valid. Only one self-adhesive system provided insufficient bond strength after 90 days storage. The results of the shear bond test cannot be transferred directly to the clinical situation, but this investigation allows for ranking and comparing different bonding concepts. The shear bond test may be affected by the bending of the individual components of the set-up (cylinder, coplanar plates, resin) under high shear forces [17]. Then the measured values represent the resistance of the single components against bending and not the shear bond strength itself. Therefore, cobalt–chromium (modulus of elasticity of about 200 GPa) was used instead of composite cylinders as described elsewhere [15, 18] in order to try to concentrate the stress in the bonding area. The present failure modes showed that the interface resin-to-alloy was stronger than the interface resin-to-zirconia. In contrast to other strength testing methods (e.g., tensile test), SBS is influenced by the roughness of the bonding area. The surface roughness which was achieved by the pre-treatment of the zirconia specimens in this study is comparable to results described in the literature (using 100–150 μm Al_2O_3) [8].

Self-adhesive composite cements offer a simple luting procedure, because they allow a bond between resin and zirconia without additional primer application. Both types of RelyX Unicem, Multilink Sprint and Panavia F seem to fulfill this promise, because they simplify the luting procedure on the zirconia surface. These systems show stable SBS values under different conditions or at least sufficient values after 90 days of storage in water. The results may presumably be an effect of phosphate groups in the cement, which has been described earlier [7, 13, 16,

19]. Therefore, phosphate monomer-containing resin cements may be promising for long-term stability of the bond between zirconia and metal. Indeed, the low results for Maxcem may allow to assume that phosphate components alone may not guarantee a sufficient bond to zirconia. Furthermore, the results show that the bond strength is strongly material-dependent. Even both types of Unicem (hand-mixed and capsule) show different bond strengths, which may be attributed to different compositions.

This study indicated that the different bonding systems have different sensitivity to hydrolysis. Some systems showed a strong (Panavia, RelyX hand-mixed or Multilink) or even drastic (Calibra) reduction of SBS compared to the results after 24 h, but remained on a good, or at least sufficient, bonding level. This is in agreement with other studies [13, 19]. Astonishingly, one self-adhesive system totally failed after 90 days of water storage. The type of polymerisation has a strong influence on the material properties: in self-curing mode, flexural strength and the modulus of elasticity cannot develop to such a high degree as compared to the dual-curing mode. The drop of bond strength might be attributed to hydrolytic degradation especially in combination with the low pH ∼4, which is achieved 24 h after self-curing [20].

Sandblasting of zirconia results in a remarkable initial SBS to a dual-curing composite like Variolink. Sandblasting may activate and modify the zirconia surface, but sandblasting effects may not be stable and SBS may be reduced after long-term storage in water [9, 10]. The addition of a silane coupling agent does not enhance the bond strength in the long-term. The initially high SBS of Calibra with silane was not durable. This indicates that the silane coupling agent used did not bond to zirconia in contrast to silica-based ceramics. These results agree with other investigations [21] where sufficient bond strength values were reported only with special silane agents [12].

The tribochemical treatment provided no advantages in combination with the self-adhesive cement RelyX and only some minor advantages when it was combined with the resin cement Variolink. These results may be explained by the hard/inert zirconia surface and support earlier investigations, where tribochemical treatment did not enhance bond strength [3] or even did not result in durable bonding [13]. A similar result is reported on alloys, where silica coating works more successfully with softer alloys than with harder ones [22]. In contrast to these results, Atsu and co-workers [18] recommend tribochemical treatment to increase the adhesive resin bond strength to zirconium oxide ceramic. These investigations were performed only after 24 h storage in water, without considering the long-term hydrolysis. Some authors even reported that an auto-polymerizing resin cement exhibited high bond strength regardless of the surface treatment such as silica coating, airborne particle abrasion, HF etching or grinding with a diamond bur [21].

5. Conclusions

Overall, within the limitations (e.g., testing methodology and number of cements) of this study, the systems with additional process steps are not superior to the simple self-adhesive methods and, therefore, the hypothesis stated in the Introduction is not found to be valid. Some self-adhesive bonding systems can successfully bond to zirconia. The use of resin cements without bonding pre-treatment should be avoided. The durability of the bonding between a resin and zirconia can only be judged after long-term water storage.

References

1. K. D. Jorgensen, *Acta Odontol. Scand.* **13**, 35–40 (1955).
2. R. P. Palacios, G. H. Johnson, K. M. Phillips and A. J. Raigrodski, *J. Prosthetic Dentistry* **96**, 104–114 (2006).
3. C. P. Ernst, U. Cohnen, W. Stender and B. Willershausen, *J. Prosthetic Dentistry* **93**, 551–558 (2005).
4. O. Zidan and P. Ferguson, *J. Prosthetic Dentistry* **89**, 565–571 (2003).
5. B. Blatz, A. Sadan and M. Kern, *J. Prosthetic Dentistry* **89**, 268–274 (2003).
6. B. Yang, S. Wolfart, M. Scharnberg, K. Ludwig, R. Adelung and M. Kern, *J. Dental Res*. **86**, 749–753 (2007).
7. M. Wolfahrt, F. Lehmann, S. Wolfart and M. Kern, *Dental Mater*. **23**, 45–50 (2007).
8. Y. Tsou, K. Yoshida and M. Atsuta, *Dental Mater. J.* **25**, 669–674 (2006).
9. I. L. Denry and J. A. Holloway, *J. Biomed. Mater. Res*. **76**, 440–448 (2006).
10. Y. Zhang, B. R. Lawn, E. D. Rekow and V. P. Thopson, *J. Biomed. Mater. Res.* **71B**, 381–386 (2004).
11. S. Debnatha, S. L. Wunder, J. I. McCool and G. R. Baran, *Dental Mater.* **19**, 441–448 (2003).
12. J. P. Matinlinna, T. J. Heikkinen, M. Özcan, L. V. Lassila and P. K. Vallittu, *Dental Mater*. **22**, 824–831 (2006).
13. M. Kern and S. M. Wegner, *Dental Mater*. **14**, 64–71 (1998).
14. H. Lüthy, O. Loeffel and C. H. Hämmerle, *Dental Mater*. **22**, 195–200 (2006).
15. T. Derand, M. Molin and K. Kvam, *Dental Mater*. **21**, 1158–1162 (2005).
16. K. Yoshida, Y. Tsuo and M. Atsuta, *J. Biomed. Mater. Res.* **77B**, 28–33 (2006).
17. B. W. Darvell, *Mechanical Testing*, 7th ed, Chapter 1, pp. 11–23. The University of Hong Kong, Hong Kong (2003).
18. S. S. Atsu, M. A. Kilicarslan, H. C. Kucukesman and P. S. Aka, *J. Prosthetic Dentistry* **95**, 430–436 (2006).
19. K. Yoshida, M. Yamashita and M. Atsuta, *Am. J. Dentistry* **17**, 249–252 (2004).
20. E. Saskalauskaite, L. E. Tam and D. McComb, *J. Prosthodont.* **17**, 262–268 (2008).
21. P. Derand and T. Derand, *Int. J. Prosthodont.* **13**, 131–135 (2000).
22. M. Behr, M. Rosentritt, G. Gröger and G. Handel, *J. Dentistry* **31**, 33–42 (2003).